
# SYNTHESIS AND BIOLOGICAL EVALUATION OF NEW TITANIUM(IV) COMPLEXES AND THEIR USE IN ANTI-CANCER TREATMENT

By

**Mohammed Adnan Abid**

B.Sc. (Chemistry), M.Sc. (Chemistry)

Thesis submitted to the University of Nottingham
for the degree of Doctor of Philosophy

**February 2021**

## Abstract

This thesis considers the synthesis, and characterisation of new fulvene ligands and titanium(IV) complexes and evaluation of their potential as anti-cancer agents. It contains the *in vitro* cell results from different techniques used to investigate their biological mechanisms of action and their activity against human cancer cell lines.

**Chapter One** covers an introduction to the PhD project, including a literature search focusing on previously synthesised titanium anti-cancer compounds (1979-2020), and a description of the aims of the thesis.

**Chapter Two** discusses the synthesis and characterisation of novel (*R*)-3-(cyclopenta-2,4-dien-1-ylidene)-2,3-dihydro-1*H*-inden-1-ol ligand precursors (two X-ray structures reported) attained *via* iminium-based organo catalysis in 53-78% yield (> 99% *er*). Unsuccessful attempts to form new titanocene complexes from these ligands are also discussed.

**Chapter Three** discusses the synthesis and characterisation of novel titanium(IV) complexes, using [ONO] donor atom sets from underutilised 2,2'-((methylazanedyl) *bis*(methylene)diphenol ligands. Complexes featuring different substituents (e.g. Cl, Me, OMe) *ortho* and *para* to the phenolic donors can be prepared in good yield (66-89%, eight examples). The structures of these complexes were proved by X-ray crystallography in four cases and studies of their hydrolysis in DMSO/water mixtures have conducted by $^{1}$H NMR spectroscopy and LCMS. In one case a [(ONO-ligand)Ti (OH)($OH_2$)]$^{+}$ intermediate can be detected. Biological studies, including MTT and clonogenic techniques, show high anti-cancer activity for these species ($GI_{50}$ values down to 1 μM for the MCF-7 cell line). The mode of action of these agents was studied by annexine-V, cell cycle analysis, γ-H2AX, and caspase

techniques. The antiproliferative activity of the new [ONO] donor atom titanium complexes compares favourably or outperforms cisplatin, in five carcinoma cell lines: HCT-116 (colorectal cancer) MCF-7 (breast cancer), MDA-MB-468 (breast cancer), PANC-1 (pancreatic cancer), and HT-29 (colon cancer). Thus, the new [ONO] donor atom complexes developed herein are some of the most active anti-cancer titanium species presently known.

**Chapter Four** presents the experimental details and characterisation data for all compounds described in Chapters Two and Three. It also provides protocols for all biological studies.

**Appendix** introduces additional figures relating to Chapter Three and a summary of crystallographic data for the X-ray structures obtained within this work.

# Declaration

I confirm that the work described in this thesis was conducted by ***Mohammed Adnan Abid***, the results of his own investigations at the University of Nottingham and are not being concurrently submitted in for any other degree. It has been our privilege to act as ***Mohammed Adnan Abid`s*** academic supervisors.

Yours sincerely,

Supervisor Signature:

Simon Woodward,

Professor,

School of Chemistry.

Supervisor Signature:

Tracey Bradshaw,

Assistant Professor,

School of Pharmacy.

# Acknowledgements

*Praise should be to **Almighty Allah** the Lord of the World, for he is the source of all knowledge, for giving me the patience, power and willingness to complete my PhD studies.*

*I would like to express my sincere gratitude to my supervisors, **Prof. Simon Woodward** and **Assistant. Prof. Tracey Bradshaw**, for their guidance, judicious advice, and unlimited support they have provided to me throughout my studies. I am truly grateful to them for giving me this opportunity to study at the University of Nottingham under their supervision and they will be blessed abundantly for all the advice, encouragement, and the support given to me throughout my studies.*

*I wish to expand my sincere gratitude and appreciation to my **parents**, my wife "**Hamsa Saadoon Abed**", to my kids "**Yazen, Rawan, Aiham**", to my brother **Dr. Ali Adnan Abid** and his family, and to my brother in law **Prof. Ahmed M. Turke** and his wife (my sister) **Tamara Adnan Abid** and their kids for their abundant support, patience, understanding, and for their love. I love you all.*

*I would like to express my thanks to: **Dr. Liam Ball**, **Dr. Mohannad Qazzaz**, **Dr. Melchior Cini** and **Dr. Huw Williams** for their support and advice given to me throughout my studies.*

*I also would like to express my thanks to my lab colleagues: **Dr. Mustafa Aljumaili**, **Dr. Ryan Nouch**, **Dr. Alexander Kingsbury**, **Dr. Mark Jurrat**, **Dr. Aimie Garces**, **Mustapha Musa**, **Thomas Barber, Lorenzo Maggi**, **Aaron Senior**, **Teresina Ambrosio**, **Kaouthar Bouzinab** and **Haneen Abuzaid**.*

*I would like to express my special thanks to* ***Dr. Saddam Almudadi***, ***Dr. Ayad Subhy***, ***Dr. Sean Goodwin*** *and* ***Dr. Daniel Smith*** *for their help and valuable advice throughout my study journey.*

*I am also grateful to the University of Nottingham for the scholarship provided (IDB 600032659), additional appreciation goes to the University of Anbar for providing study leave and additional funding to me during my period of study. I am also grateful to Nottingham Trent University (NTU) for their cooperation and assistance for allowing us to use some of their facilities to evaluate the anti-cancer properties of some my compounds.*

*For all my friends and those who I have not had space to specifically mention here, I am also truly grateful.*

***Mohammed Adnan Abid*** ***2021***

# Dedication

*I dedicated this work to my soul (**My Parents**) specifically my mother. She is suffering from breast cancer and I have been driven to work in this area hoping that one day I will able to find a cure to such malignant diseases for the good of humanity.*

## List of Abbreviations

| | |
|---|---|
| 1° Ab | Primary antibody |
| 2° Ab | Secondary antibody |
| bzac | Benzoylacetonate |
| ATCC | American Type Culture Collection |
| CpR | Substituted cyclopentadienyl, $\eta^5$-$C_5H_4R$ |
| Cp* | 1,2,3,4,5-Pentamethylcyclopentadienyl, $\eta^5$-$C_5Me_5$ |
| DBU | 1,8-Diazabicyclo[5.4.0]undec-7-ene |
| DMSO | Dimethyl sulfoxide |
| DNA | Deoxyribonucleic acid |
| EELS | Electron energy loss spectroscopy |
| *er* | Enantiomeric ratio |
| ESI | Electrospray ionization |
| η | Hapticity of ligand donor atoms π-coordinated to metal |
| FBS | Foetal bovine serum |
| G1 phase | Cell cycle, gap 1 phase |
| G2/M phase | Cell cycle, gap2/mitosis phase |
| $GI_{50}$ | Concentration of species inhibiting growth of cells by 50% |

| | |
|---|---|
| h | Hour |
| HCT-116 | Colorectal carcinoma wildtype |
| HPLC | High performance liquid chromatography |
| $IC_{50}$ | Half maximal inhibitory concentration |
| LCMS | Liquid chromatography mass spectroscopy |
| MAPK | Mitogen-activated protein kinase |
| MCF-7 | Michigan Cancer Foundation-7 (breast ductal carcinoma) |
| MDA-MB-468 | Breast adenocarcinoma |
| mg | Milligram |
| ml | Millilitre |
| µl | Microlitre |
| µM | Micromolar |
| MRC-5 | Medical Research Council strain 5 (normal lung tissue) |
| MTT | 3-(4,5-Dimethylthiazol-2-yl)-2,5-diphenyltetrazolium bromide |
| n.O.e. | nuclear Overhauser effect |
| *n*-Bu | Butyl |
| p53 | Tumour protein 53 |
| PANC-1 | Pancreas adenocarcinoma |

| | |
|---|---|
| PBS | Phosphate-buffered saline |
| PI | Propidium iodide |
| $pK_a$ | $-Log_{10}$ of the acid dissociation constant |
| PS | Phosphatidylserine |
| PCD | Programmed cell death |
| RPMI-1640 | Roswell Park Memorial Institute |
| S phase | Cell cycle, synthesis phase |
| $T_0$ | Time zero |
| THF | Tetrahydrofuran |
| Tf | Transferrin |
| TFA | Trifluoroacetic acid |
| TMEDA | *N*,*N*-tetramethylethylene diamine |
| Ts | Tosyl |

## Table of Contents

# Chapter 1

# 1. Introduction

## 1.1. Cancer

'Cancer' is the term given to a group of diseases deriving from the mutation of cells in the body that were initially derived from normal cells. These transformed cells grow and divide in an uncontrolled manner.[1] Cancer is a widespread health problem globally and is a major cause of death worldwide.[2] According to Cancer UK Research (a UK based cancer research and awareness charity), there are more than 200 different types of cancer. In the UK, there were about 363,000 cases of diagnosed cancer between 2014 and 2017; 164,901 cases led to death in the same period. [see:www.cancerresearchuk.org/health-professional/cancer-statistics-for-the-uk].

Cancer is a complex disease, identified by abnormality in cell growth, in which such abnormal cells can attain the ability to metastasise (transfer) from their origin site (primary tumour) to secondary site in other parts of the body (secondary tumours).[3] Tumours can be categorised into two types: malignant and benign.[3-4] Benign tumours are characterised by normal chromosomes, division is rare, the cells are differentiated, and growth is slow. These benign tumours do not metastasise.[1] In contrast, tumours that spread into or invade adjacent tissues are called invasive and cells that migrate to other parts of the body to create new secondary tumours are called metastatic.[4]

### 1.1.1. Cancer classifications

Although there are many types of cancers, from a histological perspective they can be grouped into five classifications:[5]

1) **Leukaemia**: "blood cancers" or "liquid cancers" are cancers of immature WBCs (white blood cells) that grow in the bone marrow and accumulate significantly in the bloodstream.

2) **Carcinomas**: refer to cancers of the external or internal lining of organs in the body, which constitutes around 90% of all cancer cases. Examples include, lung, colon and breast cancer.

3) **Lymphomas**: originate or establish in the nodes or glands of the lymphatic system.

4) **Myeloma**: are cancers initiating from plasma cells of the bone marrow, these cells generate certain kinds of proteins known as paraproteins which have no beneficial function and circulate in the blood.

5) **Sarcomas**: are cancers that arise in connective and supportive tissues of the body such as tendons, muscle, bones, fat, and cartilage.

## 1.2. Treatment of cancer

Many drugs have been used in the treatment of cancer. The mode of treatment of cancer depends on the type of cancer, grade of cancer, location, the stage of the disease, and the drug used. Treatment of cancer can be achieved by surgery, chemotherapy, radiation therapy, hormonal therapy and molecularly targeted therapy. Generally several types of treatment are used in combination to give optimal effects.[6] This thesis specifically discusses anti-cancer compounds which contain transition metal elements within their structure. These are attractive and promising for many reasons: adjustable ligands, structural diversity, interesting exchange kinetics, and fine tuneable redox properties. Such useful properties make them exciting chemical scaffolds in new potential cancer therapies.[7]

## 1.3. Historical non-metal and metal-based compounds used to treat cancer and other diseases

### 1.3.1. Nitrogen mustards

Nitrogen mustards (**Figure 1**) were first prepared in 1930s-1940s as chemical warfare agents, due to their toxicity being similar to that of sulfur mustards.[8] They were the first anti-cancer agents to be utilised. Early (1940s) trials showed their chemotherapeutic effects in the treatment of lymphosarcoma.[9] Their mode of action involves DNA alkylation. The nitrogen mustard, forms an aziridinium ion intermediate by intramolecular displacement of a chloride atom by the nucleophilic nitrogen atom. This reactive intermediate ion then reacts most frequently with, the guanine base in DNA at the *N7* position, forming a covalent bond to the nitrogen mustard agent. Bifunctional crosslinking of two strands of DNA results and prevents cell growth, leading to apoptosis. While nitrogen mustards have been shown to be

effective against lymphoid malignancies and leukaemia, they exhibit significant side effects, such as killing the white blood cells, and they have an extreme effect on bone marrow.[10]

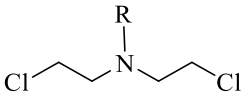


**1** R = Me
**1a** R = Et
**1b** R = $CH_2CH_2Cl$

**Figure 1.** Nitrogen mustard structure.

From the introduction into the clinic of the first antineoplastic chemotherapeutic nitrogen mustard agent in 1942, many metal-free anti-cancer agents have arisen in the last 80 years.[11] These include the use of other alkylating agents, antimetabolites, natural products and hormones.[12] Below are such examples of, drugs used to treat different cancer types:

Temozolomide is an alkylating agent used in treatment of glioblastoma multiforme.[13] The proposed mechanism of action is that it methylates *N7*, *N3*, *O6* sites in guanine and *N3* in adenine. It is the *O6*-methylguanine adduct that is the primary cytotoxic lesion. However, if the tumour expresses the direct repair protein *O6*-methylguanine-DNA methyltransferase (MGMT), resistance to temozolomide is conferred.[14] Another front line anti-cancer drug, Taxol (paclitaxel) is a natural product and one of the chemotherapy drugs derived from plant alkaloids. Taxol was isolated from Pacific Yew *Taxus brevifolia*.[15] This drug acts as a microtubule disrupting agent, which means that it stabilises the microtubules and inhibits microtubule depolymerisation. It leaves cells stranded in mitosis and leads to a

mitotic catastrophe and apoptosis.[16] It is often used in combination with cisplatin for treatment of solid cancers such as ovarian, breast carcinoma, and lung.[17] A final front line example, Glivec (Gleevec, Imatinib) is used in treatment of chronic myeloid leukaemia and also in treatment of gastrointestinal stromal tumours (GISTs).[18] It is a tyrosine kinase inhibitor and specifically inhibits the constitutively active protein product of the *bcr-abl* oncogene. Bcr-abl oncoprotein is produced as a result of a chromosome translocation between chromosomes 9 and 22 which give rises to the Philadelphia chromosome and results in constitutive activation of bcr-abl tyrosine kinase. Glivec also inhibits other protein tyrosine kinases such as the product of *c-kit* oncogene.[18] Taxol and Temozolomide are termed cytotoxic antitumour agents, whereas Glivec is a molecularly-targeted antitumour agent. However, as the focus of this thesis is exclusively on metal-based therapies only these are discussed in detail in the next sections.

### 1.3.2. **Metal-based drugs**

Many metal compounds have been proposed to treat cancer (and other diseases) over the last century, and this field is active and still growing.[19] Transition metal complexes are important compounds in the field of biology and can play a role in disease treatment. As early as 1910 the use of metal-based complexes in medicine had been initiated, when arsphenamine, an arsenic containing therapeutic agent (**Figure 2**), was first used to treat syphilis.[20] Arsphenamine ('Salvarsan') consists of cyclic trimers and pentamers (**Figure 2**) but is too toxic for modern use.[21] Subsequently other metal-based complexes were used to treat many diseases.[22]

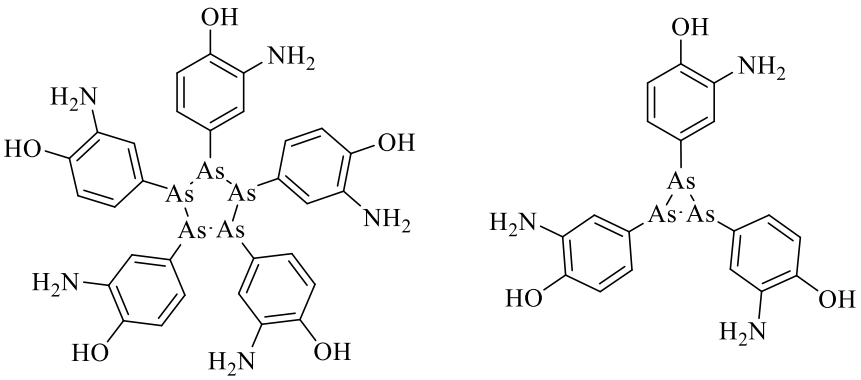

**2** **2a**

**Figure 2.** Cyclic arsphenamine structures.[21]

### 1.3.3. Platinum compounds as anti-tumour drugs

The complex *cis*-diamminedichloroplatinum(II) *or* cisplatin (**3**) (**Figure 3**) was first discovered in 1845 and was coined "Peyrone's salt".[23] In 1893 Werner derived the structure of cisplatin when he proposed the theory of coordination chemistry. He demonstrated that ammonia can bind to the Pt(II) by donating its lone pair in a coordination or dative bond.[24] However, it was not until the late 1960s that cisplatin's anti-tumour efficacy was established by Rosenberg.[25] This discovery was made serendipitously during an experiment to measure the effect of electrical currents on bacterial cell growth in *E. coli* using an aqueous solution of ammonium chloride and platinum electrodes.[24] Since that time **3** has been used to treat many different human malignancies, but especially testicular cancer. In addition to its remarkable success in testicular cancer, **3** is active against a wide variety of solid tumours, *i.e.* lung, cervical, ovarian, head and neck, and bladder.[26] Although **3** is highly efficient, it has drawbacks such as nephrotoxicity, neurotoxicity, vomiting, cancer resistance and these all remain major challenges for **3**-based anti-tumour therapy.[23, 26] For this reason, numerous other platinum complexes (2$^{nd}$ and 3$^{rd}$ generation species), have been studied in an attempt to defeat these problems (**Figure 3**).

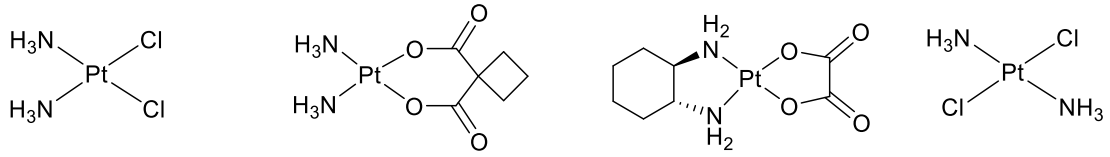


**3** Cisplatin
1st generation

**3a** Carboplatin
2nd generation

**3b** Oxaliplatin
3rd generation

**3c** *trans*-DDP
3rd generation

**Figure 3.** Structures of some platinum compounds investigated for biological activity.[25]

The compounds in **Figure 3** displaying anti-tumour activity share the same sub-structure as **3** (*cis*-amine ligands). Carboplatin **3a** has increased activity compared to **3**, due to the cyclobutanedicarboxylate ligand which is more stable vs. the chloride ligands of **3**. This increased stability is due to slower hydrolysis *in vivo* which allows more time for the complex to reach the target before the ligand is displaced. Another advantage of **3a** is its lower toxic side effects, allowing the drug to be administrated in higher dosage compared to **3**. However, **3a** induces greater bone marrow toxicity.[27] Oxaliplatin **3b** also provided lower toxic side effects than **3** and also displayed a lack of cross resistance, leading to it being preferred to treated colorectal cancer.[25, 27] In contrast, **3c** (*trans*-DDP), the geometric isomer of **3**, does *not* follow the patterns as those found for cisplatin and its analogues. Although **3c** is kinetically more reactive than **3**, it is clinically ineffective. This is despite the fact that **3c** can form more varied platinum-DNA adducts than the other cisplatin analogues.[27-28]

### 1.3.4. The mechanism of cisplatin (mode of action)

Once cisplatin (**3**) enters the body and reaches the target organs, it passes through the cell membrane by passive transport. Once inside the cell hydrolysis of **3** is rapid as the concentration of chloride ions is low in the cell cytoplasm, enabling water molecules to replace the labile chloride ligands (**Scheme 1-A**).[29] The cisplatin becomes extremely electrophilic through the aquation process and facilely binds to different biomolecules within the cell, particularly DNA bases. Cisplatin interacts specifically with *N*7-sites of the purine bases. This results in two types of DNA adducts. If the purines are located on the same strand, this generates intrastrand adducts. By contrast, an interstrand crosslink is produced if the purines are located on opposite strands (**Scheme 1-B**). This causes structural changes to the DNA strand preventing replication; the cross-linking then prevents cell division and leads to arrested tumour growth.[26]

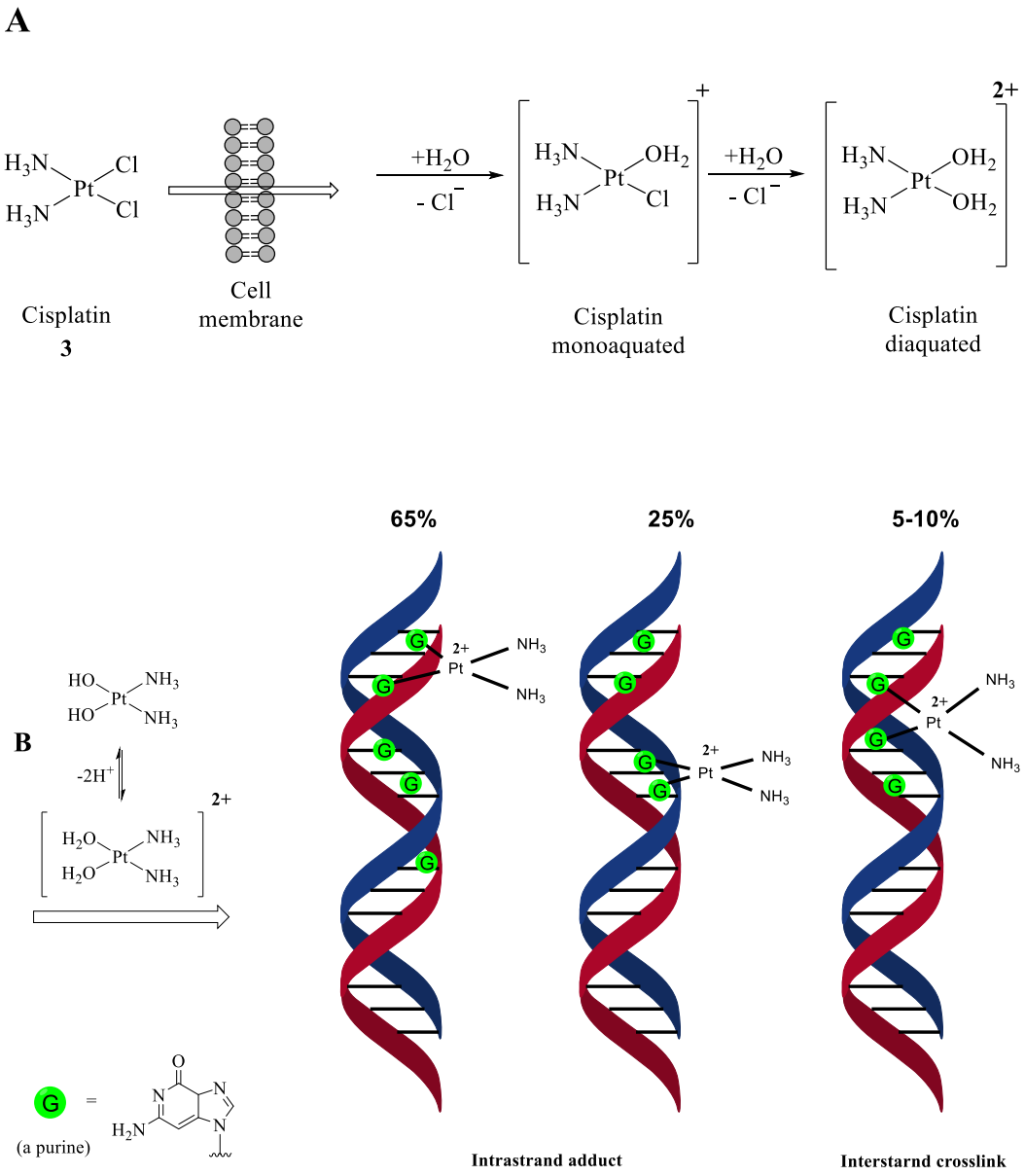


**Scheme 1.** Cisplatin **A**) Aquation inside the cell results in two chlorides being replaced by two molecules of water. **B**) Formation of covalent bonds with DNA, 90% of DNA lesions are intrastrand DNA adducts, and ~5-10% are interstrand, crosslinked adducts.[26]

As stated previously, **3** reacts with purines and binds more readily to guanine over other bases, e.g. adenine. This is due to the higher nucleophilicity of the *N7* of guanine and stronger hydrogen bonding of the ammonia NH-amine to the *O6* of the guanine (**Figure 4**).[30]

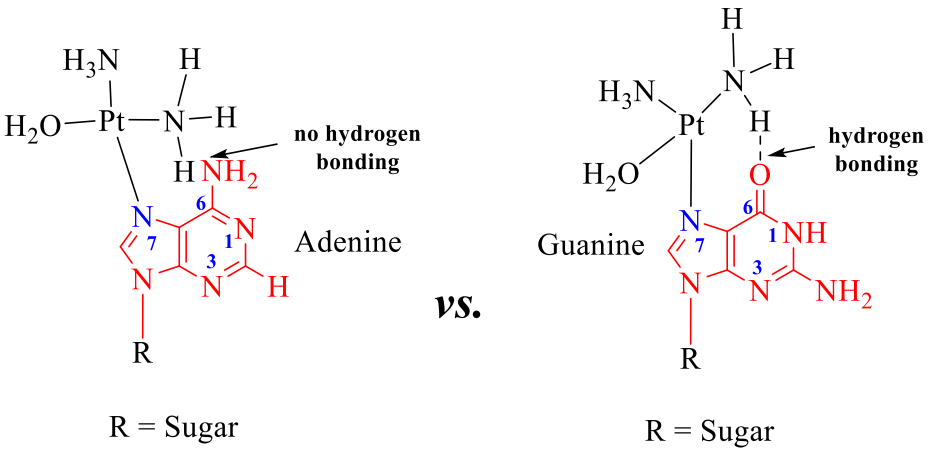


**Figure 4.** Platinum binding to *N7* guanine is kinetically favoured due to hydrogen bonding between the NH-amine of diaqua form of cisplatin and ketone *O6* of guanine.[30]

Cisplatin prevents the DNA synthesis and transcription, which in turn triggers an intricate intracellular signal transduction cascade as the cell attempts to remove the Pt-lesions. The cell cycle is arrested, providing time for attempted DNA repair mechanisms to eliminate the lesions. Ultimately, when this fails, apoptosis is activated and programmed cell death ensues.[26, 31]

### 1.3.5. Cisplatin resistance

Even though cisplatin is highly effective, resistance is frequently acquired during cancer treatment cycles. Both acquired and initial resistance are common and remain a considerable challenge for cisplatin based anti-cancer therapy. There are many

opportunities for cells to deactivate cisplatin including: down-regulation of the chloride transport receptor 1 (CTR1) and Cu-transport pump thus decreasing intracellular cisplatin levels.[26] Cisplatin resistance may also be conferred by increased levels of glutathione (GSH), glutathione *S*-transferase (GST) and the ATP-dependent glutathione S-conjugate export pump (GS-X) pump. Finally, up-regulation of the multidrug resistance-associated protein 1 (MRP-1) also reduces intracellular cisplatin levels, and thus sensitivity to this agent.[26, 32] However, when cisplatin reacts with DNA, leading to different DNA lesions, unless this is repaired, the extensive damage to the DNA causes the cells undergo to apoptosis (**Scheme 2**).[26]

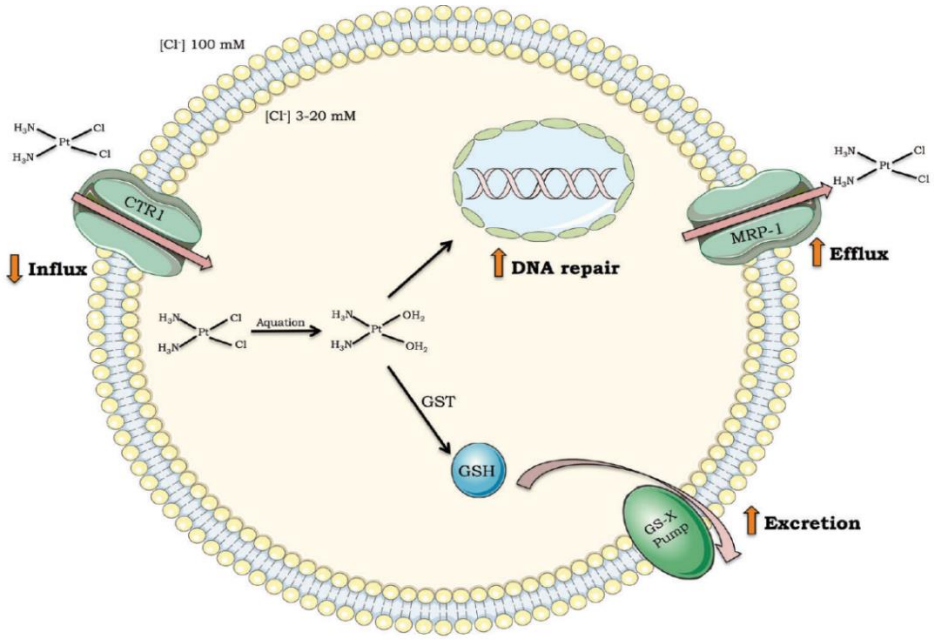


**Scheme 2.** Mechanisms of cancer cell resistance to cisplatin. Chloride transport receptor 1 (CTR1); glutathione (GSH); glutathione S-transferase (GST); multidrug resistance-associated protein 1 (MRP-1); ATP-dependent glutathione S-conjugate export pump (GS-X pump).[26, 32]

## 1.4. Titanium(IV) complex based anti-cancer agents

Over the last 60 years many metal complexes, other than platinum species, have been screened for anti-cancer activity, but their development to viable therapies has been at a very slow pace. Part of the reason for this is that most new complexes show varying mechanisms of action depending on metal Lewis acidity, surrounding ligands and oxidation state.[33] An exact understanding of a drug candidate's mechanism of action is a requirement for it to pass key legislation associated with use in patients. The mechanistic complexity of many metal therapies has slowed their development. For over three decades, transition-metal complexes containing multi-dentate ligands have generated considerable interest as their hydrolytic decomposition pathways are minimised.[34] Considerable advances have been made in understanding and developing the structures and reactivity of these species. Titanium, ruthenium, and Pt-based metals complexes are at the forefront of these developments.[35] One popular ligand in titanium-based anti-cancer compounds are functionalised derivatives of cyclopentadienyl ($\eta^5$-$C_5H_5$) ligands. As these are commonly derived from fulvene derivatives these are considered next.

### 1.4.1. Fulvenes (pentafulvenes)

The word fulvene (pentafulvene) was coined by Thiele in 1900 from the Latin word (fulvus) meaning yellow. Pentafulvene is the name for the unsubstituted parent compound $C_6H_6$ (**4**) (**Scheme 3**), which can be derivatised by the addition of substituents (R) (**Scheme 3**). Because of the resonance forms of **4**, pentafulvenes are potential precursors to the types of substituted cyclopentadienyl ligands initially needed for this PhD project. Although pentafulvenes are isoelectronic with benzene they show profound differences in reactivity and colour to benzene.[36]

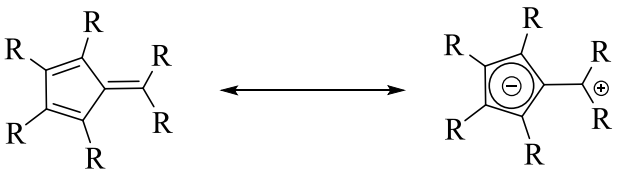

**4** R = H
**5** R = Me

**Scheme 3.** The structure of fulvene and its resonance.

Fulvenes are powerful precursors to a wide range of cyclopentadienyl derivatives and are attractive as they are typically relatively easy to prepare, e.g. **5** (**Scheme 4**).[37] A common approach is the condensation of cyclopentadiene (CpH) **6** with a carbonyl derivative in the presence of base, usually piperidine or pyrrolidine (**Scheme 4**). A large range of functionalised fulvenes bearing thiols, halogens, cyclopropyls, and alcohols can be made this way.[36a, 38]

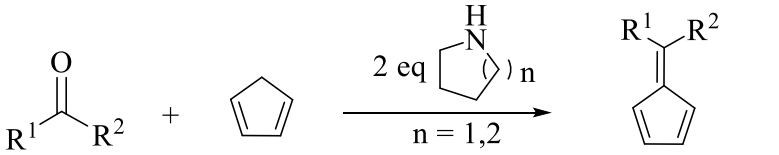

**6** **5** R = Me

**Scheme 4.** Synthesis of fulvenes by condensation of **6** with carbonyl compounds in the presence of base.

Pyrrolidine acts as an organocatalyst in the condensation of **6** with a carbonyl containing substrate and not just as a base. The iminium formed from the pyrrolidine and substrate carbonyl has a much lower LUMO than the carbonyl alone, enabling the double bond of **6** to attack the electrophilic carbon of carbonyl group as a nucleophile. The pyrrolidine also acts as a base deprotonating **6** to form the active nucleophile.

Using benzaldehyde derivatives such as **7**, the condensation leads to the formation of benzylidene fulvenes, as can be seen in **Scheme 5-A**. By reacting such fulvenes sequentially with $LiBHEt_3$ and $TiCl_4$ many benzyl-substituted titanocene dichloride compounds have been synthesised.[39] The hydride transfer reagent $LiBHEt_3$, results in the formation of the substituted lithium cyclopentadienyl intermediate **8a**. Reaction of (2 equiv.) of **8a** with (1 equiv.) of titanium tetrachloride (by transmetallation reaction) in THF under reflux resulted in non-bridge substituted titanocene dichloride **9** (**Scheme 5-B**).[40] More recently, novel methods starting from fulvenes (which will be discussed later in Chapter Two) and other precursors allow direct access to substituted titanocenes *via* reductive dimerisation with titanium dichloride, carbolithiation or hydridolithiation of the fulvene, followed by transmetallation with titanium tetrachloride.[37]

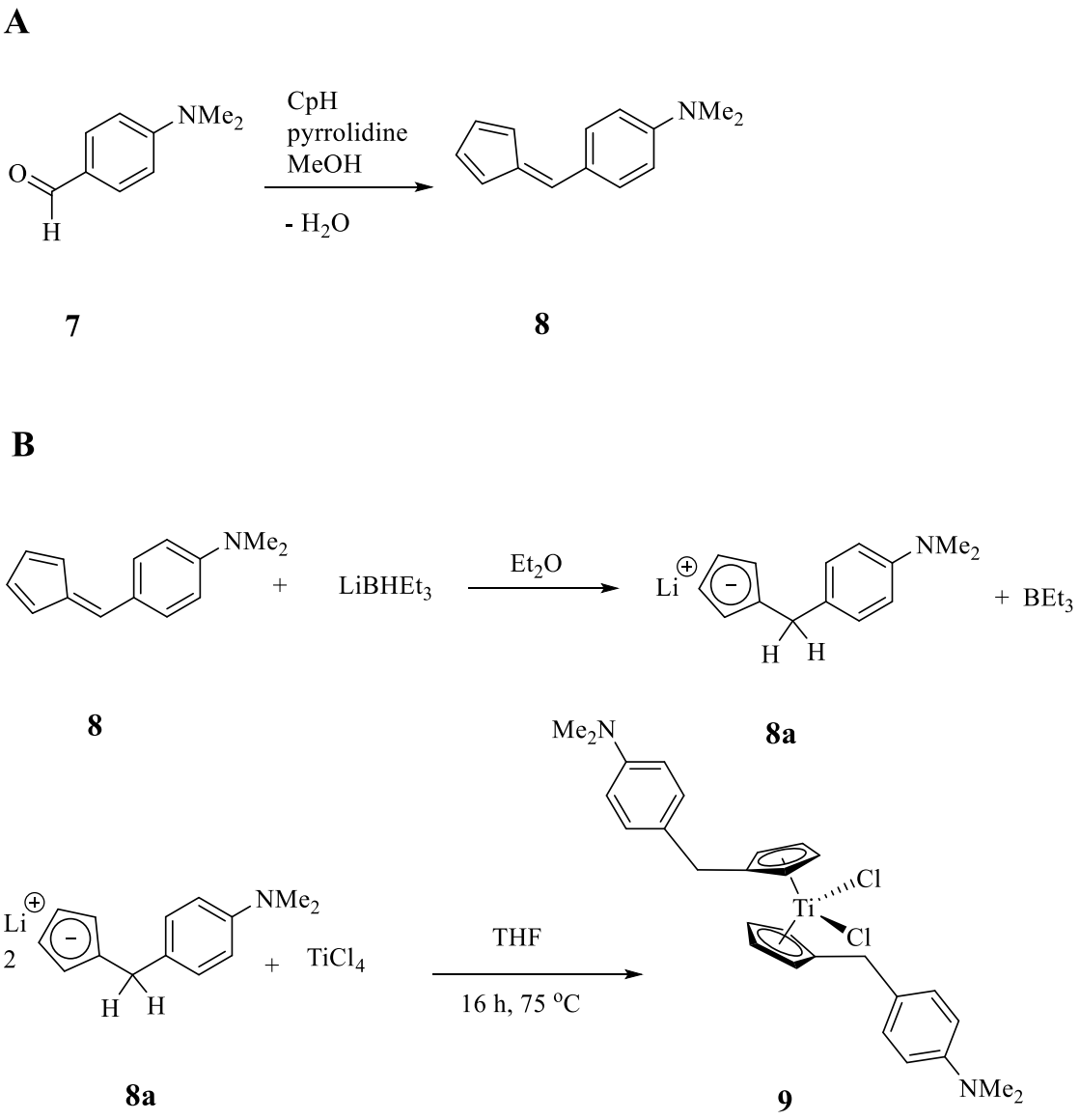


**Scheme 5. A**) Synthesis of 6-aryl fulvenes. **B**) Synthesis of "non-bridged" benzyl-substituted titanocene dichlorides.[37]

### 1.4.2. Metallocene as anti-tumour drugs

Generally, the metallocene motif of organometallic chemistry refers to *bis*(cyclopentadienyl)metal complexes (so called 'sandwich' complexes), but a wider usage is now accepted and includes mono cyclopentadienyl complexes ('half sandwich' complexes) and multicyclopentadienyl complexes ('multidecker sandwich' complexes) as well as complexes with additional substitution at the metal centre. In fact, metallocene-like complexes are now known for >50 elements in the periodic table.[41] The general structure of the metallocene typically consists of two cyclopentadienyl anions (Cp) ($\eta^5$-$C_5H_5$) unit. Attaching various Cp units to metals (M) in different oxidation states forms the final structure of most metallocenes. For example, the most relevant metallocene to this thesis is dichloro *bis*($\eta^5$ cyclopentadienyl)titanium (titanocene dichloride) **10** (**Figure 5**).

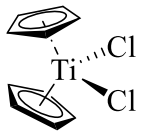


**10**

**Figure 5.** The structure of (titanocene dichloride) **10**.

#### 1.4.2.1. Cytostatic activity of titanocene dichloride

Titanocene dichloride (**10**) was first reported in 1955, and its cytostatic activity has remained under almost continuous investigation since 1979.[42] It was anticipated that **10** should show anti-cancer activity, since it contains *cis*-dichloro ligands in a neutral complex.[43] The mechanism was initially thought to be similar to that of well-known anti-tumour agent cisplatin (**3**) involving hydrolysis of the chloride ligands (**Scheme 6**, **10b**).[42, 44]

In 1979 Köpf-Maier investigated the anti-tumour activity of many types of metallocenes. In particular, they reported in detail the anti-tumour activity of **10** (**Figure 5**) which was tested on Ehrlich ascites tumour cells implanted into $CF_1$ mice, which showed a remarkable cure rate of over 80%.[45] Complex **10** showed promise against a diverse range of human carcinomas, including breast and gastrointestinal cancer.[45] It progressed successfully through phase I clinical trials into phase II in the late 1980s, but the trials were stopped due to the low efficacy in human subjects.[46] Despite cisplatin (**3**) being the first species used in metal based cancer therapeutic agents, titanium complexes, especially derivatives of titanocene dichloride **10**, have always had a significant profile in this area. Among all of the metals studied to date, which comprise much of the periodic table, complexes of titanium have shown particular promise due to significant activity against tumours that are resistant to cisplatin combined with very low *in vivo* toxicity; particular for the titanium complexes **10** (**Scheme 6**).[47]

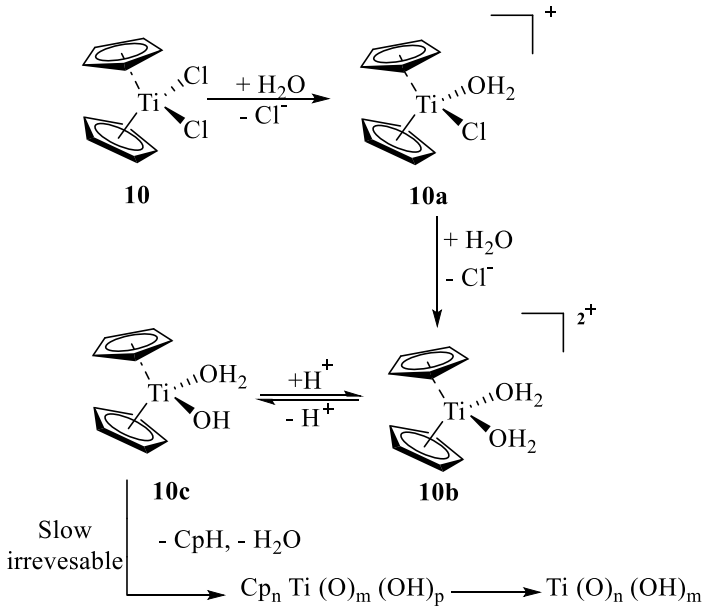


**Scheme 6.** The hydrolysis of titanocene dichloride **10**.

Although hydrolysis likely plays a significant role in the activation of titanocene derivatives as tumour inhibitors few studies, as yet, reliably support this postulate due to the complexity of the hydrolysis events (**Schemes 6-7**).[46] Based on comparison of titanocene dichloride (**10**) with cisplatin (**3**), Jeffrey *et al.* suggested that the hydrolysis of the chloride ligands in **10** occurred faster than in the case of **3**.[43, 48] The formation of unknown aggregates also obstructs therapeutic use and mechanistic investigation.[49]

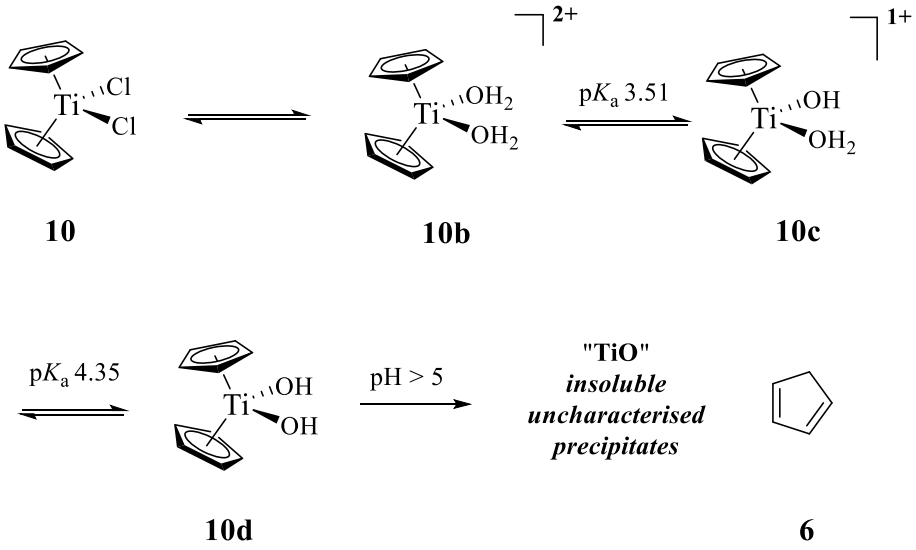


**Scheme 7.** The major species present during physiological pH hydrolysis of **10**. The structure of the precise species in an aqueous solution depends on pH, concentration and salt.[48]

Sadler *et al.* proposed that DNA is the main cellular target of **10**.[50] Additionally, Köpf-Maier initially suggested **10** inhibits DNA synthesis rather than protein and RNA synthesis and that titanium accumulates in nucleic acid-rich regions of tumour cells.[51] However, unlike **3**, **10** does not bind strongly to DNA bases at physiological pH but forms strong complexes with nucleotides solely at pH values below 5.[52] Hydrolysis of the chloride ligands of **10** (as mentioned above) happens very rapidly in aqueous solutions, resulting in the formation of aqua-, hydroxo-, μ-hydroxo or

μ-oxo bridged species, depending on the pH value and concentration.[53] It is potentially possible that inhibition of DNA replication is triggered by phosphate coordination to these species.[54]

### 1.4.3. Titanocene dichloride derivatives

Complex **10** was the earliest Ti-anti-cancer complex to be developed, and demonstrated significant activity against lung, colon, and breast cancers.[55] Unfortunately, the performance of **10** with metastatic renal-cell carcinoma and metastatic breast cancer in Phase II clinical trials in patients was unsatisfactory.[56] Therefore, many efforts to increase the cytotoxicity of **10** through analogues were made and several hundred substituted titanocenes have been developed over the last 30 years.[57] More efforts are still required to attain species showing low toxicity and high uptake inside the human body. For this reason, McGowan *et al.* established an elegant synthesis of ring-substituted cationic titanocene dichloride analogues, which are all water-soluble and show significant activity against ovarian cancer and some other cell lines.[58] In recent years, a variety of titanocene dichloride derivatives with interesting cytotoxic properties have been synthesised, including benzyl-substituted titanocene, titanocene derivatives with alkylammonium substituents on the cyclopentadienyl rings, alkenyl-substituted titanocenes, and amide functionalised titanocenyls (**Figure 6**).[51] Some of these titanocenes showed higher activity than **10**, e.g. while the $IC_{50}$ of **10** against kidney cancer is above 2000 μM, that of the titanocene dichloride analogue **11** showed 100-fold improvement in activity against same cell line.[37]

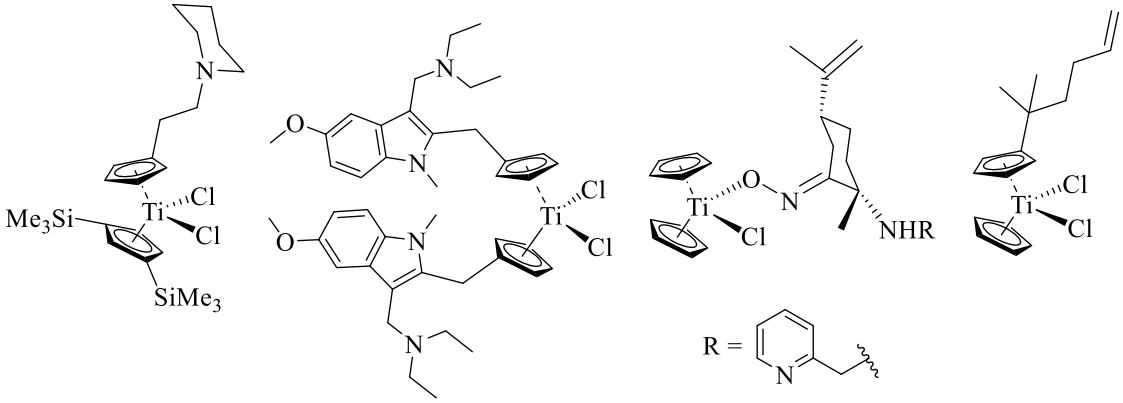


**11** **12** **13** **14**

**Figure 6.** Literature titanocene derivatives that have been screened for cancer cell line inhibition: **11** titanocene derivative with alkylammonium substituents,[23] **12** (*bis*-[((5-methoxy-1-methyl,3-diethylaminomethyl)indol-2-yl)methylcyclopentadienyl]-tanium(IV) dichloride),[59] **13** (2-picolylamine) titanocene,[60] **14** alkenyl-substituted titanocene derivative.[23]

### 1.4.3.1. **Chiral titanocene derivatives**

A new class of titanocenes has emerged recently which are optically active and more water soluble than **10** and show moderate to good anti-cancer activity.[61] In medicinal chemistry stereochemistry plays a significant role in biological efficacy as biological targets are typically chiral.[62] A range of chiral metal complexes have been the subject of anti-cancer studies, e.g. the *trans* form of 1,2-diaminocyclohexane of oxaliplatin.[63] However the function of the stereochemistry in non-platinum based compounds, for example Ti(IV), in biological activity has been less examined.[64] In 2011 Manna *et al.* suggested that stereochemistry plays a significant role in biological recognition when identifying cytotoxicity, and that this has to be considered in the modification, design, and enhancement of active compounds.[65] For example, Cini (2016) found that cytotoxic activity is enantiomer-dependent for the chiral substituted titanocene compound of $TiCl_2[\eta\text{-}C_5H_4CHEt(2\text{-}MeOPh)]_2$ [abbreviated $(CpR)_2TiCl_2$].

The (*S*,*S*) enantiomer of $CR_2TiCl_2$ (**15**) being twice as effective as the (*R*,*R*) isomer towards pancreatic, colon and breast cancer cell lines (**Figure 7**).[61] This is due to the biological targets, such as nucleic acids and proteins, being chiral. Clearly chiral **15** interacts with biological targets in different ways depending on its chirality.[63]

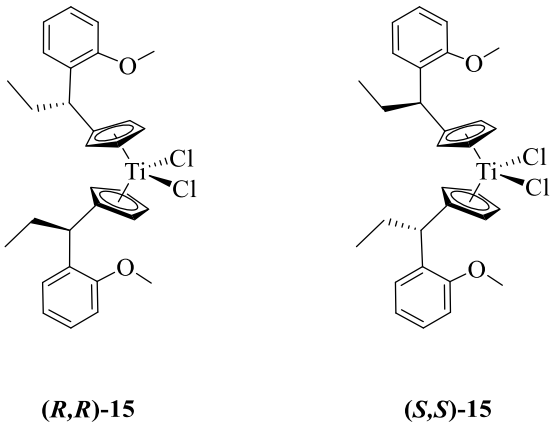


**(*R*,*R*)-15** **(*S*,*S*)-15**

**Figure 7.** The enantiomers of **15**.

During the last four decades, chiral and achiral analogues of **10** titanocene dichloride have attracted considerable interest as potential alternate chemotherapeutic agents to cisplatin (**3**).[66] New species, based on pentafulvene derived titanocenes, in the last 15 years were reported by Tacke and his group (see Chapter Two). These species include *ansa*-titanocenes (**16**) (*ansa*-titanocenes are characterised by a C─C bridge between Cp (cyclopentadienyl) rings, leading to restriction of the conformation of the Cp rings), 6-*N*,*N*-dimethylamino titanocene (**16a**), and benzyl substituted titanocenes (**16b, 16c**) (**Scheme 8**). These structures showed modest, e.g. with (**16**) $GI_{50}$ ~ 210 µM, or high activity e.g. for (**16a-c**) $GI_{50}$ ~ 5.5, 26, and 21 µM respectively against LLC-PK cells (pig kidney cancer).[37] However, all of Tacke's procedures lead only to attain achiral titanocenes or mixtures of stereoisomers.

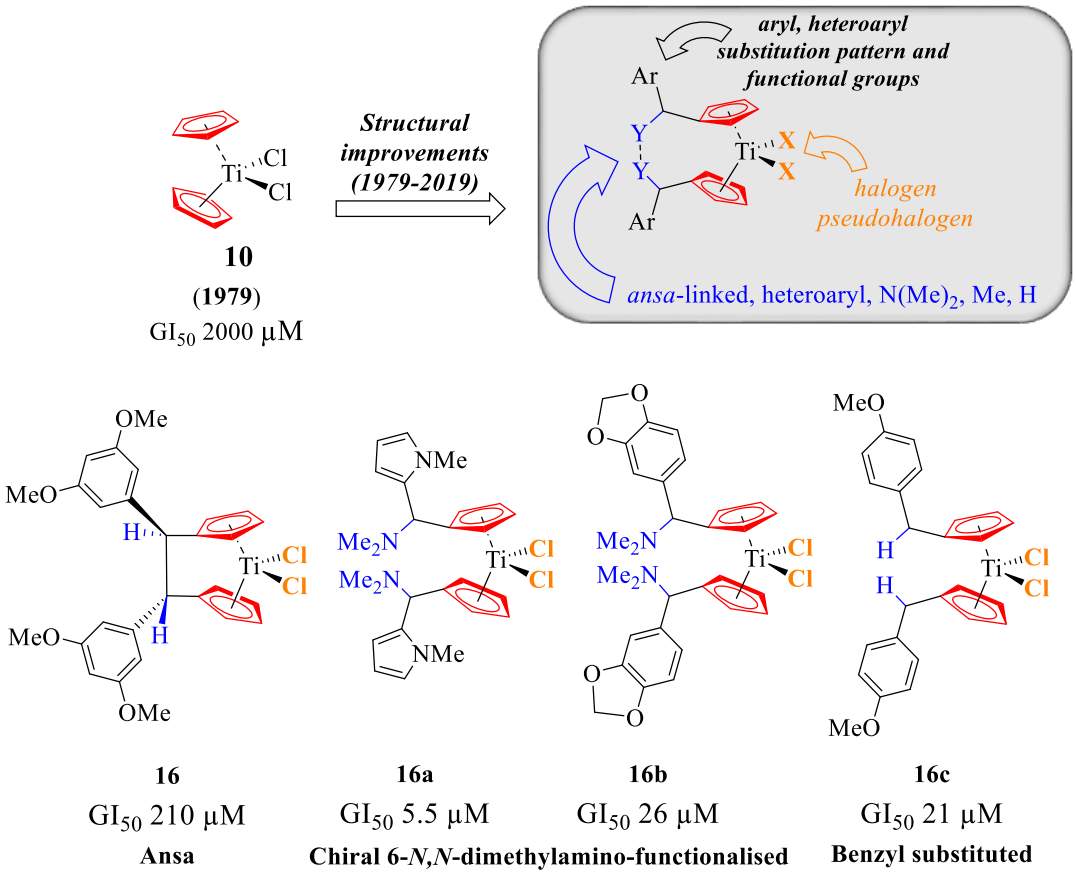


**Scheme 8.** The titanocene structural improvements. Biological activities against LLC-PK cells (pig kidney cancer) which cisplatin shows a $GI_{50}$ value of 3.3 µM.

## 1.5. Budotitane

Along with cisplatin and titanocene dichloride, the *bis* (*β*-diketonate) titanium(IV) motifs (**Figure 8**) have also been used to formulate anti-cancer drugs.[67] Budotitane $[Ti(bzac)_2(OEt)_2]$ **17** was the first non-platinum complex to enter clinical trials (**Figure 8**). It has been used against a wide variety solid tumours and showed significant activity during its preclinical evaluation.[33, 68] Keppler *et al.* have studied the anti-tumour activity of this complex using different tumours.[69] It was shown to be effective against Walker 256 carcinosarcoma ascitic tumours, and sarcoma 180 ascitic tumour.[69] Budotitane entered phase I trials in the 1990s and these studies showed it was fairly well tolerated, with nephrotoxicity and liver toxicity being the main side-effects.[69-70] The dose limiting toxicity was associated with cardiac arrhythmia.[67] However, clinical trials for phase II and III stopped due to a consequence of problems with formulation.[55, 71]

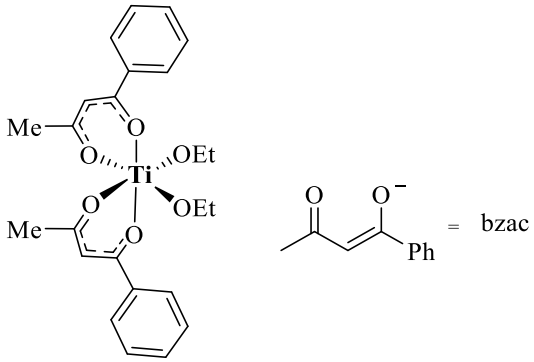


**17**

**Figure 8.** Structure of budotitane **17**.

The mechanism of budotitane towards cancer is poorly understood. It was suggested that budotitane initially loses the two ethoxide ligands followed by bzac ligands, leading to the eventual formation of $TiO_2$ (titanium dioxide) (**Scheme 9**).[69]

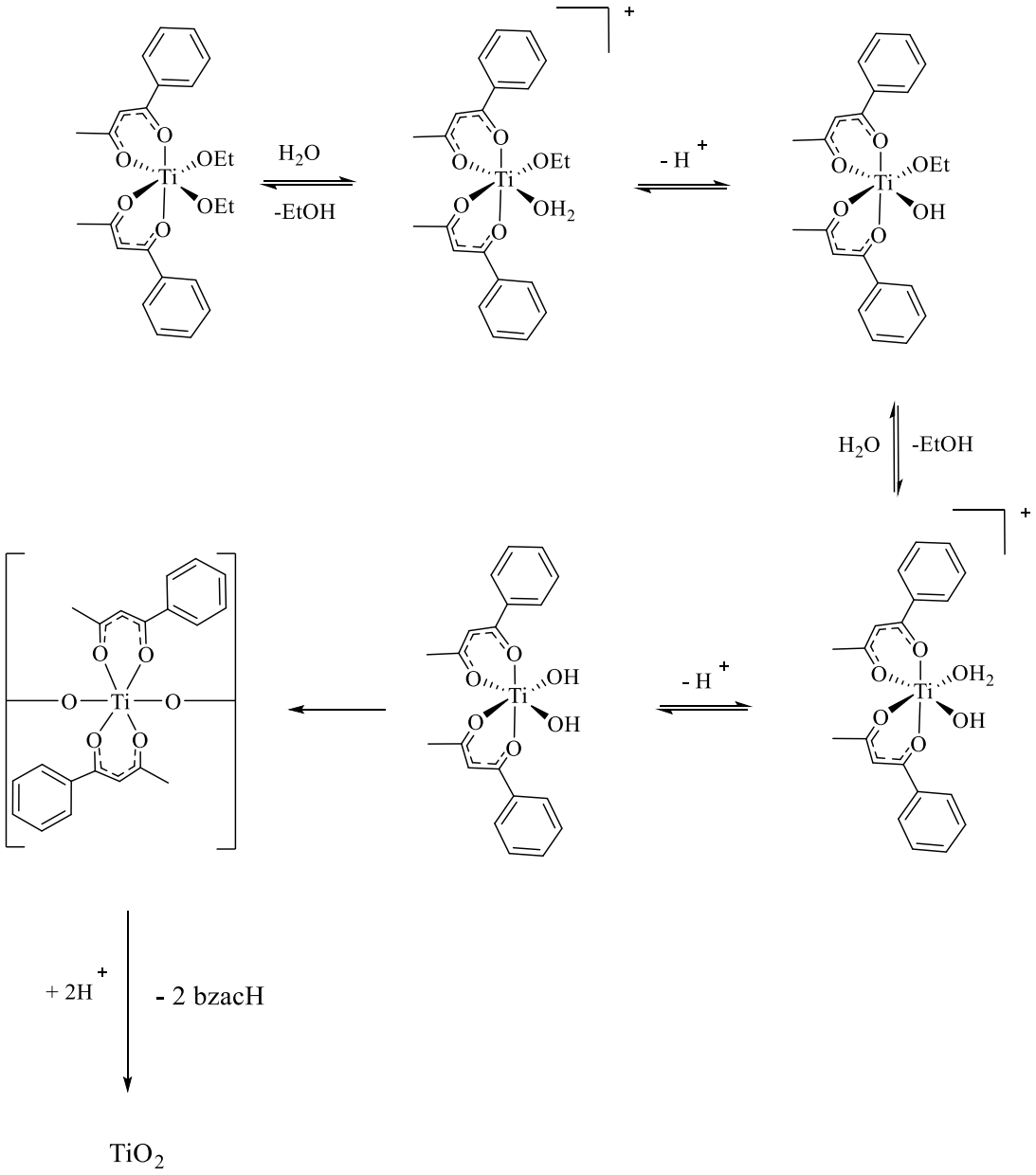


**Scheme 9.** The suggested hydrolysis of budotitane.

The major drawback in the use of budotitane in clinical trials is the existence of stereoisomers. Budotitane can exist as the five isomers shown in **Figure 9**, and this makes it hard to identify which isomer exhibits specific anti-cancer activity. A study conducted by Dubler *et al.* showed that a favoured geometry for budotitane is *cis-cis-trans* (**17a**, X = OEt) in the solid state. In comparison to the titanium chloride derivative which assumed a *cis-trans-cis* (**17b**, X = Cl) arrangement.[70]

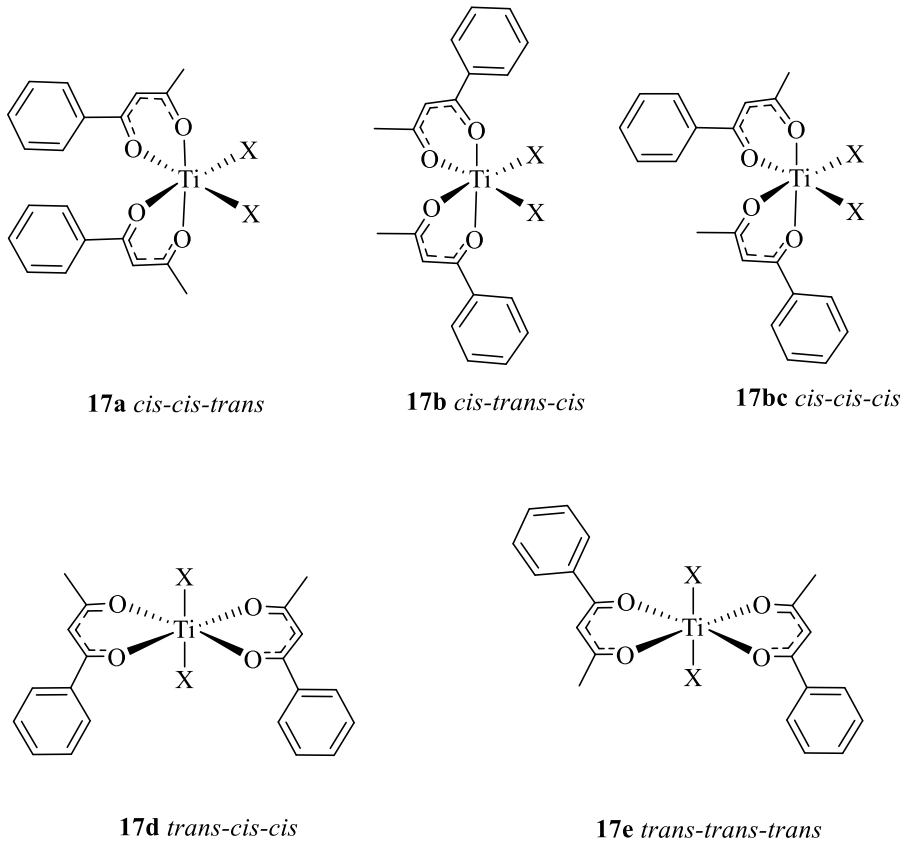


**Figure 9.** Five isomers of budotitane.

In solution phase experiments, studies have shown that all synthetic routes result in the formation of multiple isomers, and it is difficult to separate these. Another issue is that **17a** and **17b** are formed as enantiomeric pairs (Λ, Δ)[70], which further complicates the separation and purification. Finally, studies *in vitro* and *in vivo* conducted by Frühauf *et al.* using budotitane showed no DNA damage.[72] Derived problems in formulation *i.e.* the difficulty in separating, characterising and analysing the isomers present contributed to the end of budotitane clinical trials.[69] Fast hydrolysis and poor water solubility are also major issues for the use of all titanium-based as anti-cancer agents. Research conducted between 1980 and 2020 focused on finding new anti-cancer agents to overcome these features, as described below.

## 1.6. Amine-diamine *bis*(phenolate) titanium(IV) complexes

Titanium complexes of aryloxide and alkoxide ligands exhibit rich coordination chemistry and have applications in numerous fields.[73] In the last decade, researchers in the titanium anti-cancer agents have chosen to work with amine- and diamine-*bis*(phenolato) ligands due to both the basicity of the nitrogen and phenolato donors creating strong covalent bonds to the oxophilic titanium(IV) centre.[74] In addition, different constitutions of bonding modes and branching motifs can be employ by changing the connectivity of the *N*-*O* linking units (**Figure 10**).[47]

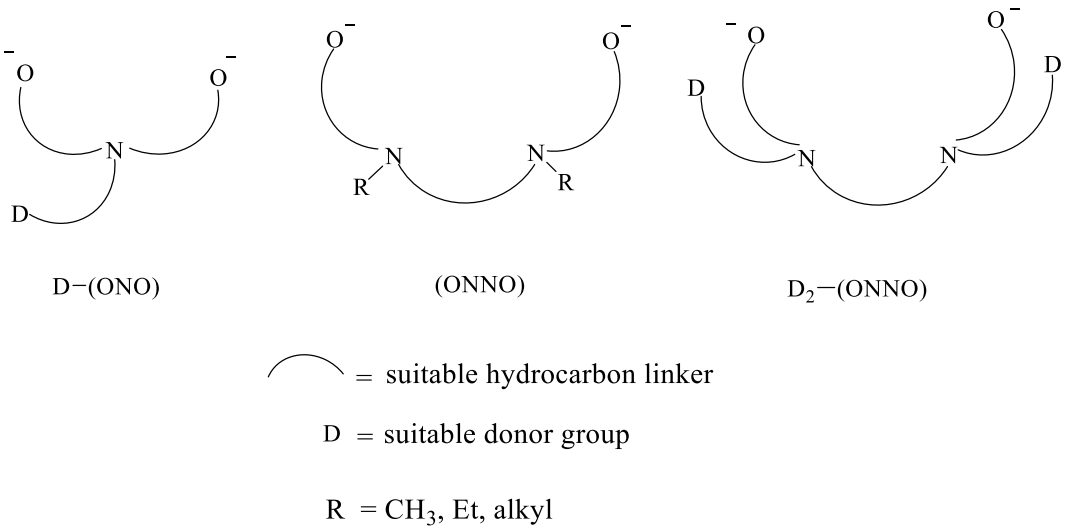


**Figure 10.** Variable connectivity for N and O donor atom sets.

### 1.6.1.1. Survey of ONNO - and ONO-type titanium complexes

Salan ligands, *bis*(phenolato)ethylenediamine, are commonly referred to as ONNO donor atom ligands due to their characteristic tetradentate oxygen, nitrogen, nitrogen, oxygen coordination sites.[75] ONO ligands can be regarded as a smaller, tridentate derivatives. Examples of these ligand types were first synthesised in 1960s for polymerisation and catalysis studies.[76] Both ligands types can be easily produced by heating the mixtures of parent phenol with formaldehyde, primary amine or diamine, and a suitable solvent (**Scheme 11**).[77] These classes of 'salan-type' ligands typically have ONNO and ONO donor sets. The term 'salan' is specifically used for compounds incorporating the ligand set (diamine- amin-*bis*(phenolato)Ti(IV).[76, 78]

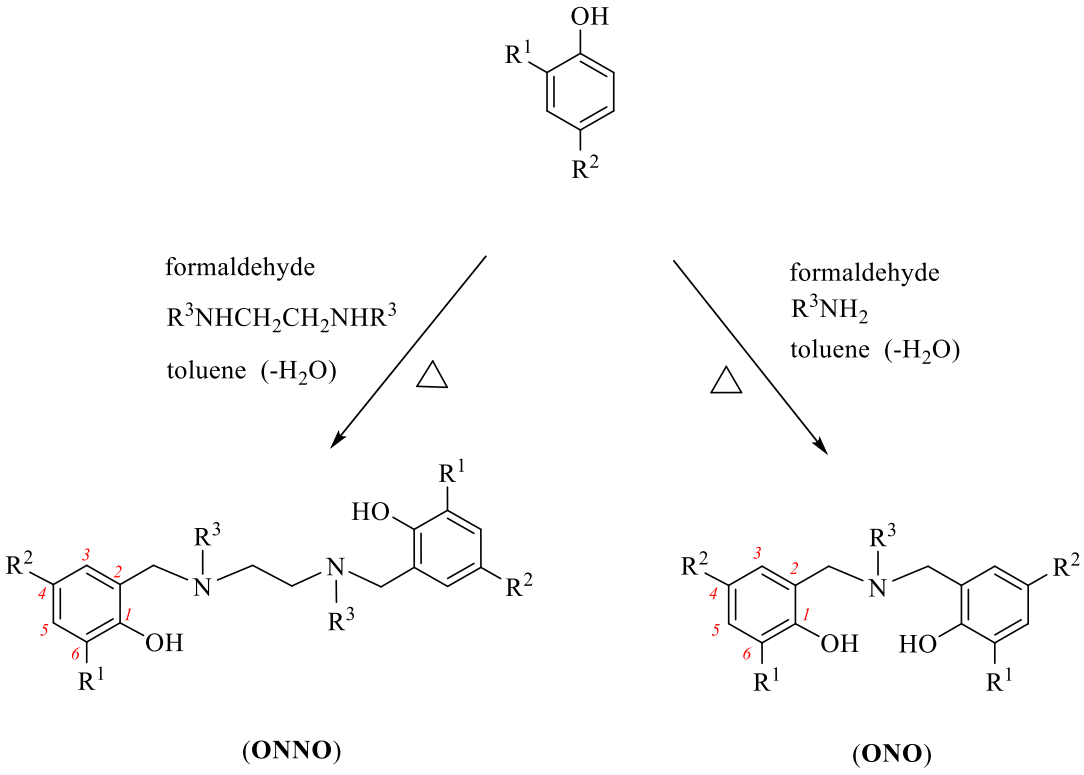


**Scheme 10.** Formation of representative ONNO and ONO donor type ligands. The former type (ONNO) is much more commonly used.

Although numerous reports of ONNO and ONO ligands precursors were published before 1990s,[76-77] they were not utilised as ligands for group IV transition metals (as complexes) prior to 1999.[73] Most of the work with these types of complexes has been described by Tshuva.[79] In 1999 and 2001 Tshuva *et al*. synthesised mainly tetradentate [ONNO] ligands by reacting with $TiX_4$ to form the [ONNO]-$TiX_2$ **18** complexes (salan complexes), where X is a hydrolysable ligand (**Figure 11**).[73-74, 80] Tshuva *et al*. designed many of these new ligands after considering certain parameters aiming to enhance their hydrolytic stability specifically: 1) the favoured geometry of titanium(IV) centre is octahedral[47]; 2) neutral complexes are preferred allowing cell penetration *via* passive diffusion; 3) the most stable oxidation state they have been employed for the Ti center is (IV); 4) geometries based on [ONNO]-$TiX_2$ donor sets favour stable *cis* configurations. These factors allow multidentate binding to the titanium for stability, as in structure **18** (**Figure 11**).[47]

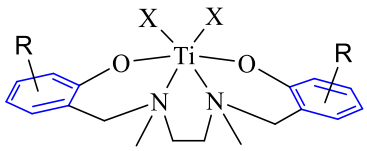


**18**

**Figure 11.** The first complex based on diamine *bis*(phenolato) ligands titanium(IV) ( [ONNO]-$TiX_2$).[47]

Most of these Ti(IV) salan complexes have been synthesised using these ONNO ligands by use of specific numbers of equiv of Ti(O*i*Pr)$_4$ to afford the desired products (**Scheme 11**).[74, 81] Interestingly, we noticed that compared to ONNO ligand set no anti-cancer studies had been carried out for Ti-ONO species.

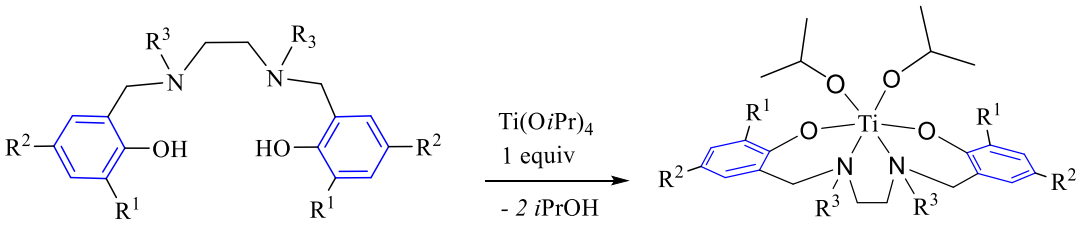


**18**

$R^1$, $R^2$ = H, Me
$R^3$ = Me, $CH_2CH_3$

**Scheme 11.** Formation of ONNO-(tetradentate ligand) Ti complexes.

The major obstacle which needs to be overcome when making Ti(IV) complexes for biological studies is their hydrolytic instability. The binding of the ligands to the metal [Ti(IV)] needs to be optimised to manage this. The activity of ONNO-ligand anti-tumour drugs **18** were not established until 2007, when Tshuva and her research group trialled these complexes against various type of cancer cells, such as HT-29 (colon cancer cell line) and OVCAR-1 (ovarian cancer cell line).[81] These complexes exhibited promising and attractive anti-tumour activity against these different cell lines.[81] Initially, Tshuva trialled *cis*-*bis*(isopropoxide)Ti(IV) complexes **18a-c** which contain diamine *bis*(phenolato) ligands (**Figure 12**). Unsurprisingly, the activity of the complexes was affected by the substituents attached to the ligand, e.g. bulky complex **18a** was inactive. However, somewhat less hindered **18b** around the metal led to significant improvement. The $IC_{50}$ of **18b** was 12±1 µM for both cell lines tested and the $IC_{50}$ of **18c** was 12±1 µM against HT-29 and 14±1 µM against

OVCAR-1. For comparison the $IC_{50}$ values of cisplatin against both cancer cell lines are ~33±3 and 17±4 µM respectively (**Figure 12**).

| | | | | $IC_{50}$ µM | |
|---|---|---|---|---|---|
| **18** | $R^1$ | $R^2$ | $R^3$ | HT-29 | OVCAR-1 |
| **a** | *t*Bu | *t*Bu | Me | inactive | inactive |
| **b** | Me | Me | Me | 12±1 | 12±1 |
| **c** | H | Me | Me | 12±1 | 12±1 |
| **3** | | | | 33±3 | 17±4 |

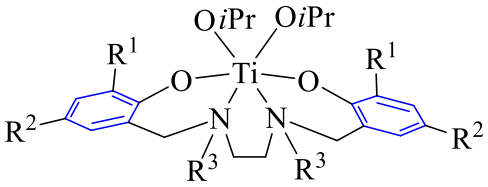


**18a-c**

**Figure 12.** The first complex based on diamine *bis*(phenolato) ligands titanium(IV) **18a-c** evaluated against colon and ovarian cancer cell lines.[81]

It is worthy of mention that there is a correlation between hydrolytic stability of these Ti-salans and their cytotoxic activity. The cytotoxic activity of tetradentate and tridentate Ti(IV)-salan compounds relies on electronic effects engendering specific ligand lability, supported by steric bulk at various ring locations.[81-82] In structures **18** (**Figure 12**) those with $R^1$, $R^2$ = H or Et, $R^3$ = Me were less cytotoxic (inactive) and less stable towards hydrolysis. Those with $R^1$, $R^2$, $R^3$ = Me were even more stable towards hydrolysis and showed higher cytotoxicity.[82-83] In comparison with Tshuva's complexes, Huhn *et al.* in 2009 suggested that the electronic effect in his (ONNO)Ti $X_2$ class did not have a major influence on overall activity (cytotoxicity). They reported that the $IC_{50}$ values of complexes **18b**, **d-f** (**Figure 13**) were ~2±0.1, 1.6±0.1, 5±0.2, and 13±1 µM respectively against the Hela S3 cell line and were ~2±0.2, 2.2±0.2, 4±0.4, and 40±4 µM respectively against Hep G2 (**Figure 13**). The $IC_{50}$ values of cisplatin (as a reference) against both cancer cell lines are ~1.2±0.4 and 3±1.3 µM respectively.[84]

| 18 | $R^1$ | $R^2$ | $R^3$ | $IC_{50}$ μM Hela S3 | $IC_{50}$ μM Hep G2 |
|---|---|---|---|---|---|
| **b** | Me | Me | Me | 2±0.1 | 2±0.2 |
| **d** | F | F | Me | 1.6±0.1 | 2.2±0.2 |
| **e** | Cl | Cl | Me | 5±0.2 | 4±0.4 |
| **f** | Br | Br | Me | 13±1 | 40±4 |
| **3** | | | | 1.2±0.4 | 3±1.3 |

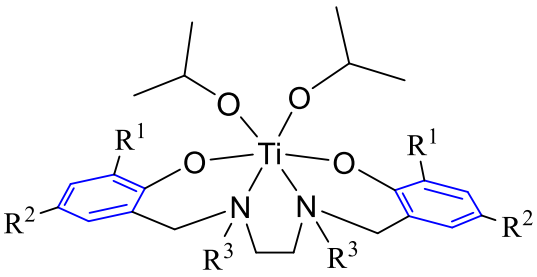

**18b**, **d-f**

**Figure 13.** The structure of the **18b**, **d-f** salan Ti(IV) complex with different substituents against Hela S3 and Hep G2 cell lines.

Until recently, the problem of moderate activity (cytotoxicity) and lower hydrolytic stability of the salan Ti(IV) based complexes had been not resolved, despite many efforts to find improvements. However, in 2016 Meker *et al.* was able to find new salan Ti(IV) based complexes which showed increased biological accessibility and water solubility. The ligands were designed to be tetra (anionic) and hexadentate and these appear particularly effective (**Figure 14A-B**). The geometry of these neutral Ti(IV) complexes is octahedral, thus facilitating diffusion through the hydrophobic cell membrane.[85]

**A**

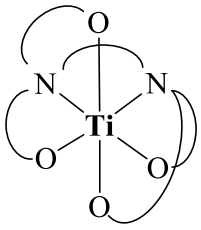

**B**

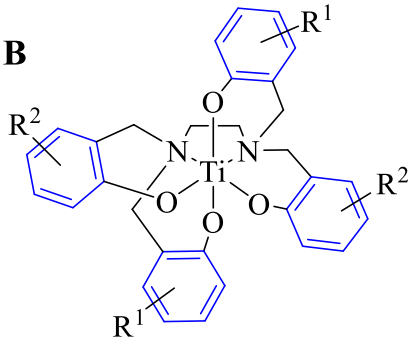

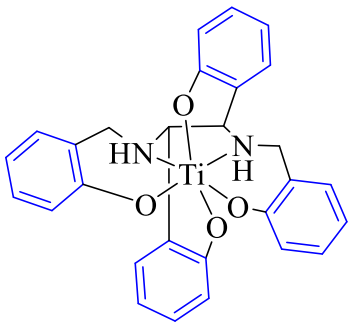

**19** $R^1 = R^2 = o,p$-Me

**19a** $R^1 = o,p$-Br; $R^2$ = H

**19b**

**Figure 14.** (**A**) Coordination mode for hexadentate complexes, (**B**) some examples of this type of Ti(IV) compounds.[85]

The cytotoxicity of these ONNO complexes is shown in **Figure 15** towards HT-29 (human colon) and A2780 (human ovarian) cancer cell lines. The complexes (**19c-e**) revealed high potency against both cell lines. The $IC_{50}$ values of **19c-e** against HT-29 were ~5.7±0.4, 6.4±0.9, and 0.74±0.08 µM respectively while, the $IC_{50}$ values against A2780 were ~6.4±0.7, 1.5±0.8, and 0.43±0.03 µM respectively.[85-86] This confirms that solubility together with steric and electronic factors all affect cytotoxicity.[87]

| | $IC_{50}$ µM | |
|---|---|---|
| **19** | HT-29 | A2780 |
| **c** | 5.7±0.4 | 6.4±0.7 |
| **d** | 6.4±0.9 | 1.5±0.8 |
| **e** | 0.74±0.08 | 0.43±0.03 |

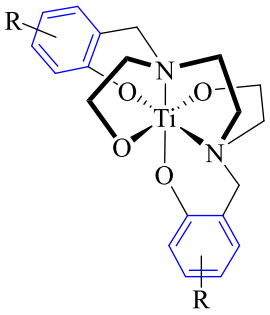


**19c** R = *m,p* = Me
**19d** R = *o* = Cl, p = F
**19e** R = *p* = $NO_2$

**Figure 15.** Ti(IV) complexes of *bis*(alkoxo)*bis*(phenolato) ligands **19** and their cytotoxicity against HT-29 and A2780 cell lines.[85]

### 1.6.1.2. **Salen complexes**

In parallel to the studies of Tshuva, other researchers using related ONNO donor analogues, have described new *trans*-salen complexes.[88] Tzubery *et al*. (2011) introduced this type of anti-cancer complex for titanium(IV), as they suggested that using *trans*-complexes may help to gather additional information regarding the mechanism of action and possible diversity of activity for diamino *bis*(phenolato)titanium complexes against variable cancer cell lines such as HT-29 (human colon) and OVCAR-1 (human ovarian). These salen *bis*(phenolato)Ti-based complexes are shown in **Scheme 12**. They are similar to the salan family but afford equatorial binding because of the planar imine moiety, resulting in *trans* labile

ligands. In addition, this class of Ti(IV) compounds can demonstrate good anti-tumour activity (cytotoxicity), aquatic solubility, and hydrolytic stability.[88-89]

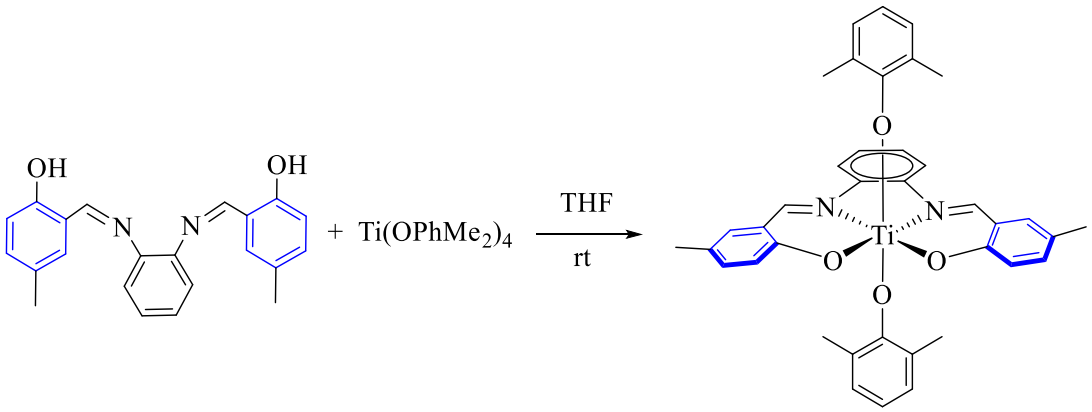


**20a**

**Scheme 12.** The preparation of salen diamino *bis*(phenolato)Ti-based complexes.[88]

The use of a phenylenediamine rather than an ethylenediamine linker further enforces the equatorially geometry for such complexes. Although transplatin (the geometric analogue of cisplatin) is ineffective clinically, *trans*-salen Ti(IV) complexes with this motif showed good anti-tumour activity against some cancer cell lines (**Figure 16**). This class of Ti(IV) complexes exhibited particularly high activity against HT-29 (human colon) and OVCAR-1 (human ovarian) cell lines.[88] Their stability is similar to the salan complexes **18** described earlier with regard to their hydrolysis. Sometimes these *trans* species also showed activity greater than cisplatin. Compounds **20a-d** (**Figure 16**) when tested against both cell lines HT-29 and OVCAR-1 showed variable activity. Complex **20c** (*para*-chloride) revealed the highest activity, whereas **20d** (*ortho*-chloride) was inactive (**Figure 16**). This may be due to adverse steric effects at the *ortho* position. The $IC_{50}$ values of **20a-c** (**20d** was inactive) complexes were ~10±2, 3.5±0.6, and 1.2±0.3 µM against HT-29 while, the $IC_{50}$ values of **20a-c**

(**20d** was inactive) complexes against OVCAR-1 were ~9±1, 3.3±0.5, and 1±0.3 µM respectively.[88] The $IC_{50}$ values of cisplatin (as a reference) against both cancer cell lines are ~20±2 and 13±1 µM respectively.[90]

| | $IC_{50}$ µM | |
|---|---|---|
| **20** | HT-29 | OVCAR-1 |
| **a** | 10±2 | 9±1 |
| **b** | 3.5±0.6 | 3.3±0.5 |
| **c** | 1.2±0.3 | 1±0.3 |
| **d** | inactive | inactive |
| **3** | 20±2 | 13±1 |

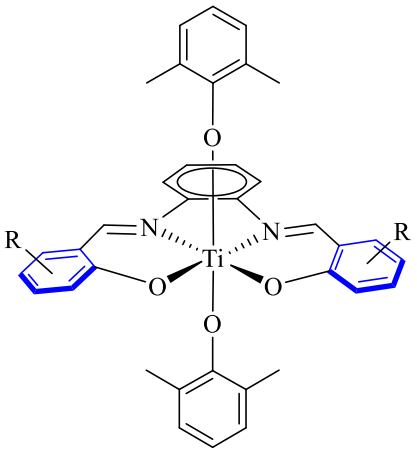


**20a** R = *p*-Me, **20b** R = H
**20c** R = *p*-Cl, **20d** R = *o*-Cl

**Figure 16.** Salen **(**salophen) Ti(IV) complexes containing a phenylenediamine bridge with different substituents.

Despite their variable diamino bridges, different labile ligands, and different geometries, the $IC_{50}$ values gained from these *trans* complexes **20** and their analogues are comparable with those attained for other *cis* salans **18**. For example, a comparison in activity (cytotoxicity) between all these Ti(IV) compounds can be seen in **Figure 17** against HT-29 (colon cancer cell line) and OVCAR-1 (ovarian cancer cell line).

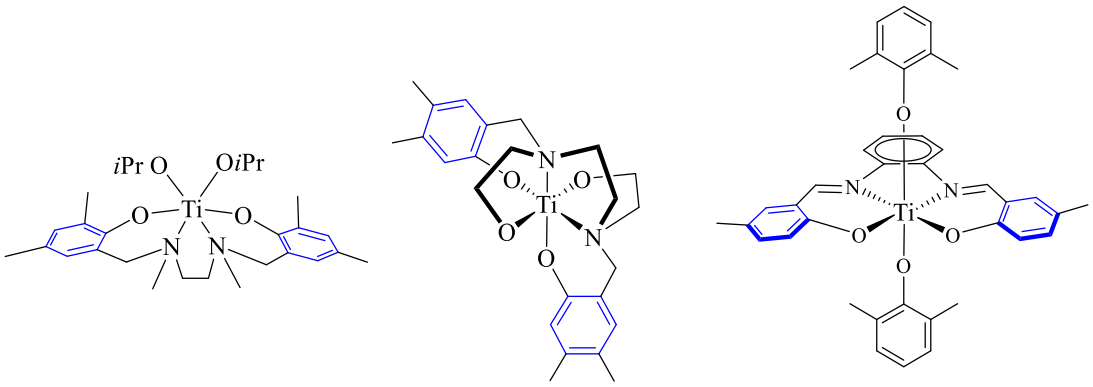

**18b** **19c** **20a**

| | $IC_{50}$ μM | |
|---|---|---|
| | HT-29 | OVCAR-1 |
| **18b** | 12±1 | 12±1 |
| **19c** | 5.7±0.4 | 6.4±0.7 (against A2780) |
| **20a** | 10±2 | 9±1 |

**Figure 17.** Comparison between all salan and salen complexes against HT-29 and OVCAR-1 cancer cell lines.[85, 88]

Tzubery *et al*. in 2017 found new Ti(IV) compounds (**Figure 18**) which are a combination of two main Ti(IV) multidentate structures. 'Salalen' Ti(IV) compounds are the combination of half salan and half salen. This new class of compounds exhibits: a) moderate to good anti-tumour activity, b) decreased complex lability leading to increased hydrolytic stability, c) higher steric (bulky) group, which usually increases kinetic stability towards hydrolysis.[91]

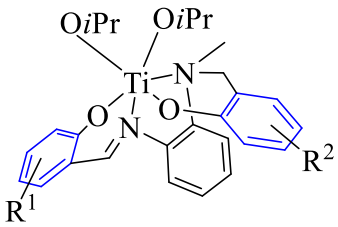


**20e**

**20e** $R^1$ = *o,p*-*t*Bu, $R^2$ = *p*-$NO_2$

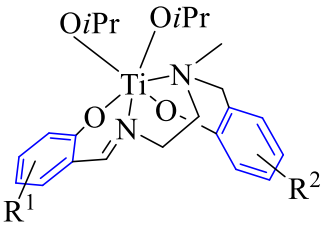


**20f**

**20f** $R^1$ = *o,p*-H, $R^2$ = *p*-$NO_2$

**20fa** $R^1$ = *o,p*-F, $R^2$ = *p*-$NO_2$

**20fb** $R^1$ = *p*-Cl, $R^2$ = *p*-$NO_2$

| | $IC_{50}$ µM |
|---|---|
| **20** | HT-29 |
| **e** | 51 ± 11 |
| **f** | 10 ± 3 |
| **fa** | 6 ± 1 |
| **fb** | 17 ± 5 |

**Figure 18.** Shows different *bis*(isopropoxido)(salalen)Ti(IV) complexes and their activity against HT-29 cell line.

Manne *et al*. in the early part of 2019[92] and Shpilt *et al*. in 2020[93] reported that new dianionic tridentate acylhydrazone ligands (featuring the ONO motif). Their complexes prepared by the chemistry of **Scheme 13**,[92] show improved hydrolytic stability. They were stable in cell growth medium and at least comparable with ONNO complex stability. However, their low solubility led to reduced cytotoxicity. The complexes show moderate activity against HT-29 (human colon) and A2780 (human ovarian) cancer cell lines (**Scheme 13**).[92-93] Despite evidence of activity towards cancers, the mechanism (mode of action) of all these Ti(IV) complexes discussed above and initial metallocene such as **10** and its analogues and **17** are still unknown. Nevertheless, these Ti(IV) complexes do represent some of the most active experimental anti-cancer agents amongst metal complex therapies as have been seen.

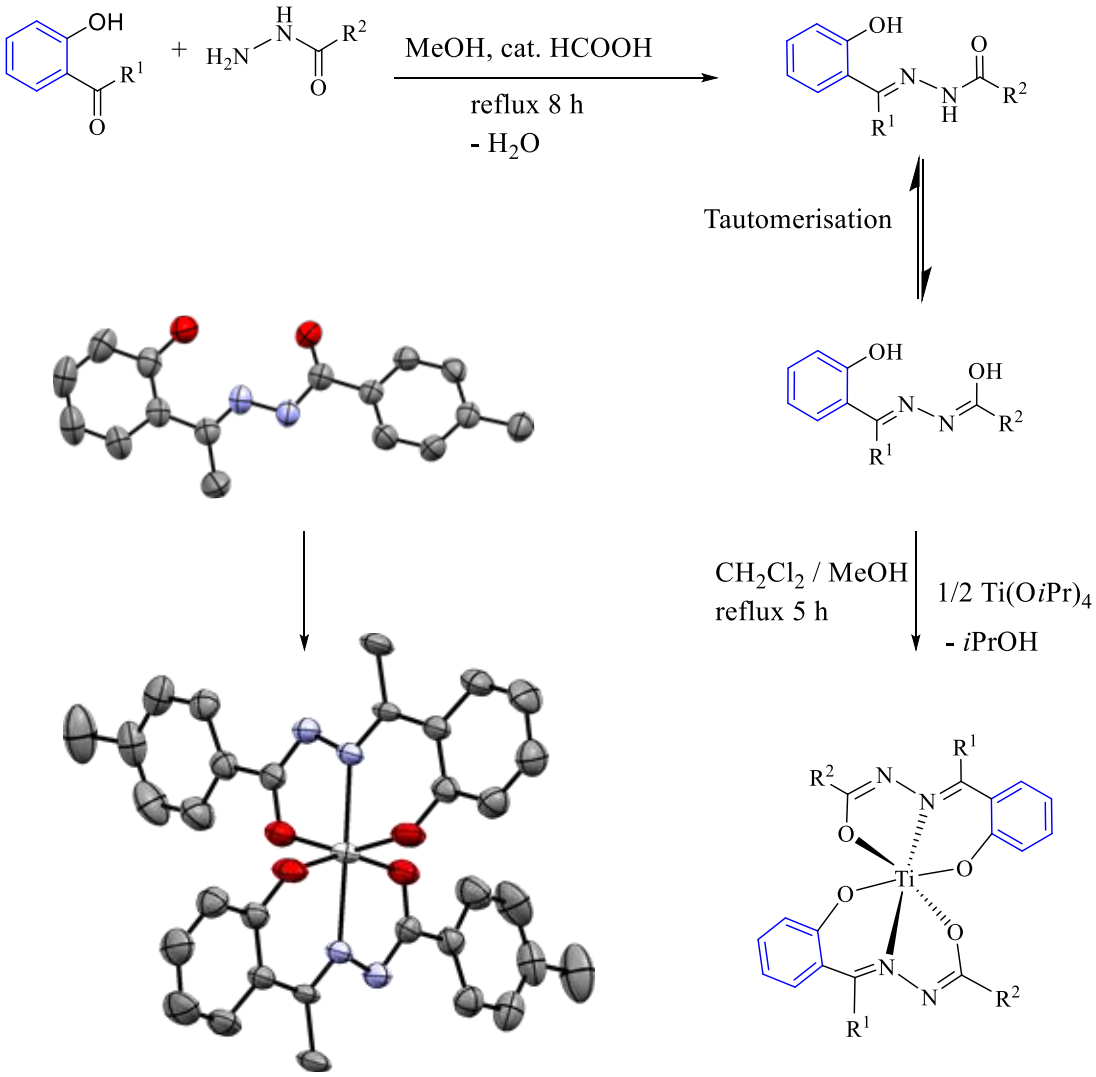


**Scheme 13.** Preparation of rare ONO Ti(IV) complexes and representitive crystal structures of ligand ($R^1$ = Me; $R^2$ = 4-Me $C_6H_4$)and complex. These crystal structures have been plotted from the cif files which are available at The Cambridge Structural Database (CSD).[92]

## 1.7. Titanium(IV) complexes and their mode of action

All chemical substances need to be verified (tested) for their environmental and toxicological properties before being permitted for clinical use. The most important part of this is understanding how such chemical substances behave inside the cell.[94] The term mode of action, or mechanism of action is used to describe this. As has been seen above, for metal complexes, the best understood mode of action is for cisplatin (**3**). For many other metal compounds, especially titanium(IV) species, this remains under scientific investigation in both biology and chemistry.[95] Although **10** reached phase II clinical evaluation, it did not progress due to the deficiency in patient effectiveness. Ehrlich ascites (a mouse tumour cell line) was used for preliminary mode of action studies of **10**. Köpf-Maier suggested that compound **10** is a DNA-binding agent, similar to **3**. Unfortunately, due to the low signal-to-noise intensity of the EELS (electron energy loss spectroscopy) technique used to study this hypothesis they were forced to use high concentrations of **10** (up to 10 mM) which consequently led to questionable observations of high levels of **10** in the nucleic acid of cells.[51] In 2017 Cini *et al*. showed that **10** is significantly insoluble in either cellular growth media or water at this concentration and it makes colloidal suspensions invalidating the assay.[51] Alternative attempts to characterise titanium DNA binding with cells were conducted by fluorescences studies. In 2005 Waern *et al*. showed that using V79 (hamster lung cells) treated with 100 µM of **10** indicated no significant Ti-uptake compared to cells treated with other non-Ti complexes or to those not exposed at all. Overall studies, thus far, suggest that titanocene dichloride (**10**) exhibits a different mode of action to cisplatin and that DNA is not the main cellular target causing the anti-cancer efficacy of **10**.[96] However, Sadler suggested that the transferrin iron transport protein (Tf) might be used as a mediator for titanium(IV) species to

transport in to tumour cells as a "Trojan horse". He elucidated that under physiological conditions, **10** is rapidly acquired by apo-transferrin as $Ti^{4+}$ resulting from fast loss of both cyclopentadienyl ligands and chloride. Model NMR studies showed that Tf metal-adducts underwent conformational alteration that strongly supporting the idea that in titanium binding to Tf the $Ti^{4+}$ is loaded first, and this results in a stable Ti-Tf complex. Afterward, this complex is transported intercellularly in endosomes (membrane-bound compartments) and proposed to release the $Ti^{4+}$ ions on direct contact with adenosine triphosphate (ATP) and eventually binding to DNA/RNA (**Scheme 14**) although no direct evidence is available to support this latter idea.[52]

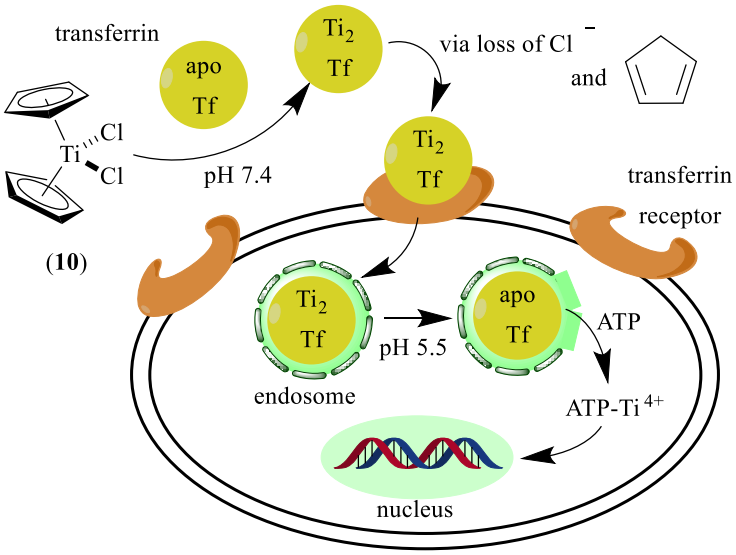


**Scheme 14.** Proposed uptake of **10** by Tf and the suggestion that this supplies a toxic intracellular $Ti^{4+}$ species that reacts with DNA (and/or RNA).

Tacke *et al.* in 2009 suggested an alternative mechanism for titanocene activity that uses serum albumin (SA) instead of Tf as a cellular transporter. This was suggested to bind the titanocenes, on the basis of the low level computational modelling, and potentially supply the nucleus with $Ti^{4+}$ species for eventual interaction with DNA.[68]

Other titanium(IV) complexes (non-titanocene) have been proposed to show various mode(s) of action, some with similarity to titanocene, while others not. The mechanism of action of budotitane **17** (**Figures 8-9**) has been suggested to involve initial loss of two ethoxide ligands followed by the bzac ligands, leading to the eventual formation of $TiO_2$ (**Scheme 9**). However, it is not know which of these is the biologically active and what its biological target is. The existence of multiple isomers also makes it hard to identify which isomer delivers the anti-cancer activity. Miller *et al.* (2016) presented trials of complex **18h** (**Figure 19**) against two different cancer cell lines, HT-29 and A2780. The $IC_{50}$ values of **18h** against HT-29 and A2780 were 0.9±0.2 and 0.5±0.04 µM respectively. Both cell lines were tested using cell cycle assay and both showed cell cycle arrest in the G1 phase. This might suggest that complex **18h** gets inside the nucleus and interacts with DNA leading to check point cell cycle arrest.[97] Additionally, Manna *et al.* (2012) noted upregulation of p53, which is followed by cell cycle arrest in G1 phase, although full details of the mode of action of this salan compound still remain to be defined.[98]

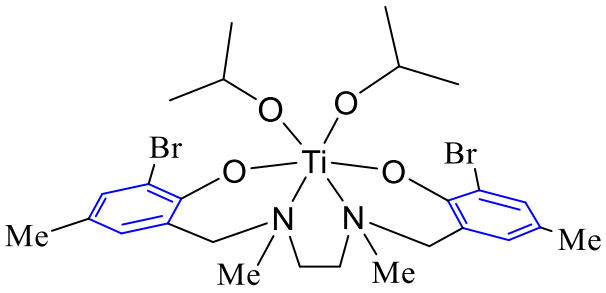


**18h**

**Figure 19.** Structure of complex **18h**.

While there are numerous examples of partial mode of action studies of promising Ti(IV) compounds the overall picture is far from complete. In general, the mode(s) of action for Ti(IV) initially proposed in the 1970s still remain poorly understood and how the titanium species are delivered through the cell to the DNA (or other targets) is still more speculative than definitive.

## 1.8. Mode of action and programmed cell death (PCD)

Most anti-cancer modes of action end in the death of the tumour cell, so it is important to understand this fundamental process. There are three main categories of programmed cell death (PCD) specifically: apoptosis, autophagy and paraptosis (or necrosis) that occur, and these are briefly overviewed in **Scheme 15**.[99] Individual PCD types are identified by distinct biomolecular/biochemical changes and cellular morphological alterations. The most common process is apoptosis (which is the PCD most often suggested for **10** and other titanium(IV) analogues).[51] Apoptotic cells are characterised by membrane blebbing (formation of cell membrane protrusions), nuclear fragmentation and formation of apoptotic bodies, cell shrinkage, and chromatin condensation (**Scheme 15**). Apoptosis acts as a natural barrier to cancer cell proliferation as confirmed in early studies.[100] Nevertheless, cancer cells can overcome this barrier *via* obtaining resistance to apoptosis.[101] Regulators of the apoptotic cascade are known and these can be divided into two sub-types: intrinsic, which is responsible for the intracellular pathway of apoptosis, and extrinsic, which regulates the extracellular pathway of apoptosis. The main role for intrinsic apoptosis is to provide a protective system against cancer pathogenesis.[102] A second type of PCD, autophagy can be identified by the accumulation of autophagolysosomes formed by the fusion of autophagosomes with lysosomes and autophagosomes in the cytoplasm, and protein degradation (**Scheme 15**). Autophagy is a typical response to

cellular stress when nutrient resources are low leading to 'self-eating' as the organism's cells try to manage depleted resources. Sometimes, however, chemical agents can also trigger this response. Necrosis is a type of cell death which is morphologically identified (distinct from apoptosis) by rupture of the plasma membrane, cellular swelling, and loss of cytoplasmic components. Inflammatory necrotic cell death is usually categorised as non-programmed cell death (PCD) caused by trauma damage to the cell. However, necrotic PCD is also known and is called necroptosis. This PCD is controlled by particular signal pathways and the metabolic breakdown of signal molecules. Some cytotoxic agents have been reported to induce necroptosis rather than apoptotic pathways, and this can happen when a cell cannot die by type 1 PCD (apoptosis) (**Scheme 15**). To exemplify, Cini's Ti(IV) complex[61] (**Scheme 15**) triggers paraptotic (type three) cell death involving MAP kinase signal transduction.[51, 99] Paraptosis is a biochemically and morphologically distinct from apoptosis and caspase-independent and is accompanied by cytoplasmic vacuolisation before membrane rupture (**Scheme 15**).[51]

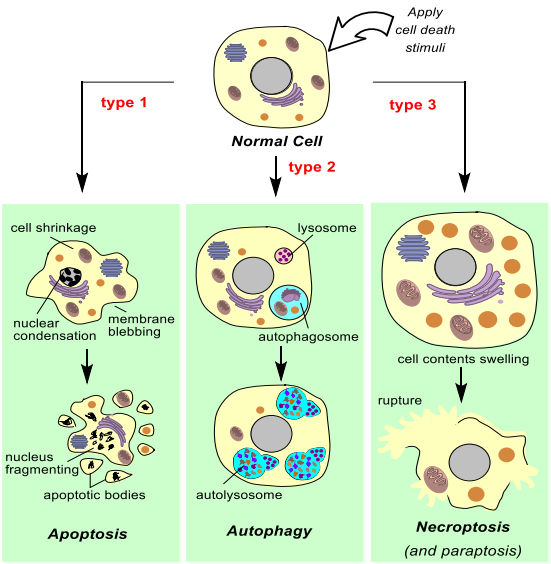


**Scheme 15.** Three main categories of programmed cell death (PCD) induced *via* titanium(IV)-based analogues.[51]

## 1.9. Aims of the study

### The aims of this thesis were:

- To synthesise new fulvene ligands, potentially aiming at making new titanium complexes (titanocene based) and if possible to test their activity towards cancers.

- To synthesise new underrepresented tridentate *bis*(phenolate) ligands with [ONO] donor ligand sets.

- To synthesise new titanium complexes able to show high stability in aqueous media which are also not air sensitive.

- To test the new titanium complexes for high activity and selectivity against cancer cell lines, typically HCT-116 (colon cancer) and MCF-7 (breast cancer), using MTT and clonogenic assays.

- To study the mode of action of this type of complexes, using cell cycle, annexin-V, γ-H2AX, and caspase assays.

- To characterise the behaviour of these complexes in aqueous solution models.

## 1.10. Cell lines used in this research

**HCT-116**: This cell line is one of the colorectal carcinoma cell lines isolated from adult male primary cells with human colonic carcinoma. These cells shown high colony formation in both confluent fibroblasts and agarose with a short doubling time of ~ 21 h.[103]

**MCF-7**: A breast cancer cell line, Michigan Cancer Foundation-7. The first breast cancer cell (MCF-7) was isolated in 1970 by Dr. Soule,[104] from a Caucasian woman who was 69 years old and suffering from pleural effusion.[105]

**MDA-MB-468**: A breast cancer cell line,[106] isolated in 1979, from a 51 years old black female patient with metastatic adenocarcinoma of the breast from pleural effusion by Pathak *et al.*[107]

**PANC-1**: An E-cadherin-negative adherent ductal adenocarcinoma. This cell under the microscope shows three different morphological configurations: small morula (small cells), stellate (intermediate cells), and isolated (large cells).[108]

**HT-29**: A human colon adenocarcinoma cell line, which was isolated from a primary tumour from a 44 years old Caucasian female in 1964 by Fogh and Trempe.[109]

**MRC-5**: The MRC-5 is an abbreviation of Medical Research Council strain-5 cell line. It is a fibroblast cell line and was isolated from the lung tissue of a 14-week old foetus aborted from 27 year old woman in 1966 by J. P. Jacobs and colleagues. It has a population doubling time of ~42-84 h.[109]

The communication resulting from this chapter is presented in a final Appendix:

R. Nouch, M. Cini, M. Magre, **M. Abid,** M. Diéguez, O. Pàmies, W. Lewis, S. Woodward, "Enantioselective Synthesis of 6,6-Disubstituted Pentafulvenes Containing a Chiral Pendant Hydroxy Group" *Chem. Eur. J.* **2017**, 23, 1-5.

# Chapter two

## 2. Pentafulvenes and their applications

Pentafulvene derivatives have interesting roles in cycloaddition reactions and as models for aromaticity theories (see **Scheme 3** earlier).[110] They also possess significant applications in organometallic chemistry, either as versatile ligands for a variety of transition metal complexes or as easy-to-handle precursors for an enormous variety of cyclopentadienyl ligands, providing multiple reactivity patterns.[37, 111] This is due to the nature of pentafulvenes, as they can react with both nucleophiles and electrophiles (**Scheme 16**).[110, 112]

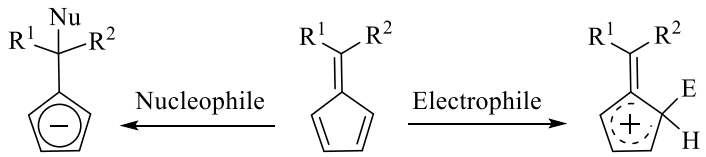


$R^1$, $R^2$ = H, alkyl group

**Scheme 16.** Shows the reactivity of pentafulvenes toward nucleophiles and electrophiles.[110]

Because of their unique cross-conjugated system pentafulvenes display a broad manner of coordination modes.[113] The most common are the so called *exo* and *endo* binding modes although others are known (**Figure 20**).[110]

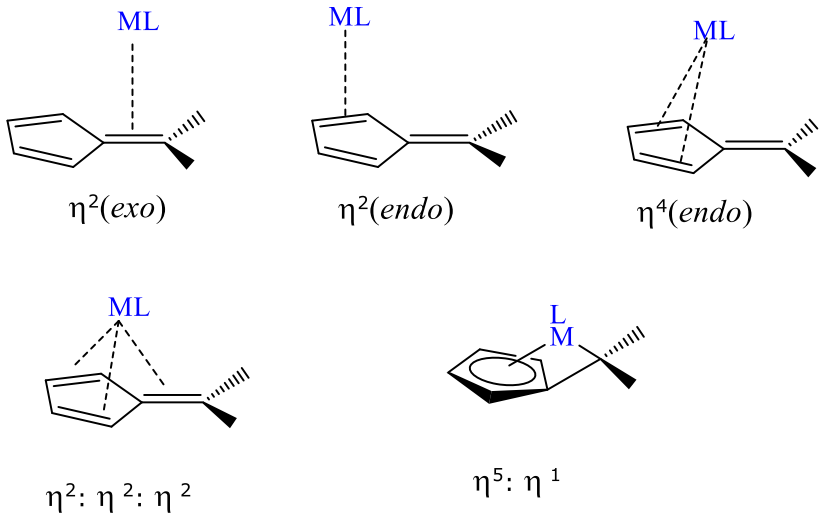


**Figure 20.** Representative binding modes of transition metals of pentafulvenes.[110, 113]

Importantly, the addition of organometallic reagents to fulvenes provides access to various substituted cyclopentadienyl metal precursors *via* salt metathesis reactions with suitable transition metal $MX_n$ sources. Tacke *et al.* describes many titanocene complexes produced from the reaction of 6-arylfulvenes with aryllithium reagents and subsequent transmetalation with titanium tetrachloride ($TiCl_4$).[37] The cytotoxicity of these compounds has been examined against cancer cells during the investigations. For example, the $IC_{50}$ value of **16d** in **Scheme 17** was 270±0.1 µM against LLC-PK cells (pig kidney cancer) which is a 10-fold increase in cytotoxicity compared to **10** (titanocene dichloride).

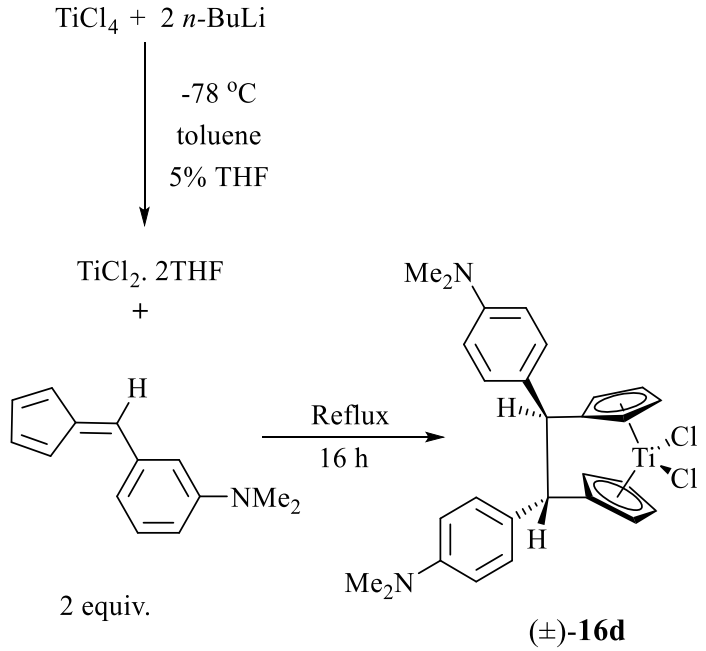


**Scheme 17.** Synthesis of *ansa*-titanocene dichloride.[37]

Reduction of metal precursors in the presence of pentafulvenes has been reported by Beckhaus in 2001 using Cp*$TiCl_3$ (**10a**) and Mg in the presence of fulvenes. This led to the isolation of a Cp*($\eta^5$-fulvene)TiCl (**10aa**) complex in a highly diastereoselective manner (**Scheme 18**).[114]

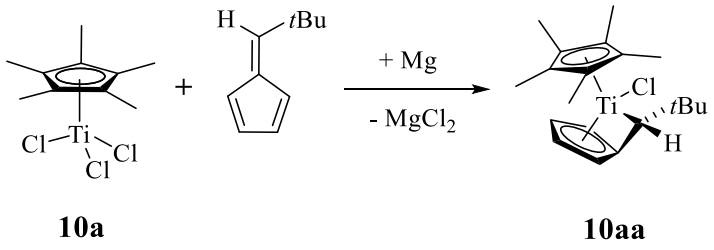


**10a** **10aa**

**Scheme 18.** Synthesis of complex **10aa**.[114]

In 2001, Kim *et al*. proposed a new type of complex by reacting *N*-alkyl-diethanolamine with **10a** in the presence of trimethylamine. This opened a new method for the synthesis of alkoxy cyclopentadiene titanium complexes that can

mimic the activity of titanocene dichloride **10** against cancer cells both *in vitro* and *in vivo* (**Scheme 19**).[115]

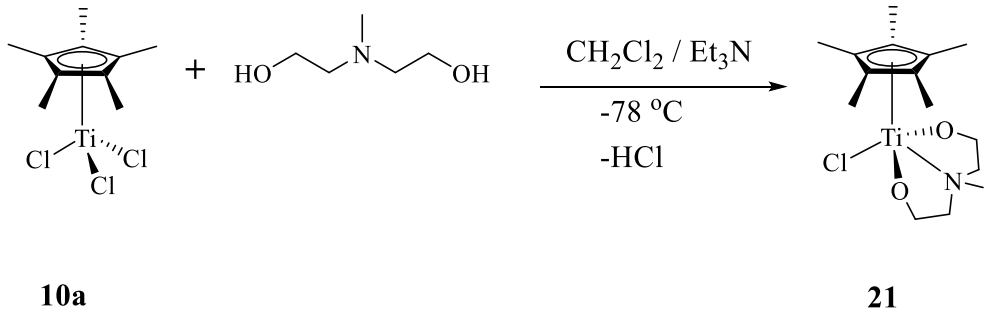


**10a** **21**

**Scheme 19.** The formation a new half metallocene by reaction of *N*-alkyl-*N*,*N*-diethanolamine with $Cp^*TiCl_3$ (**10a)** in the presence of triethylamine.[115]

## 2.1. Results and Discussion

Although pentafulvenes allow organometallic formation of cyclopentadiene ligands for titanocene dichlorides, there are few readily available chiral versions. The primary objective behind this PhD work was to synthesise enantioselectivity 6,6-disubstituted pentafulvenes containing a chiral pendant hydroxy group, such as **24-27** (**Scheme 20**), as potential precursors to titanium complexes. Our research was aimed at providing a new scaffold for the addition of organometallics to substituted fulvenes. Our postulate was to develop a new approach to form titanocene dichlorides **24a-27a** through transmetallation process of 6,6-disubstituted pentafulvenes **24-27** using *in situ* titanium dichloride (**Scheme 20**). Significant experimental effort is needed to prepare **24-27**, as most of these materials (and their starting materials) are expensive or unknown. Therefore, initial attempts focused on making the key precursors needed. **Scheme 20** outlines the approach taken towards synthesis of the **24-27** from the starting materials, and then to the desired titanocene complex.

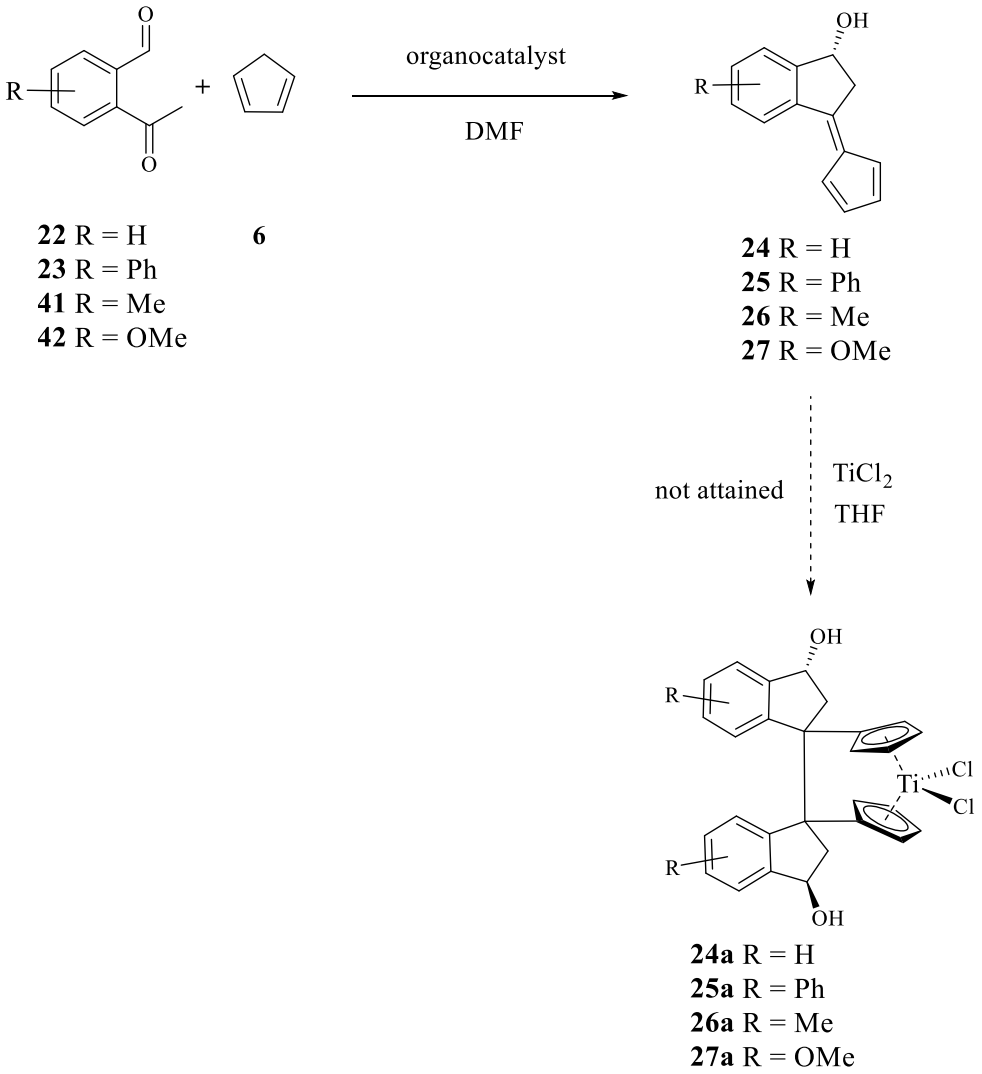


**Scheme 20.** Proposed reaction to synthesis of fulvene **24-27** from 2-acetyl-benzaldehyde and its elaboration to form the titanocene **24a-27a**.

## 2.1.1. **Synthesis and optimisation the catalysts**

Numerous efforts were undertaken to identify an appropriate organocatalyst for the proposed fulvene preparation. Prior to my project a range of organocatalysts (**Figure 21**) had been trialled for their ability to form **24** by Dr Ryan Nouch of the Woodward team, but these underperformed, so additional pentafulvene and organocatalyst conditions were screened within this PhD project (**Figure 21**). This was the starting point for our work.

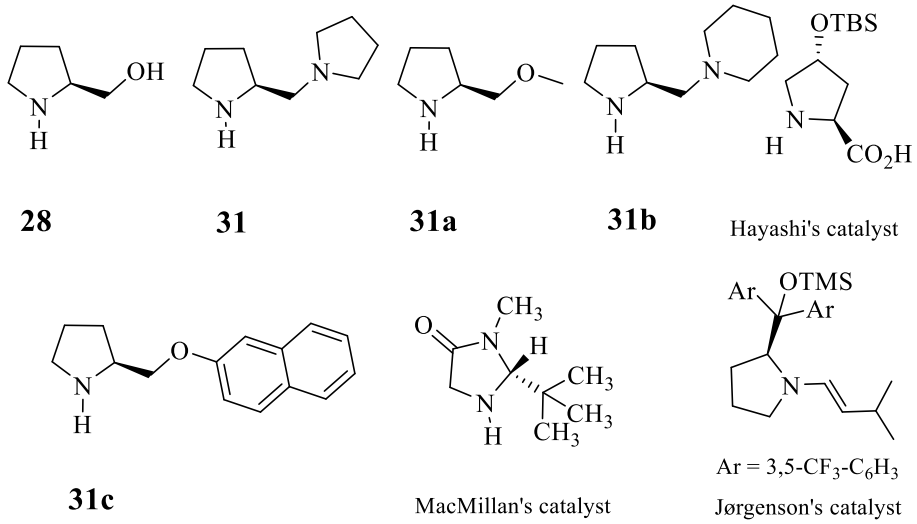


**Figure 21.** Different organocatalysts have been trialled at the outset of this project.[116]

Under the initial chemistry of **Scheme 20**, the catalysts of **Figure 21** were screened for formation of **24** from **22**. As can be seen (**Table 1**) the optimal yield of **24** was with catalyst **28** (highlighted in orange). However, optimal stereoselectivity was attained with (*2S*)-1-(pyrrolidin-2-ylmethyl) pyrrolidine **31** showing higher *er*, (**Table 1**, highlighted in green).[117] The optimal number of equivalents of the catalyst **31** was found to be ~0.38. Below this amount while the *er* remained high, the reaction conversion suffered.[116] Sterically bulky catalysts such as **31c**, used by Jørgenson,[118] Hayashi,[119] and MacMillan[120] (**Figure 21**) had also been trialled previously, but they showed less selective and reactive (these attempts were conducted by Dr. Ryan Nouch).[120]

**Table 1.** Various catalysts were trialled for synthesis of **24**. *[n.d: not determined]

| Catalyst | Acid | *t*[h] | T[°C] | Yield [%] | *er* |
|---|---|---|---|---|---|
| **31** | AcOH (0.38) | 2 | 25 | 71 | 86:41 |
| **31** | AcOH (0.26) | 2 | 22 | 76 | 89:11 |
| **31** | AcOH (0.13) | 6 | 15 | 78 | 94:6 |
| **28** | AcOH (0.38) | 24 | 25 | 90 | 79:21 |
| **31a** | AcOH (0.13) | 24 | 22 | 69 | 80:20 |
| **31b** | AcOH (0.13) | 2 | 22 | 71 | 90:10 |
| **31c** | AcOH (0.13) | 4 | 22 | <5 | n.d.* |

Unfortunately, although **31** is commercially available (Sigma-Aldrich-Merck), it is very expensive (~£140 per g in 2020). An initial project goal was to find an approach giving a cost and time effective synthesis of fulvene **24** and large amounts of catalyst **31** were needed. Many potential synthetic routes exist to convert (*S*)-proline to the optimal catalyst **31**, however, most of these provide poor yields and have imprecise experimental details, costing time and resources. The route of **Scheme 21** developed as optimal for synthesis of catalyst **31**.

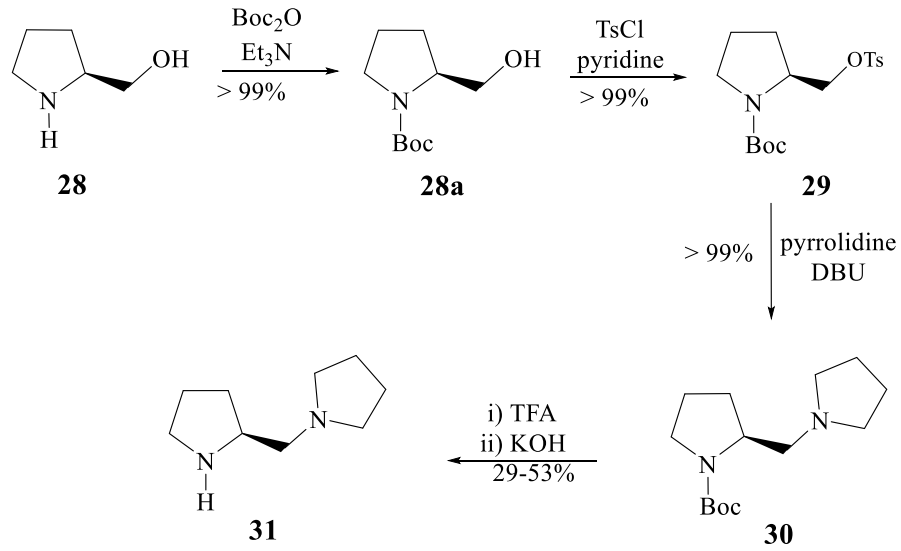


**Scheme 21.** Optimal route to **31** proceeding *via* (*S*)-prolinol.

Commercial (*S*)-prolinol **28** was protected by $Boc_2O$, to prevent nitrogen being attacked, affording **28a**.[121] Subsequently, the primary alcohol group was tosylated under standard conditions to yield **29**.[122] Using pyrrolidine as a nucleophile and DBU as a base the OTs group was displaced to provide **30**,[123] all of these steps occurred quantitatively. In the final step TFA was used to remove the protecting group. This required the reaction to be left overnight. After careful removal of the high corrosive TFA solvent, the mixture then was treated with 4 M aqueous KOH to

remove residual TFA, leaving a pale brown solid. Kügelrohr distillation was used to yield the final product as a colourless oil **31**.[117b]

### 2.1.2. Synthesis and optimisation of 2-acetyl benzaldehyde and its derivatives toward synthesis of fulvenes

Initially two published procedures were followed to form the diols **32** and **33** in **Scheme 22**, using the chemistry of Piazza *et al*. 2002[124] and Lambert[125]. In our hands a more attractive procedure was the approach of Lambert *et al*. 1987.[125] This involved the use of *n*-BuLi activated with TMEDA, so that the benzyl alcohols were *ortho*-lithiated before quenching with ether solutions of acetaldehyde to yield the final diols **32** and **33** (**Scheme 22**, **A**). The next step was to oxidise the diols **32** and **33** *via* a Swern reaction to provide the reactive carbonyls **22** and **23** respectively needed for preparing the fulvene **24**. Even though good yields were typically achieved from this procedure, keeping these products at RT resulted in their decomposition as indicated by darkened sample colours and NMR assay. This is because **22** and **23** are self-reactive (to form condensation polymers, see **Scheme 22**, **B**). If stored at -20 $^{o}$C samples of **22-23** were usable for at least 4 weeks (**Scheme 22**).

**A**

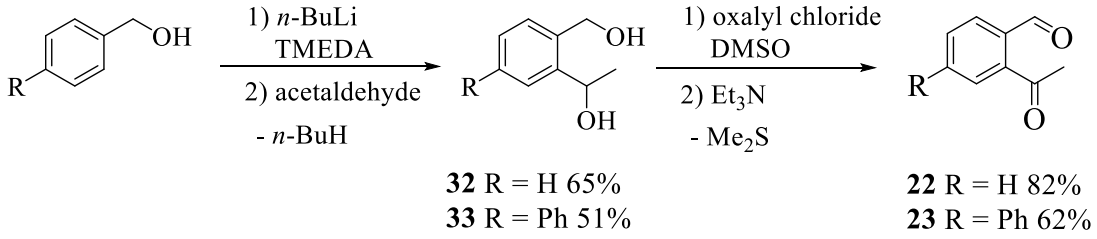


**32** R = H 65%
**33** R = Ph 51%

**22** R = H 82%
**23** R = Ph 62%

**B**

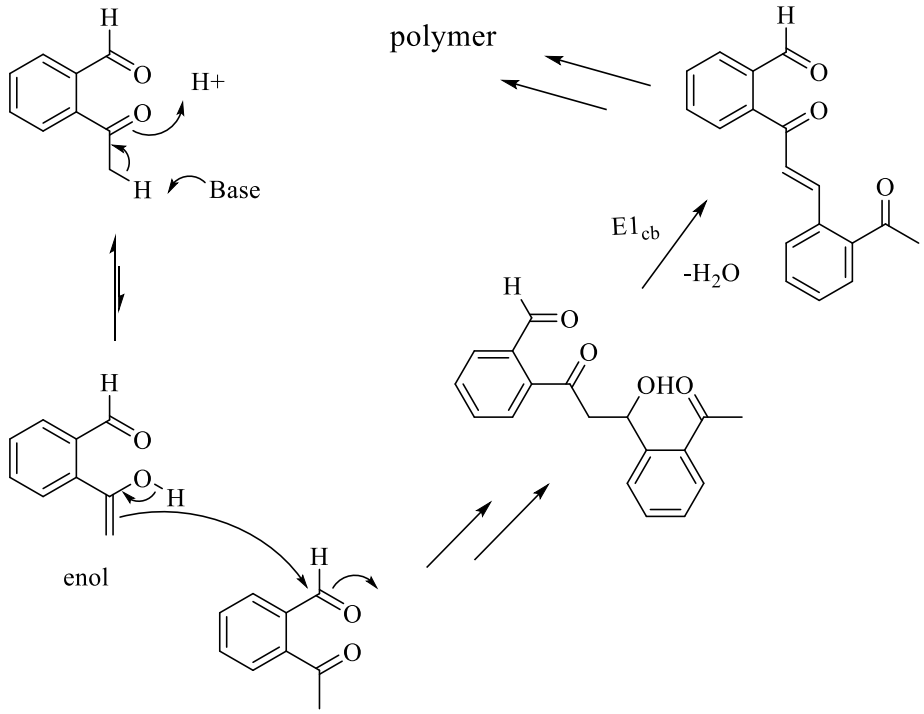


**Scheme 22.** (**A**) Synthesis of 2-acetyl-benzaldehydes **22** and **23** with two steps, starting from benzyl alcohol (**B**) self-reactive (form condensation polymers).

## 2.1.3. Synthesis and optimisation of fulvene 24 and its derivatives

Our main approach to synthesising fulvene **24** has been given (**Scheme 20**). However, the aim of this chapter was to build a library of compounds, which requires the capability to make a broad variety of derivatives of **24**. The route of **Scheme 22** is quite limited in substrate scope, so another alternative method was sought. Phan's attractive approach[126] (**Scheme 23**) was followed to achieve this. This route involves the *ortho* formylation of a wide range of phenol analogues, followed by condensation reaction with **37** (acetic acid hydrazide). The resulting compounds **38**-**40** underwent an uncommon lead(IV) acetate promoted rearrangement to yield the final products **41-43** by replacing the hydroxyl group of the phenol with an acyl unit (**Scheme 23**).[126]

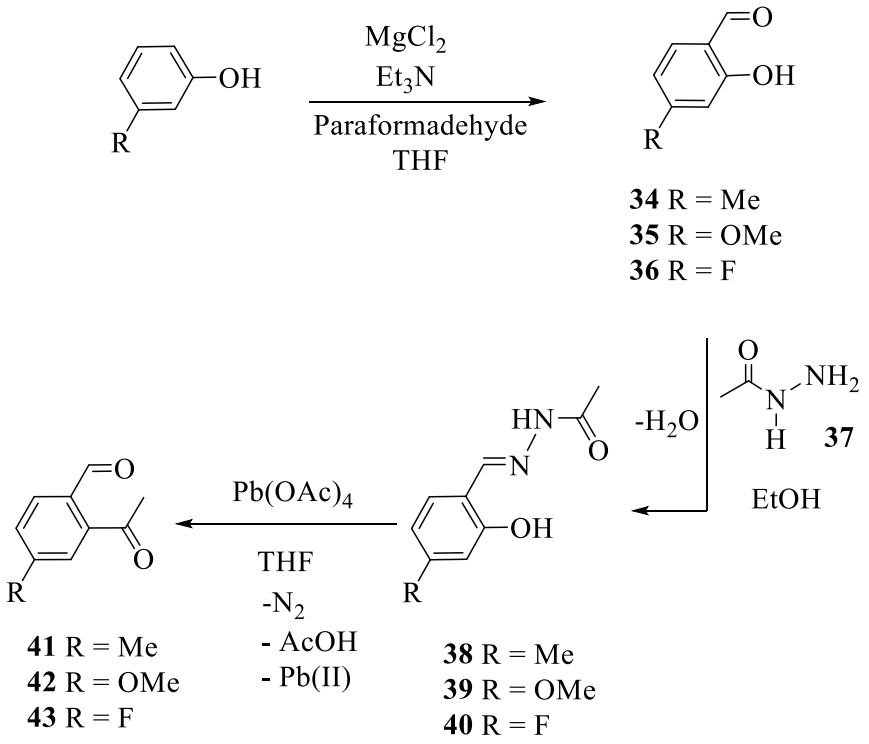


**Scheme 23.** Alternative synthetic route for making 2-acetyl benzaldehyde analogues to access additional derivatives of fulvene **24**.[126]

Surprisingly, the mechanism of formation of **24-27** does not involve condensation of the aldehyde unit in **22-23** or **41-42** with cyclopentadiene (**Scheme 24**). Formyl groups are normally regarded as much more electrophilic than acyl units. However, under equilibrium conditions the cyclopentadiene undergoes a condensation reaction with the acyl group (ketone moiety) of 2-acetylbenzaldehyde triggering formation of the pentafulvenes, as catalyst **31** was added to the aldehyde group forming iminium ions **22a**-**23a**, **41a**-**42a** (**Scheme 24**). The iminium ions promote C-C bond formation from the resulting pentafulvene stabilised carbanion (p$K_a$ *ca.* 22.1 in DMSO)[127]. This proceeds with the carbanion attacking on the bottom face of iminium ion because of a blocking group effect (steric hindrance effect) of the catalyst (**Scheme 24**).

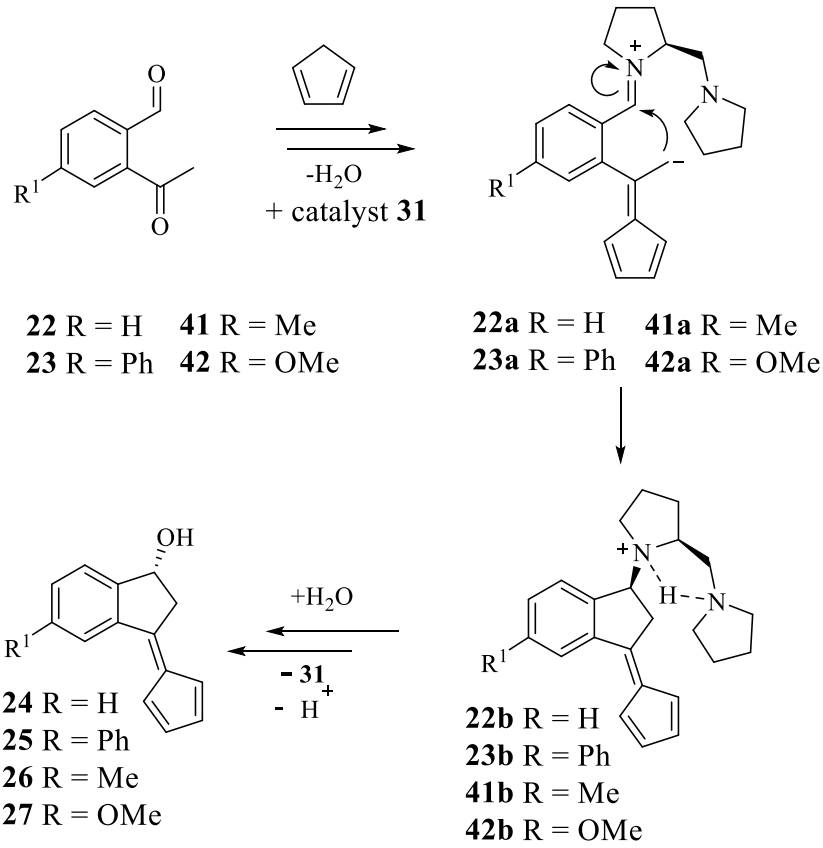


**Scheme 24.** Proposed mechanism for the formation of pentafulvenes **24-27**.[116]

Hydrolysis of the amine is then proposed to yield pentafulvene **24-27** with the correct stereochemistry and regiochemistry. The formation of fulevenes from **41-42** (**Scheme 23**) confirms that the mechanism of **Scheme 24** is correct. If the CHO group (formyl group) reacted first with the cyclopentadiene, different regio and stereo isomers would have been attained (**Scheme 25**). Additionally, crystallography studies have shown that none of the alternative pentafulvenes in **Scheme 25** such as **42f** were made.

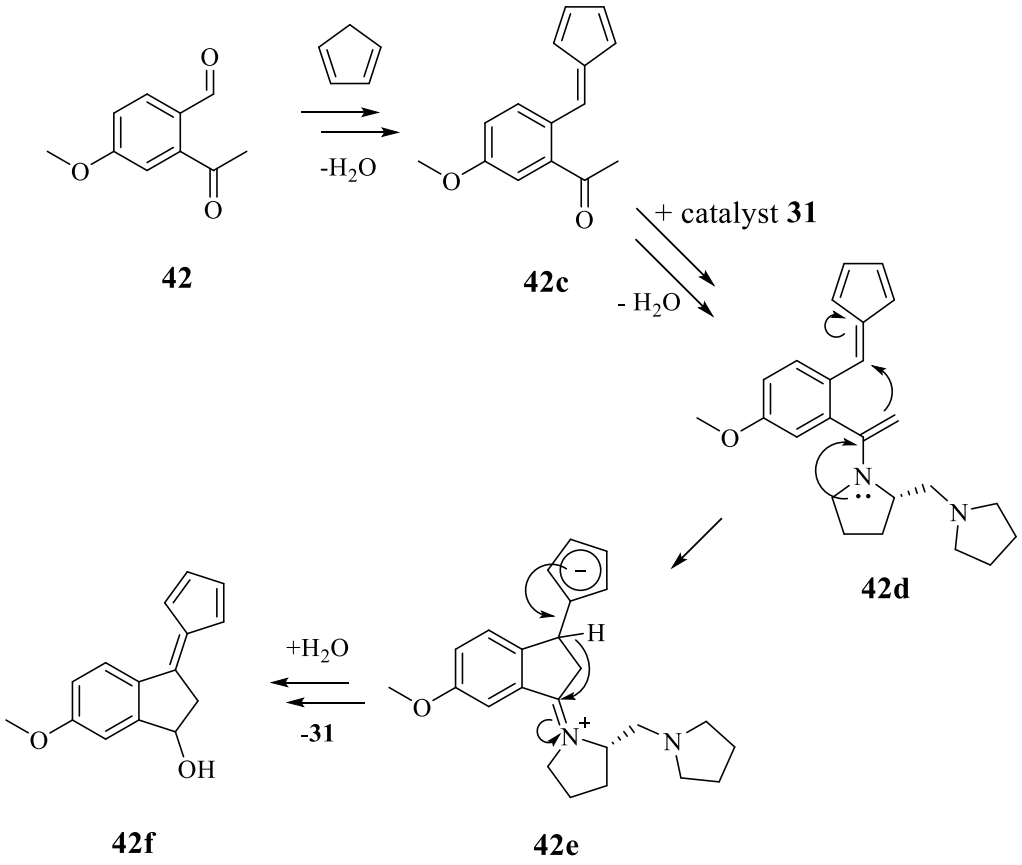


**Scheme 25.** Alternative mechanistic proposal for making pentafulvenes which involved the condensation of aldehyde group of 2-acetyl benzaldehyde first to make the pentafulvene. The resulting CpH **42e** after cyclization would undergo a 1,3-hydride shift and following hydrolysis of **31** to yield pentafulvene **42f**.

Initially fulvene **24** and its derivatives were produced in low yield which was due to the formation of the two by-products **24b** and **24c** in significant quantities (**Scheme 26**). This was overcome by optimisation of the reaction conditions. Finally, all of the fulvenes synthesised here are temperature sensitive compounds which must to be stored at -20 $^{o}$C, otherwise they darken in colour.[36a] Proton NMR spectra of these materials indicated once decomposition of fulvene **24**-**27** has started (*via* intermolecular condensation) they cannot be used for the next step effectively.[36a]

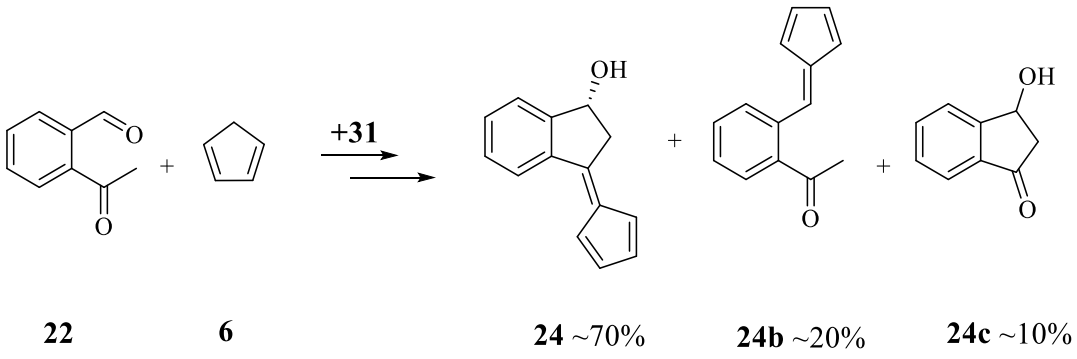


**Scheme 26.** The ratio of proposed product and by-product during the synthesis of fulvene **24**.

The optimised reaction conditions were then applied to afford the pentafulvenes **24-27** (**Figure 22**). Yields of aryl, alkyl, and methoxy substituted fulvenes and the reaction conditions and stereoselectivities are summarised in **Table 2** while the structures of the new pentafulvenes can be seen in **Figure 22**.

**Table 2.** New pentafulvenes **24-27**, using optimised conditions.

| Compound | Temp (˚C) | Time (h) | Yield (%)[a] | Initial *ee* | Recrystallised *ee* |
|---|---|---|---|---|---|
| **24** | 15 | 6 | 78 | 88 | >99 |
| **25** | 15 | 6 | 53 | 76 | >99 |
| **26** | 15 | 6 | 72 | 82 | -[b] |
| **27** | 15 | 6 | 54 | 82 | >99 |

[a] Isolated yields; [b] *ee* not improved by recrystallisation.

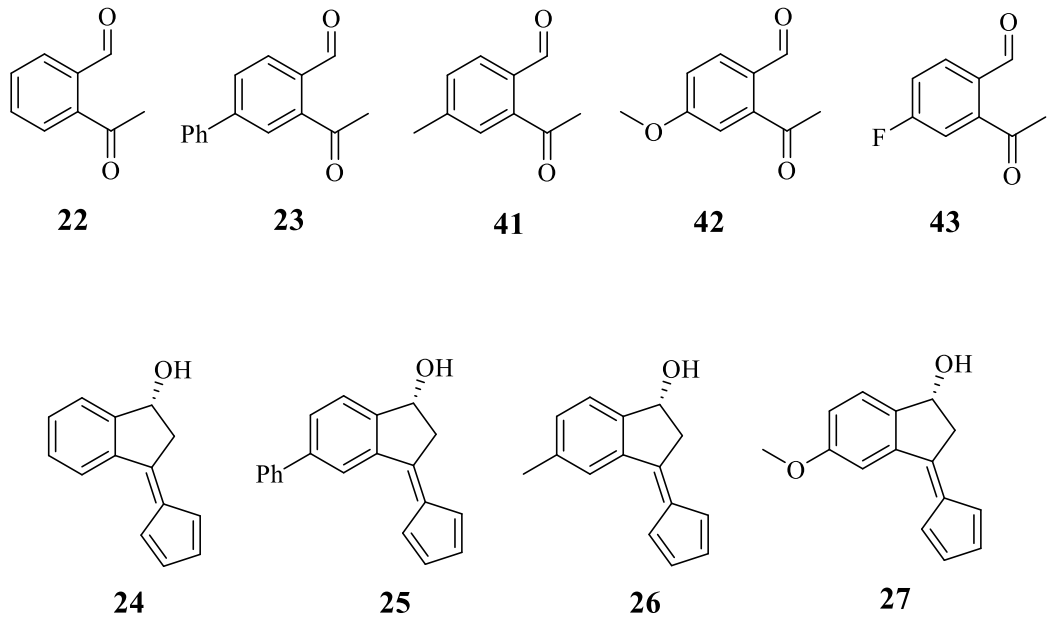


**Figure 22.** The derivatives of 2-acetyl-benzaldehyde (**22**-**23**, **41**-**43**) and the pentafulvenes (**24**-**27**) which were achieved in this study.

### 2.1.4. Attempted complexation studies using ligands derived from 24

Although they were ultimately unsuccessful, some initial studies towards titanium complexes derived from the pentafulvene **24** were made using methodology built on that of Tacke *et al*.[128] The final steps of the cyclopentadienyl ligand preparation was a collaboration carried out with Dr Ryan Nouch, as described in his thesis;[116] so only an outline of this ligand synthesis is given here. Nouch was able to alkylate the pendant hydroxyl group of **24** with either triethylsilyl chloride (TESCl) or chloromethyl methyl ether (MOM-chloride), providing **24aa** and **24ab** (**Scheme 27**) which he fully characterised.[116] These protected pentafulvenes **24** were reduced using the 1,2-hydride addition methodology developed by Tacke[128] using $LiBHEt_3$ (Super-Hydride®).[129] Nouch was able to show that a >16:1 mixture of a single diastereomer was formed for **24ac** and **24ad** (**Scheme 27**). This was assigned as the *syn* stereoisomer on the basis of the appearance of an n.O.e. effect between the 1,3-related CHY (Y = OR, Cp) units.[116] Together with Nouch, I made repeated attempts to complex ligands of this class to titanium. It was quickly noticed that, even at room temperature, **24ac** and **24ad** begin to decompose to mixtures of species soon after they are isolated. For this reason, crude samples of the ligands **24ac/d**, or their lithium cyclopentadienides, had to be used. We assume that this instability of **24ac/d**, is due to β-elimination of '$Et_3SiOH$' or 'MOMOH' leading decomposition to intractable mixtures (**Scheme 27**).[130]

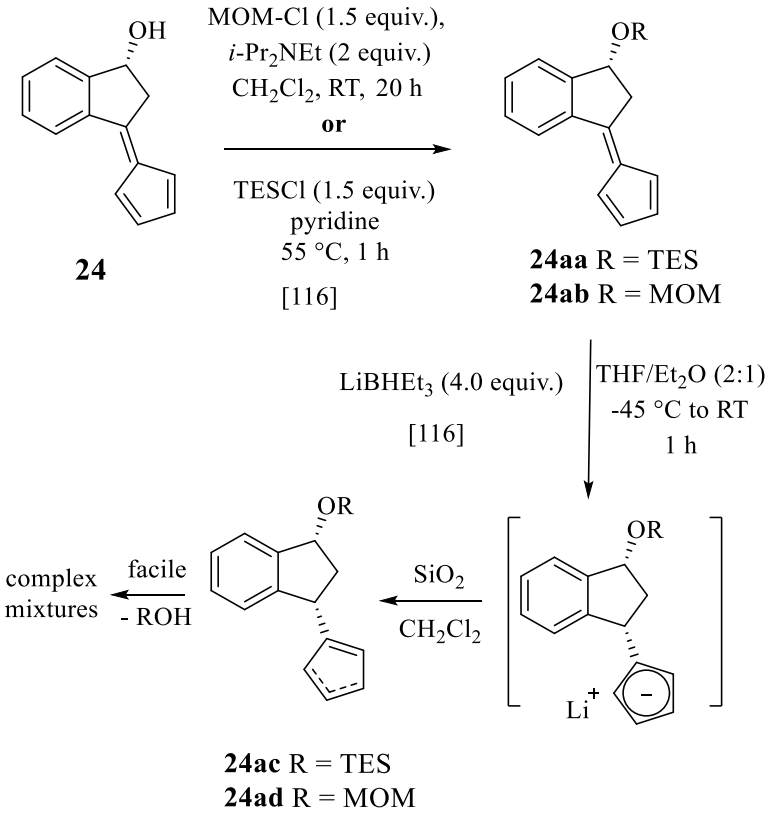


**Scheme 27.** Summary of the unstable ligands **24ac** and **24ad** provided by Nouch[116] for complexation studies.

Initially, the reaction of fulvene **24ab** with freshly prepared "$TiCl_2$" was attempted using the method of Tacke *et al.*[128] Nominal titanium(II) dichloride was thus obtained *in situ* by reaction of titanium tetrachloride with (2 equiv.) of *n*-BuLi in toluene-THF mixtures (**Scheme 28**). Unfortunately, the addition of **24ab** resulted only in the formation of complex mixtures from which nothing could be crystallised using either literature conditions,[128] or modifications thereof. It is likely that decomposition of the ligands resulted.

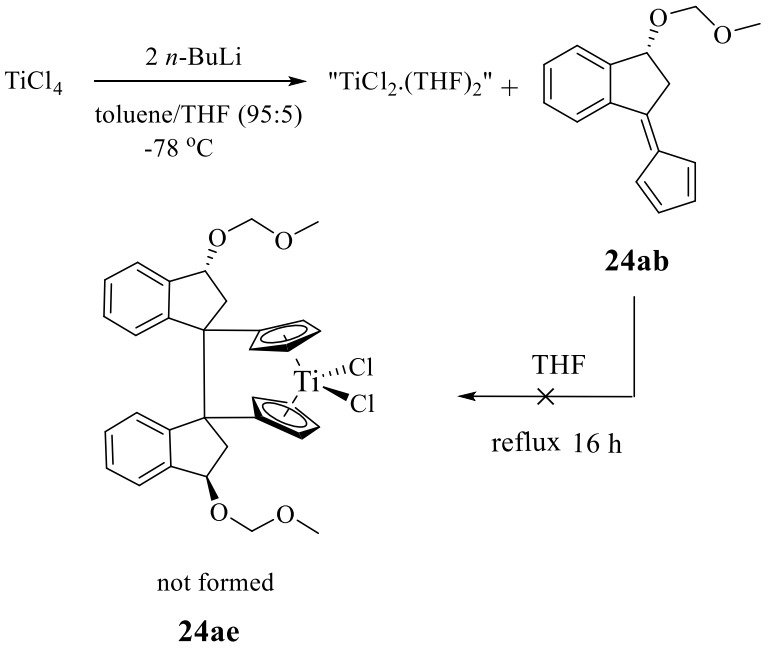


**Scheme 28.** Representative attempt at preparation of *ansa*-type complexes.

As the fragility of our pentafulvene derived ligands became readily apparent in the attempted chemistry of **Scheme 28** (and related studies), we first confirmed that the formation of cyclopentadienyl anions could be achieved. Deprotonation of both **24ac** and **24ad** with *n*-BuLi (1 equiv.) at 0 °C in $Et_2O$ followed by addition of pH 7 buffer led to quantitative recovery of the ligands by $^1$H NMR spectroscopy. Quench of the putative anions with $D_2O$ led to mass spectra consistent with mono deuteration. To avoid the formation of diasteroisomers the cyclopentadienide of **24ac** was first reacted with commercial $CpTiCl_3$ under mild conditions (**Scheme 29**). A representative $^1$H NMR spectrum of the crude reaction mixture resulting is shown in **Scheme 29**. Nothing could be isolated from these complex mixtures. All variants that were tried (reaction temperatures -78 °C to RT, concentrations 0.1 to 0.01 M THF, and other solvents) failed. At best, we could identify a trace of a signal at *m/z* 309.0753, than might be assignable to the fragment shown in **Scheme 29** by +ESI mass spectrometry in one run when using ligand **24ac**.

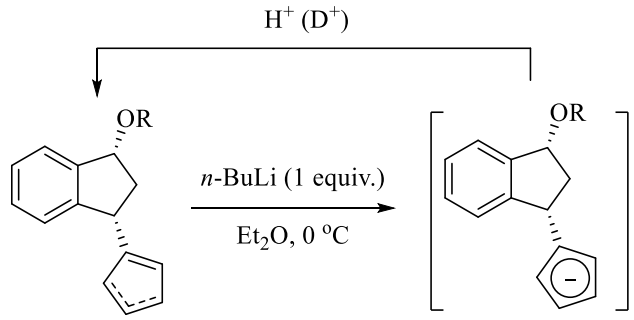


**24ac** R = TES
**24ad** R = MOM

$CpTiCl_3$ (0.5 equiv.), 0 °C to RT

complex mixture (representative $^1H$ NMR spectrum below)

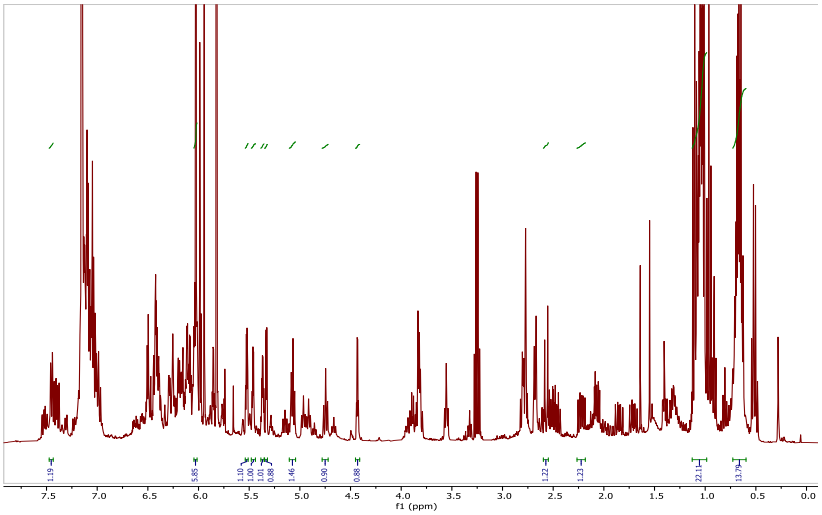

By +ESI MS possible traces of:

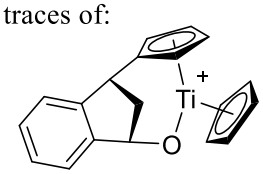


Exact Mass: 309.0753
when using ligand **24ac**

**Scheme 29.** Representative attempts at titanium complexation studies using $CpTiCl_3$ and ligands **24**.

Of many alternative attempts, the most tractable outcome resulted from the use of **24ad** in the presence of $TiCl_4$. The cyclopentadienide of **24ad** was formed in the usual way (**Scheme 30)** but the supernatant ether layer syringed away (by cannula syringe). This led to a large loss of material when the remaining solids were weighed under vacuum. Assuming the desired anion was present when this was formed, then this was in ca. 30-60% yield. Adding THF solutions of $TiCl_4$ (0.5 equiv.) led to red-brown solutions. The $^1H$ NMR spectra (**Figure 23**) of these mixtures could, sometimes, be assigned to contain significant amounts of one of the two diastereomers of product **24af**. In all trials other products were always present and the reaction was not at all reproducible. On one occasion when nominal **24af** was formed we could attain an +ESI consistent with a $[M - Cl]^+$ formula. All attempts to isolate putative **24af** from these reaction mixtures led to the decomposition of the compounds observed in the crude reaction mixtures. No tractable data were apparent beyond **Figure 23**.

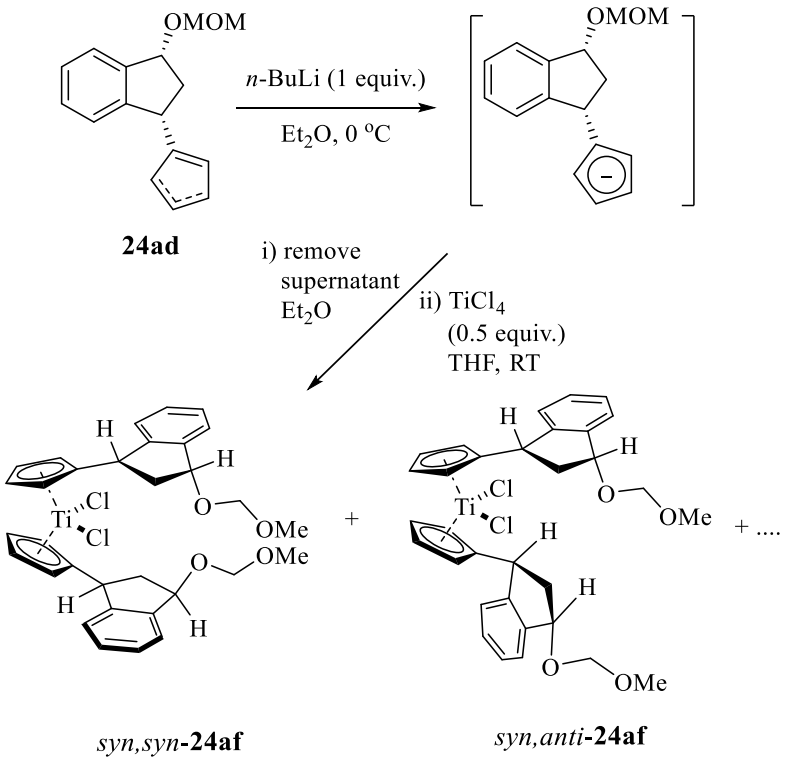


**Scheme 30.** Attempted formation of *bis*-ligated titanium complexes.

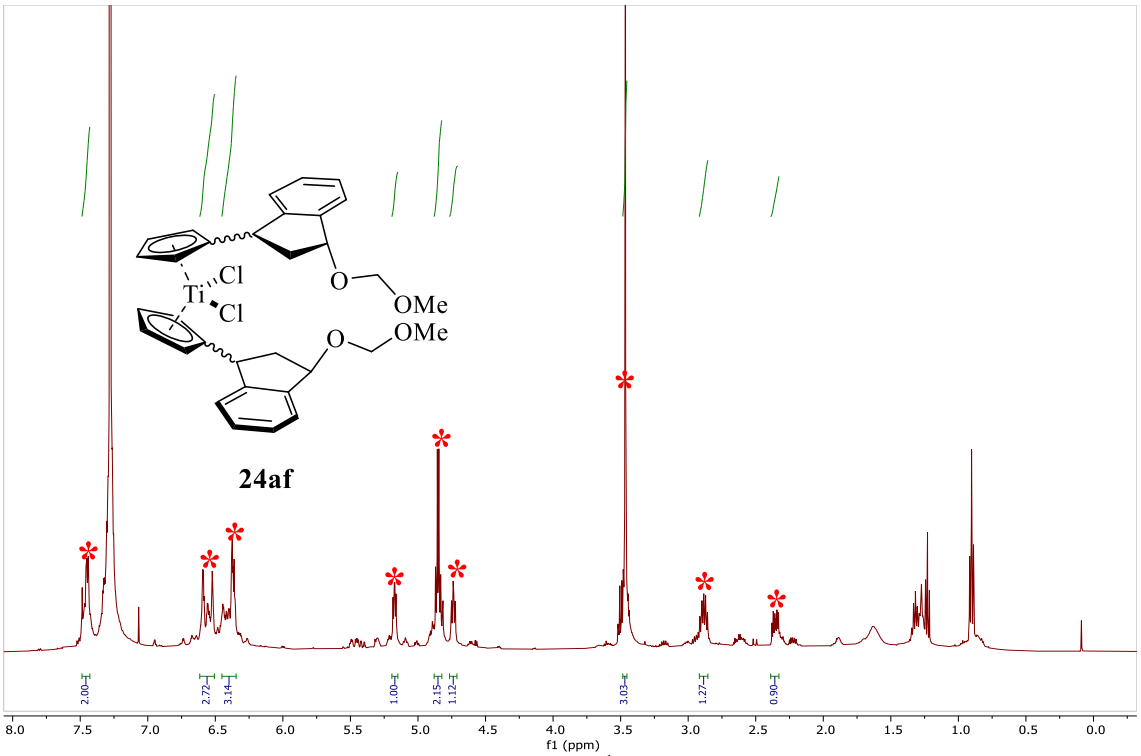


**Figure 23.** The best crude reaction mixture $^{1}$H NMR spectrum we could attain supporting formation of complex **24af**. Peaks potentially associated with the major diastereoisomer of the target are marked (*).

The non-reproducibility and poor stability of these compounds to normal work-up conditions was a source of great frustration to us. Our forward biological studies required compounds considerably more robust than those that were being (at best) observed. At this time I had already uncovered an alternative lead compound for anti-cancer studies based on titanium phenolate structures that was highly robust under physiological conditions. Faced with an ongoing struggle to isolate the cyclopentadienyl targets of this chapter or to move to the more promising phenolate-derived lead, the latter was chosen. These results are discussed in Chapter Three. I believe the correct decision was made as subsequent investigations by other researchers of the group also led to no tractable products from attempted titanium complexation by ligands based on **24ac/d**. It is possible that other metals may be more suitable for their complexation, but that is not in line with the focus on titanium proposed for this thesis.

## 2.2. Conclusions

We were able to synthesise and optimise 6,6-disubstituted pentafulvenes bearing a chiral pendant hydroxy group **24-27**. This unique class of compound appears interesting as it is easy to crystallise to a single enantiomers that are potentially synthetically useful. The product gained from this approach gave >99:1 *er*. Attaining the titanocene complexes **24ac**, **24ae** and **24af** or related derivatives were unsuccessful. The air sensitivity and short stability (facile decomposition) of these compounds are not appropriate for biological studies and led us to consider alternative classes of compounds.

Preliminary results led to a switch to Ti-phenolate species that are much more stable than the metallocenes targeted here. In the next chapter it will be seen these gave high stability, air-stable complexes with good solubility in most solvents. The class of Ti(IV) compounds proposed were diamine–amine-*bis*(phenolato) Ti(IV) complexes which exhibited a range of co-ordination chemistries for Ti(IV), with variable cytotoxicities and reactivities.

The communication resulting from this chapter presented in a final Appendix:

**M. Abid**, R. Nouch, T. D. Bradshaw, W. Lewis, S. Woodward, "Tripodal O-N-O *bis*-Phenolato Amine Titanium(IV) Complexes Show High *In Vitro* Anti-Cancer Activity" *Eur. J. Inorg. Chem.* **2019**, 2774-2780.

# Chapter three

## 3. Amine-diamine *bis*(phenolate) Ti(IV) complexes (salan)

Some titanium(IV) compounds are found in nature[131] and have been used (particularly $TiO_2$) for a range of purposes including in foods, cosmetics and drugs.[132] Medically, titanium compounds were first used in 1911-1918 both for treating mustard gas injuries and as agents against some types of bacteria.[132] The first reported Ti(IV) anti-cancer trials (in rats) date to 1937.[132] There are many reasons for using titanium complexes to treat cancer, one is their high activity against tumours which are resistant to compound **3** (cisplatin), along with low toxicity towards normal cells.[47, 133] As discussed in Chapter One, there were initially two main families of titanium(IV) compounds used as anti-cancer agents: titanocene dichloride (**10**) and budotitane (**17**).[37] Although these two families showed high activity against certain types of tumours,[134] their rapid hydrolysis, low solubility, poor stability, and problems with formulation caused them to fail in clinical trials.[67] In contrast, amine-diamine *bis*(phenolate) Ti(IV) 'salan' complexes (described in Chapter One), that were first synthesised in 1990s, are often much more stable. In 2007 their anti-tumour efficacy was established by Tshuva and her group.[81] They also exhibit high stability in aqueous media, and are much more stable than titanocene dichloride and budotitanes.[135] These new complexes also exhibited higher biological activity than early generations [e.g. titanocene dichloride (**10**) and budotitane (**17**)] against wide range of cancer cell lines.[81] For example, the $IC_{50}$ value of **18b** (**Figure 24**) against HT-29 (colon cancer) and OVCAR-1 (ovarian cancer) is 12±1 μM for both cell lines tested, while the $IC_{50}$ values of **10** is 710±120 and 870±90 μM respectively. The $IC_{50}$ value of **17** is 53±1 μM against both cell lines tested (**Figure 24**).[81]

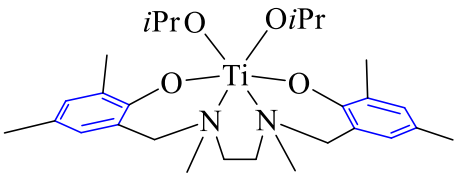


**18b**

| | $IC_{50}$ µM | |
|---|---|---|
| | HT-29 | OVCAR-1 |
| **18b** | 12±1 | 12±1 |
| **10** | 710±120 | 870±90 |
| **17** | 53±1 | 53±1 |

**Figure 24.** Salan complex **18b** and its activity against two cancer cell lines, HT-29 and OVCAR-1 in comparison to titanocene dichloride (**10**) and budotitane (**17**).[81]

In 2011 Immel *et al.* showed that the new family of titanium(IV) compounds (salan) which containing tetradentate ligands (ONNO coordination) also display very good activity against different cancer cell lines.[135] For example, the $GI_{50}$ values of **18e** against HCT-116 (colon cancer) and MDA-MB-468 (breast cancer) were 29.2±0.1 µM and 9.9±0.2 µM respectively (**Figure 25**). Additionally, these salan complexes also showed high stability in aqueous environments compared to titanocene dichloride **10**.[135]

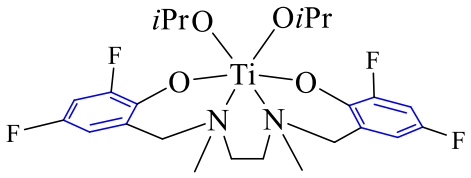


**18e**

| | $IC_{50}$ µM | |
|---|---|---|
| | HCT-116 | MDA-MB-468 |
| **18e** | 29.2±0.1 | 9.9±0.2 |

**Figure 25.** The structure of salan complex **18e** and its activity against two cancer cell lines, HCT-116 and MDA-MB-468.[135]

Many examples of this new generation of titanium(IV) complexes (salan) has been developed between 2007 and 2019 by Tshuva *et al.* and other co-workers, and most of these complexes have tetradentate ligands (ONNO coordination).[81, 98, 135-136] These tetradentate phenolato ligands can be divided into two sub-ligands, ligands of type $\mathbf{L_A}$ and $\mathbf{L_B}$ (**Figure 26**).[137]

All of the titanium complexes achieved from these ligands $\mathbf{L_A}$ and $\mathbf{L_B}$ have been examined against various cancer cell lines both *in vitro* and *in vivo*, and showed moderate to good activity.[81, 98, 135-136, 138]

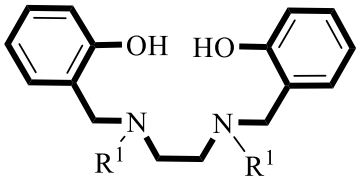


$\mathbf{L_A}$ $R^1$ = Me
$\mathbf{L_B}$ $R^1$ = $CH_2CH_2OH$

**Figure 26.** Tetradentate phenolato (ONNO coordination) ligands, types $\mathbf{L_A}$ and $\mathbf{L_B}$.[98, 138]

Conversely, phenolato complexes with ONO donor atom coordination[139] are tridentate and are little studied in the anti-cancer area. Ligands of the $\mathbf{L_C}$ core, shown in **Figure 27**, were first prepared in the 1990s for titanium(IV) catalysed alkene polymerisation studies.[73] To the best of our knowledge, they have never been used in anti-cancer trials prior to our work (see later, Section 3.2.2).[74]

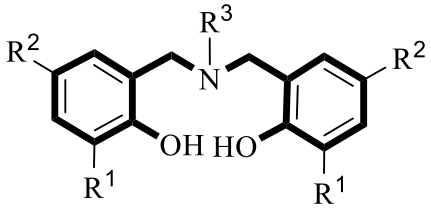


$\mathbf{L_C}$ $R^1$ $R^2$ = Me, OMe, OEt, Cl, F
$R^3$ = Me, Et, *n*-Pr

**Figure 27.** An un-trialled ONO donor atom class of ligand cores ($\mathbf{L_C}$) for anti-cancer use with titanium(IV) complexes.

## 3.1. Aims of this Chapter

We were interested to investigate if the use of ligand cores $\mathbf{L_C}$ (**Figure 27**), after coordination to titanium(IV) could lead to highly active anti-cancer titanium(IV) complexes. They had not previously been trialled in biological studies, although examples of such complexes have been identified in the fields of catalysis and coordination chemistry since the 1990s.[73, 140] The aim of this chapter was to synthesise new titanium complexes with ligands $\mathbf{L_C}$. We hoped these would show not only high activity against cancer cell lines, but limited toxicity to normal cells, good solubility in most solvents, high stability in aqueous media, and prove easy to handle. Additionally, we wished to understand the mechanism of action of such complexes, in actual cell media against cancer cell lines and to gain some insights how such complexes interact with target bio-molecules. The $R^1$-$R^3$ substitutions of $\mathbf{L_C}$ were chosen to cover a range of steric and electronic factors. Both electron withdrawing and donating groups for $\mathbf{L_C}$ were selected: Cl, F, Me, OMe (methoxy), and OEt (ethoxy). At the outset of our studies no examples containing 'OMe' donating groups in either the ligands $\mathbf{L_C}$ or their titanium complexes were known. As show earlier $R^1$-$R^3$ ligand substitutions can both increase or decrease both the cytotoxicity and stability of titanium phenolate complexes, but this must be experimentally determined.

## 3.2. Results and Discussion

### 3.2.1. Literature approaches to the synthesis of parent phenols and ligands

Most of the parent phenols needed to form the 4,6-substituted ligands were available commercially. However, **46d** and **46e** (**Scheme 31**) were not available or were prohibitively expensive. We obtained these phenols using Baeyer-Villiger oxidation of the parent aldehydes in quantitative yield.[141]

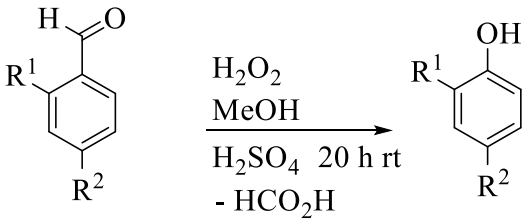


**45c** $R^1$ = Me, $R^2$ = OMe
**45d** $R^1$, $R^2$ = OMe

**46d** $R^1$ = Me, $R^2$ = OMe
**46e** $R^1$, $R^2$ = OMe

**Scheme 31.** Synthesis of phenols of **46d-e**.[141]

While there are thousands of examples containing the sub-structure core $\mathbf{L_C}$ reported, only a few examples have this structure when $R^1$ and $R^2$ are limited to Cl, Br, *t*Bu, Me and none with $R^1$, $R^2$ = OMe.[73, 142] These few examples were prepared generally for studies of alkene polymerisation catalysis only.[143] No example of the titanium complexes of $\mathbf{L_C}$ was reported for use in anti-cancer studies. The substructures $\mathbf{L_C}$ were identified through Scifinder search in 2019 and prepared by simple Mannich chemistry.[73, 76] It is preferable for biological studies to block both *para* and *ortho* sites to the OH to minimise oxidative degradation of the phenol and to restrict $R^3$ in $\mathbf{L_C}$ to a methyl group (**Scheme 32**). Failing to block the $R^1$, $R^2$ sites leads to

undesirable compounds being formed e.g. polymers, due to the hydroxyl group on the phenols activating the *para* and *ortho* sites to attack. We synthesised a small library containing 4,6-substituted versions of core the **L**$_C$: **47a-f**,**h**, of which only **47a** and **47g** were already known (**47**, **Scheme 32**).[78]

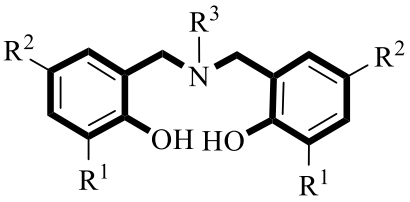


**L**$_C$

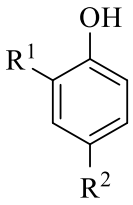


(**46a-h**)

i) paraformaldehyde
$R^3NH_2$
toluene (-$H_2O$)
ii) 150 °C

| **L**$_C$ | $R^1$ | $R^2$ | $R^3$ | Recrystallised yield (%) | Ref. |
|---|---|---|---|---|---|
| **47a** | Me | Me | Me | 46 | [78] |
| **47b** | MeO | Me | Me | 62 | |
| **47c** | MeO | Me | Et | 80 | |
| **47d** | Me | MeO | Me | 54 | |
| **47e** | MeO | MeO | Me | 55 | |
| **47f** | Me | F | Me | 56 | |
| **47g** | Cl | Cl | Me | - | [78] |
| **47h** | EtO | EtO | Me | 40 | |

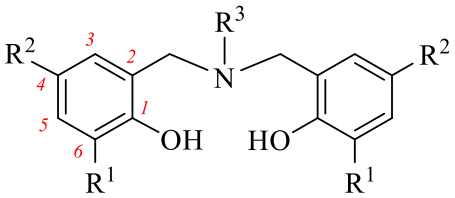


**L**$_C$ (**47a-f,h**)

**Scheme 32.** Proposed general structure of ligand **L**$_C$ with *para* and *ortho* sites blocked and the specific **L**$_C$ library prepared in this study.

The ligands **47a-f,h** were attained using the Mannich condensation reaction.[144] This reaction begins with the formation of an iminium ion from the formaldehyde and the amine (**Scheme 33**). The iminium is formed by protonation of an initially formed imine. The low energy $\pi^*$ LUMO of the iminium is attacked by the electron-rich $\pi$-bond of the phenol leading to amine formation. Such acid promoted processes, however, can also suffer deactivation through protonation of any amine intermediate, as these are better bases. General literature procedures[144] report that the final products typically attained after heating the bulk material to 150 ºC for 1 h, followed by recrystallisation from diethyl ether.[144] Unfortunately, we found that such procedures did not give pure products, and that significant amounts of undefined by-products were present. Therefore, we tried an alternative work up, filtering the crude mixture (dissolved in diethyl ether) through Celite®, and covering this with pentane. As the layers diffuse together crystals form. This gave analytically pure materials as can be seen in the exemplary spectra of **47b** (**Figure 28**), in 40-80% yield.

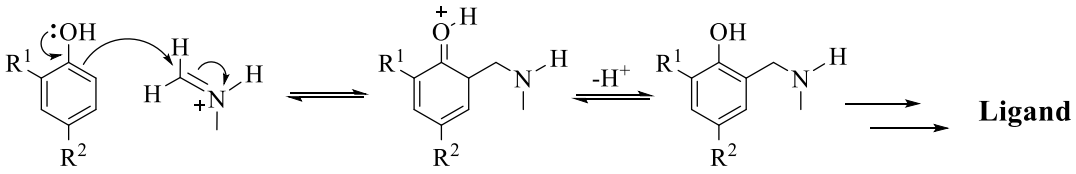


**Scheme 33.** Mechanism of the *bis*(phenolato) ligand formation.

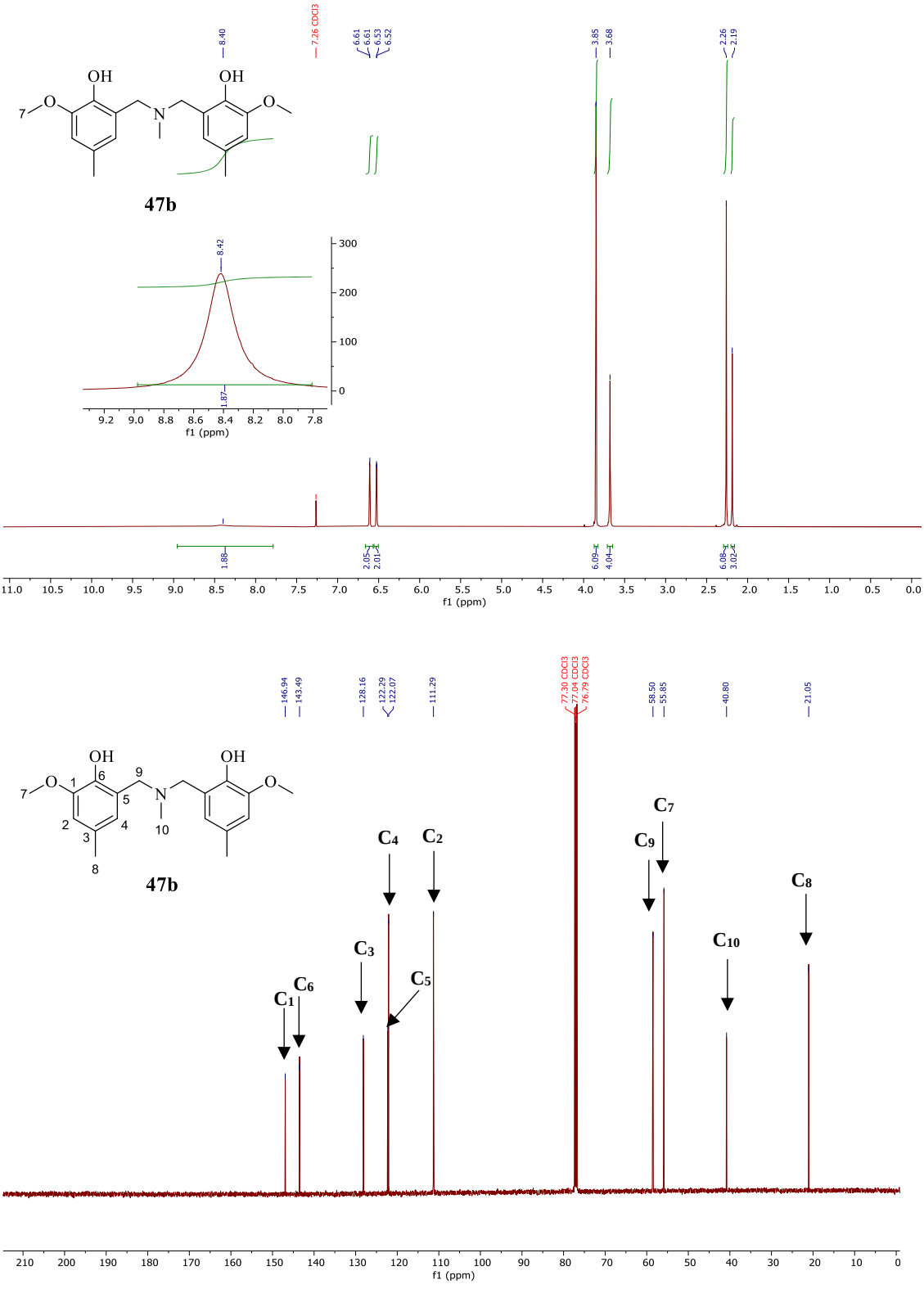


**Figure 28.** Representative **$^{1}$H** (top) and **$^{13}$C NMR** (bottom) spectra of **47b** demonstrating ligand purity.

Complex **47h** was achieved in only moderate 40% yield (see the table within **Scheme 32**). Additionally, none of our attempts to isolate **47g** were successful, although we could see it was present in the reaction mixture. We were unable to purify it, although its isolation was already described in literature.[76] The poor behaviour of **47g** is due to the electron withdrawing nature of the chloride substituents. These reduce the π-electron density of the phenol making it a poorer nucleophile to the iminium electrophile in the Mannich reaction.[145] Consistent with this picture, only some compound **47g** was found to be present in the crude mixture (around 40-60%) by $^{1}$H NMR spectroscopy (**Figure S1** in Appendix). This mixture was therefore used directly in subsequent complexation studies with Ti(O*i*Pr)$_4$.

In an attempt to extend the library of **Scheme 32**, compound **44** was prepared by reacting 4-amino-2-chlorophenol with sodium acetate and isobutyryl chloride in acetone (**Scheme 34**). The addition of isobutyryl group was used to protect the amine through amide formation by reducing its *N*-nucleophilicity. Unfortunately, onward attempts to synthesise a 4,6-substituted ligand from compound **44** were not successful. In all our ligand preparation reactions we need to heat the bulk materials at 150 $^{o}$C for one hour to promote the π bond by the aromatic *ortho* site attacking the iminium ion promoted by donation of a lone pair of oxygen (**Scheme 34**, **A**). However, compound **44** did not behave in this way. We propose that the nitrogen in the amide group donates its electrons to the carbonyl group facilitating *O*-alkylation. The π bond of the carbonyl group attacks the iminium ion, resulting in a thermal unstable product (**Scheme 34**, **B**), which decomposed to dark uncharacterised products (**Figure 29**).

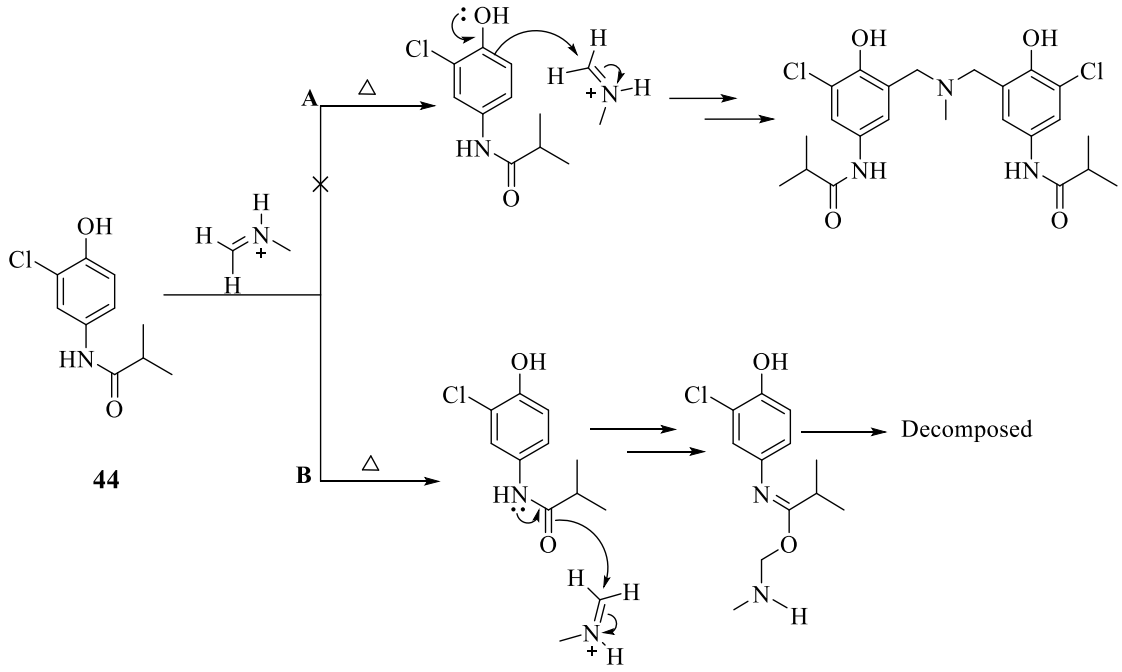


**Scheme 34.** (**A**) Desired mechanism **44** to afford the preferred product. (**B**) The alternative mechanism thought to occur.

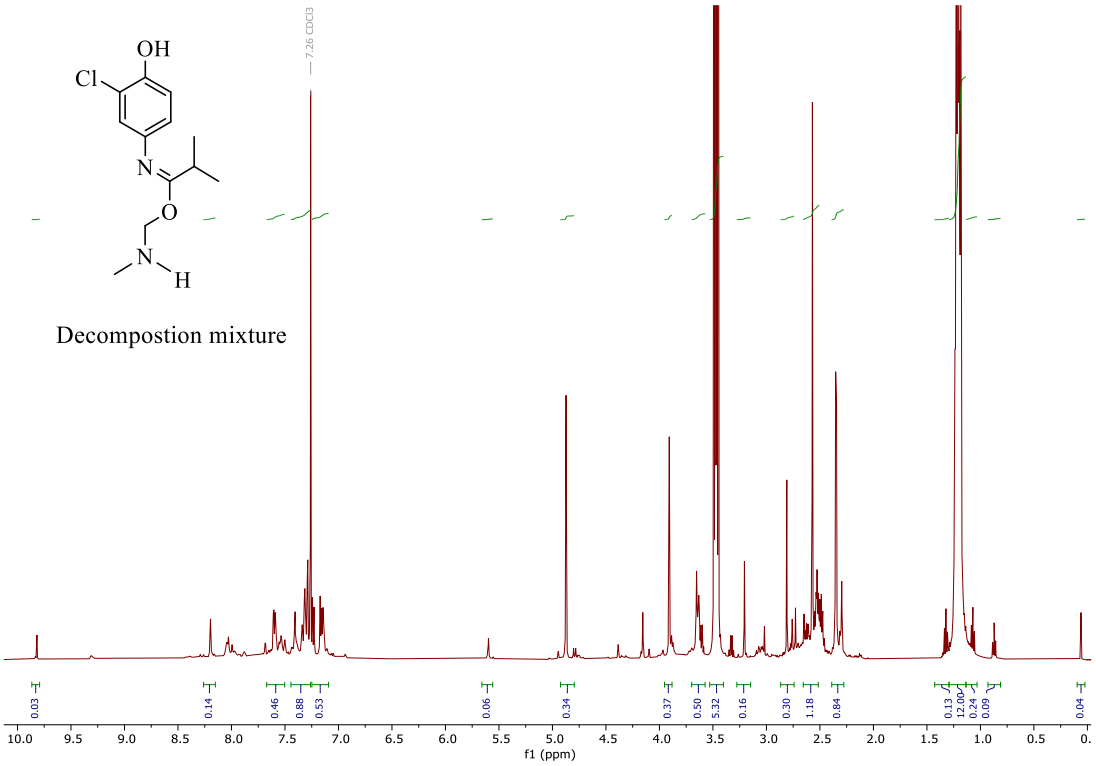


**Figure 29.** **$^{1}$H NMR** spectrum of the decomposed mixture from compound **44**.

Finally, we synthesised compound **45** by reducing the carbonyl group of vanillin using sodium borohydride. We chose this motif as it possesses two hydroxyl groups, so the product after complexation would expected to be more hydrophilic than other complexes we have made. Potentially, this might aid dissolution in the aqueous media used in biology studies. However, ligand **45a** could not be isolated (**Scheme 35**).

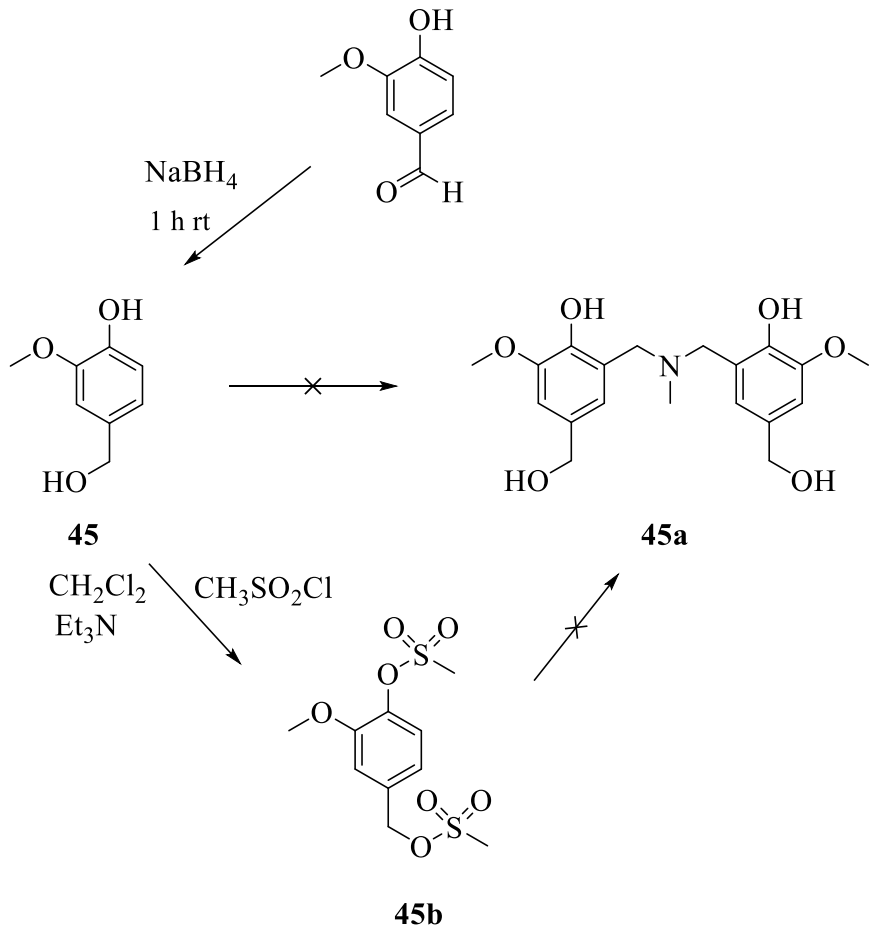


**Scheme 35.** Desired product of **45a** (not formed) after attempted Mannich condensation of **45** or **45b**.

The addition of a mesyl group for the protection of the OH groups, was attempted for compound **45**, and using $CH_3SO_2Cl$ resulted in compound **45b**. Our concept of protecting both OH groups was that these would not be subsequently involved in iminium mediated formation of the nitrogen methylene bridge. It was proposed the reaction would form the required *N*-methylene bridge on the *ortho* site of phenol, but this was also unsuccessful. This may be due to the fact that the reactants were decomposed during heating instead of giving the final product. This was confirmed by $^1$H NMR monitoring of the reaction mixture as the reaction developed a dark colour; leading to a dark polymer finally being achieved (**Figure 30**).

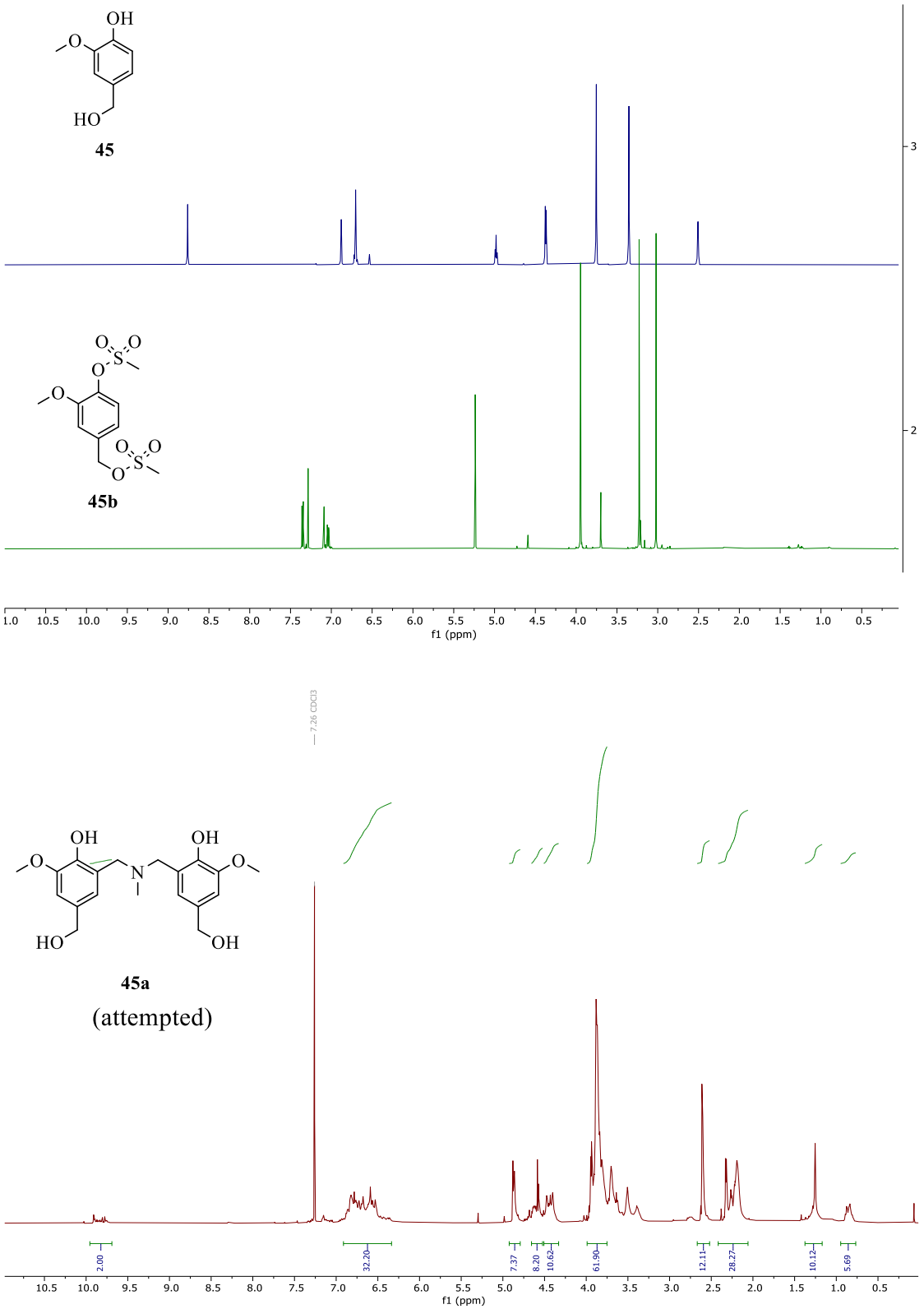


**Figure 30.** **$^{1}$H NMR** spectra of **45**, **45a-b** confirm starting compounds **45** and **45b** were pure, but decomposed to intractable polymeric mixtures on heating.

### 3.2.2. Complexation studies

We next investigated the formation of a variety of titanium(IV) complexes, derived from amine *bis*(phenolate) ligands **47** and Ti(O*i*Pr)$_4$. Thus, reacting ligands (**47a-h**) (**Scheme 32**) with Ti(O*i*Pr)$_4$ at a 2:1 ratio in toluene at ambient temperature for 4 h under a nitrogen atmosphere led to the formation of the titanium(IV) complexes **48a-h** (**Scheme 36**). We utilised trap to trap distillation to remove the reaction solvent. Our optimal conditions resulted in intense red coloured solutions, from which complexes **48a-h** were isolated in good yield as rhomboidal crystals or orange powders, by recrystallisation from appropriate solvents. The preparation and purification of complexes **48** are either completely absent or only poorly described in limited cases.[74, 98, 146] We found liquid-liquid diffusion optimal for recrystallisation, often with dichloromethane and pentane (**Figure 31**).

**Figure 31.** Representative recrystallisation by liquid-liquid diffusion for compound **48f**.

Ligands of type **47** (**L**$_C$) complex readily to a wide variety of transition metals including: Fe,[147] Mo,[148] Zr,[143] Cu,[149] Mn,[150] and V.[151] Nevertheless for Ti, only the preparation of **48a**[143] is known together with three related Ti(substituted-**L**$_C$)$_2$ complexes using ligands correlated to **47** with R$^1$, R$^2$ = Me[143], *t*Bu[152] and R$^3$ = Et,

*n*Pr, $CH_2CH_2NMe_2$ being known.[74] None of these complexes have been used in anti-cancer studies. The nearest other titanium complexes we could classify (ca. 180 examples) were those showing the motifs (**A**) (**Scheme 36**), which have been prepared typically for studies of alkene polymerisation catalysis.[139] Complexes **48** are chiral (but racemic) and this causes observation of characteristic diastereotopic aryl C-H (four $^4J$ coupled doublets in the range $\delta_H$ 6.61-6.44) and $NCH_2$ (at $\delta_H$ 4.85-3.30 showing $^2J$ ~12.8 Hz or second order behaviour) signals (**Figure 32**). Conveniently, complexes **48** are all highly crystalline so that they can be easily purified for both biological and mechanistic studies.

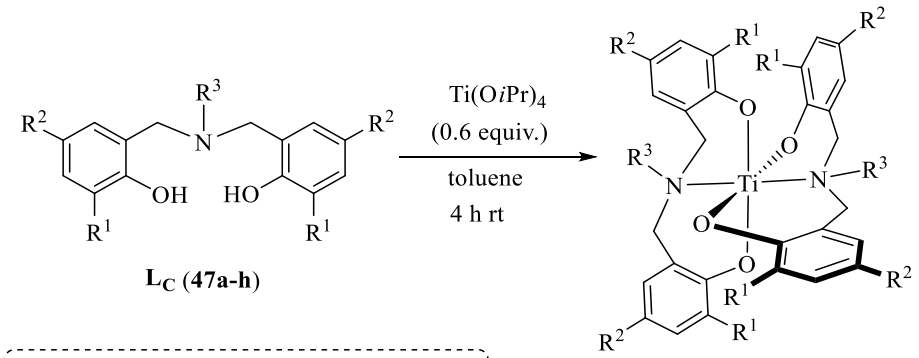


| | $R^1$ | $R^2$ | $R^3$ | Recrystallised yield (%) | Ref |
|---|---|---|---|---|---|
| **48a** | Me | Me | Me | 88 | [143] |
| **48b** | MeO | Me | Me | 88 | |
| **48c** | MeO | Me | Et | 66 | |
| **48d** | Me | MeO | Me | 81 | |
| **48e** | MeO | MeO | Me | 76 | |
| **48f** | Me | F | Me | 83 | |
| **48g** | Cl | Cl | Me | 85 | |
| **48h** | EtO | EtO | Me | 89 | |

**Scheme 36.** Titanium complexes **48** prepared in this study and comparison to the more commonly targeted motifs (**A**).

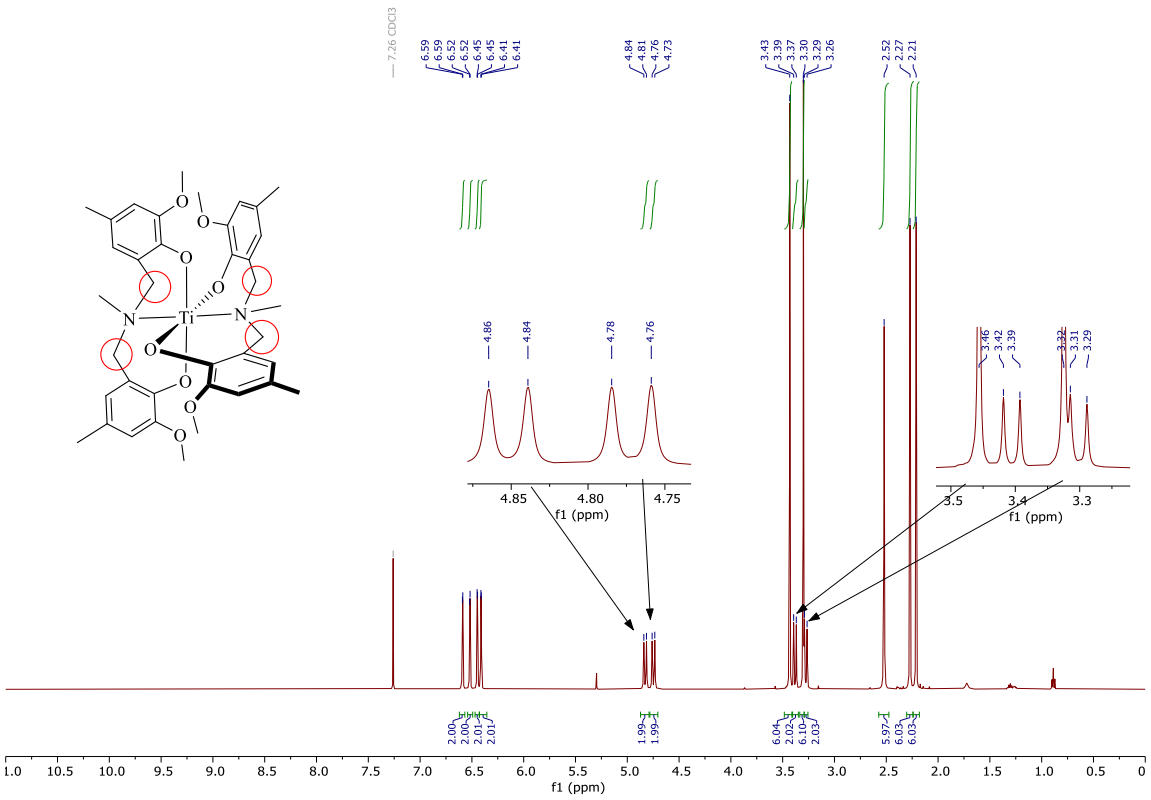


**Figure 32.** Observation of the diastereotopic $CH_2NMeCH_2$ bridge of **48b** as an example.

### 3.2.3. Crystallographic studies

Using a liquid-liquid diffusion technique by dissolving the crude product in dichloromethane and layering pentane, crystalline pure products are isolated. For example see **Figure 33**, **A**. Alternatively, for X-ray examination, single crystals were obtained by liquid-vapour diffusion using same mixture, as shown in **Figure 33**, **B**.

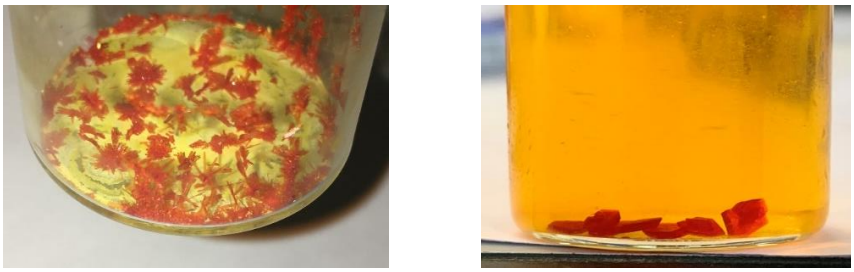

**(A)** **(B)**

**Figure 33.** (**A**) The crystal morphology of **48f**, attained by liquid-liquid diffusion and (**B**) **48f** attained by liquid-vapour diffusion.

The molecular structure of complex **48b** was determined by X-ray studies and is shown in **Figure 34**. The same *trans,mer* geometry has been seen in related crystallographic studies (for more information see the Appendix) of **48d**, **48e**, **48f**, (**Figure 34**) and for the literature structure of **48a**.[143] The ligands in this series **48** contain a common $CH_2NMeCH_2$ arm linker so that electronic effects on bonding to the $TiO_4N_2$ core (see scheme within **Figure 34**) induced by the aryl substituents could be examined. Comparing the angle data and bond distance for these five complexes (**Table 3**) exposes a very similar range of geometries for all these species.

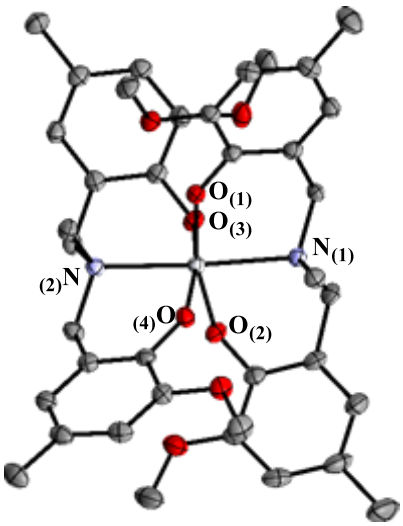


**48b**

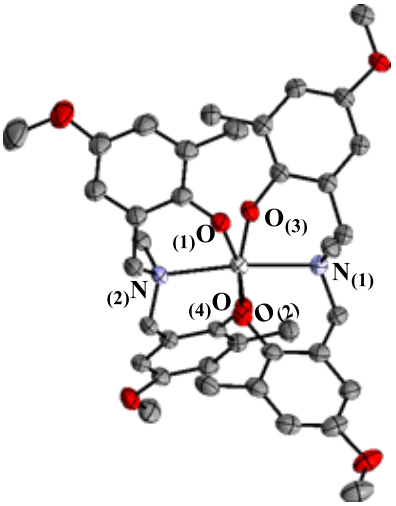


**48d**

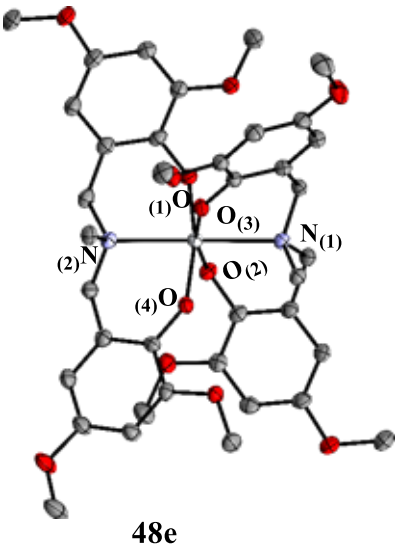


**48e**

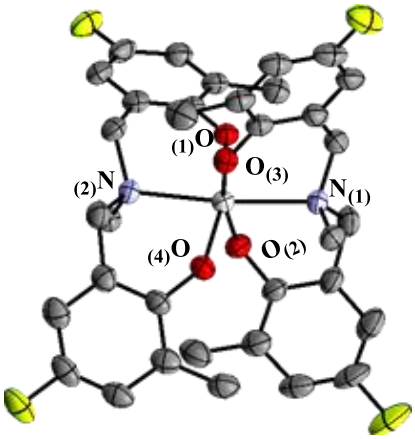


**48f**

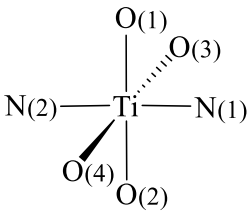


**Figure 34.** Molecular structures of titanium complexes **48b, d-f**; CCDC codes: 1915855, 1915856, 1915857, and 1915858 respectively.

**Table 3.** Selected comparison of angle data and bond distance for titanium complexes **48a-48b** and **48d-f** for their $TiO_4N_2$ cores.[a]

| Complex | **48a**[b] | **48b**[c] | **48d**[c] | **48e** | **48f** |
|---|---|---|---|---|---|
| $R^1$ (*ortho*) | Me | MeO | Me | OMe | Me |
| $R^2$ (*para*) | Me | Me | OMe | OMe | F |
| ***Bond lengths (Å)*** | | | | | |
| Ti(1)-O(1) | 1.892 | 1.909 | 1.881 | 1.921 | 1.880 |
| Ti(1)-O(2) | 1.882 | 1.859 | 1.889 | 1.874 | 1.876 |
| Ti(1)-O(3) | 1.892 | 1.873 | 1.894 | 1.867 | 1.880 |
| Ti(1)-O(4) | 1.882 | 1.900 | 1.878 | 1.887 | 1.876 |
| Ti(1)-$O_{ave}$ | 1.887 | 1.885 | 1.885 | 1.887 | 1.878 |
| Ti(1)-N(1) | 2.264 | 2.244 | 2.244 | 2.272 | 2.247 |
| Ti(1)-N(2) | 2.264 | 2.267 | 2.265 | 2.251 | 2.247 |
| Ti(1)-$N_{ave}$ | 2.264 | 2.255 | 2.256 | 2.262 | 2.247 |
| ***Bond angles (°)*** | | | | | |
| O(1)-Ti(1) O(2) | 168.6 | 167.5 (10) | 167.1 (15) | 165.2 (5) | 167.9 (13) |
| O(3)-Ti(1)-O(4) | 168.6 | 167.6 (10) | 167.9 (14) | 166.4 (6) | 167.9 (14) |
| N(1)-Ti(1)-N(2) | 179.7 | 174.7 (9) | 173.8 (14) | 173.6 (6) | 179.8 (14) |
| O(1)-Ti(1) O(3) | 90.5 | 93.2 (10) | 89.1 (16) | 90.3 (6) | 90.6 (15) |
| O(2)-Ti(1) O(4) | 92.2 | 89.6 (10) | 93.4 (17) | 92.7 (6) | 92.0 (16) |

[a] The $TiO_4N_2$ donor set is numbered in all cases as for **48b** see scheme within Figure 34. [b] (Based on the published structure.[143]) [c] Average of two independent molecules within unit cell.

### 3.2.4. Solution stability studies of 48b-h

Our compounds show interesting results in preliminary hydrolysis investigations. Firstly, all the complexes remain completely intact in the absence of water. Preliminary $^{1}$H NMR studies were carried out using dry samples of **48** prepared as 10 mM DMSO-$d_6$ solutions (simulating the stock solutions used in all biological studies, page 97 onwards). Such solutions were stable in all cases (**48a-h**) for at least five days e.g. complex **48e** in **Figure 35**, **A-B**. These **48** solutions (10 mM in DMSO-$d_6$) were further diluted using $D_2O$ (20:80 DMSO-$d_6$:$D_2O$) to 150 µM, which resulted in slow hydrolysis (3 days) of the complexes **48**. The $^{1}$H NMR spectra typically show that only the free ligands **47** are identified in these e.g. for complex **48e Figure 35 C-D**.[153] Understanding the biological mode of action complexes **48** requires characterisation of the biologically active species formed through hydrolysis. Attempts have been conducted to characterise the active species derived from all the complexes **48**, they all show variable, but low, aqueous solubility. Amongst these compounds **48b** was the most soluble, suggesting there is a positive correlation between the biological activity and the aqueous solubility of the compound (**Table 4**). For **48b** alone, we could confirm by $^{1}$H NMR spectroscopy and HPLC-MS techniques (**Scheme 37**), and possibly $^{1}$H NMR spectroscopy, after 24 h in water an intermediate titanium complex in addition to formation of **47b**. We propose the formation of structure **48ba**, which is supported by the molecular weight studies using HPLC-MS (**Scheme 37**). We further proposed that this is likely to be the true biologically active species, or closely related to it, as it is formed under conditions that closely mimic the *in vitro* biological environments. We cannot clearly see **48ba** in the proton spectrum, but once all **48b** is consumed trace extra signals at ca. 6.37 and 6.39 ppm remain.

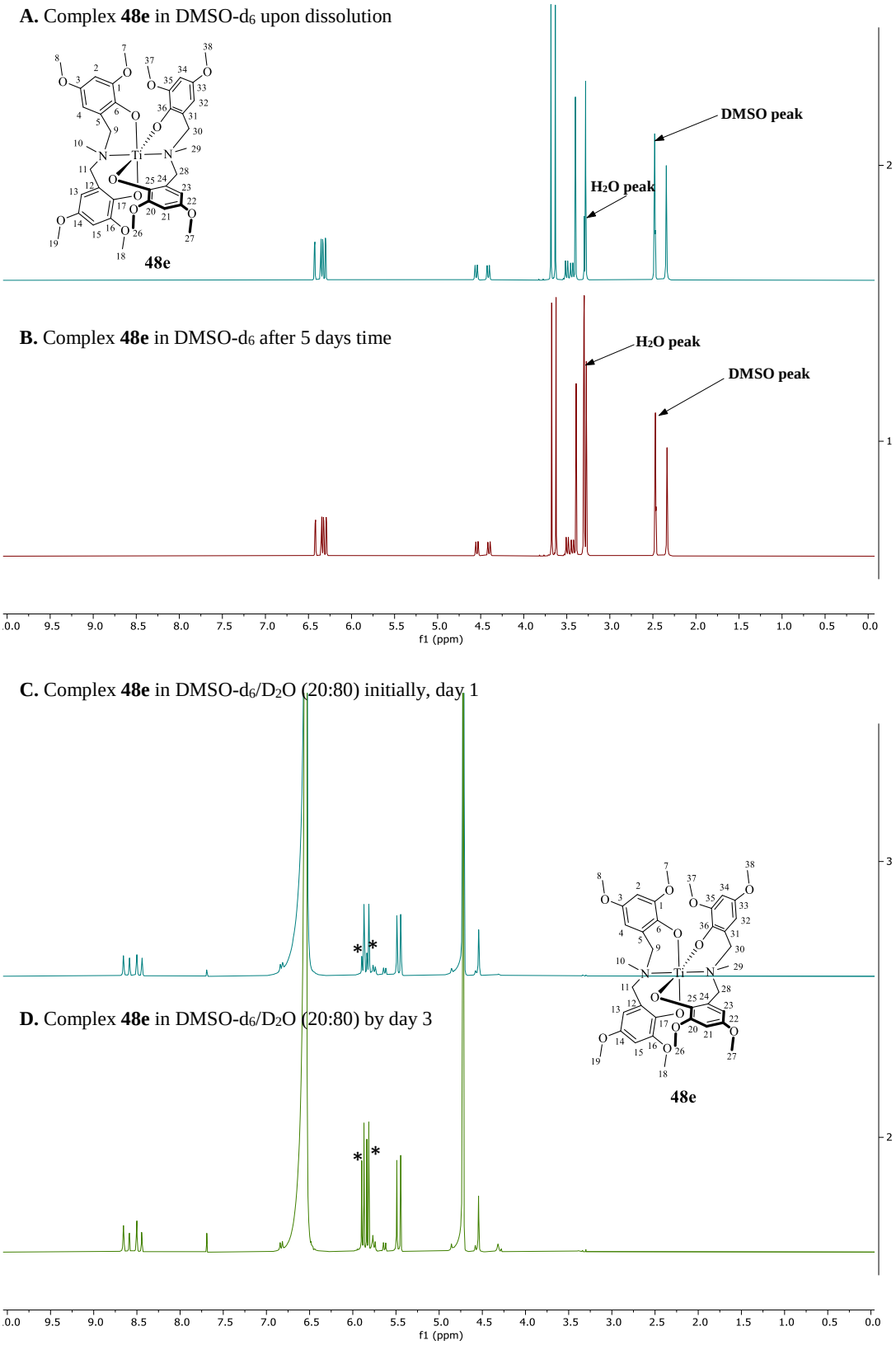


**Figure 35.** **$^1$H NMR** spectra of complex **48e**, initially in DMSO-$d_6$ (**48e** 10 mM) (**A**); after 5 days in DMSO-$d_6$ (**B**); initially in DMSO-$d_6$/$D_2O$ (20:80 with **48e** 150 µM) (**C**); after 3 days, resonances marked (*) indicate non overlapped ligand (**47e**) signals (**D**). No other signals for species other than **47e** and **48e** were detected in these studies.

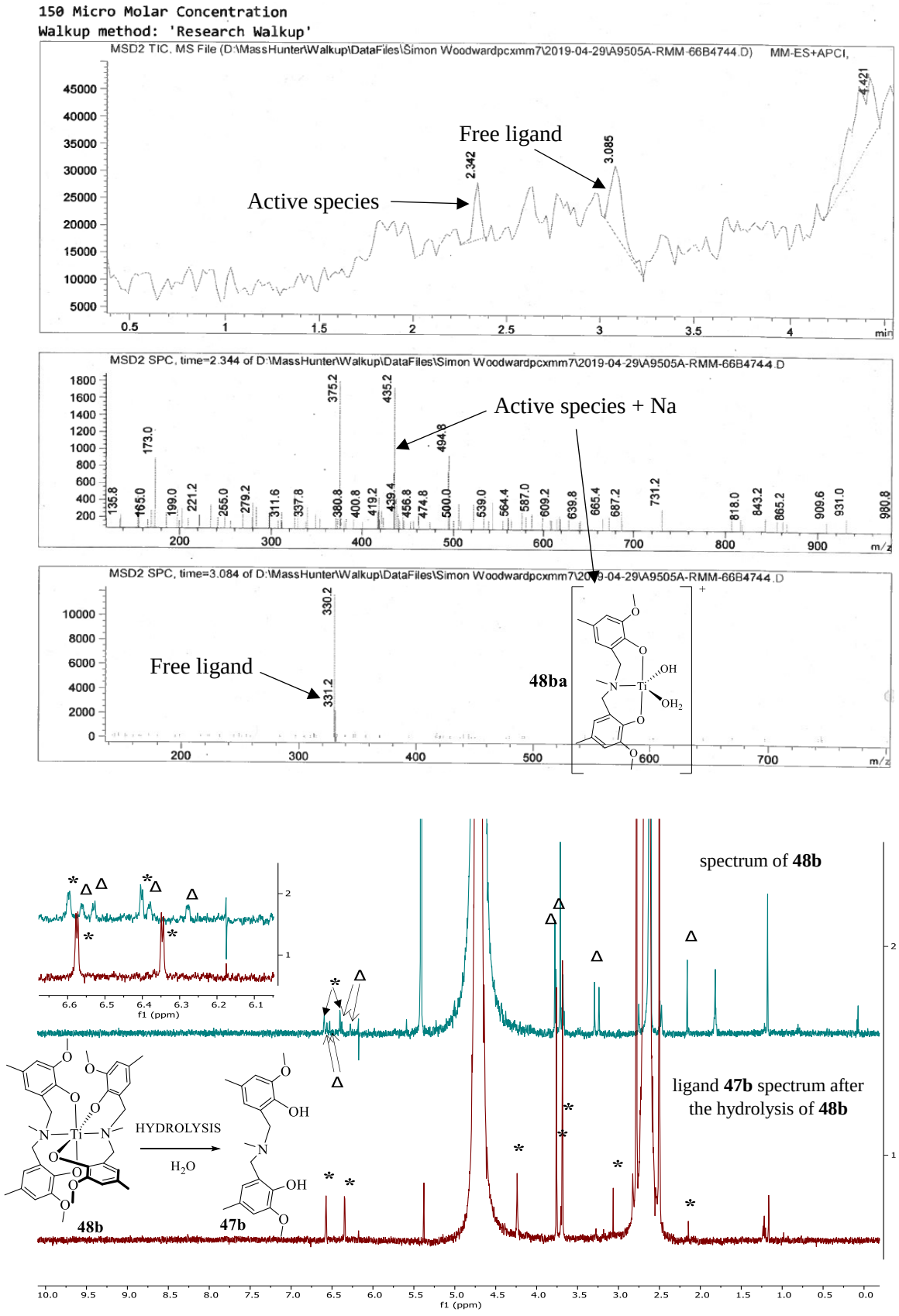


**Scheme 37.** Hydrolysis of the complex **48b** (150 µM) under aqueous conditions provides ligand **47b** by reversed phase and active species by **HPLC-MS**, and the **$^1$H NMR** for the **48b** (Δ) and the ligand **47b** (*) for 24 h.

### 3.2.5. Synthesis and optimisation of 4,4-difluoro-1,3,5,7 tetramethyl-8-(4ethynylphenyl) boradiazaindacene [BODIPY]

Although titanium anti-cancer compounds have been known since 1979, there is still no general agreement regarding the mechanisms of these compounds inside cells. A variety of modes of action have been suggested including: inhibition of mitochondrial activity, the triggering of apoptosis by DNA binding, the inactivation of topoisomerases, cell death by iron deprivation, and induction of paraptosis (by kinase activation).[51] In recent years, a number of newer very promising techniques have been used to investigate proposed mechanisms action, one of which is using trackable metal agents.[154] To date, a few trackable Ti complexes have been prepared, primarily using $^{45}$Ti (3.1 h half-life).[155] Although $^{45}$Ti studies are highly informative, the availability of this isotope is very limited. Martin and his group in 2015 developed some trackable complexes of late transition metals to find their mechanism of action using BODIPY fluorescent probe (**Figure 36**).[156]

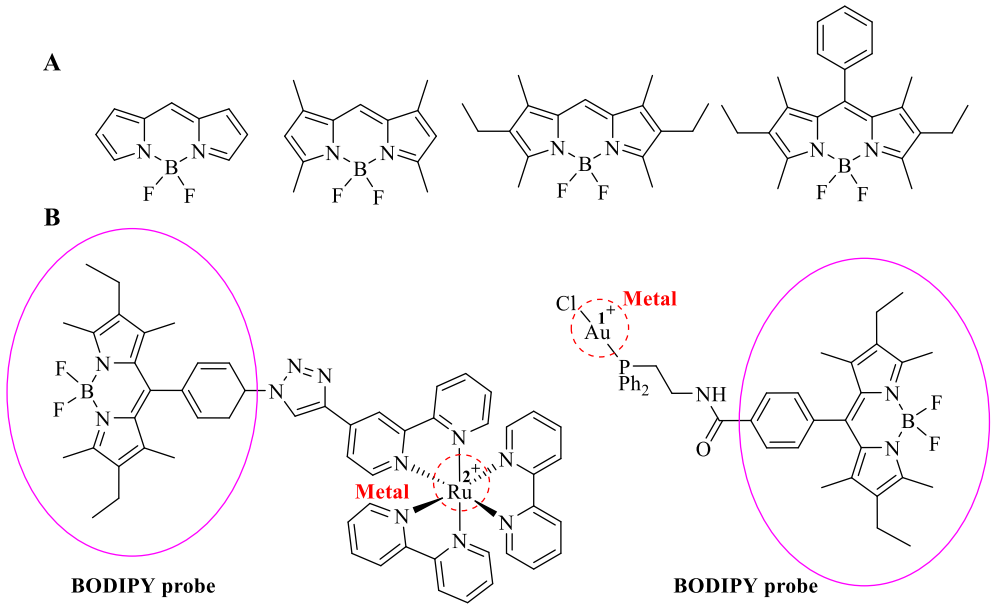


**Figure 36.** Different BODIPY structures (**A**); different metal BODIPY complexes (**B**).[157]

Recently, Florès *et al.* described trackable titanium complexes using the fluorescent probe, BODIPY.[158] Therefore, we decided to design trackable titanium complexes using BODIPY to visualise our compounds and their hydrolysis products inside the cancer cell. The reasons behind using the BODIPY fluorescent probe are that: 1) it has been used as a reliable trackable metal agent e.g. specifically with 'salan' complexes.[155] 2) it has a good lipophilicity, which can enhance the cell uptake.[158] 3) *in vitro* and *in vivo*, BODIPY derivatives are trackable even at low concentrations. Finally, BODIPY can be combined into different alkyl or phenyl groups, which easily and efficiently form range of analogues.

We proposed to make the BODIPY dye required compounds **49** and **50** (**Scheme 38**, **39**). These are available commercially, but they are not cheap: **49** is ~£75 for 5 g and **50** is ~£390 for 5 g. Thus, compound **49** was synthesised following a literature procedure.[159] It was prepared by decarboxylation of diethyl 3,5-dimethyl-*1H*-pyrrole-2,4-dicarboxylate to give the desired compound **49** in 45% yield (**Scheme 38**).

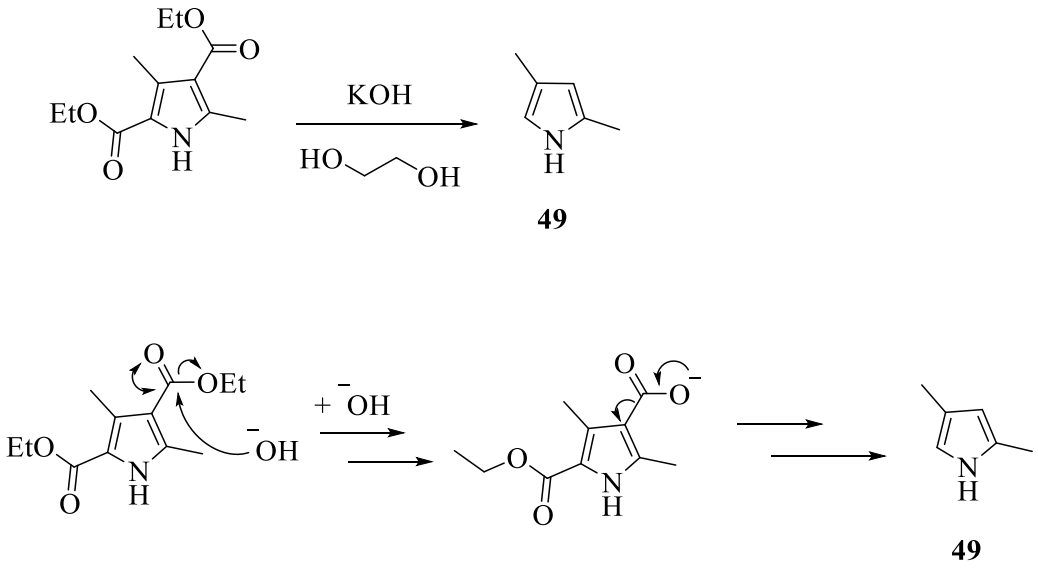


**Scheme 38.** Proposed mechanism preparation of compound **49**.

Compound **50** was prepared by a Sonogashira coupling.[160] This reaction involved the palladium catalyst and copper co-catalyst to make a new C-C bond between aryl halide and the terminal alkyne (**Scheme 39**).

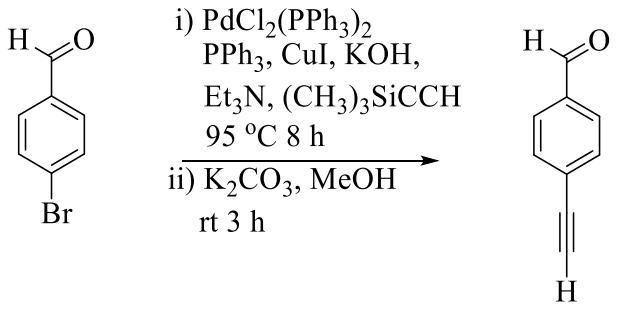


**50**

**Scheme 39.** Sonogashira reaction to form compound **50**.[160]

Finally, compound **51** was synthesised by literature reaction of compounds **49** and **50** in dichloromethane with trifluoroacetic acid (**Scheme 40**).[160-161] The addition of acid is to catalyse condensation of the aldehyde group of the 4-ethynylbenzaldehyde. Thus, the carbonyl group is protonated, which promotes the amine group of the pyrrole to attack the empty $\pi^*$-orbital of carbonyl group. Subsequently, compound **51** is isolated after addition of *p*-chloranil and boron trifluoride diethyl etherate in the presence of base. This reaction gives low ~26% yields, but is comparable to those reported in the literature protocols.[160-161]

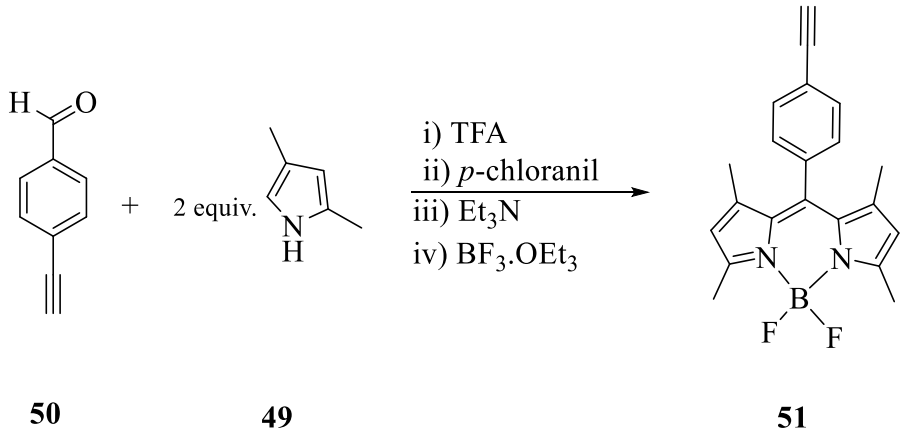


**50** **49** **51**

**Scheme 40.** Literature route to form BODIPY **51**.[160-161]

Although we do not have a convincing explanation for why the yield is low, we found that we could improve the purification in the work up of this compound by simply washing the crude solid with methanol. This enables us to isolate **51** in > 99% purity, which is not mentioned in the literature approaches.[160-161] These used column chromatography to purify compound **51**. In our hands it was not easy to separate the desired layer. Thus, we tracked the required band using a UV light source and the correct layer was then obtained (**Figure 37**).

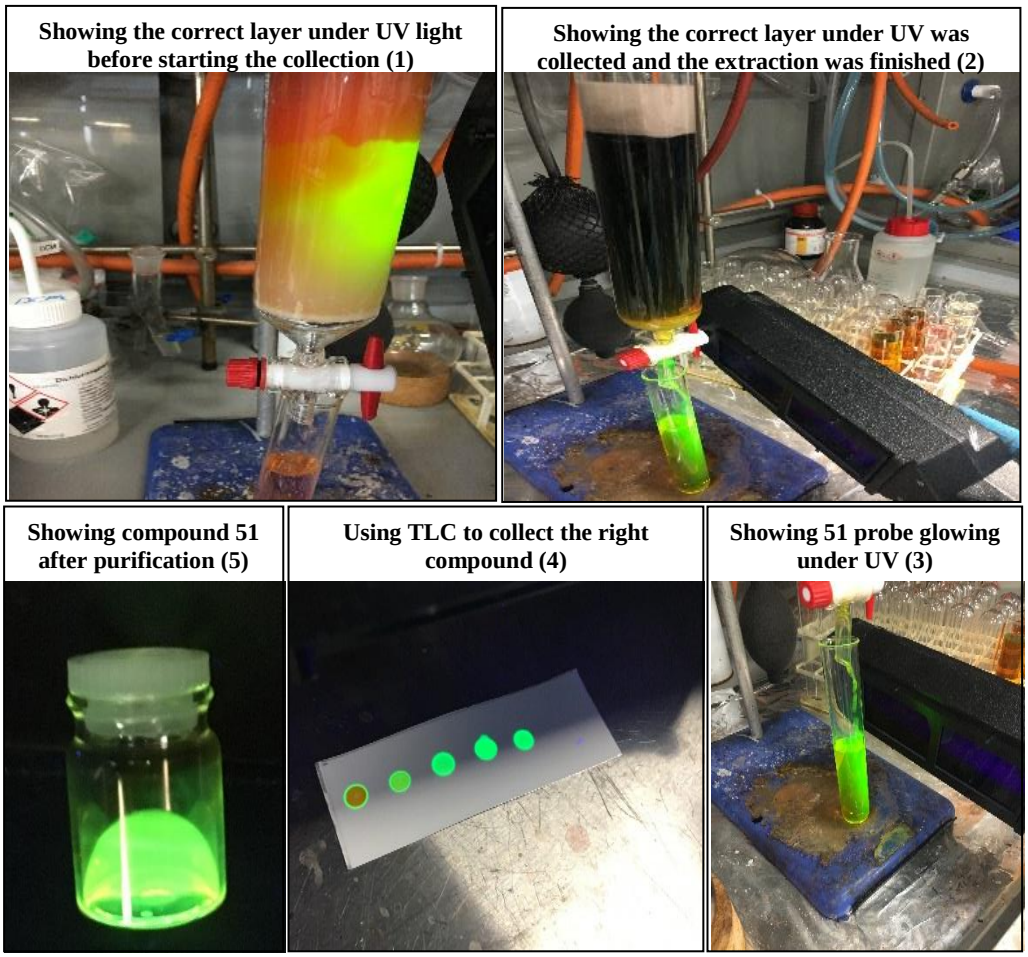


**Figure 37.** Using UV light to detect the right layer of BODIPY dye **51**.

Having made our BODIPY dye (**51**), we then investigated attaching the dye to our compounds. Starting materials (**52-54**) were made by the synthetic method outlined in **Scheme 41**. Compound **52** was synthesised by Mr Mustapha Musa of our group. We then proposed to prepare compound **53** by use of *m*CPBA[162] to convert the allyl group in compound **52** to the epoxide **53** (**Scheme 41**).[163] Subsequently, we planned opening of compound **53** with sodium azide to afford **54**.[164] Coupling of **54** with **51** (BODIPY) by 'click' reaction should afford compound **55**, which upon complexation would give the BODIPY-Ti complex (**56**) (**Scheme 41**).[157, 165] Due to time constraints at the end of this PhD only preliminary investigations in this area were possible.

Although we were able to synthesise compounds **51** and **52** (**Scheme 41**), thus far, we were unsuccessful in isolating **53** and **54** due to the epoxidation reaction not occurring as proposed. Based on $^{1}$H NMR data we believe, it is probably the lone pair of nitrogen of **52** that is attacked rather than the allyl group during the attempted epoxidation. However, colleagues in our group are still attempting to isolate this class of compound by alternative approaches that can access compound **54** and favour attachment of the fluorescent compound (see Future Work). Attaining compound **53** and **54** would require two more steps to make the desired compound **56** (**Scheme 41**). Even allowing for ligand dissociation, as proposed earlier in **Scheme 37** one fluorescent ligand would be bound to the [**L**$_{C}$Ti (OH)(OH$_2$)]$^+$ complex in the active species (*i.e.* compound **48ba** in **Scheme 37**). If this active species binds to specific target e.g. a protein, this would help us to tag the protein and isolate it by tracking it using the BODIPY probe visible under UV or confocal assay.

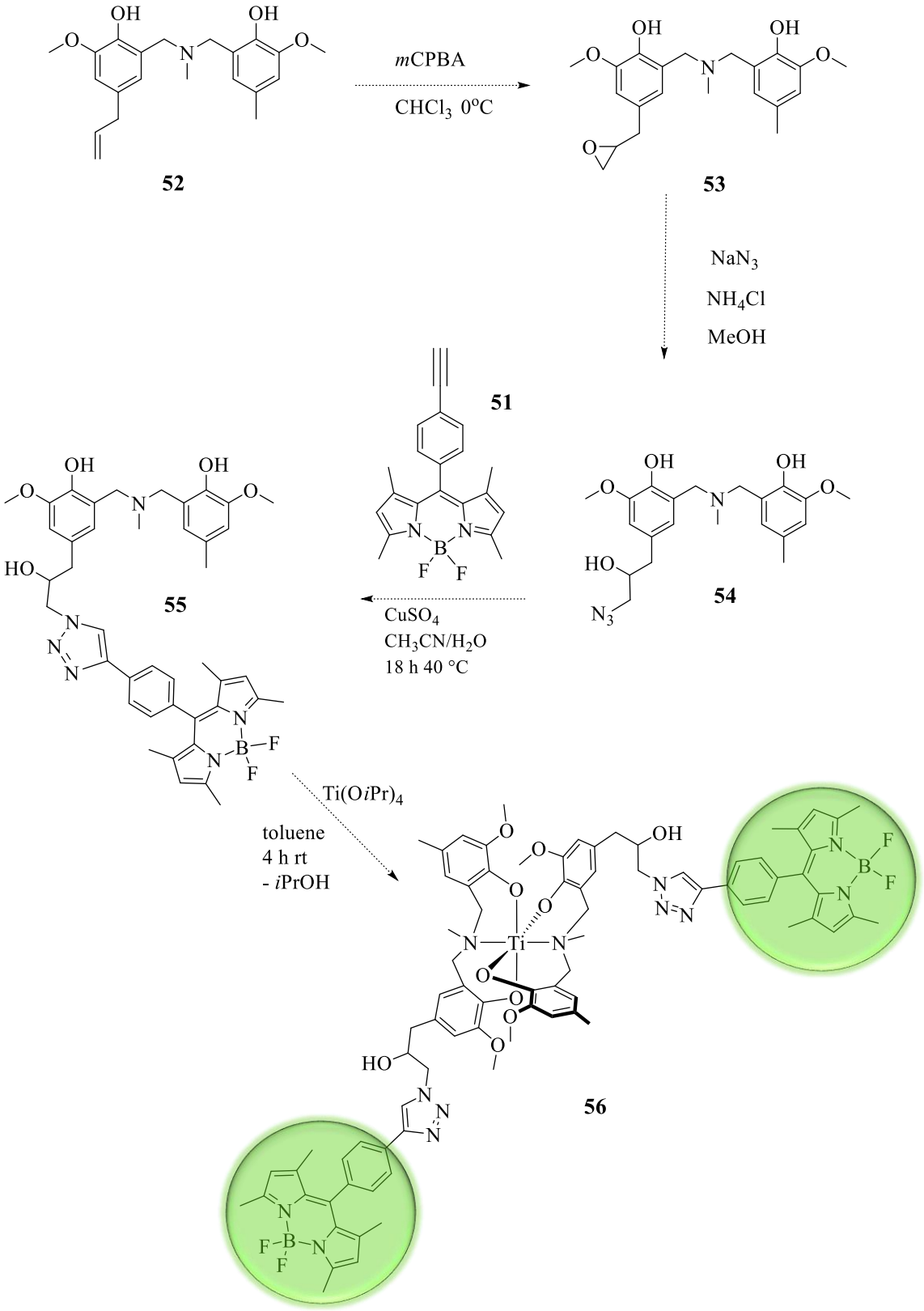


**Scheme 41.** Proposed route to form a **BODIPY**-tagged titanium compound.

## 3.3. Titanium(IV) complexes in biological studies

In the last ten years, Ti(IV) complexes have re-emerged as a 'hot' area in bio-inorganic chemistry.[166] This is due, in part, to their potential lower toxicity towards normal tissues and an ability to tune cellular action through suitable ligand modification. To advance the Ti(IV) complexes that are active into the clinic requires two key requirements to be met. The first key point is a need for selective cytotoxicity to be attained for the chosen compound, and the second (and the most important key point), is that its pharmacokinetic behaviour must be well defined (*i.e.* its mode of action must be understood). Studies with 3-[4,5-dimethylthiazol-2-yl]-2,5 diphenyl tetrazolium bromide (MTT) and clonogenic assays are initial starting points towards these goals. Therefore, MTT and clonogenic assays were utilised to understand the activity of complexes **48**. In addition, to help characterise the activity of **48**, cell cycle, annexin-V/PI, γ-H2AX, and caspase assays were also set up to provide initial indications of these compounds' biological mode of action.

### 3.3.1. Growth inhibitory activity of 48a-h against MCF-7 and HCT-116 (MTT assay)

Use of 3-[4,5-dimethylthiazol-2-yl]-2,5 diphenyl tetrazolium bromide (MTT) allows quantitative, economical, reproducible and rapid colorimetric assay of cell metabolic activity. This means that it can be used to measure growth inhibitory or the cytotoxic activity of the test agents when cell proliferation is suppressed.[167] It was established by Mosmann in 1983[168] that MTT assays work by conversion of tetrazolium MTT into formazan crystals by viable cells.[169] *In vitro* anti-tumour activity of all compounds (**48**) (**Figure 38**) was assessed using the MTT assay against two human-derived cancer cell lines: MCF-7 (breast) (Michigan Cancer Foundation-7) and HCT-116 (colon) (Human Colon), with cisplatin as a positive control for all tests. Compound **48a** previously has been reported in the literature,[143] but its anti-cancer properties were not determined in those studies. Trials of **48a** revealed low activity ($GI_{50}$ values 35-40 μM) against both of these cell lines. Exchange of a single methyl for methoxy group in complex **48b** resulted in >10-fold increase in anti-cancer activity. The $GI_{50}$ values of **48b** were ~1±0.04 μM for MCF-7 and ~3.4±0.07 μM for HCT-116 (**Table 4**). The growth inhibitory activities of **48a** and **48b** are compared in (**Figure 39**, **A**-**B**).

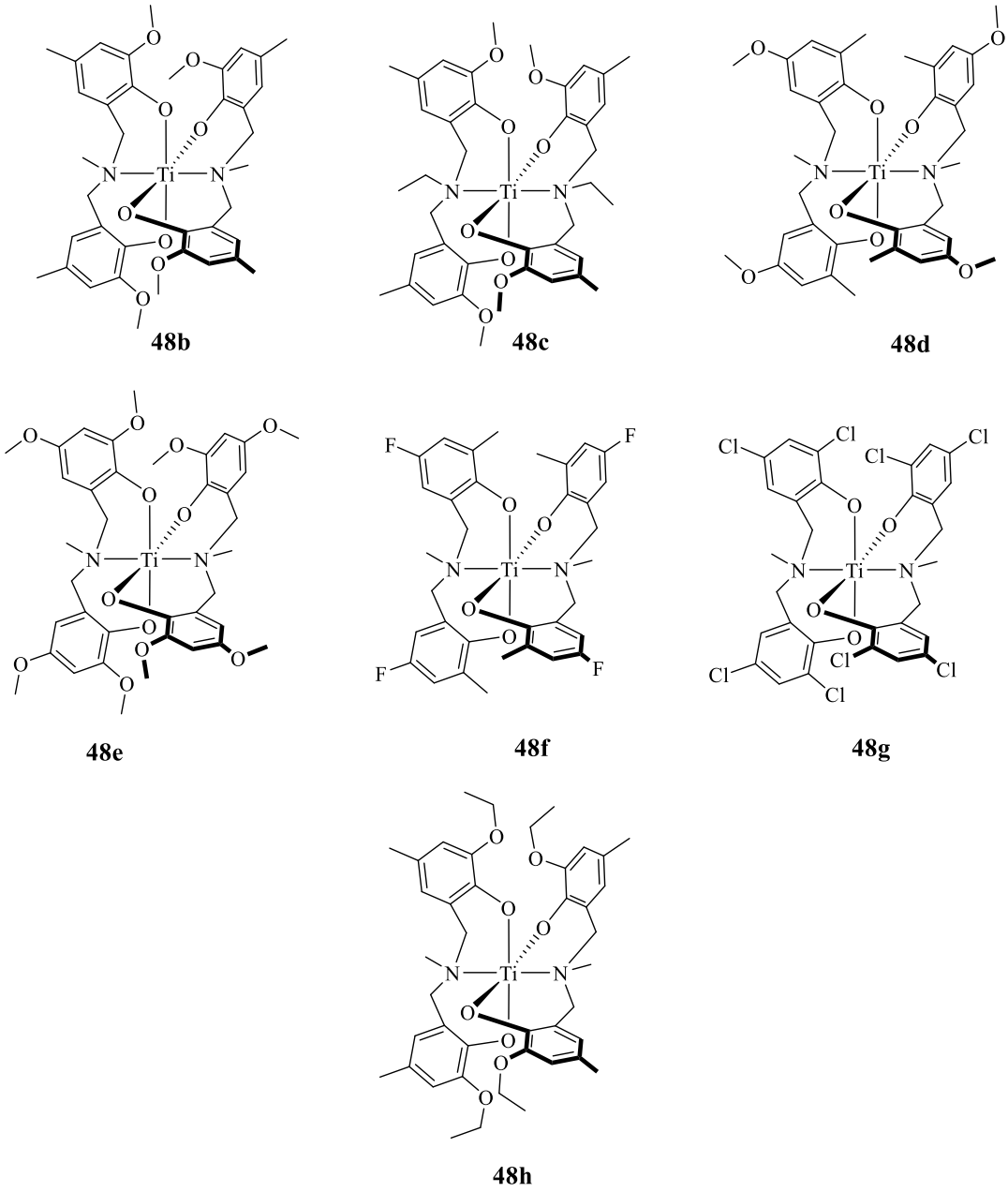


**Figure 38.** Structures of complexes **48b-h**.

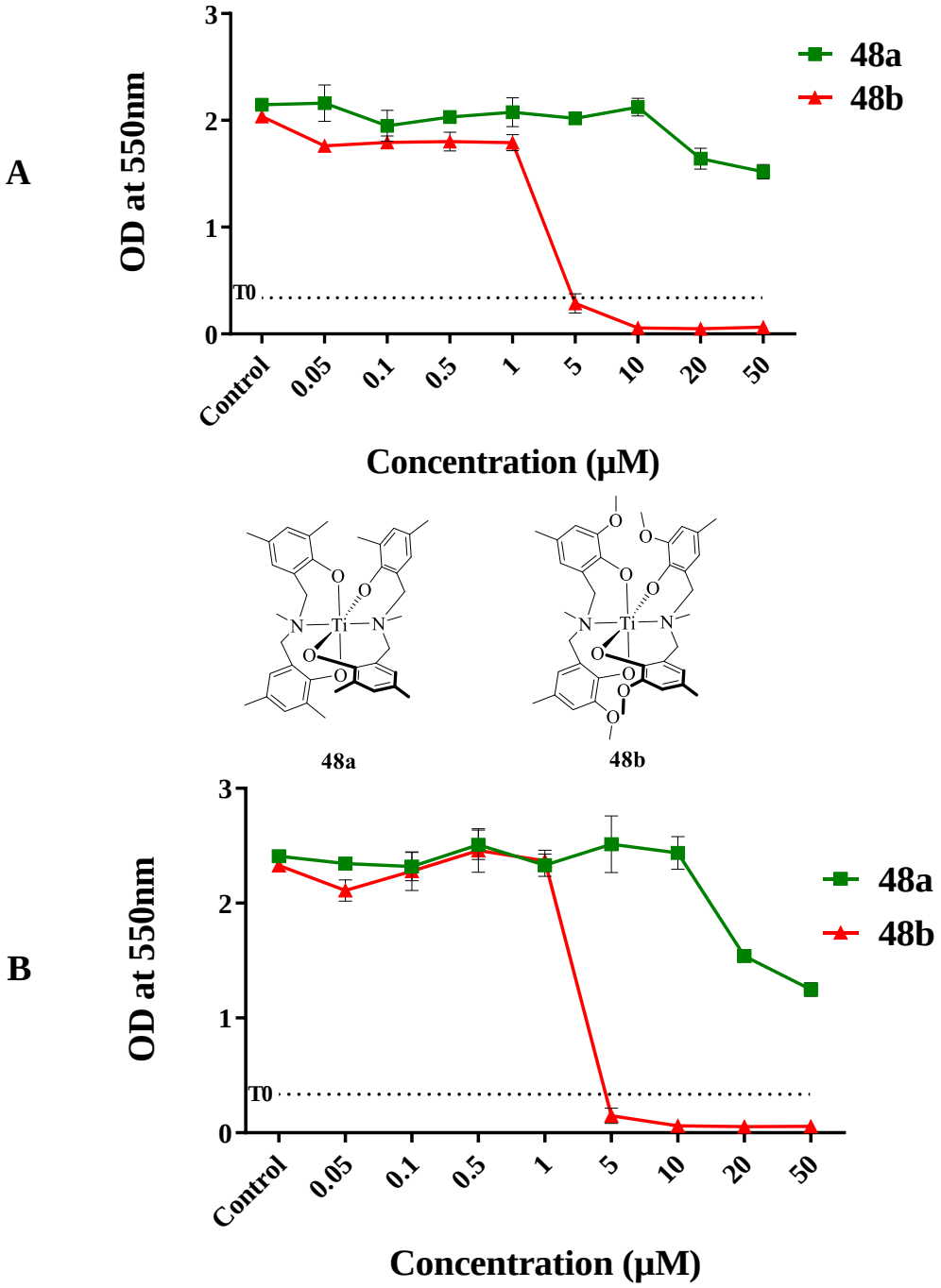


**Figure 39.** Representative MTT graphs displaying the dose-dependent growth inhibitory properties of **48a-b** against MCF-7 (**A**) and HCT-116 (**B**) cell lines. Cells were seeded in 96-well plates at a density of 3 x $10^3$ cells/well. After allowing 24 h for adherence, cells were treated with the specified compound and incubated for 72 h. Data points depict mean ±S.D. n = 8; MTT assays were repeated >3 times.

The MTT derived $GI_{50}$ values of the electronically diverse complexes **48b-f** are shown in **Figure 38**. Complex **48b** was confirmed as the most active with $GI_{50}$ values of ~1±0.04 μM for MCF-7 and ~3.4±0.07 μM for HCT-116 (**Table 4**). Other compounds in the series showed moderate to good activity in anti-cancer performance (**Figure 40** and **Table 4**). Structural modification was made to the compound **48b** at the nitrogen donor (e.g. $R^3$), and preliminary studies indicated that changing the methyl group at $R^3$ within **48b** to the ethyl derivative **48c** negatively affected the compound class, reducing potency. The activity of **48c** is similar to cisplatin, whose control $GI_{50}$ values in our studies were 6.6±0.07 μM for MCF-7 and 9.2±0.09 μM for HCT-116 (**Figure 40**, **A-B**). We suspect **48c** of being less soluble in aqueous media, leading to reduced activity. Our results show that Ti(IV) complexes **48b-f** are among the most active thus far reported in the literature (e.g. compared to other active salan complexes[37, 47, 51, 85, 170]) and that this activity is strongly dependent on the ligand structure. While **48b** is the most potent compound, **48d** showed good activity with $GI_{50}$ values of 2.2±0.06 μM and 3±0.05 μM against MCF-7 and HCT-116 cell lines respectively (**Figure 40**, **A-B** and **Table 4**). Complex **48e** showed lower potency than **48b** and **48d** against the same cell lines ($GI_{50}$ values ~8.5±0.1 μM against both MCF-7 and HCT-116 cells; **Figure 40**, **A-B** and **Table 4**). Complex **48f** revealed reduced activity with $GI_{50}$ values of 11.7±0.05 μM for MCF-7 and 22±0.031 μM for HCT-116 (**Figure 40**, **A-B** and **Table 4**).

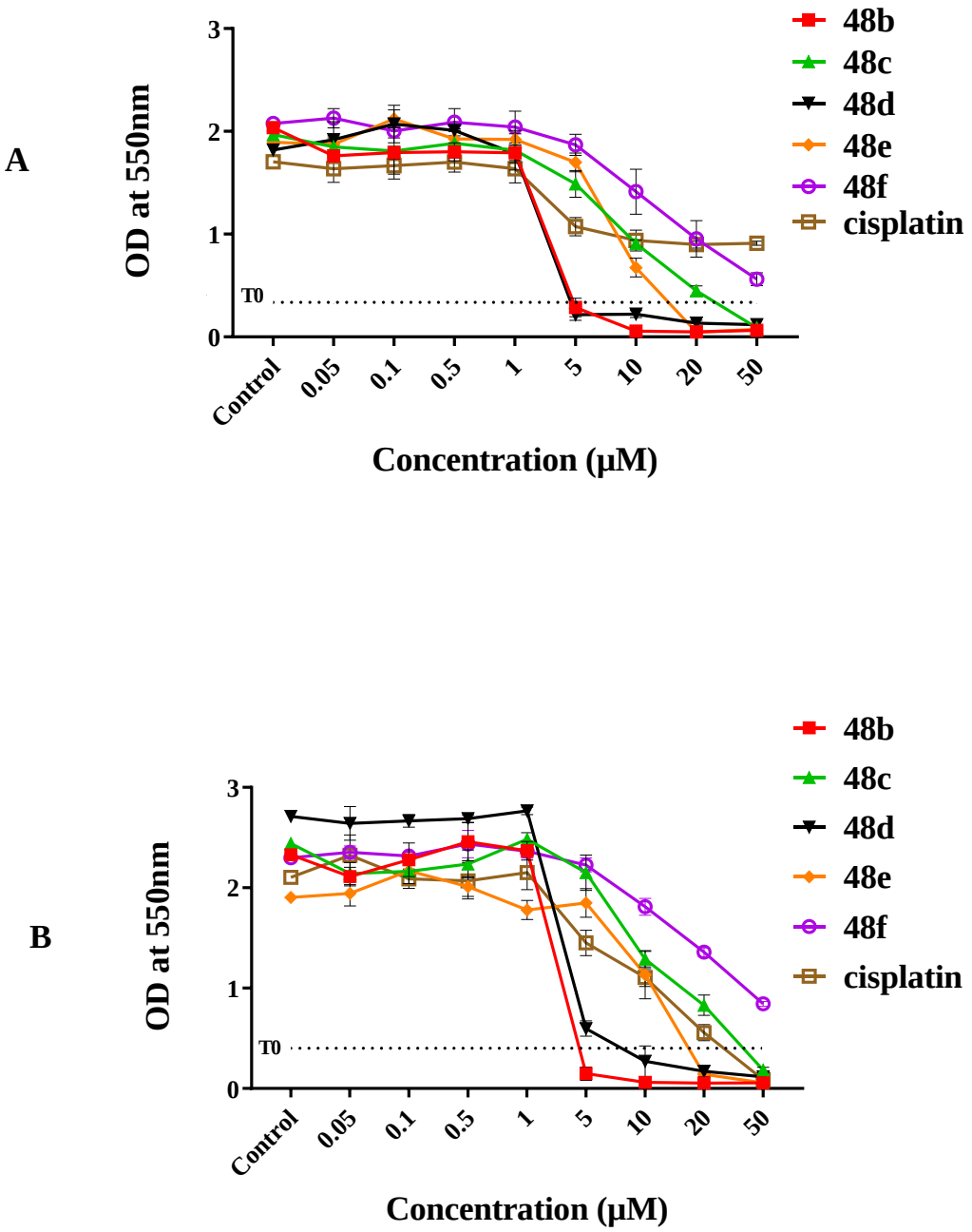


**Figure 40.** Representative MTT graphs displaying the dose-dependent growth inhibitory properties of **48b-f** against MCF-7 (**A**) and HCT-116 (**B**) cell lines. Cells were seeded in 96-well plates at a density of 3 x $10^3$ cells/well. After allowing 24 h to adhere, cells were treated with the specified compound and incubated for 72 h. Data points depict mean ±S.D. n = 8; MTT assays were repeated >3 times.

Compound **48g** showed the poorest activity (highest $GI_{50}$ value) among the complexes **48** screened and was comparable in activity to **48a**. The **48g** $GI_{50}$ values attained were: 51.5±0.1 µM for MCF-7 and 64.8±0.07 µM for HCT-116 (**Figure 41**) *i.e.* a 50-60 fold decrease in activity in comparison with **48b**.

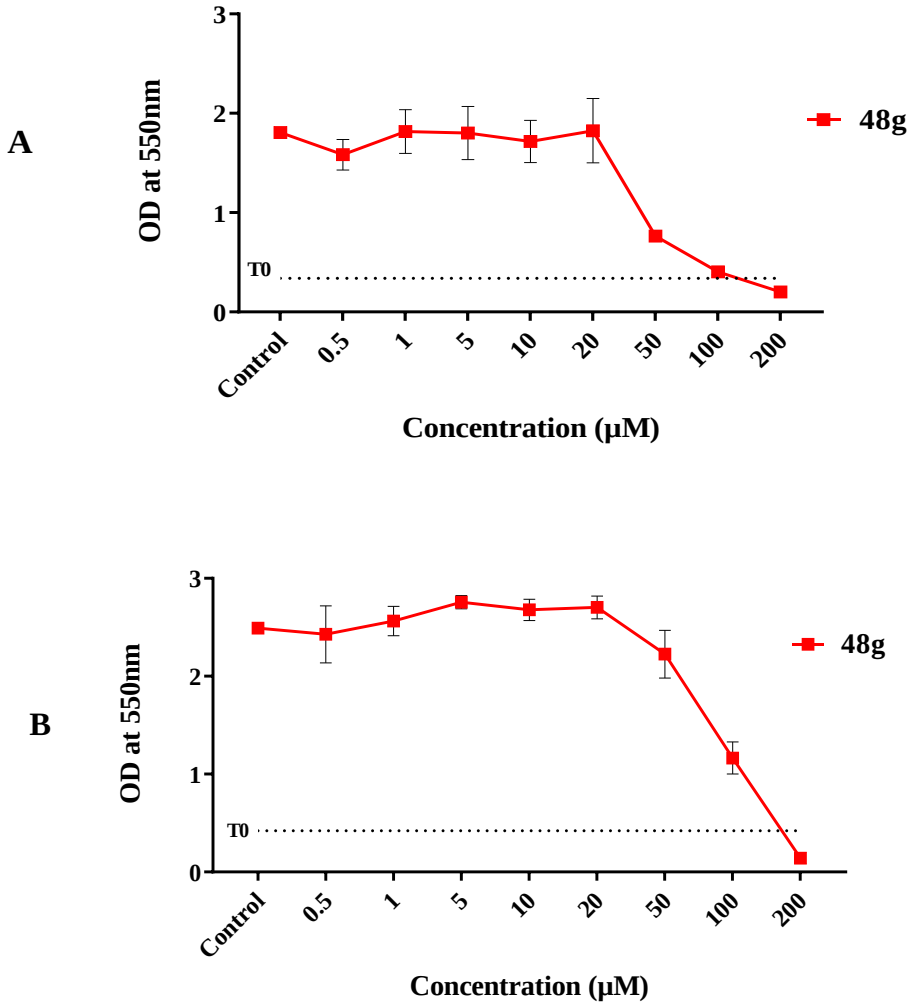


**Figure 41.** Representative MTT graphs displaying the dose-dependent growth inhibitory properties of **48g** against MCF-7 (**A**) and HCT-116 **(B**) cell lines. Both cell lines were seeded in 96-well plates at a density of 3 x $10^3$ cells/well. After allowing 24 h for adherence, cells were treated with **48g** and incubated for 72 h. Data points depict mean ± S.D. n = 8; MTT assays were repeated >3 times.

Clearly changing the *ortho* and *para* substituents of **48b** plays a key role in decreasing or increasing the compound's potency. Changing the methoxy group within **48b** to ethoxy **48h** affected the activity negatively, with the activity of complex **48h** (as assessed by MTT) being between 24-34 fold lower in comparison with **48b** against both cell lines. Compound **48h** revealed only moderate activity showing $GI_{50}$ values of 24.2±0.2 μM for MCF-7 and 33.6±0.02 μM for HCT-116 (**Table 4**).

The *in vitro* growth inhibitory activity of complexes **48a-h** are summarised in **Table 4**. An interesting correlation is seen between the cellular activity vs. the electronic properties of the phenolic substituents. Modest donation ($R^1$, $R^2$ = Me, MeO) into the phenolate results in increased potency, but if this is either further increased (**48e**) or decreased (**48a**, **48f**, **48g**, **48h**) the biological activity falls. Bulky substitution of $R^3$ (**48b** vs. **48c**) also had a negative effect on biological performance.

**Table 4.** Activity of complexes **48** ($GI_{50}$ values in μM by MTT assay) against MCF-7 and HCT-116 cancer cell lines and normal MRC-5 fibroblast cells. Data were generated from ≥3 independent trials; n = 8 per experimental condition per trial.

| **48** | **$R^1$** | **$R^2$** | **$R^3$** | **$\sigma_p(R^1)$[a]** | **$\sigma_p(R^2)$[a]** | **$GI_{50}$ (MCF-7) (μM)[b]** | **$GI_{50}$ (HCT-116) (μM)[b]** | **$GI_{50}$ (MRC-5) (μM)[b]** |
|---|---|---|---|---|---|---|---|---|
| **48a** | Me | Me | Me | -0.17 | -0.17 | 36.3±0.1 | 38.6±0.1 | >50 |
| **48b** | MeO | Me | Me | -0.27 | -0.17 | 1.0±0.04 | 3.4±0.07 | 7.33±0.04 |
| **48c** | MeO | Me | Et | -0.27 | -0.17 | 6.6±0.07 | 9.2±0.09 | 15.23±0.01 |
| **48d** | Me | MeO | Me | -0.17 | -0.27 | 2.2±0.06 | 3.0±0.05 | 8.38±0.04 |
| **48e** | MeO | MeO | Me | -0.27 | -0.27 | 8.4±0.1 | 8.6±0.15 | 16.0±0.1 |
| **48f** | Me | F | Me | -0.17 | +0.06 | 11.7±0.05 | 22±0.031 | 34±0.03 |
| **48g** | Cl | Cl | Me | +0.23 | +0.23 | 51.5±0.1 | 64.8±0.07 | >100 |
| **48h** | EtO | Me | Me | -0.27 | +0.06 | 24.2±0.2 | 33.6±0.02 | - |
| **Cis-Pt[c]** | - | - | - | - | - | 7.8±0.04 | 8.4±0.06 | 7.6±0.09 |

[a] Hammett parameter value for *para* substituent.[171] [b] As determined by MTT assay (3 replicates). [c] Cisplatin.

As a control we checked that the activity of our complexes came from the complex **48** itself, rather than just ligand **47**. The MTT data for all ligands **47** show that there was no activity for the ligands alone. For example, there was no activity for **47b** recorded against either HCT-116 or MCF-7 cell lines as shown in **Figure 42**.

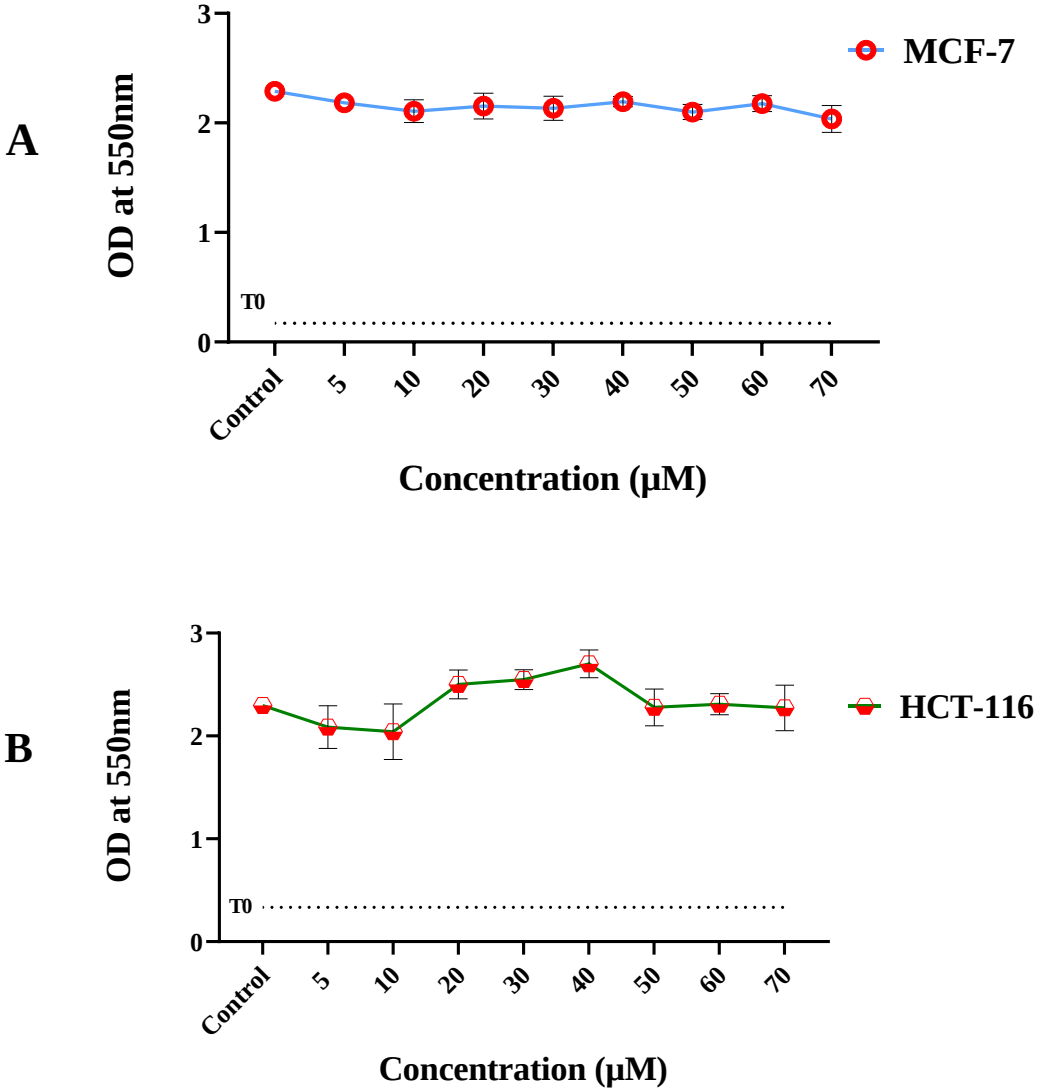


**Figure 42.** Representative MTT graphs displaying the dose-dependent growth inhibitory properties of **47b** against MCF-7 (**A**) and HCT-116 (**B**) cell lines. The both cell lines were seeded in 96-well plates at a density of 3 x $10^3$ cells/well. After allowing 24 h for adherence, cells were treated with **47b** and incubated for 72 h. Data points depict mean ± S.D. n = 8; MTT assays were repeated >3 times.

### 3.3.2. Cancer selectivity of complexes 48

Screening of complexes **48b-g** to evaluate their cellular selectivity was conducted using the MRC-5 (non-transformed foetal lung) cell line. This was to compare the cytotoxicity of **48** towards normal cell lines (e.g. MRC-5) in comparison to cancerous cell lines. The selectivity of **48b** to cancerous cells was evaluated by measuring its growth inhibitory activity ($GI_{50}$ values) in non-cancerous MRC-5 human lung fibroblast cells (**Figure 43**, **A**). Complex **48b** showed reduced activity toward these cells with a $GI_{50}$ value for **48b** in MRC-5 cells of 7.3±0.04 μM (**Table 5**), compared to 1.0±0.04 μM in the breast cancer MCF-7, indicating ~7-fold increase in activity towards the cancer cells.[137] The activities of all Ti(IV) complexes **48** were similarly evaluated against MRC-5, and consistently, reduced activities were observed against these non-tumourigenic fibroblasts. The $GI_{50}$ values for **48d**, **48e** and **48f** were 8.3±0.04 μM, 16±0.1 μM, and 34±0.03 μM respectively. These show 3.8, 1.9, and 2.9 fold selectivity against the MCF-7 based on comparison of the $GI_{50}$ values.[172] This behaviour for **48** was in complete contrast to cisplatin, which was equi-active across all three cell lines (cancerous MCF-7 and HCT-116 and benign MRC-5 fibroblasts) (**Table 5** and **Figure 43**, **B**). Based on these assays we propose the novel Ti(IV) complexes **48**, especially **48b** and **48d** demonstrate significant toxicity to cancer cells over a representative normal cell type.

**Table 5.** Shows the selectivity index for compounds **48b-f**.

| 48 | $R^1$ | $R^2$ | $R^3$ | $GI_{50}$ (MCF-7) (μM) | $GI_{50}$ (HCT-116) (μM) | $GI_{50}$ (MRC-5) (μM) | Selectivity Index for MCF-7 | Selectivity Index for HCT-116 |
|---|---|---|---|---|---|---|---|---|
| **48a** | Me | Me | Me | 36.3±0.1 | 38.6±0.1 | >50 | - | - |
| **48b** | MeO | Me | Me | 1.0±0.04 | 3.4±0.07 | 7.33±0.04 | 7.33 | 2.15 |
| **48c** | MeO | Me | Et | 6.6±0.07 | 9.2±0.09 | 15.23±0.01 | 2.3 | 1.65 |
| **48d** | Me | MeO | Me | 2.2±0.06 | 3.0±0.05 | 8.38±0.04 | 3.81 | 2.8 |
| **48e** | MeO | MeO | Me | 8.4±0.1 | 8.6±0.15 | 16.0±0.1 | 1.9 | 1.9 |
| **48f** | Me | F | Me | 11.7±0.05 | 22±0.031 | 34±0.03 | 2.9 | 1.54 |
| **48g** | Cl | Cl | Me | 51.5±0.1 | 64.8±0.07 | >100 | - | - |
| **48h** | EtO | Me | Me | 24.2±0.2 | 33.6±0.02 | - | | |
| ***Cis*-Pt** | - | - | - | 7.8±0.04 | 8.4±0.06 | 7.6±0.09 | 0.9 | 0.9 |

Investigations of the anti-cancer activity of **48b** were expanded to include the extended spectrum of cancer cell lines: MDA-MB-468, Panc1, and HT-29. The *MTT* (*only*) for these three cancer cell lines were conducted by a master's student (Jason Cheong) under my direct supervision. Cheong used only **48b** and attained identical $GI_{50}$ values to myself. These trials of **48b** revealed remarkable activity against MDA-MB-468 (triple negative breast cancer), Panc1 (pancreatic adenocarcinoma), and HT-29 (colorectal carcinoma) cell lines. The $GI_{50}$ values in these three cell lines were 3.1±1.9, 3.0±0.3, and 3.8±1.5 μM respectively (see **Figure S2**, **A** in Appendix). The data indicated that the activity of **48b** was comparable or superior to compounds described in recent related titanium literature.[61, 81, 173] In complete contrast cisplatin showed only moderate activity ($GI_{50}$ 8.1±1.6, 31.8±0.9, and 8±2.1 μM respectively) across all three of the extended scope cell lines (see **Figure S2**, **B** in Appendix).

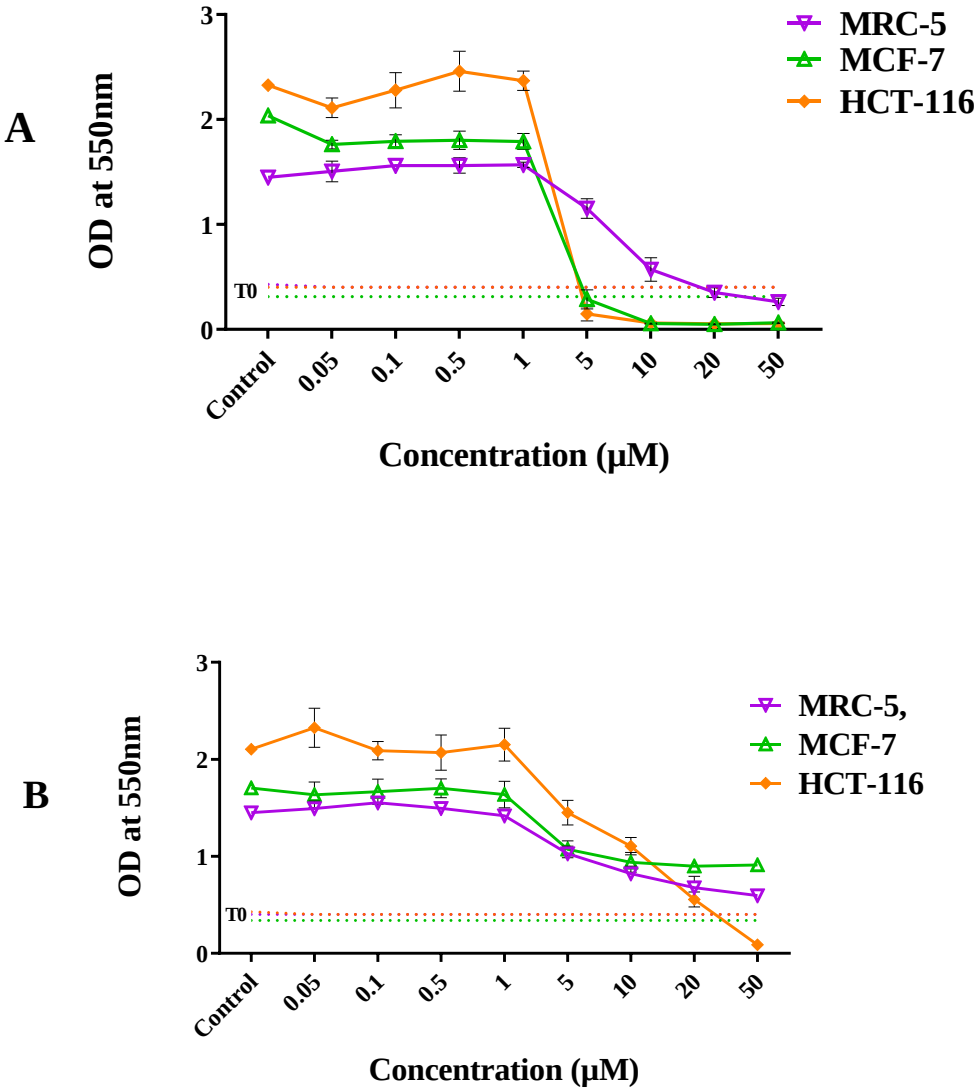


**Figure 43.** Representative dose-dependent growth inhibitory properties of **48b** (**A**) and cisplatin (**B**) against MRC-5 fibroblast, MCF-7 and HCT-116 carcinoma cell lines. Data points depict mean ± S.D. n = 8; ≥3 independent trials were conducted.

### 3.3.3. Effect of 48b and 48d-f on MCF-7 and HCT-116 colony formation

Clonogenic assays are a recognised technique to determine the cytotoxic potential of an anti-cancer agent.[174] They test the ability of cancer cells to survive and recover from a brief exposure to the test agent and subsequently form colonies containing at least 50 cells.[174] There are some differences between MTT and clonogenic assays. MTT assays are typically used to measure effects on cell proliferation, which allows

rapid investigation of agent's cytotoxicity or growth inhibitory activity against different cell lines.[167] By contrast, clonogenic assays are used to measure the ability of a single cell to survive in the presence of test compound and retain proliferative capacity to form colonies.[175] Clonogenic assays can only be used to test cell lines that are able to form colonies.[167] Having established that Ti(IV) analogues **48** cause significant selective growth inhibitory activity in two cancer cell lines, we sought to evaluate whether MCF-7 and HCT-116 cells could survive a short period (24 h) of exposure to 1 µM or 5 µM of Ti-complexes **48** and retain their proliferative capacity. These values were selected as the span the $GI_{50}$ values determined in the MTT studies. To this end, clonogenic assays were set up. The results are typically reported as a survival fraction (%) (SF) and the plating efficiency (PE) which were calculated as below:[176]

PE = (Number of colonies counted / Number of cells plated) × 100%

SF = (PE of treated sample / PE of control) × 100%

Both **48b** and **48d** significantly inhibited colony formation after 24 h treatment of cells at concentrations of 1 and 5 µM (**Figure 44**, **A-B**). Complexes **48b** and **48d** were used to test MCF-7 colony formation cell leading to 40% and 45% (at 1 µM), and 100% (at 5 µM) respectively. This is despite the fact that both MCF-7 and HCT-116 show variable sensitivities to **48b** and **48d** based on MTT assay (e.g. **48b** showed $GI_{50}$ values of 1.0±0.04 µM towards MCF-7 and 3.4±0.07 µM towards HCT-116). Both **48b** and **48d** showed similar inhibition of HCT-116 colony to the MCF-7 colony, 51% (at 1 µM), and 100% (at 5 µM) for both these compounds respectively (**Figure 44**, **A-B**).

Complexes **48e** and **48f** also inhibited colony formation in MCF-7 cells by 25% and 29% (at 1µM), and 57% and 48% (at 5 µM) respectively. The same agents inhibited HCT-116 colony formation by 16% and 22% (at 1 µM) and 49% and 28% (at 5 µM) (**Figure 44**, **A**-**B**).

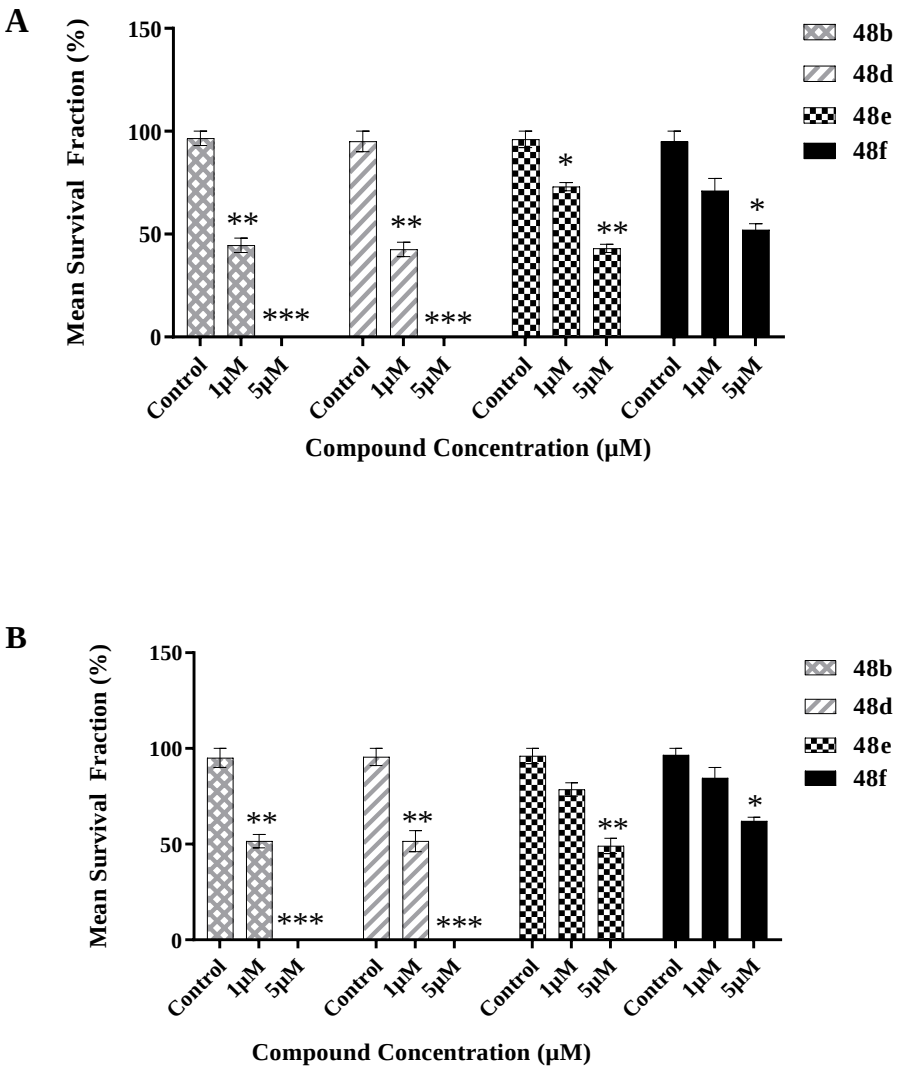


**Figure 44.** Effect of **48b**, **48d**, **48e**, and **48f** on **A**) MCF-7, **B**) HCT-116 colony formation. Graphs **A** and **B** both show the mean survival fraction of % control represented of mean ±S.D. of 5 independent trials (n = 2 per trial). Complexes **48b** and **48d** exhibited significant reduction in colony formation while **48e** and **48f** showed modest activity by comparison ($p < 0.0001$, n = 2).

Complete (100%) inhibition of colony formation was observed in HCT-116 cells and MCF-7 exposed to 5 µM **48b** and **48d**, reflecting the potency and cytotoxicity of these complexes (**Figure 45**). These data indicate that the cancer cells have either lost their ability to form progeny colonies[⊥] or have been killed.[177] In contrast, at the concentrations adopted (1 and 5 µM), **48e** and **48f** demonstrated reduced potency. Exposure of MCF-7 or HCT-116 cells to **48e** and **48f** at these concentrations failed to inhibit colony formation by >50% (**Figure 46**).[178]

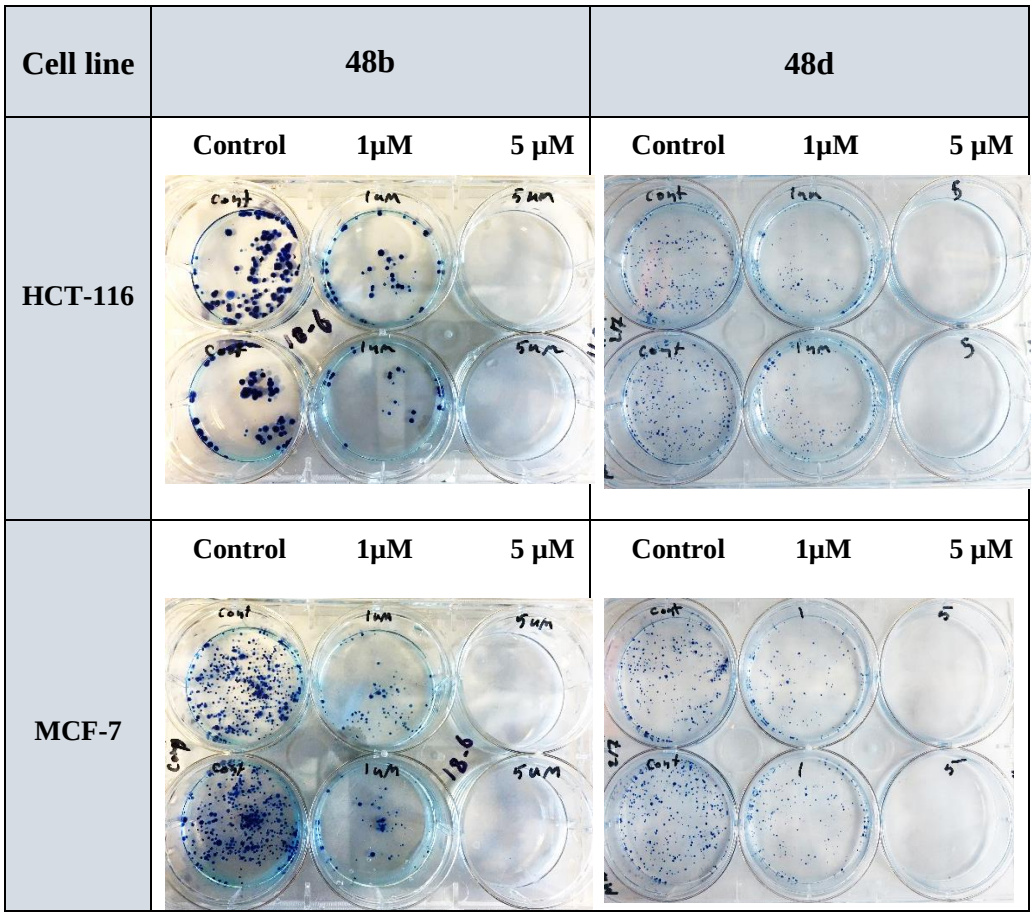


**Figure 45.** Effect of **48b** and **48d** on MCF-7 and HCT-116 colony formation at 1 and 5 µM.

[⊥] A cluster of identical cells (clones) on the surface of (or within) a solid medium, usually derived from a single parent cell.

| Cell line | 48e | 48f |
|---|---|---|
| HCT-116 | 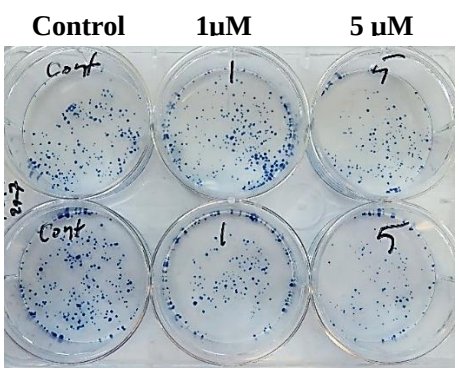  | 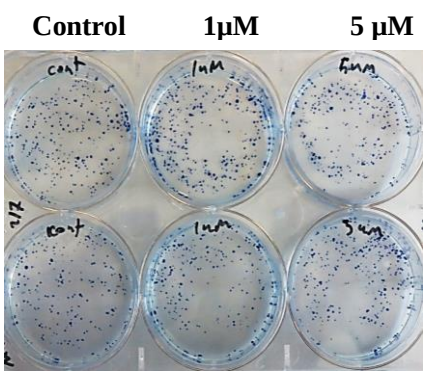  |
| MCF-7 | 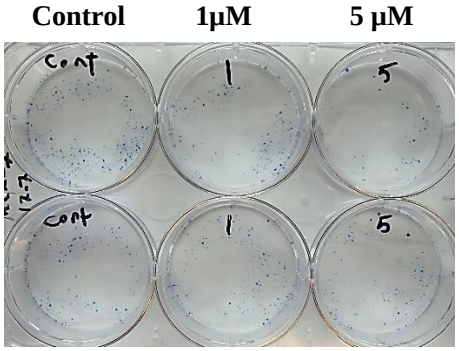  | 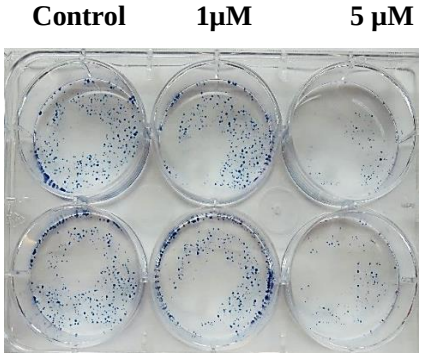  |

**Figure 46.** Effect of **48e** and **48f** on MCF-7 and HCT-116 colony formation at 1 and 5 µM.

### 3.3.4. **Cell cycle analysis**

A variety of flow cytometric methods have been developed during the last four decades to analyse cell cycle progression.[179] The method used in our study was univariate analysis of propidium iodide (PI) stained DNA content. PI is an intercalating agent that can bind to DNA and fluoresces strongly when excited with blue light (488 nm).[179] The DNA content of each cell (or event) in each cell cycle phase is proportional to the emitted fluorescence.[180] Therefore, this assay characterises the DNA content of each event in each phase of the cell cycle (Sub-G1 (G0), G1, S, G2/M) and this can therefore be used to show how a test agent perturbs the cell cycle distribution.[181] Based on the previous MTT and clonogenic assays, the

complexes **48** compromise cancer cell viability and growth. Led by these observations, we examined the effect of **48b**, and **48f** (as representative potent and modest agents respectively), and cisplatin (as a positive control) on cell cycle perturbation of HCT-116 by flow cytometry. An HCT-116 control cell cycle (no agents present) distribution profile demonstrated: 53.4±1.5 %, 24.9±1.3 % and 15.3±0.6 % events for the G1, S, G2/M phases[51] respectively. Negligible events were detected in the preG1 compartment reflecting a healthy HCT-116 population (**Figure 47** and **Table 6**). In contrast, following 72 h exposure of these cells to 10 µM cisplatin (~1.5 x $GI_{50}$), a substantial pre-G1 population was evident (25.2±0.8 % events) indicative of cells undergoing apoptosis (**Figure 47** and **Table 6**). It is known that cisplatin causes DNA inter- and intra-strand crosslinks (for an overview of DNA-drug interactions see ref.[182] and Chapter One) blocking DNA replication. The alerted DNA repair mechanisms fail to repair cisplatin-induced DNA damage (initially) initiating apoptosis. As DNA replication is blocked and repair is attempted, the cell cycle is halted during S and G2 phases. After 72 h of continued cisplatin treatment, DNA repair failure triggers programmed cell death. Miller *et al.* reported (2016) that titanium(IV) complexes affected HT-29 cell cycle distribution, as the cells demonstrated accumulation in G1 and S phases (see Chapter One, section 1.7).[97] No preG1 peak was evident in HCT-116 cells exposed to 10 µM **48b** (~3 × $GI_{50}$). Instead **48b** caused a profound accumulation of events in the G2/M phases indicates that DNA damage has occurred and DNA repair is being attempted, indicating a different/delayed mechanism of action (apoptosis) in contrast to Miller's titanium(IV) compounds and others (**Figure 47** and **Table 6**).[97] If the arrested cell cycle occurs as a result of DNA damage, its onset may be later than that caused by cisplatin (as observed in Pesch's group search, see ref.[138]). In contrast, complex **48f**

(at 10 µM; <0.5 × $GI_{50}$) caused negligible apparent HCT-116 cell cycle perturbation (**Figure 47** and **Table 6**). On the other hand, MCF-7 cells exposed to 10 µM cisplatin (~1.3 × $GI_{50}$), **48b** (~10 × $GI_{50}$) or **48f** (~0.9 × $GI_{50}$) demonstrated a modest increase in late S/G2/M events (**Figure 48** and **Table 7**).

**Table 6.** HCT-116 cell cycle distributions following treatment with cisplatin, **48b**, and **48f**.

| Time | Treatment | HCT-116 cell cycle events | | | |
|---|---|---|---|---|---|
| | | Sub G1% | G1% | S% | G2/M% |
| 72h | Control | 2.0±0.2 | 53.4±1.5 | 24.9±1.3 | 15.3±0.6 |
| 72h | Cisplatin 10 µM | 25.2±0.8 | 5.2±0.8 | 55.2±0.4 | 14.1±0.5 |
| 72h | 48b 10 µM | 1.0±0.1 | 20.2±0.5 | 51.9±1 | 26.7±0.5 |
| 72h | 48f 10 µM | 1.2±0.3 | 56.5±0.2 | 31.0±1.2 | 11±0.3 |

**Table 7.** MCF-7 cell cycle distributions following treatment with cisplatin, **48b**, and **48f**.

| Time | Treatment | MCF-7 cell cycle events | | | |
|---|---|---|---|---|---|
| | | Sub G1% | G1% | S% | G2/M% |
| 72h | Control | 0.3±0.1 | 46.2±1.5 | 23.2±0.2 | 20.5±0.9 |
| 72h | Cisplatin 10 µM | 19.5±1.3 | 48±0.9 | 18.2±1 | 14.1±0.8 |
| 72h | 48b 10 µM | 0.9±0.3 | 58.6±0.6 | 24.8±1.3 | 16.8±0.6 |
| 72h | 48f 10 µM | 1.3±0.2 | 63.8±1.1 | 19.5±0.9 | 16.5±0.2 |

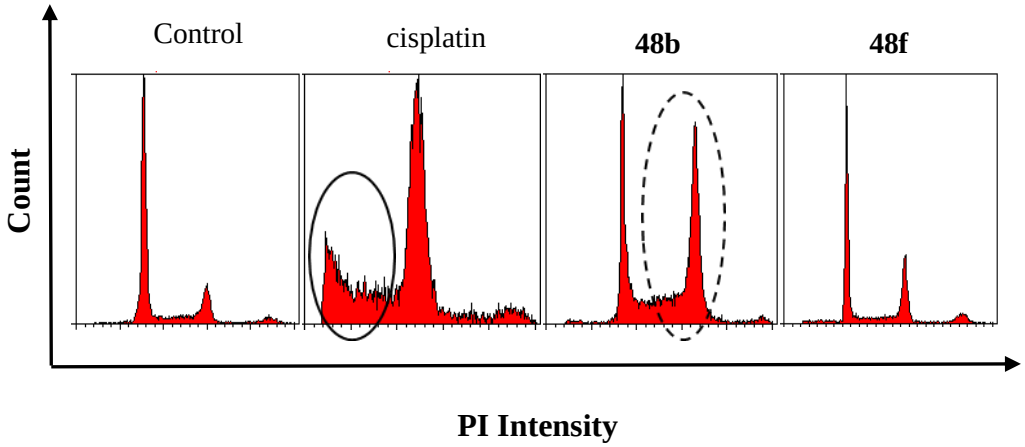


**Figure 47.** Representative cell cycle histograms of HCT-116 and cells treated with **48b**, **48f** and cisplatin at 10 µM concentrations for 72 h. Cells were seeded at a density of $4 \times 10^5$ (n = 2, for ≥3 trials). The solid ellipse **represents** the accumulation of cells in sub-G1 phase of the cell cycle affected by cisplatin. The dashed ellipse shows the accumulation of events G2/M phase of the cell cycle caused by **48b**. Events (15,000) were recorded for each sample.

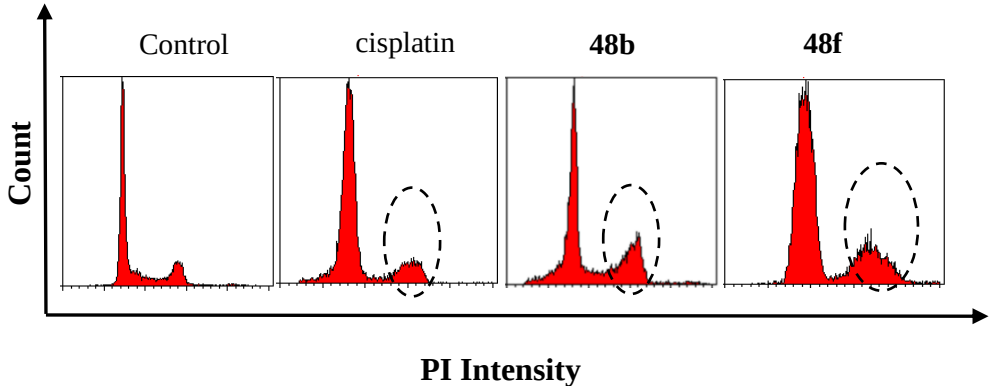


**Figure 48.** Representative cell cycle histograms from a single trial of MCF-7 cells treated with **48b**, **48f** and cisplatin at 10 x $GI_{50}$ concentrations for 72 h. Cells were seeded at a density of $4 \times 10^5$ (n = 2, for ≥3 trials). The dashed ellipse **represents** the accumulation of cells in pre G2/M phase of the cell cycle. Events (15,000) were recorded for each sample.

### 3.3.5. Induction of apoptosis in cancer cells

The annexin-V/PI assay is a technique used to measure the percentage of cells that are undergoing apoptosis.[183] The phospholipid phosphatidylserine (PS) protein is normally located at the inner surface of the plasma membrane, but during apoptosis the PS translocates to the outer surface of the plasma membrane. Annexin-V in the presence of calcium binds tightly to PS. At this stage, as an indicator of cell membrane integrity, PI is used as a DNA stain.[183] Our annexin-V/PI apoptosis assays[51] were performed to explore the apoptosis-inducing properties of **48b** and **48f**, with cisplatin being used as a positive control. MCF-7 and HCT-116 cells were exposed to both complexes (5 µM and 10 µM; 72 h). Apoptotic populations were confirmed by dual annexin V-FITC/PI staining (**Figure 49**, **A-B** and **Table 8**). As expected the majority (65%) of cells exposed to 10 µM cisplatin (72 h) were seen to be undergoing apoptosis. Both **48b** and **48f** revealed profound apoptotic MCF-7 and HCT-116 populations at the concentrations tested (**Table 8**). However, while both early and late apoptosis were evident in HCT-116 cells treated with **48b**, exposure to **48f** for 72 h revealed only a significant population of cells undergoing early apoptosis. The latter is indicative of later onset of programmed cell death (**Figure 49**, **A-B** and **Table 8**). Thus, although both **48b** and **48f** complexes trigger apoptosis, programmed cell death (**Figure 50**), the mechanism of how these complexes behave inside the cell is still ambiguous and structure-dependant. However, the cell cycle perturbations and subsequent apoptosis seen are highly suggestive of a DNA-targeting mechanism.

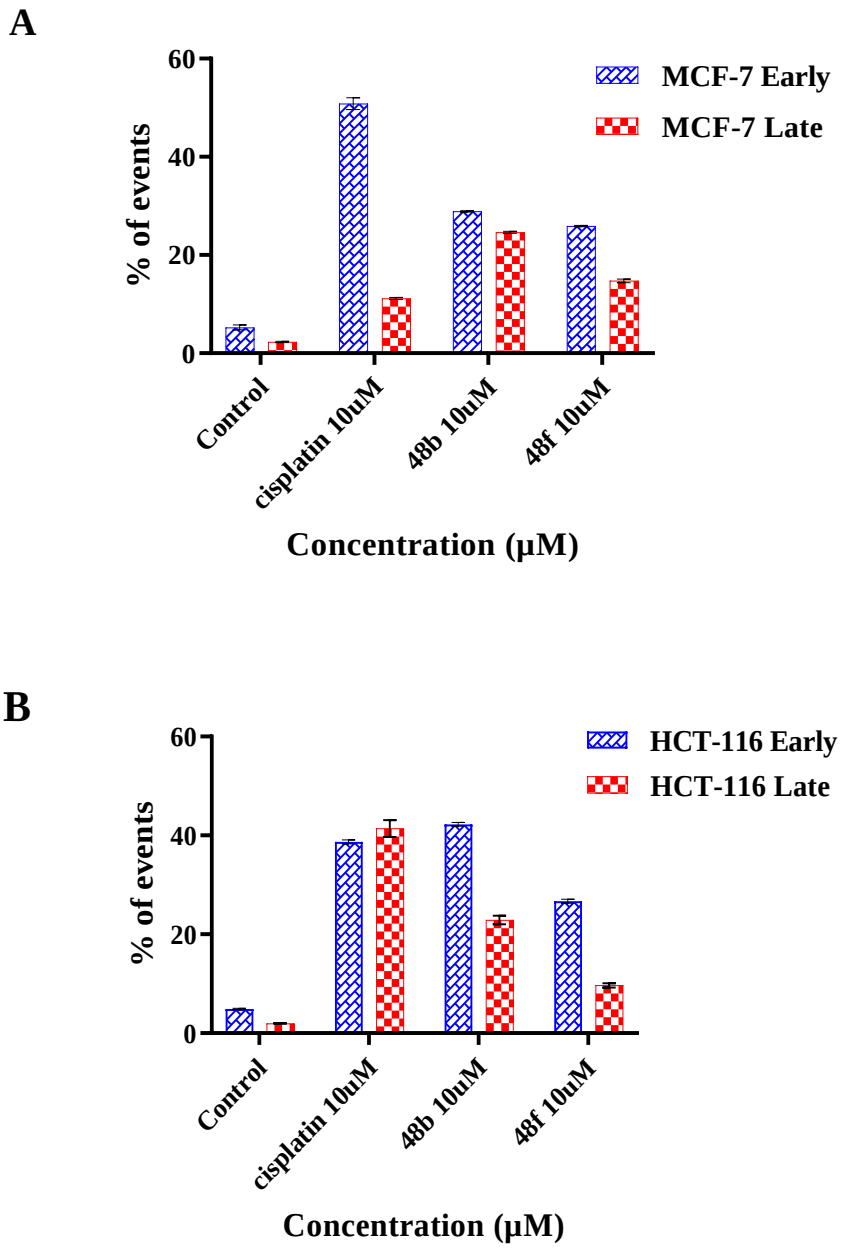


**Figure 49.** Apoptotic effects of **48b**, **48f**, and cisplatin on **A**) MCF-7 and **B**) HCT-116 cells at 10 µM. Cells were seeded at a density of $4 \times 10^5$ (n = 2, for 3 trials). Cells were treated with 10 µM for 72 h. Annexin-V/PI apoptosis assay was adopted to determine the percentage of apoptotic cells. Events (15,000) were recorded for each sample.

**Table 8.** Early and late apoptosis populations for HCT-116 and MCF-7 against **48b**, **48f**, and cisplatin.

| **Annexin-V/PI of HCT-116** | | | | |
|---|---|---|---|---|
| **Treatment** | **Live cells %** | **Early %** | **Late %** | **Dead cells %** |
| Control | 92±1.3 | 4.79±0.05 | 1.99±0.09 | 0.67±0.01 |
| Cisplatin | 16.9±0.7 | 38.4±0.3 | 42.6±3.1 | 2.19±0.4 |
| 48b | 33.8±0.9 | 42.5±1.1 | 22.3±0.9 | 1.4±1.2 |
| 48f | 61.0±1.8 | 26.4±0.5 | 9.36±0.1 | 3.23±0.8 |
| **Annexin-V/PI of MCF-7** | | | | |
| **Treatment** | **Live cells %** | **Early %** | **Late %** | **Dead cells %** |
| Control | 94.5±0.2 | 5.61±0.4 | 2.20±0.1 | 0.72±0.3 |
| Cisplatin | 35.1±0.7 | 51.7±0.5 | 11.0±0.02 | 2.29±0.3 |
| 48b | 39.8±1.4 | 29.0±0.2 | 24.5±0.2 | 6.78±0.9 |
| 48f | 53.6±0.2 | 26.0±0.9 | 14.5±0.6 | 5.92±1.2 |

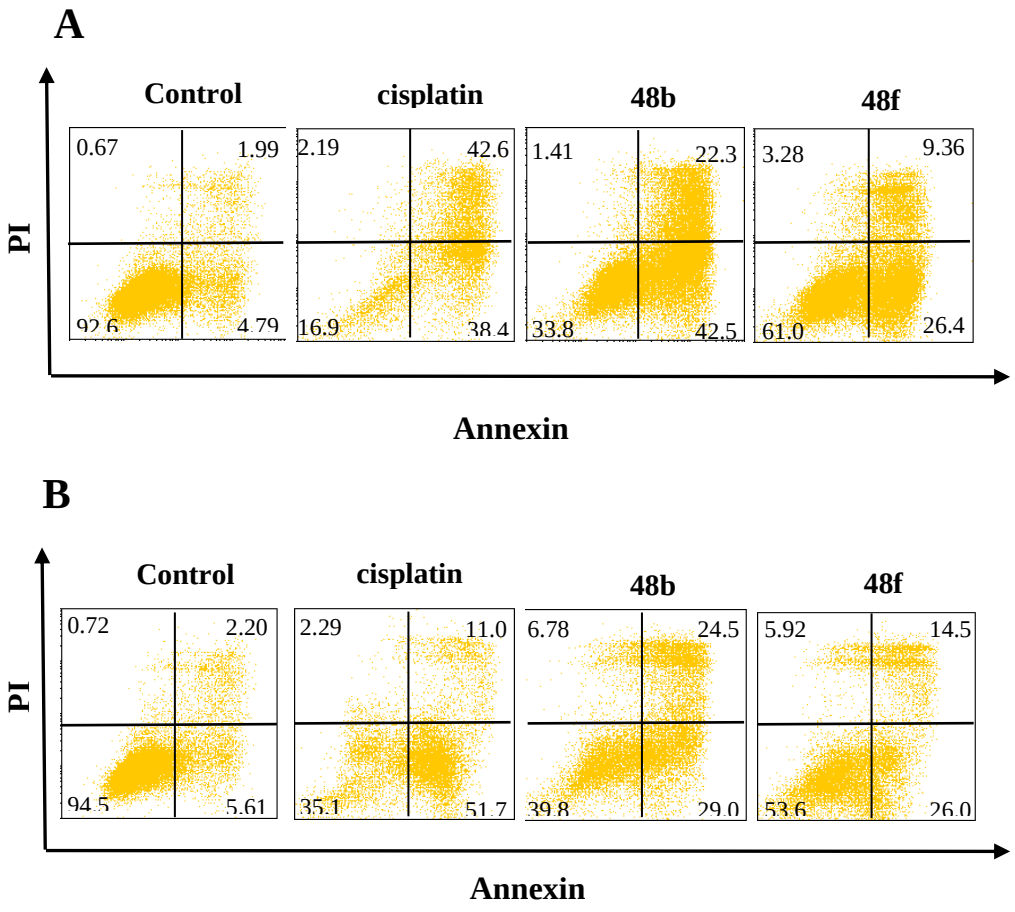


**Figure 50.** Representative apoptosis quadrant plots illustrating apoptotic effects of **48b**, **48f** and cisplatin on **A**) HCT-116 and **B**) MCF-7. Both cells were treated with 10 µM concentration of each agents for 72 h. Cells were seeded at a density of $4 \times 10^5$ (n = 2, for 3 trials). These are representative quadrant plots analysed by flow cytometry, 15,000 events were recorded for each sample.

To support our cell cycle studies simple imaging studies were undertaken using HCT-116 and **48b** to see if any morphological changes associated with apoptosis were evident (**Figure 51**). Two samples of HCT-116 cultures were set to grow in a video-monitored incubator. In an untreated control sample of HCT-116 growth continued over 72 h. However, HCT-116 treated with **48b** (5 µM) showed growth inhibition after ~12 h (**Figure 51**). By 72 h of exposure to 5 µM **48b** significant morphological changes in the cells characteristic of apoptosis were evident. Cell shrinkage and membrane blebbing can be seen clearly (**Figure 52**). We acknowledge the assistance and cooperation from Nottingham Trent University (NTU) for these real-time video recording of cells.

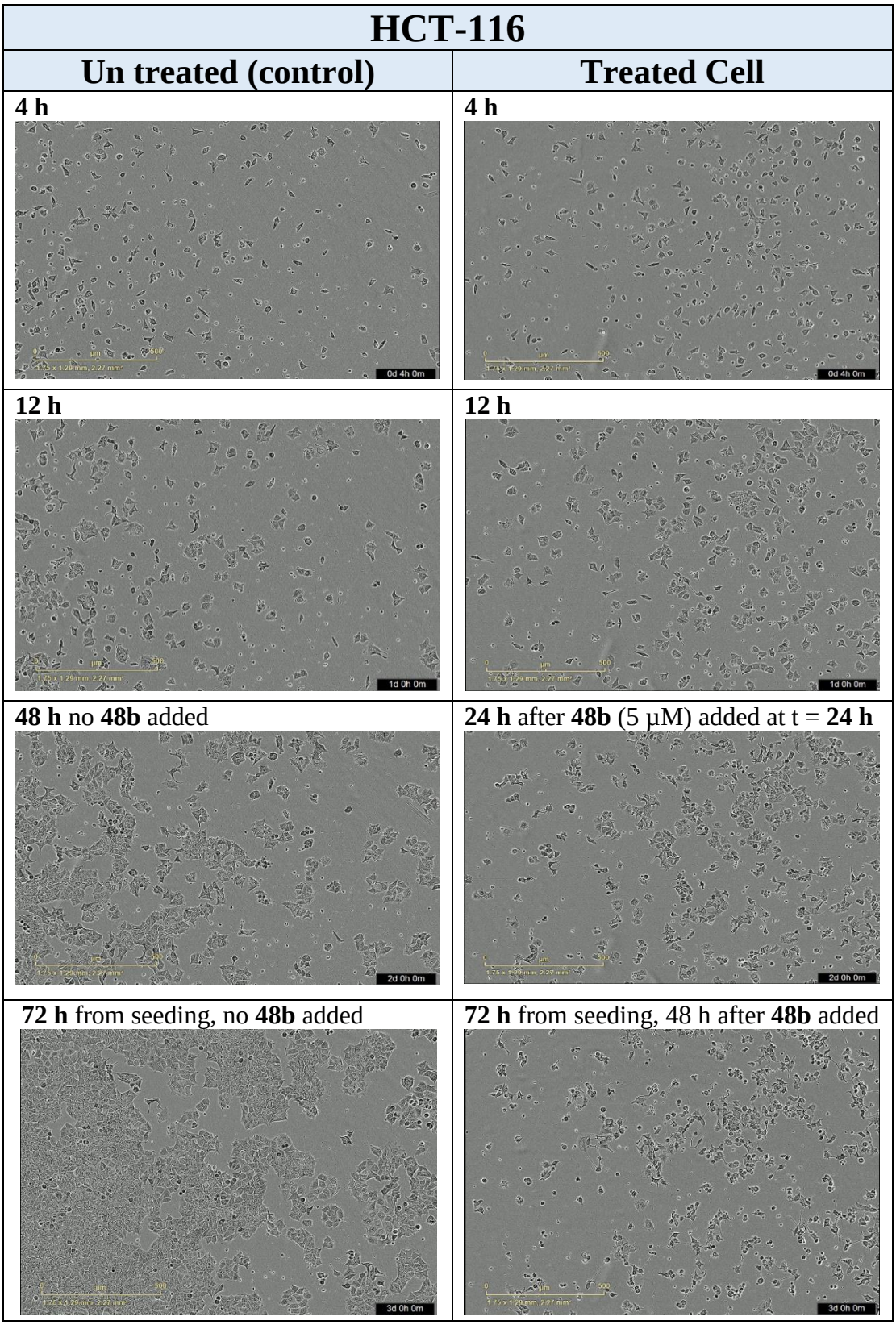


**Figure 51.** Comparison between HCT-116 control and same cell line exposure to **48b** during variable times at 5 µM.

**A** **96 h** from seeding, no **48b** added

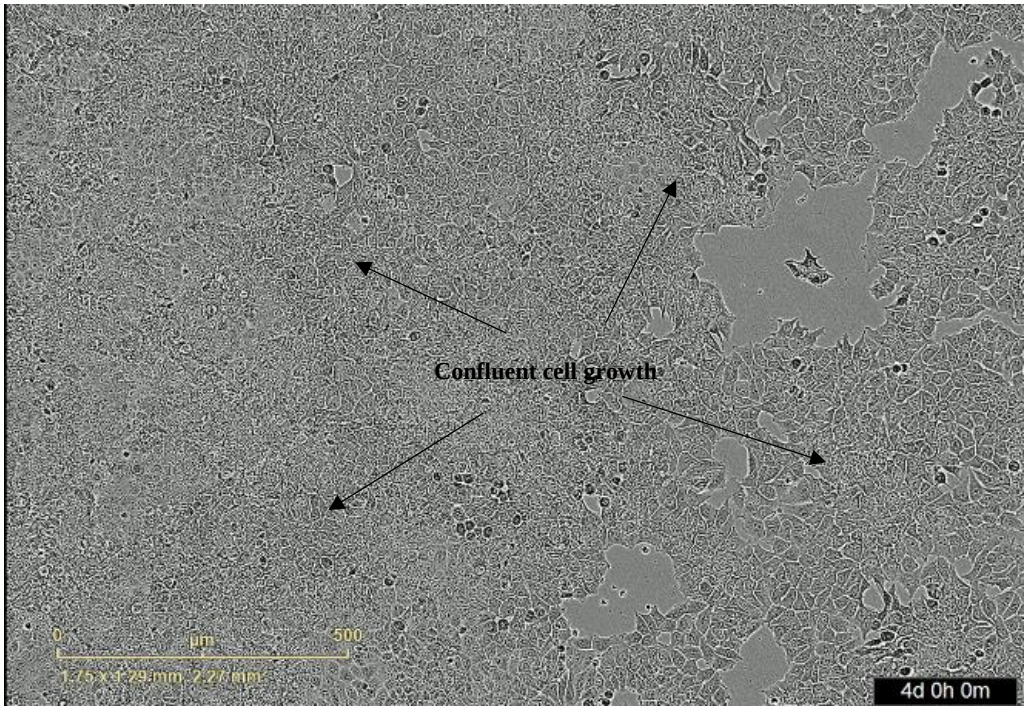


**B** **96 h** from seeding, **72 h** from **48b** added

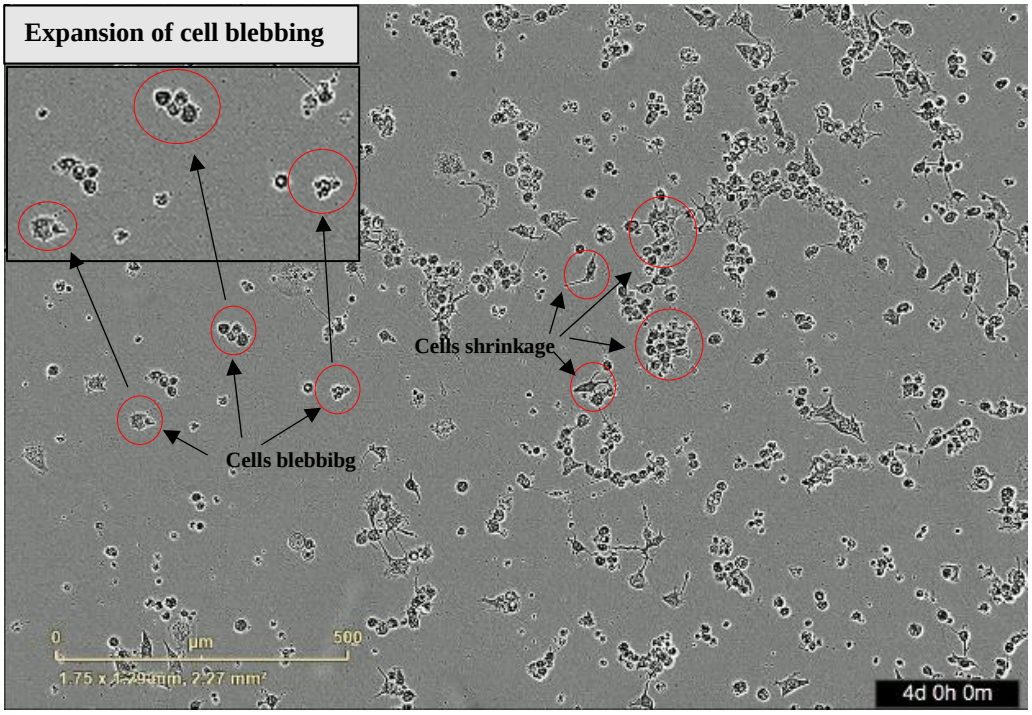


**Figure 52**. Image of HCT-116 cells: (**A**) control after 72 h from the treatment time; (**B**) following 72h exposure of cell to 5µM of **48b**. *Note: the device used to record this video (an incucyte), was provided by NTU.

### 3.3.6. Induction of DNA damage

To determine whether apoptosis is triggered by the generation of DNA double strand breaks (DSBs), flow cytometric analyses of control (untreated cells), cisplatin (a positive control), **48b** and **48f** treated HCT-116 and MCF-7 populations were performed following co-incubation with PI (propidium iodide) and a 1$^{o}$ Ab (primary antibody) recognising γ-H2AX.[51] It is well known that γ-H2AX foci appear at sites of DNA DSBs.[184] Cisplatin causes DNA damage: inter/intrastrand DNA crosslinks, and DNA monoadducts that lead to DNA DSBs. These harbingers of apoptosis are largely responsible for the Pt-drug's anti-tumour activity.[25, 182] Thus, co-incubation of cell populations with PI and the 1$^{o}$ Ab recognising γ-H2AX, prior to flow cytometry analyses, allows cell-cycle-specific detection of sites of DNA DSBs. Validating this hypothesis, accumulation of G2/M cell cycle events following exposure of HCT-116 cells to cisplatin 10 μM; 72 h was observed accompanied by γ-H2AX +ve events at sites of DNA DSBs. γ-H2AX +ve events were obviously detected in G1 and G2 cell cycle phases following exposure of MCF-7 cells to cisplatin, **48b** or **48f** (**Figure 53**, **A**). Consistent with our cell cycle analyses, dual PI/γ-H2AX labelling of HCT-116 cells supported **48b**-induced G2/M cell cycle arrest (**Figure 53**, **B**, see also **Figure S3** in Appendix). Interestingly, HCT-116 G2/M events comprised a population heavily positively stained γ-H2AX+ve (63 %) suggestive of the presence of DNA DSBs. Complex **48f**, in contrast revealed neither G2/M arrest, nor γ-H2AX+ve events associated with this cell phase consistent with HCT-116 cell cycle analysis and reduced potency. For **48f** a minority of G1 events appeared to have incurred DNA DSB damage and were γ-H2AX+ve. The current Ti complexes **48b** and **48f** clearly evoke apoptosis, but at different levels, following accumulation of DNA double strand breaks.

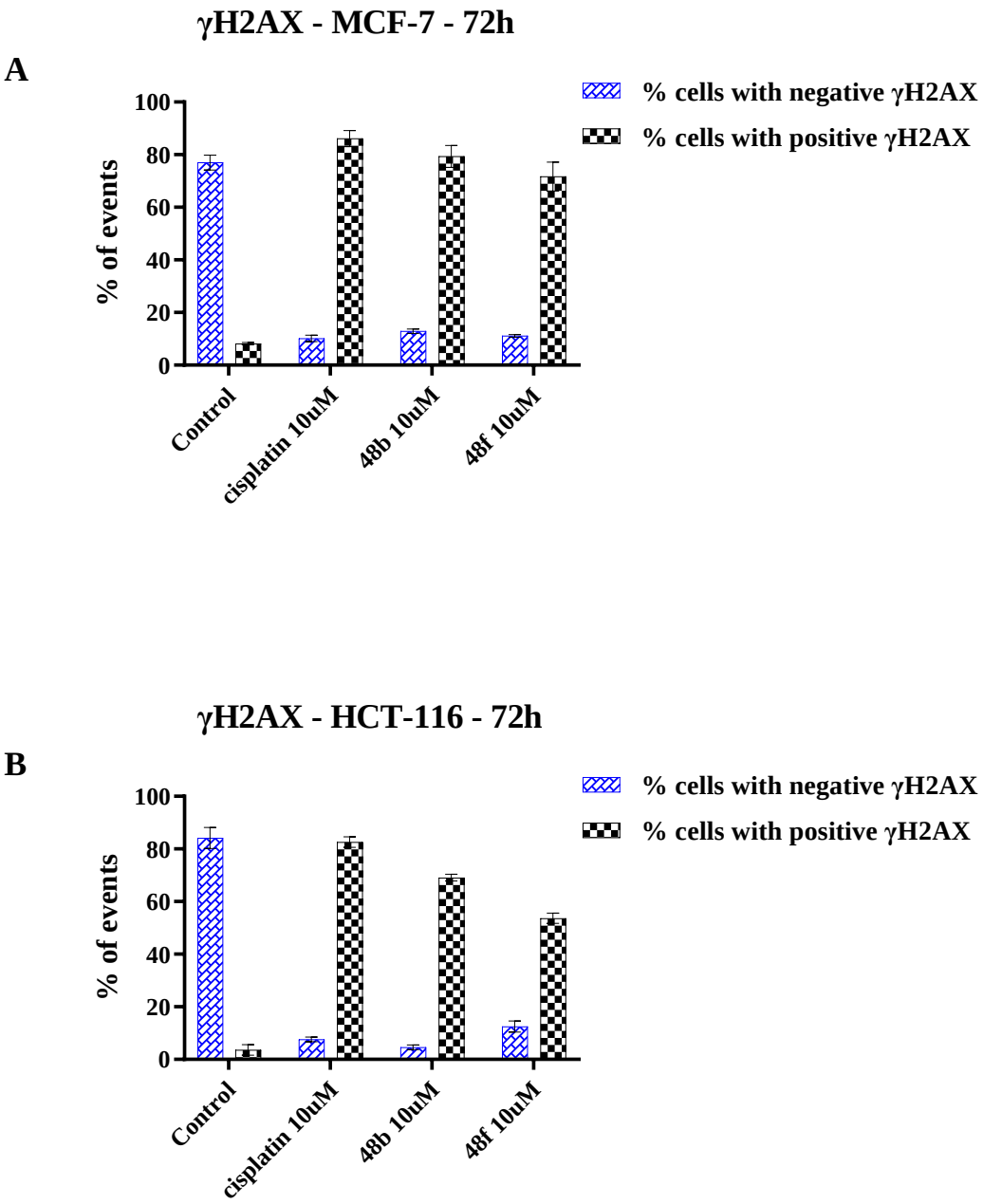


**Figure 53.** Determination of DNA double strand breaks by flow cytometric analyses of γ-H2AX cells following 72 h treatment of **48b**, **48f** with cisplatin vs. **A**) MCF-7 and **B**) HCT-116 cells. Cells were seeded at a density of $4 \times 10^5$ (n = 2, for 3 trials); 15000 events analysed per sample).

### 3.3.7. Caspase activation

Caspases are a family of conserved cysteine proteases that play an essential role in apoptosis.[185] These initiator and executioner caspases are important for hydrolytic degradation of cellular proteins and DNA.[185] Caspases will cleave a range of substrates, including downstream caspases, nuclear proteins, plasma membrane proteins and mitochondrial proteins, ultimately leading to cell death. Thus, one can monitor apoptosis by detecting cleaved (activated) caspases.[186] The data of sections 3.3.4 to 3.3.6 suggest that potent Ti-complex **48b** causes later-onset apoptosis compared to cisplatin. To irrefutably confirm an apoptotic cell fate for cells exposed to **48b**, a caspase 3/7 activation assay was performed following exposure of HCT-116 and MCF-7 cells with various concentrations of **48b**. Dose-dependent caspase activation (≥5 µM **48b** p< 0.0001; **Figure 54**) was detected following 72 h exposure of cells to **48b** consistent with apoptosis-induction. As a positive control, 50 µM cisplatin was used to confirm the assay raised caspase activation (e.g. by ~350% in HCT-116 populations; not shown). These data confirm that after 72 h exposure, **48b** triggers apoptotic cell death (**Figure 54**).[187]

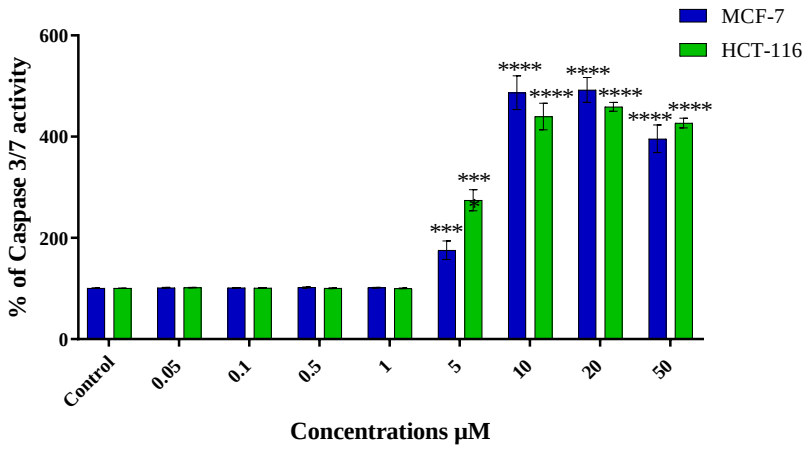


**Figure 54.** Dose-dependent elevation of caspase 3/7 activity in HCT-116 and MCF-7 cells following 72 h exposure of cells to Ti-complex **48b**. Data points are mean ±S.D; ($p < 0.0001$, $n = 8$).

## 3.4. Conclusions

A range **48b**-**h** of new titanium(IV) compounds has been synthesised and fully characterised (**48b**-**h**, in Chapter Three in **Figure 38**). All these complexes show similar $^{1}H$ and $^{13}C\{^{1}H\}$ NMR spectra with distinctive methylene bridge signals that are characteristic of complex formation. Four complexes were obtained as single crystals, with structural solutions performed in monoclinic (**48b** and **48e**), or triclinic (**48d** and **48f**) space groups. The range of compounds was synthesised included different ligand electronic properties in order to obtain an initial Structure Activity Relationships (SAR) upon complexation. The library of titanium(IV) complexes characterised in Chapter Three has been tested using the MTT, colonogenic, cell cycle, annexine-V, γ-H2AX, and caspase assays. This enabled determination of cytotoxic and mechanism of cell death, which give an indication of the complexes potential as an anti-cancer compounds. These complexes trigger apoptosis as indicated by annexine-V, γ-H2AX, and caspase activation assays. The library tested shows that complexes **48** have moderate to potent growth inhibitory activity and cytotoxicity. Complex **48b** has high potential as its $GI_{50}$ values of **48b** against MCF-7, HCT-116, MDA-MB-468, Panc1, HT-29 were: 1.0±0.04, 3.4±0.07, 3.1±1.9, 3±0.3 and 3.8±1.5 μM respectively. Complex **48b** also showed reduced toxicity toward non-tumorigenic (MRC-5) cells, thus displaying a degree of cancer cell selectivity. The $GI_{50}$ value of **48b** in MRC-5 cells was 7.3 μM, indicating a ~7-fold reduced activity when compared to activity against MCF-7 breast cancer cells. This is in complete contrast with cisplatin, where the $GI_{50}$ values in both MCF-7 and MRC-5 cells were nearly identical 7.8±0.04 vs 7.6±0.09 μM respectively. Presently, we were unable to identify the precise biological target(s) of these complexes, which would need a further future work in order to gain more information about the behaviour of

these complexes inside the cells, but it seems likely that [**L**cTi(OH)($OH_2$)]$^+$ is the active agent.

## 3.5. Future work

The key finding in this doctoral work is that the titanium complexes exemplified by our most active compound **48b** (**Scheme 32**, $R^1$ = OMe, $R^2$, $R^3$ = Me) show significant potential as anti-cancer agents. They demonstrate $GI_{50}$ values equal or better than a cisplatin (**3**) benchmark in five common human cancer cell lines. To move these *in vitro* findings towards *in vivo* studies and eventual clinical trials requires three future goals be overcome for this class of complex:

- The water solubility of **48** needs to be improved.
- The behaviour of **48** derivatives in both cell cultures and living tissue (including ultimately their pharmacokinetics) needs to be fully understood.
- The precise biological target(s) of **48** needs to be identified.

These specific, but somewhat interrelated, goals are discussed below.

### 3.5.1. Improved water solubility

The complexes **48** are freely soluble in DMSO at 10 mM, but are poorly soluble in aqueous environments. Above ca. 200 μM all examples of **48** precipitate as orange colloids in the presence of water or cellular growth media. While serial dilution of such suspensions appears to provide ‘solutions’, confirming the presence or absence of ultra-fine colloids or nanoparticles is challenging. Genuinely homogeneous systems would, of course, be preferred. The calculated logP values of the present family of **48** are appalling (Table in **Figure 55**) from a medicinal chemistry perspective, these values were estimated from the protocols within ChemDraw. Typically, an intravenous drug candidate should have a logP of <5, and more

normally this should be in the range 1-2, if formulation issues as in poorly soluble drugs such as Taxol are to be avoided.[188]

| | $R^1$ | $R^2$ | $R^3$ | ClogP | $GI_{50}$ (MCF-7, μM) |
|---|---|---|---|---|---|
| **48a** | Me | Me | Me | 14.44 | 36.3±0.1 |
| **48b** | MeO | Me | Me | 12.12 | 1.0±0.04 |
| **48c** | MeO | Me | Et | 13.18 | 6.6±0.07 |
| **48d** | Me | MeO | Me | 12.12 | 2.2±0.06 |
| **48e** | MeO | MeO | Me | 10.48 | 8.4±0.1 |
| **48f** | Me | F | Me | 13.02 | 11.7±0.05 |
| **48g** | Cl | Cl | Me | 16.16 | 51.5±0.1 |
| **48h** | EtO | Me | Me | 14.24 | 24.2±0.2 |

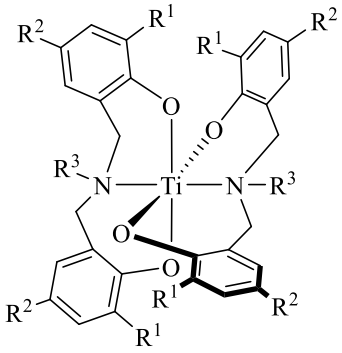

**48**

**Figure 55.** Comparison of calculated logP values and representative anti-cancer activity for complexes **48**.

For comparison, cisplatin (**3**) has a measured logP value of -2.53[189] making it almost too water soluble, the opposite of the problem we face. The intermediate **48ba** we have observed by $^1$H NMR spectroscopy and LCMS in the hydrolysis of **48b** has a ClogP value of 5.65 (**Figure 56**), suggesting that the additional water solubilising groups might bring this into a pharmaceutically useful range. For example, hypothetical complex **48i** has a ClogP of 6.62 and its derived intermediate **48ib** has ClogP = 2.90.

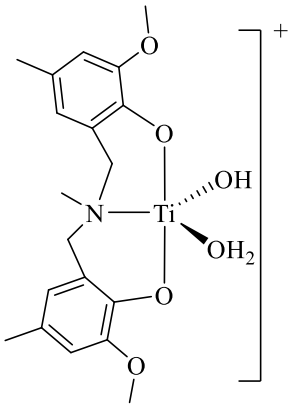

**48ba**

ClogP = 5.65

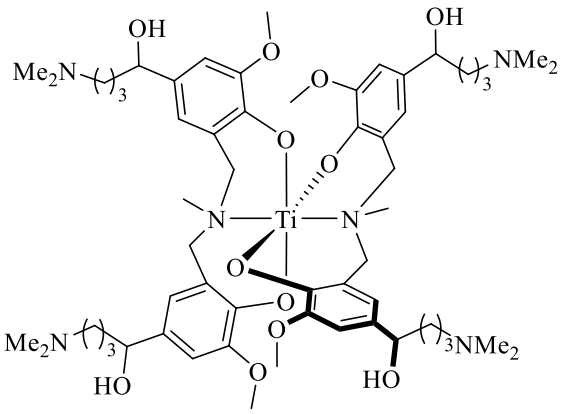

**48i**

ClogP = 6.62

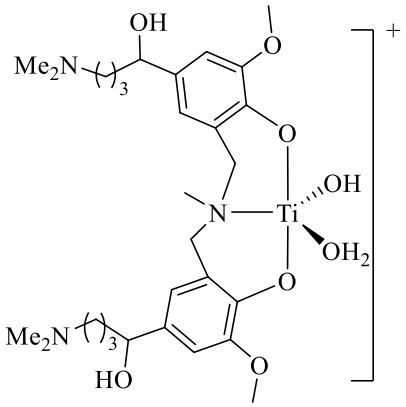

**48ib**

ClogP = 2.90

**Figure 56.** Calculated ClogP values for more pharmaceutically relevant complexes and intermediates.

Low cost vanillin is potentially a useful starting point for such chemistries (**Scheme 42**). Its modification to both ligand **47j** and complex **48j** should be possible using the approaches outlined in this thesis.

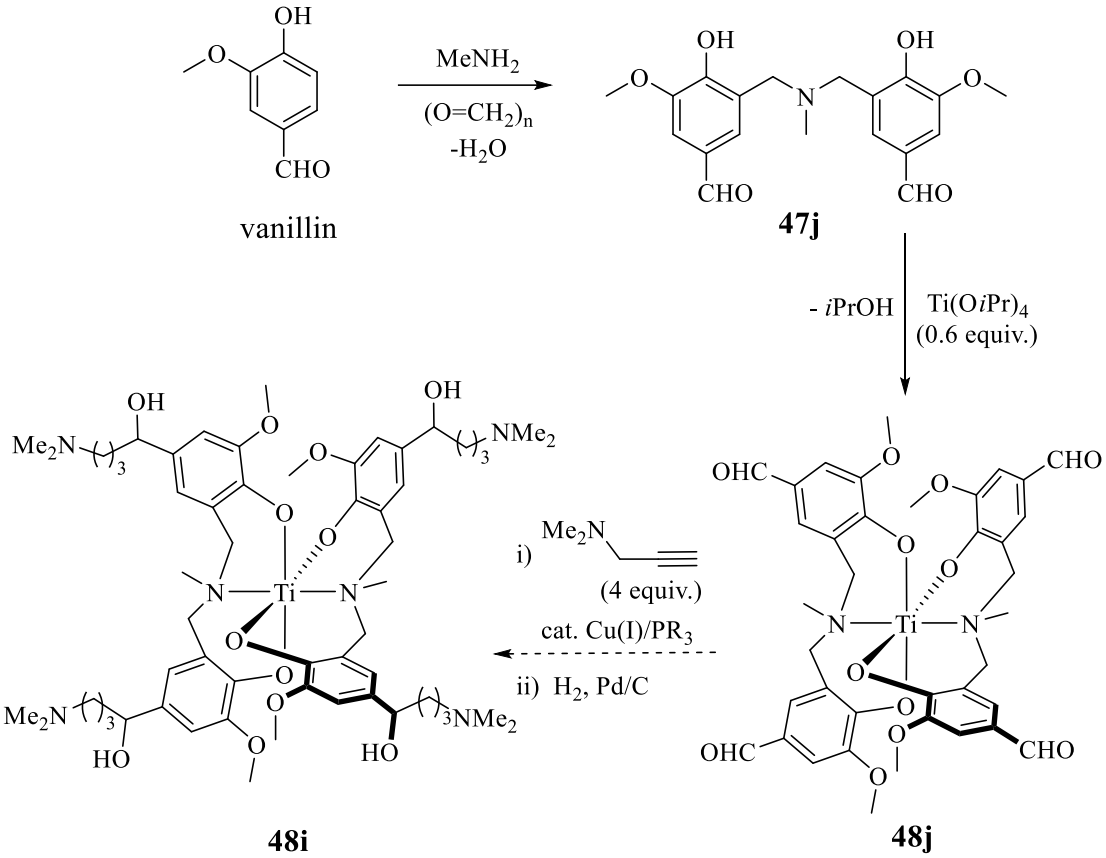


**Scheme 42.** Initial targets for vanillin-derived ligands and titanium complexes.

The *para*-formyl groups in ligand **47j** offer excellent potential for diversity in synthesis. For example, using Sawamura's[190] process for the selective addition of terminal acetylenes to aldehydes, it is likely that after *in situ* hydrogenation of the triple bond the same complex, **48i**, would be possible. This approach would also allow us to attach the fluorescent probe unit **51** already developed (see p. 92-93), through similar manipulation of its terminal acetylene. Proof-of-concept studies confirm that starting materials **47j** and **48j** can be prepared. We expect these to act as

medicinal chemistry diversity points allowing us to introduce a wider range of functional groups, some of which are exemplified **Scheme 43**. We anticipate that one or more of these classes to provide us with appropriately aqueous solubility and high activity in SAR studies.

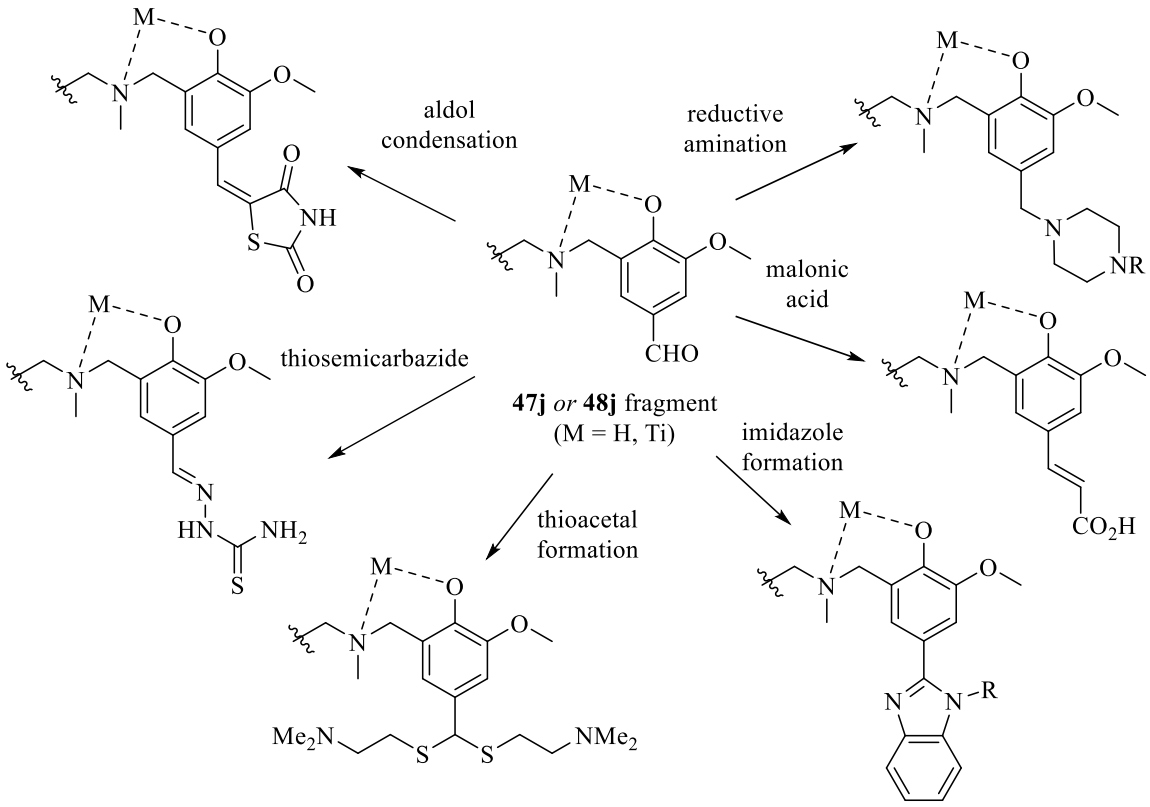


**Scheme 43.** Exemplary derivatives possible by formyl manipulation within ligand **47j** or complex **48j**.

### 3.5.2. Details of hydrolytic behaviour of complexes of type 48

Although in the case of **48b** an intermediate (nominally **48ba**) could be detected, it is far from fully characterised (**Scheme 44**). For other complexes in this class fast hydrolysis to just the ligands **47** and, presumably, $TiO_2$ is observed by $^1H$ NMR spectroscopy. However, by LCMS we could, in some runs, detect signals whose low

resolution mass spectra could be assigned as traces of [**L**cTi(OH)($OH_2$)+Na]$^+$ species. These preliminary investigations need to be repeated in the presence of a $Me_3SiCD_2CD_2CO_2Na$ internal standard, allowing us to accurately quantify the amounts of **48b**, **48ba** and **47b** present in the reaction mixture as a function of time. Using kinetic modelling akin to the studies made by us before[61] will allow us to understand the speciation present when the anti-cancer activity of **48b** maximises (up to 24 h after its addition).

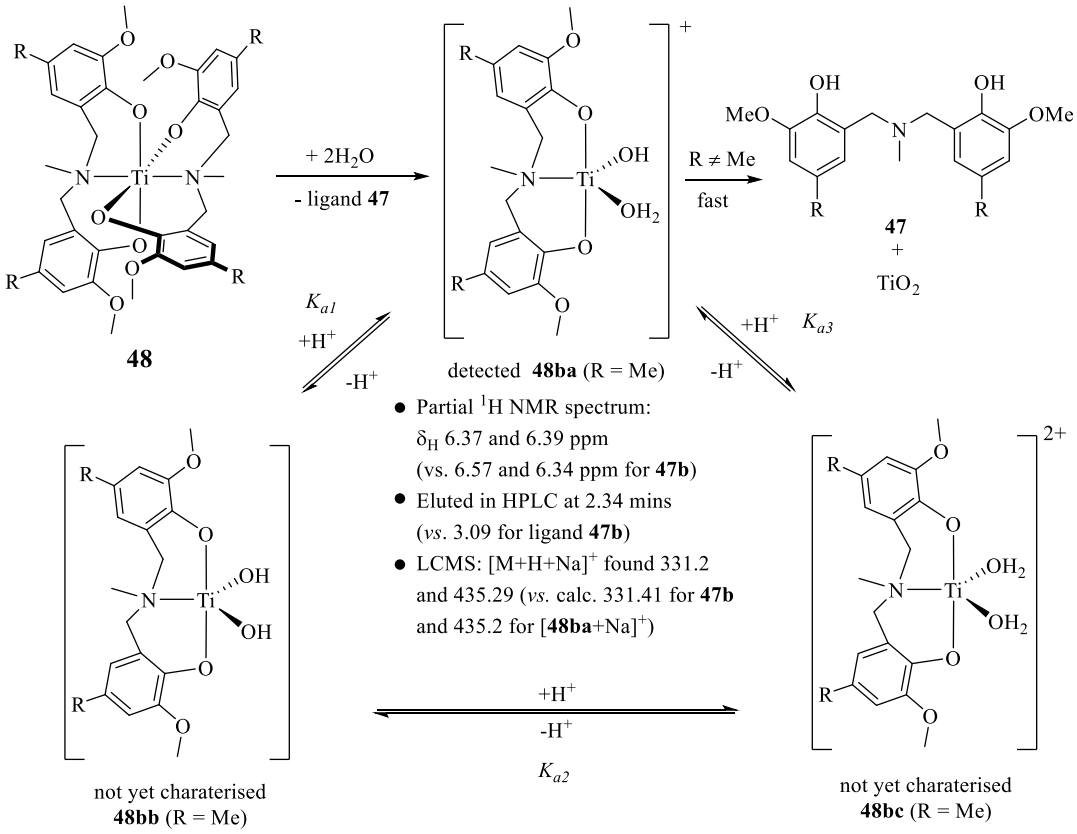


**Scheme 44.** Summary of preliminary hydrolysis data.

Studies of the hydrolysis of complexes **48** is complicated by their 2:1 ligand:Ti stoichiometry, meaning that excess free ligand is always present during NMR studies. In particular, this leads to complications in analysing the aromatic region of the spectra. We propose that use of the new starting material **i**[191] will allow us to prepare the mixed species **ii**. We predict that the higher basicity of the $sp^3$ alkoxides will lead to its preferential hydrolysis providing selective loss of the non-aryl ligand allowing clean formation of the putative biologically active species. Such controlled release may allow us to significantly increase the populations of active intermediates we can attain allowing studies with models for various biological targets.[191a, 192]

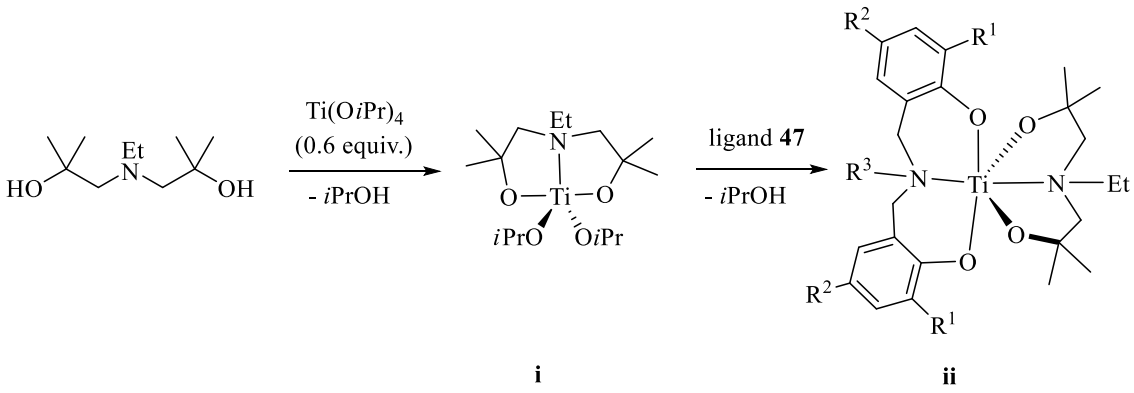


**i** **ii**

**Scheme 45.** Proposed hydrolysis leading to loss of the non-aryl ligand.

### 3.5.3. Biological target studies

Fluorescent labelling of **48** would allow us to visualise the intracellular localisation of the compound after treatment of the cells and this has been achieved in related systems.[158, 173a] Provided the label does not perturb the distribution/activity of the drug. Our studies show that complexes **48** trigger apoptotic responses in the cell lines we have studied. However, we have not shown if these outcomes are due to DNA alkylation or not. Typically, a *Thermo aquaticus* (TAQ) polymerase stop assay is used for detection of DNA alkylation.[193] This assay shows the stop sites on DNA where alkylated adducts have formed. To determine whether alkylation occurs at *N7* of guanine or not a piperidine cleavage assay can be used for more information of both assays (see reference 193). Conversely, we also plan to study human protein kinase in appropriate cell lines.[61] Apoptosis triggered by **48** occurs with very different characteristics to classic DNA alkylators (e.g. cisplatin **3**). While unusual, kinase triggered apoptosis is known and this possibly needs to be identified or refuted. Finally, we should aim to use proteomic profiling to further understand the biological mechanisms of the tested agents and find biomarkers of both the cancer states and their therapeutic responses. Using SWATH Acquisition, we could quickly create proteomic profiles of a large range of proteins in each sample (up to 4,500 in an hour's LC gradient).[194]

# 4. Experimental

## 4.1. General Experimental Procedures

Reactions involving air or moisture sensitive reagents were carried out under nitrogen atmospheres using flame-dried Schlenkware. All temperatures refer to the thermostated cooling/heating baths used (±2 °C). All solvents and liquid reagents were dried over 4 Å molecular sieves prior to use. Hydrogen peroxide (typically '100 volume', ca. 30% w/w, 0.8 M) was titrated against a sodium iodide by a known method.[195] Thin layer chromatography was performed on foil-backed plates coated with Merck silica gel 60 F254. The plates were visualised using ultraviolet light and basic aqueous potassium permanganate. Liquid chromatography was performed using forced flow (flash column) techniques with the solvent systems indicated. The stationary phase used was silica gel 60 (220-240 mesh) supplied by Fluorochem. Lead (IV) acetate was used as supplied if received as a colourless or off white solid impure samples (typically darker brown/black in colour) were recrystallised from hot glacial acetic acid.

## 4.2. Instrumentation

Infrared spectra were recorded on a Bruker Alpha Platinum spectrometer by ATR (for neat samples) or by transmission (if solutions). Nuclear magnetic resonance spectra were recorded on Bruker AV(III)400 (400.1 MHz), Bruker AV400 (400.1 MHz), Bruker Ascend™ 400 (400.2 MHz) or Bruker Ascend™ 500 (500.1 MHz) spectrometers at ambient temperature (unless otherwise stated). Chemical shifts are quoted in parts per million (ppm) and were referenced to residual solvent peaks using values provided by the MestReNova processing software. Coupling constants (*J*) are quoted in Hertz. Couplings are written using the following abbreviations: br (broad),

s (singlet), d (doublet), t (triplet), q (quartet), m (multiplet) and app (apparent). Carbon NMR multiplicities and connectivities were assigned using DEPT and the relevant 2D NMR experiments. Mass spectrometry was performed using a VG Micromass AutoSpec spectrometer (EI) or Bruker MicroTOF (ESI) as noted. Theoretical HRMS molecular weights were taken from the spectrometer output file, for HRMS analyses deviations from expected values (σ) are given in ppm. Melting points were measured on a Gallenkampf melting point apparatus. Liquid chromatography-mass spectrometry (LCMS) analysis using an Agilent 1260 Infinity HPLC with a 6120 Quadrupole mass spectrometer with a multimode source. Chromatography conditions: XBridge C18 3.5µm 2.1 x 30 mm column. Mobile phase A: 0.1% ammonia in water, mobile phase B: acetonitrile. Flow rate 0.8 ml/min in a gradient of 5 – 95 % mobile phase B over 3.5 minutes with UV detection at 210 – 400 nm reported at 254nm. Column temperature 40 $^{o}$C.

## 4.3. X-Ray Crystallography

X-ray diffraction data were collected (*via* the University of Nottingham, X-ray Crystallographic Service). A suitable single crystal was selected and immersed in an inert oil. The crystal was then mounted on a glass capillary and attached to a goniometer head. Data were collected on a Bruker X8 Apex or an Agilent Supernova diffractometer using graphite monochromated Mo-$K_{\alpha}$ radiation ($\lambda$ = 0.71073 Å) using 1.0° $\phi$-rotation frames. The crystal was cooled to 100 K by a Oxford Cryostream low temperature device.

## 4.4. New compounds made and first reported within this PhD

**The following new chemical entities were created during this doctoral work:**

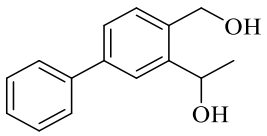


**33**

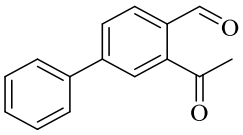


**23**

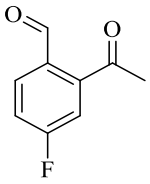


**36**

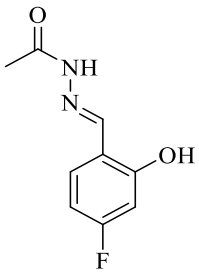


**40**

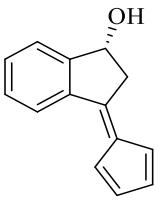


**24**

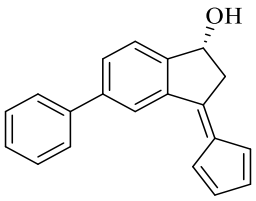


**25**

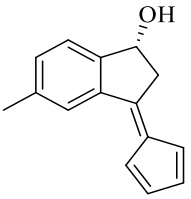


**26**

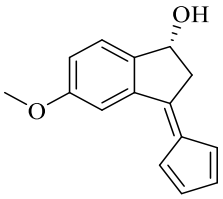


**27**

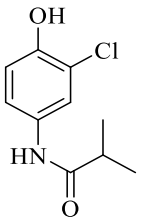


**44**

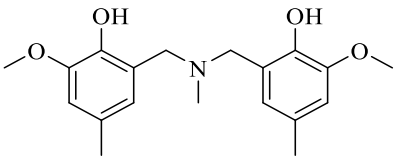


**47b**

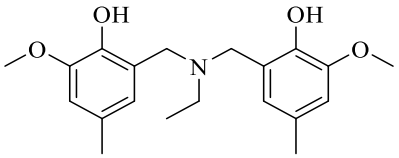


**47c**

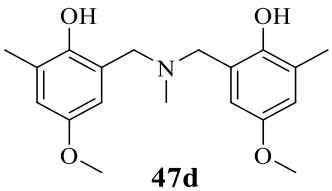


**47d**

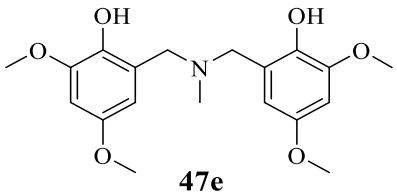


**47e**

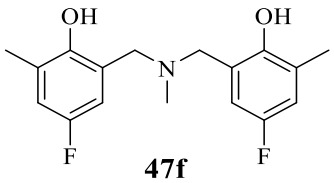


**47f**

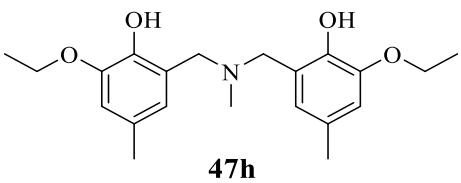


**47h**

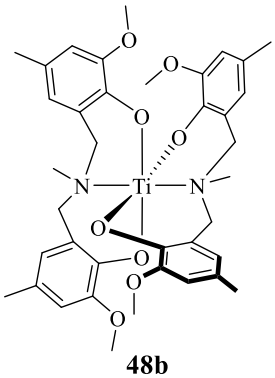

**48b**

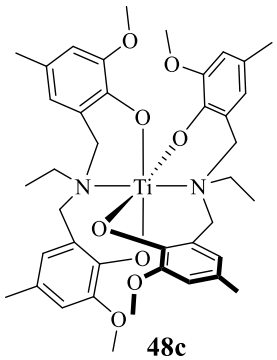

**48c**

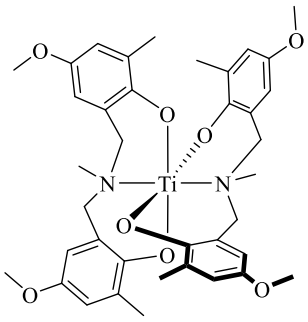

**48d**

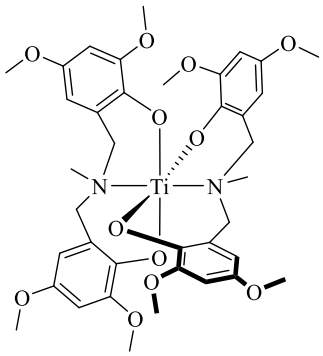

**48e**

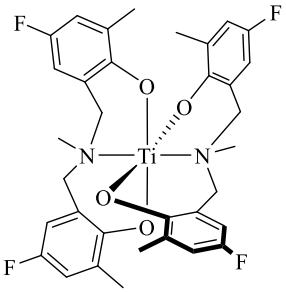

**48f**

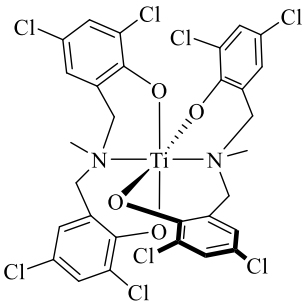

**48g**

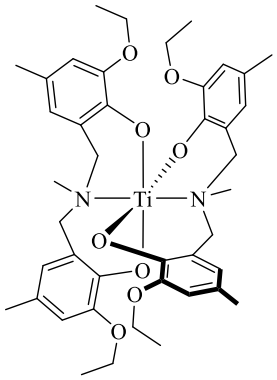

**48h**

Preparative details for these compounds, and their supporting reagents, are fully described in this experimental section. All compounds are named on the basis of IUPAC nomenclature. In order to provide unique atom numbering for all NMR assignments the auto-numbering feature of Chemdraw 19.1 has been used for convenience and consistency in atom/fragment identification.

## 4.5. Experimental Data for Chapter 2

**2-Acetyl-benzaldehyde (22)**

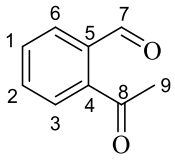


**22**

Compound **22** was prepared by a modification of a literature route.[196] A solution of oxalyl chloride (3.1 ml, 36 mmol) in dichloromethane (56 ml) was cooled to -78 °C before the dropwise addition of a solution of DMSO (5.2 ml, 73 mmol) in dichloromethane (8.5 ml). The resulting mixture was stirred at this temperature for 45 minutes before the addition of a solution of diol **32** (2.25 g, 14.8 mmol) in dichloromethane (20 ml). The resulting mixture was stirred at this temperature for 90 minutes before the addition of triethylamine (9.8 ml, 70 mmol). The reaction was then allowed to slowly warm to RT and stirred for 30 minutes before quenching *via* the addition of HCl (1 M, 50 ml). The reaction was extracted with dichloromethane (50 ml), washed with water (50 ml), dried over anhydrous magnesium sulfate and the solvent removed *in vacuo* to yield the crude product as a brown oil. The crude product was purified *via* flash column chromatography (eluent: 5:1 pentane:ethyl acetate) to give the product as a yellow oil in 82% yield (1.81 g, 12.2 mmol). NOTE: The product is unstable at RT and darkens in colour if left. It can be stored at -20 °C where it solidifies. Samples of **22** stored thus should be used within four weeks. **$R_f$** (3:2 ethyl acetate:pentane): 0.76; **$^1$H NMR** (400.2 MHz, $CDCl_3$): $\delta_H$ 10.20 (s, 1H, *H*CO), 7.85-7.61 (m, 4H, Ar*H*), 2.63 (s, 3H, C$H_3$); **$^{13}$C{$^1$H} NMR** (100.05 MHz, $CDCl_3$): $\delta_C$ 201.1 (C=O, $C_8$), 192.3 (C=O, $C_7$), 140.6 (C, $C_4$), 136.3 (C, $C_5$), 133.1

(CH, $C_2$), 131.9 (CH, $C_1$), 129.7 (CH, $C_6$), 128.6 (CH, $C_3$), 28.9 ($CH_3$, $C_9$); **IR $\nu_{max}$** (neat): 3068, 2861, 2750, 1761 (CO, $C_7$), 1694 (CO, $C_8$), 1594, 1573, 1359, 1262, 1197, 767, 642 $cm^{-1}$; **HRMS** found 171.0424 $C_9H_8O_2Na^+$ requires 171.0417 ($|\sigma|$ = 4.1 ppm). As of 2019 only a $^1H$ NMR spectrum and MS data had been published for **22**.[197]

**2-Acetyl-4-phenyl-benzaldehyde (23)**

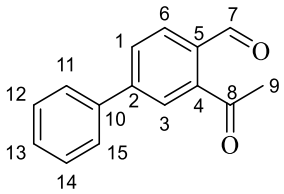


**23**

Compound **23** was prepared analogously to **22**. A solution of oxalyl chloride (1.4 ml, 16 mmol) in dichloromethane (26 ml) was cooled to -78 °C before the dropwise addition of a solution of DMSO (2.4 ml, 34 mmol) in dichloromethane (4.3 ml). The resulting mixture was stirred at this temperature for 45 minutes before the addition of a solution of diol **33** (1.50 g, 6.58 mmol) in dichloromethane (9 ml). The resulting mixture was stirred at this temperature for 90 minutes before the addition of triethylamine (4.6 ml, 33 mmol). The reaction was then allowed to slowly warm to RT and stirred for 30 minutes before quenching *via* the addition of HCl (1 M, 40 ml). The reaction was extracted with dichloromethane (50 ml), washed with water (50 ml), dried over anhydrous magnesium sulfate and the solvent removed *in vacuo* to yield the crude product as a brown oil. The crude product was purified *via* flash column chromatography (eluent: 4:1 pentane:ethyl acetate) to give the product as an orange oil in 62% yield (0.91 g, 4.06 mmol). NOTE: The product is unstable at RT and darkens in colour if left. It can be stored at -20 °C where it solidifies. Samples of **23**

stored thus should be used within four weeks. **$R_f$** (1:1 ethyl acetate:pentane): 0.85; **$^1$H NMR** (400.2 MHz, $CDCl_3$): $\delta_H$ 10.25 (s, 1H, *H*CO), 7.98 (dd, 1H, $^3J$ ($^1$H-$^1$H) = 7.9, 0.7 Hz, Ar*H*), 7.87-7.81 (m, 2H, Ar*H*), 7.65-7.60 (m, 2H, Ar*H*), 7.54-7.43 (m, 3H, Ar*H*), 2.70 (3H, s, C$H_3$); **$^{13}$C{$^1$H} NMR** (100.05 MHz, $CDCl_3$): $\delta_C$ 201.5 (C=O, $C_8$), 191.8 (C=O, $C_7$), 146.4 (C, $C_2$), 141.8 (C, $C_{10}$), 139.1 (C, $C_4$), 134.4 (C, $C_5$), 130.8 (CH, $C_1$), 130.1 (CH, $C_3$), 129.3 (CH, $C_{11}$), 129.0 (CH, $C_{15}$), 127.5 (CH, $C_{12}$ or $C_{14}$), 127.1 (CH, $C_{13}$), 29.4 ($CH_3$, $C_9$); **IR $\nu_{max}$** (neat): 3061, 3033, 2921, 2854, 1759 (CO, $C_7$), 1688 (CO, $C_8$), 1599, 1357, 1306, 1274, 1239, 1204, 761, 696 cm$^{-1}$; **HRMS** found 247.0728 $C_{15}H_{12}O_2Na^+$ requires 247.0730 (|σ| = 0.8 ppm).

## 4.5.1. Preparation of pentafulvene derivatives

**General Procedure A: Synthesis of derivatives of pentafulvene 24-27**

The corresponding 2-acetyl-benzaldehyde (1 equiv.) derivative and cyclopentadiene (6.5 equiv. freshly distilled, or stored at -20 °C for no more than two weeks) were dissolved in DMF at temperature T $^o$C. Acetic acid (0.13 equiv.) was added followed by the dropwise addition of 1-(pyrrolidin-2-ylmethyl)pyrrolidine (0.38 equiv.). The reaction was stirred for 2-6 h, after which it was diluted into ethyl acetate (150 ml), washed with pH 7.4 phosphate buffer (3 × 50 ml) and the solvent removed *in vacuo*. The crude product was then purified *via* flash column chromatography (eluent:dichloromethane) to afford the product. The product could be further purified *via* liquid-liquid diffusion (4:1 pentane:dichloromethane) or cold (r.t. to 4 $^o$C) recrystallisation from dimethoxyethane for larger scales.

**(*R*)-3-(Cyclopenta-2,4-dien-1-ylidene)-2,3-dihydro-1*H*-inden-1-ol (*R*)-(24)**

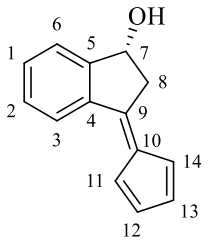


**(*R*)-24**

Synthesised according to **General Procedure A** using 2-acetyl-benzaldehyde (200 mg, 78% purity, 1.05 mmol), cyclopentadiene (0.62 ml, 7.37 mmol), DMF (2.6 ml), acetic acid (7.70 µL, 0.134 mmol), *(2S)*-1-(pyrrolidin-2-ylmethyl)pyrrolidine (65.0 µL, 0.40 mmol) at 15 °C for 6 hours to afford the crude product as an orange solid in 78% yield (161 mg, 0.82 mmol) which was further purified by recrystallisation to give the product as red needles (120 mg, 0.61 mmol, 75% recovery). **M.p.**: 130-140 °C (darkens from this temperature); **$R_f$** (dichloromethane): 0.30; **$^1$H NMR** (400.2 MHz, $CDCl_3$): $\delta_H$ 7.96 (dd, 1H, $^3J$ ($^1$H-$^1$H) = 6.6 Hz and $^4J$ ($^1$H-$^1$H) = 1.9 Hz, Ar*H*), 7.58-7.55 (m, 1H, Ar*H*), 7.48-7.38 (m, 2H, Ar*H*), 6.92 (app dt, $^{3,4}J$ ($^1$H-$^1$H) = 5.3, 1.7 Hz, 1H, Cp*H*), 6.59-6.55 (m, 1H, Cp*H*), 6.53- 6.49 (app t, $^{3,4}J$ ($^1$H-$^1$H) = 1.7 Hz, 2H, Cp*H*), 5.35 (ddd, 1H, $^3J$ ($^1$H-$^1$H) = 7.0, 7.0, 3.7 Hz, C*H*OH), 3.72 (dd, 1H, $^2J$ ($^1$H-$^1$H) = 17.5 Hz and $^3J$ ($^1$H-$^1$H) = 7.0 Hz, C$H_a$H$_b$ *anti* to OH), 3.09 (dd, $^2J$ ($^1$H-$^1$H) = 17.5 Hz and $^3J$ ($^1$H-$^1$H) = 7.0 Hz, 1H, CH$_a$*H*$_b$ *syn* to OH), 2.01 (d, 1H, $^3J$ ($^1$H-$^1$H) = 3.7 Hz, O*H*); **$^{13}$C{$^1$H} NMR** (100.05 MHz, $CDCl_3$): $\delta_C$ 151.2 (C, $C_9$), 149.5 (C, $C_5$), 139.4 (C, $C_4$), 138.7 (C, $C_{10}$), 132.8 (CH, $C_{11}$), 131.1 (CH, $C_{12}$), 131.0 (CH, $C_{13}$), 129.4 (CH, $C_{14}$), 126.5 (CH, $C_1$), 125.4 (CH, $C_2$), 123.4 (CH, $C_6$), 120.0 (CH, $C_3$), 72.9 (CH, $C_7$), 44.0 ($CH_2$, $C_8$); **IR $\nu_{max}$** ($CHCl_3$): 3614 (OH), 3590, 3070, 3045, 3008, 2960, 2927, 2873, 1630, 1476, 1458, 1389, 1368, 1239, 1050, 1021, 997 cm$^{-1}$; **HRMS** found 197.0959 $C_{14}H_{13}O^+$ requires 197.0961 (|σ| = 1.0 ppm); **$[\alpha]_D^{23}$**: +68.0 (*er* >99:1,

*c* = 0.50 in $CHCl_3$); **Anal**: Calcd. (%) for $C_{14}H_{12}O$, C, 85.68; H, 6.16; found C, 85.20; H, 6.47.

**(*R*)-3-(Cyclopenta-2,4-dien-1-ylidene)-5-phenyl-2,3-dihydro-1*H*-inden-1-ol (*R*)-(25)**

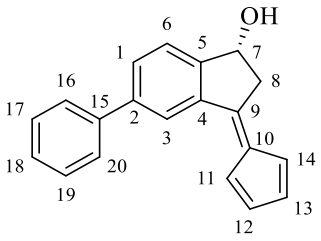


**(*R*)-25**

Synthesised according to **General Procedure A** using 2-acetyl-4-phenylacetyl-benzaldehyde (312 mg, 78% purity, 1.09 mmol), cyclopentadiene (0.62 ml, 7.37 mmol), DMF (2.6 ml), acetic acid (7.7 µL, 0.13 mmol) and *(2S)*-1-(pyrrolidin-2-ylmethyl)pyrrolidine (65 µL, 0.40 mmol) at 15 °C for 4.5 h to afford the crude product as an orange solid in 53% yield (157 mg, 0.57 mmol) which was further purified by recrystallisation to give the product as orange needles (90.3 mg, 0.332 mmol, 58% recovery) and *er* >99:1. **M.p.**: 140-150 °C (darkening observed from this temperature); $\mathbf{R_f}$ (dichloromethane): 0.18; **$^1$H NMR** (400.2 MHz, $CDCl_3$): $\delta_H$ 8.12 (d, $^4J$ ($^1$H-$^1$H) = 1.6 Hz, 1H, Ar*H*), 7.71-7.57 (m, 4H, Ar*H*), 7.52-7.45 (m, 2H, Ar*H*), 7.41 (tt, 1H, $^3J$ ($^1$H-$^1$H) = 4.5 Hz and $^4J$ ($^1$H-$^1$H) = 1.3 Hz, Ar*H*), 6.98 (app ddt, $^{3,4}J$ ($^1$H-$^1$H) = 5.3, 1.7 Hz, 1H, Cp*H*), 6.60-6.57 (m, 1H, Cp*H*), 6.54-6.52 (m, 2H, Cp*H*), 5.39 (dd, 1H, $^3J$ ($^1$H-$^1$H) = 6.9 Hz and $^4J$ ($^1$H-$^1$H) = 3.8 Hz, C*H*OH), 3.74 (dd, 1H, $^2J$ ($^1$H-$^1$H) = 17.5 Hz and $^3J$ ($^1$H-$^1$H) = 6.9 Hz, C$H_a$H$_b$ *anti* to OH), 3.12 (dd, 1H, $^2J$ ($^1$H-$^1$H) = 17.5 Hz and $^3J$ ($^1$H-$^1$H) 3.8 Hz, CH$_a$$H_b$ *syn* to OH), 2.03 (br s, 1H, O*H*); **$^{13}$C{$^1$H} NMR** (100.05 MHz, $CDCl_3$): $\delta_C$ 150.2 (C, $C_9$), 149.2 (C, $C_4$), 142.8 (C, $C_5$), 140.8 (C, $C_2$), 140.0 (C, $C_{15}$), 138.9 (C, $C_{10}$), 132.9 (CH, $C_{12}$), 131.1 (CH, $C_{13}$), 130.4 (CH,

$C_{17}$ or $C_{19}$), 129.1 (CH, $C_{18}$), 127.9 (CH, $C_{16}$), 127.4 (CH, $C_{20}$), 125.6 (CH, $C_6$), 125.0 (CH, $C_1$), 123.4 (CH, $C_3$), 120.0 (CH, $C_{11}$ or $C_{14}$), 72.7 (CH, $C_7$), 44.2 ($CH_2$, $C_8$); **IR** $\nu_{max}$ ($CHCl_3$): 3590 (OH), 3109, 3066, 3008, 2925, 1702, 1631, 1603, 1477, 1464, 1389, 1368, 1055, 1021, 1001, 910, 861, 840, 803, 790, 779 $cm^{-1}$; $[\alpha]_D^{23}$: -12.8 (*er* >99:1, *c* = 0.47 in $CHCl_3$).

**(*R*)-3-(Cyclopenta-2,4-dien-1-ylidene)-5-methyl-2,3-dihydro-1*H*-inden-1-ol (*R*)-(26)**

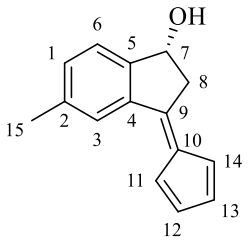


**(*R*)-26**

Synthesised according to **General Procedure A** using 2-acetyl-4-methylbenzaldehyde (120 mg, 78% purity, 0.58 mmol), cyclopentadiene (0.34 ml, 4.05 mmol), DMF (1.5 ml), acetic acid (4.2 µL, 0.07 mmol) and *(2S)*-1-(pyrrolidin-2-ylmethyl)pyrrolidine (36 µL, 0.23 mmol) at 15 °C for 6 h to afford the product as an orange solid in 72% yield (87.6 mg, 0.41 mmol) and 91:9 *er*. **M.p.**: 167-170 °C; **$R_f$** (dichloromethane): 0.29; **$^1$H NMR** (400.2 MHz, $CDCl_3$): $\delta_H$ 7.77 (d, 1H, $^4J$ ($^1$H-$^1$H) = 1.4 Hz, Ar*H*), 7.44 (d, 1H, $^3J$ ($^1$H-$^1$H) = 7.8 Hz, Ar*H*), 7.28-7.26 (m, 1H, Ar*H*), 6.94 (app ddt, 1H, $^{3,4}J$ ($^1$H-$^1$H) = 5.3, 1.7 Hz, Cp*H*), 6.59-6.55 (m, 1H, Cp*H*), 6.52-6.48 (m, 2H, Cp*H*), 5.31 (ddd, 1H, $^3J$ ($^1$H-$^1$H) = 7.3, 6.9, 3.7 Hz, C*H*OH), 3.71 (dd, 1H, $^2J$ ($^1$H-$^1$H) = 17.5 Hz and $^3J$ ($^1$H-$^1$H) = 6.9 Hz, C$H_a$H$_b$ *anti* to OH), 3.08 (dd, 1H, $^2J$ ($^1$H-$^1$H) = 17.5 Hz and $^3J$ ($^1$H-$^1$H) = 3.7 Hz, CH$_a$$H_b$ *syn* to OH), 2.43 (s, 3H, $CH_3$), 1.92 (d, 1H, $^3J$ ($^1$H-$^1$H) = 7.3 Hz, O*H*); **$^{13}$C{$^1$H} NMR** (100.05 MHz, $CDCl_3$): $\delta_C$ 150.7 (C, $C_9$), 148.7 (C, $C_4$), 139.6 (C, $C_5$), 139.4 (C, $C_2$), 138.5 (C, $C_{10}$), 132.6 (CH,

$C_{12}$), 132.3 (CH, $C_{13}$), 130.9 (CH, $C_1$), 126.8 (CH, $C_3$), 125.1 (CH, $C_6$), 123.4 (CH, $C_{11}$), 120.0 (CH, $C_{14}$), 72.7 (CH, $C_7$), 44.3 ($CH_2$, $C_8$), 21.7 ($CH_3$, $C_{15}$); **IR** $\nu_{max}$ (neat): 3178 (OH), 3122, 3062, 2979, 2917, 2855, 1625, 1602, 1488, 1460, 1367, 1326, 1290, 1064, 1008, 761 $cm^{-1}$; **HRMS** found 191.0870 $C_{15}H_{11}^-$ requires 191.0866 (|σ| = 2.1 ppm); $[\alpha]_D^{20}$: +16.0 (*er* >91:9, *c* = 0.50 in $CHCl_3$).

**(*R*)-3-(Cyclopenta-2,4-dien-1-ylidene)-5-methoxy-2,3-dihydro-1*H*-inden-1-ol (*R*)-(27)**

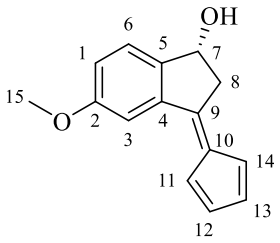


**(*R*)-27**

Synthesised according to **General Procedure A** using 2-acetyl-4-methoxybenzaldehyde (250 mg, 78% purity, 1.09 mmol), cyclopentadiene (0.64 ml, 7.61 mmol), DMF (2.7 ml), acetic acid (8.0 µL, 0.14 mmol) and *(2S)*-1-(pyrrolidin-2-ylmethyl)pyrrolidine (68.0 µL, 0.41 mmol) at 15 °C for 5 h to afford the crude product as an orange solid in 54% yield (134 mg, 0.59 mmol) which was further purified by recrystallisation to give the product as red needles (76.0 mg, 0.33 mmol, 57% recovery) and *er* >99:1. **M.p.**: 186-190 °C; $\mathbf{R_f}$ (dichloromethane): 0.41; **$^1$H NMR** (400.2 MHz, $CDCl_3$): $\delta_H$ 7.46 (d, 1H, $^3J$ ($^1$H-$^1$H) = 8.4 Hz, Ar*H*), 7.42 (d, 1H, $^4J$ ($^1$H-$^1$H) = 2.4 Hz, Ar*H*), 7.03 (dd, 1H, $^3J$ ($^1$H-$^1$H) = 8.4 Hz and $^4J$ ($^1$H-$^1$H) = 2.4 Hz, Ar*H*), 6.91 (app ddt, 1H, $^{3,4}J$ ($^1$H-$^1$H) = 5.3, 1.7 Hz, Cp*H*), 6.59-6.55 (m, 1H, Cp*H*), 6.53-6.48 (m, 2H, Cp*H*), 5.29 (ddd, 1H, $^3J$ ($^1$H-$^1$H) = 7.1, 6.9, 3.4 Hz, C*H*OH), 3.89 (s, 3H, OC$H_3$), 3.71 (dd, 1H, $^2J$ ($^1$H-$^1$H) = 17.6 Hz and $^3J$ ($^1$H-$^1$H) = 6.9 Hz, C$H_a$H$_b$ *anti* to OH), 3.09 (dd, 1H, $^2J$ ($^1$H-$^1$H) = 17.6 Hz and $^4J$ ($^1$H-$^1$H) 3.4 Hz, CH$_a$$H_b$ *syn* to OH), 2.11 (d, 1H, $^3J$ ($^1$H-$^1$H) = 7.8 Hz, O*H*); **$^{13}$C{$^1$H} NMR** (100.05 MHz,

$CDCl_3$): $\delta_C$ 161.2 (C, $C_9$), 150.0 (C, $C_4$), 144.5 (C, $C_5$), 141.2 (C, $C_2$), 139.1 (C, $C_{10}$), 133.2 (CH, $C_{12}$), 131.4 (CH, $C_{13}$), 126.6 (CH, $C_1$), 123.9 (CH, $C_3$), 120.1 (CH, $C_{11}$), 119.0 (CH, $C_{14}$), 110.5 (CH, $C_6$), 72.8 (CH, $C_7$), 56.2 ($CH_3$, $C_{15}$), 44.9 ($CH_2$, $C_8$); **IR** $\nu_{max}$ (neat): 3317 (OH), 2956, 2922, 2853, 2834, 1624, 1601, 1487, 1463, 1366, 1288, 1234, 1099, 1029, 759, 613 $cm^{-1}$; **HRMS** found 227.1069 $C_{15}H_{15}O_2^+$ requires 227.1067 (|σ| = 0.9 ppm); $[\alpha]_D^{23}$: +9.9 (*er* >99:1, *c* = 0.81 in $CHCl_3$); **Anal**: Calcd. (%) for $C_{15}H_{14}O_2$ C, 79.62; H, 6.24; found C, 79.24; H, 6.20.

## 4.5.2. Preparation of catalyst (31)

**(*2S*)-1,1-Dimethylethyl ester-2-(hydroxymethyl)-1-pyrrolidinecarboxylic acid (28a)**

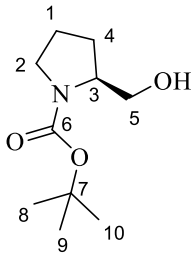


**28a**

Compound **28a** was prepared by a modification of a literature procedure as described below.[121] To a solution of commercial (*2S*)-2-pyrrolidinemethanol **28** (4.00 g, 39.5 mmol) and triethylamine (21.8 ml, 156 mmol) in dichloromethane (250 ml) was added di-*tert*-butyl dicarbonate (10.4 g, 47.7 mmol). The resulting mixture was stirred at RT, open to air, for 24 h before being quenched by the addition of water (250 ml) with stirring for 30 minutes. The aqueous layer was extracted with dichloromethane (3 × 100 ml), dried over anhydrous sodium sulfate and the solvent removed *in vacuo* to give the crude product, as a pale yellow oil, in quantitative yield which was used without further purification (8.25 g). $R_f$ (1:1 ethyl acetate:pentane): 0.37; **$^1$H NMR**

(400.1 MHz, $CDCl_3$): $\delta_H$ 4.72 (app d, 1H, $^3J$ ($^1$H-$^1$H) = 7.7 Hz, O*H*), 3.96 (m, 1H, C*H*N), 3.68-3.55 (m, 2H, C$H_2$OH), 3.45 (ddd, 1H, $^2J$ ($^1$H-$^1$H) = 10.7 and $^3J$ ($^1$H-$^1$H) = 6.7, 6.6 Hz, C$H_a$H$_b$N), 3.30 (ddd, 1H, $^2J$ ($^1$H-$^1$H) = 10.7 and $^3J$ ($^1$H-$^1$H) = 6.7, 6.6 Hz, CH$_a$$H_b$N), 2.05-1.96 (m, 1H, C$H_2$CH$_2$), 1.85-1.73 (m, 2H, C$H_2$CH$_2$), 1.58-1.50 (m, 1H, C$H_2$CH$_2$), 1.47 (s, 9H, C(C$H_3$)$_3$); **$^{13}$C{$^1$H} NMR** (100.05 MHz, $CDCl_3$): $\delta_C$ 157.0 (C=O, $C_6$), 80.1 (C, $C_7$), 67.4 ($CH_2$, $C_5$), 64.8 (CH, $C_3$), 55.3 ($CH_2$, $C_2$), 47.5 (3 × $CH_3$, $C_{8,9,10}$), 28.6 ($CH_2$, $C_4$), 28.4 ($CH_2$, $C_1$). These data were in agreement with reported properties for **28a** allowing its forward synthetic use.[121]

**(*2S*)-1,1-Dimethylethyl ester-2-[[[(4-methylphenyl)sulfonyl]oxy]methyl]-1 pyrrolidinecarboxylic acid (29)**

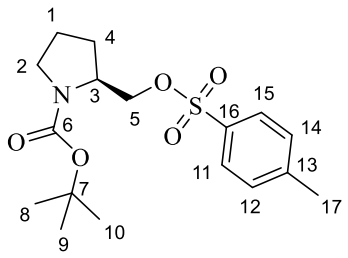


**29**

Compound **29** was prepared by a modification of a literature procedure as described below.[122] To a solution of crude **28a** (5.80 g, 28.8 mmol) in pyridine (18 ml) was added a solution of 4-toluenesulfonyl chloride (6.2 g, 32.5 mmol) in pyridine (18 ml) portionwise over 15 minutes at 0 °C. The resulting solution was stirred at 0 °C for another hour before being allowed to warm to RT and stirred for additional 18 h. The reaction was monitored *via* TLC, once complete, the solvent was removed *in vacuo* and the reaction redissolved in ethyl acetate (150 ml). This was then washed with HCl (100 ml, 0.5 M), saturated sodium hydrogen carbonate (100 ml) and water (100 ml) before being dried over anhydrous sodium sulfate and the solvent removed *in vacuo* to give the crude product in quantitative yield, as a yellow oil, which was

identified *via* $^{1}$H NMR spectrum and used without further purification (10.9 g). **R$_f$** (1:1 ethyl acetate:pentane): 0.71; **$^{1}$H NMR** (400.2 MHz, $CDCl_3$): $\delta_H$ 7.77 (d, 2H, $^{3}J$ ($^{1}$H-$^{1}$H) = 8.1 Hz, *ortho*-Ar*H*), 7.30 (br s, 2H, *meta*-Ar*H*), 4.15-4.05 (m, 2H, C$H_2$O), 3.93 (br s, 1H, C*H*N), 3.38-3.22 (m, 2H, C$H_2$N), 2.44 (s, 3H, C$H_3$), 1.98-1.74 (m, 4H, C$H_2$C$H_2$), 1.43-1.33 (m, 9H, C(C$H_3$)$_3$); **$^{13}$C{$^{1}$H} NMR** (100.05 MHz, $CDCl_3$): $\delta_C$ 154.4 (C=O, $C_6$), 154.4 (C, $C_{16}$), 154.0 (C, $C_{13}$), 144.8 (CH, $C_{12}$ or $C_{14}$), 144.5 (CH, $C_{11}$ or $C_{15}$), 79.6 (C, $C_7$), 67.3 (CH, $C_3$), 64.6 ($CH_2$, $C_5$), 55.3 ($CH_2$, $C_2$), 47.3 ($CH_3$, $C_{8,9,10}$), 28.5 ($CH_2$, $C_4$), 28.3 ($CH_2$, $C_1$), 21.2 ($CH_3$, $C_{17}$). These data were in agreement with reported properties for **29** allowing its forward synthetic use.[198]

**(*2S*)-1,1-Dimethylethyl ester-2-(1-pyrrolidinylmethyl)-1 pyrrolidine-carboxylic acid (30)**

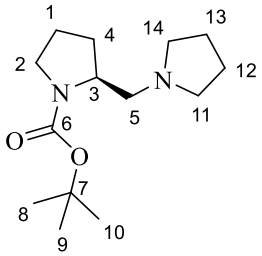


**30**

A solution of crude **29** (10.9 g, 30.7 mmol), pyrrolidine (10.1 ml, 123 mmol) and DBU (0.46 ml, 3.08 mmol) in toluene (120 ml) was heated at reflux for 42 h. After removal of all solvents *in vacuo*, the mixture was redissolved in ethyl acetate (100 ml), washed with water (3 × 50 ml), dried over anhydrous sodium sulfate and the solvent removed *in vacuo* to give the crude product, as a light brown solid, in quantitative yield which was identified by $^{1}$H NMR spectroscopy and used in immediate subsequent deprotection without further purification (8.01 g). **$^{1}$H NMR** (400.2 MHz, $CDCl_3$): $\delta_H$ 4.00-3.77 (m, 1H, C*H*N or C$H_aH_b$N), 3.37-3.27 (m, 2H,

C*H*N or C*H*$_2$N), 2.65-2.40 (m, 6H, C*H*$_2$N), 2.00-1.65 (m, 8H, C*H*$_2$CH$_2$), 1.46 (s, 9H, C(C*H*$_3$)$_3$). These data were in agreement with reported properties for **30**.[123, 199]

**(*2S*)-1-(Pyrrolidin-2-ylmethyl)pyrrolidine (31)**

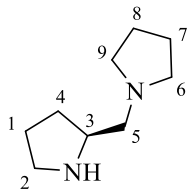


**31**

The compound was prepared by a slight adaptation of a literature procedure as described below.[200] To a solution of crude **30** (8.01 g, 31.5 mmol) in dichloromethane (136 ml) was added TFA (48 ml, ca. 627 mmol) **(CARE! – Corrosive)**. The resulting solution was stirred at RT, open to air, for 24 h before removal of all solvents *in vacuo* to yield the product as the corresponding TFA salt. This residue was dissolved in sodium hydroxide (4 M, 200 ml) and stirred for 30 minutes before extraction with diethyl ether (3 × 200 ml). The organic extracts were dried over anhydrous sodium sulfate before removal of the solvent *in vacuo* to give the crude product which was purified by Kügelrohr distillation (2 mbar, 1.5 mmHg) to afford **31** as a colourless oil in 54% yield (2.64 g, 17.1 mmol). **B.p.**: 75 °C at 1.5 mmHg; **$^1$H NMR** (400.2 MHz, $CDCl_3$): $\delta_H$ 3.16 (dtd, 1H, $^3J$ ($^1$H-$^1$H) = 8.8, 7.2, 5.3 Hz, C*H*N), 2.93 (ddd, 1H, $^2J$ ($^1$H-$^1$H) = 10.2 and $^3J$ ($^1$H-$^1$H) = 7.2, 5.9 Hz, C*H*$_a$H$_b$N), 2.80 (app dt, 1H, $^2J$ ($^1$H-$^1$H) = 10.2 and $^3J$ ($^1$H-$^1$H) = 7.2 Hz, CH$_a$*H*$_b$N), 2.56-2.28 (m, 7H, 2 × C*H*$_2$N, CH$_2$ and NH), 1.84 (dddd, 1H, $^2J$ ($^1$H-$^1$H) = 12.4 and $^3J$ ($^1$H-$^1$H) = 8.7, 7.2, 5.3 Hz, CH$_a$*H*$_b$CH$_2$), 1.81-1.63 (m, 6H, 3 × CH$_2$), 1.29 (app ddt, 1H, $^2J$ ($^1$H-$^1$H) = 12.4 and $^3J$ ($^1$H-$^1$H) = 8.8, 6.9 Hz, C*H*$_a$H$_b$CH$_2$); **$^{13}$C{$^1$H} NMR** (100.05 MHz,

$CDCl_3$): $\delta_C$ 62.2 ($CH_2$, $C_5$), 57.5 (CH, $C_3$), 54.7 ($CH_2$, $C_6$ or $C_9$), 46.2 ($CH_2$, $C_2$), 30.2 ($CH_2$, $C_4$), 25.1 ($CH_2$, $C_1$), 23.5 ($CH_2$, $C_7$ or $C_8$); $[\alpha]_D^{23}$: +10.0 (*c* = 1.00 in $CHCl_3$). These data were in agreement with published properties for **31**.[200]

### 4.5.3. Synthesis of 2-Acetyl-benzaldehyde and Derivatives (32-43)

**1-(2-(Hydroxymethyl)phenyl)ethan-1-ol (32)**

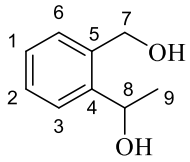


**32**

Dry TMEDA (9.8 ml, 64.0 mmol) was added dropwise to *n*BuLi (1.6 M in hexane, 40.0 ml, 64.0 mmol) at RT and the resulting yellow solution was stirred for 5 minutes. Dry benzyl alcohol (2.9 ml, 27.9 mmol) was then added dropwise, at RT, before heating the resulting brown mixture at reflux for 3 h or until all gas (butane) evolution ceased. After cooling the resulting brown suspension to -78 °C, a solution of freshly distilled acetaldehyde (3.6 ml, 64 mmol) in diethyl ether (20 ml) was cooled to -78 °C and then added dropwise to the lithiated benzyl alcohol. The reaction quickly changed to a pale yellow colour and was allowed to warm to RT before being stirred overnight. The resulting orange reaction mixture was quenched *via* the addition of water (60 ml) before being extracted with ethyl acetate (2 × 50 ml), dried over anhydrous magnesium sulfate and the solvents removed *in vacuo* to yield the crude product as an orange oil. The crude product was purified *via* flash column chromatography (eluent: 1:1 ethyl acetate:pentane) to give the product as a yellow oil which crystallised slowly to give a yellow solid in 65% yield (2.90 g, 19.1 mmol). **M.p.**: 64-66 °C [Lit M.p. 64-66 °C[201]]; $\mathbf{R_f}$ (ethyl acetate): 0.70; **$^1$H NMR** (400.2 MHz, $CDCl_3$): $\delta_H$ 7.46 (d, 1H, $^3J$ ($^1$H-$^1$H) = 7.6 Hz, Ar*H*), 7.36-7.26 (m, 3H, Ar*H*),

5.15 (q, 1H, $^{3}J$ ($^{1}$H-$^{1}$H) = 6.5 Hz, C*H*OH), 4.79 (d, 1H, $^{2}J$ ($^{1}$H-$^{1}$H) = 12.1 Hz, C$H_aH_b$), 4.62 (d, 1H, $^{2}J$ ($^{1}$H-$^{1}$H) = 12.1 Hz, C$H_aH_b$), 3.08 (m, 2H, 2 × O*H*), 1.57 (d, 3H, $^{3}J$ ($^{1}$H-$^{1}$H) = 6.5 Hz, C$H_3$); **$^{13}$C{$^{1}$H} NMR** (100.05 MHz, $CDCl_3$): $\delta_C$ 143.4 (C, $C_5$), 138.1 (C, $C_4$), 130.0 (CH, $C_6$), 128.7 (CH, $C_1$), 128.0 (CH, $C_2$), 126.0 (CH, $C_3$), 67.2 (CH, $C_8$), 63.9 ($CH_2$, $C_7$), 23.0 ($CH_3$, $C_9$); **IR $\nu_{max}$** (neat): 3331(OH, $C_8$), 2974 (OH, $C_7$), 1453, 1371, 1213, 1119, 1078, 1006, 896, 763 cm$^{-1}$; **HRMS** found 175.0724 $C_9H_{12}O_2Na^+$ requires 175.0730 (|σ| = 3.4 ppm). These data were in agreement with reported properties for **32**.[201-202]

**1-(4-Hydroxymethyl)-[1,1'-biphenyl]-3-yl)ethan-1-ol (33)**

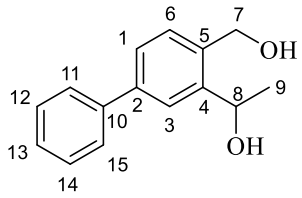


**33**

Dry TMEDA (9.8 ml, 65.3 mmol) was added dropwise to *n*BuLi (1.6 M in hexane, 43.8 ml, 70.1 mmol) at RT and the resulting yellow solution was stirred for 5 minutes. 4-biphenylmethanol (5.47 g, 29.7 mmol) was then added portionwise, at RT, before heating the resulting dark purple mixture at reflux for 3 h or until all gas (butane) evolution ceased. After cooling the resulting dark purple suspension to -78 °C, a dry solution of acetaldehyde (3.7 ml, 66.2 mmol) in diethyl ether (20 ml) was cooled to -78 °C and then added dropwise to the lithiated benzyl alcohol. The reaction quickly changed to a pale yellow colour and was allowed to warm to RT before being stirred overnight. The resulting orange reaction mixture was quenched *via* the addition of water (50 ml) before being extracted with ethyl acetate (2 × 50 ml), dried over anhydrous magnesium sulfate and the solvents removed *in vacuo* to yield the crude product as a red oil. The crude product was purified *via* flash column chromatography

(eluent: 1:1 ethyl acetate:pentane) to give the product as a yellow oil which crystallised slowly to give an orange solid in 51% yield (3.46 g, 15.2 mmol). **$R_f$** (1:1 ethyl acetate:pentane): 0.26; **$^1$H NMR** (400.2 MHz, $CDCl_3$): $\delta_H$ 7.71 (d, 1H, $^3J$ ($^1$H-$^1$H) = 1.9 Hz, Ar*H*), 7.59 (m, 2H, Ar*H*), 7.52-7.26 (m, 5H, Ar*H*), 5.26 (q, 1H, $^3J$ ($^1$H-$^1$H) = 6.5 Hz, C*H*OH), 4.87 (d, 1H, $^2J$ ($^1$H-$^1$H) = 12.1 Hz, C$H_a$H$_b$OH), 4.74 (d, 1H, $^2J$ ($^1$H-$^1$H) = 12.1 Hz, C$H_a$H$_b$), 2.78 (br s, 1H, O*H*), 2.70 (br s, 1H, O*H*), 1.65 (d, 3H, $^3J$ ($^1$H-$^1$H) = 6.5 Hz, C$H_3$); **$^{13}$C{$^1$H} NMR** (100.05 MHz, $CDCl_3$): $\delta_C$ 143.9 (C, $C_2$), 141.6 (C, $C_{10}$), 140.9 (C, $C_5$), 137.1 (C, $C_4$), 130.5 (CH, $C_3$), 128.9 (CH, $C_1$), 127.5 (CH, $C_{12}$), 127.2 (CH, $C_{14}$), 126.6 (CH, $C_{15}$), 124.9 (CH, $C_{11}$), 67.4 (CH, $C_6$), 63.7 ($CH_2$, $C_7$), 23.2 ($CH_3$, $C_8$); **IR $\nu_{max}$** (neat): 3329 (OH, $C_8$), 3058 (OH, $C_7$), 3030, 2972, 2926, 2249, 1667, 1600, 1566, 1485, 1450, 1104, 1022, 941, 852, 760, 698 cm$^{-1}$; **HRMS** found 251.1042 $C_{15}H_{16}O_2Na^+$ requires 251.1043 ($|\sigma|$ = 0.4 ppm).

**General Procedure B: *ortho*-Formylation of Phenols**

Anhydrous magnesium chloride (1.5 equiv.) was dried further by heating under vacuum (2 mbar) until free-flowing. To this was added THF (4 ml per mmol of phenol), phenol derivatives (1 equiv.), triethylamine (2.5 equiv.) and paraformaldehyde (4.5 equiv.). The mixture was heated to reflux for 18 h – **CARE! Carcinogenic α-chloroalkyl ether by-products may be formed, use an efficient hood!** Upon completion the reaction was quenched *via* the slow addition of excess HCl (2 M, 50 ml). The reaction was extracted with ethyl acetate (2 × 50 ml), dried over anhydrous sodium sulfate and the solvent removed *in vacuo* to yield the crude product which could be used without further purification. Essentially quantitative yields were attained.

**2-Hydroxy-4-methyl-benzaldehyde (34)**

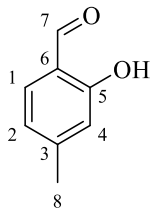


**34**

Synthesised according to **General Procedure B** using anhydrous magnesium chloride (2.86 g, 30.0 mmol), THF (80 ml), *m*-cresol (2.1 ml, 20.0 mmol), triethylamine (10.6 ml, 76.0 mmol) and paraformaldehyde (4.20 g, 140.0 mmol) to afford the crude product as a pale pink solid in a quantitative yield (2.81 g, 20.6 mmol) which was identified *via* $^{1}$H NMR spectroscopy and used without further purification. **$R_f$** (8:1 pentane:ethyl acetate): 0.83; **$^{1}$H NMR** (400.2 MHz, $CDCl_3$): $\delta_H$ 11.08 (s, 1H, O*H*), 9.81 (s, 1H, C*H*O), 7.42 (d, 1H, *J* = 7.9 Hz, Ar*H*), 6.85-6.77 (m, 2H, Ar*H*), 2.38 (s, 3H, C$H_3$); **$^{13}$C{$^{1}$H} NMR** (100.05 MHz, $CDCl_3$): $\delta_C$ 194.2 (C=O, $C_7$), 163.8 (C, $C_5$), 145.8 (C, $C_3$), 131.3 (CH, $C_1$), 123.0 (CH, $C_2$), 119.7 (CH, $C_4$), 118.5 (C, $C_6$), 21.2 (C, $C_8$). These data were in agreement with reported properties for **34** allowing its forward synthetic use.[126]

**2-Hydroxy-4-methoxy-benzaldehyde (35)**

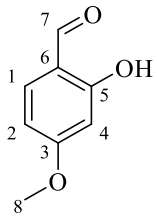


**35**

Synthesised according to **General Procedure B** using anhydrous magnesium chloride (2.86 g, 30.0 mmol), THF (80 ml), 3-methoxyphenol (2.2 ml, 20.0 mmol), trimethylamine (10.6 ml, 76.0 mmol) and paraformaldehyde (4.20 g, 140.0 mmol) to afford the crude product as a pale brown solid in a quantitative yield (3.20 g, 21.0 mmol) which was identified *via* $^{1}$H NMR spectroscopy and used without further purification. **$R_f$** (6:1 pentane:ethyl acetate): 0.69; **$^{1}$H NMR** (400.2 MHz, $CDCl_3$): $\delta_H$ 11.48 (s, 1H, O*H*), 9.72 (s, 1H, C*H*O), 7.43 (d, 1H, $^{3}J$ ($^{1}$H-$^{1}$H) = 8.7 Hz, Ar*H*), 6.54 (dd, 1H, $^{3}J$ ($^{1}$H-$^{1}$H) = 8.7 Hz and $^{4}J$ ($^{1}$H-$^{1}$H) = 2.3 Hz, Ar*H*), 6.43 (d, 1H, $^{4}J$ ($^{1}$H-$^{1}$H) = 2.3 Hz, Ar*H*), 3.86 (s, 3H, C$H_3$); **$^{13}$C{$^{1}$H} NMR** (100.05 MHz, $CDCl_3$): $\delta_C$ 194.5 (C=O, $C_7$), 167.8 (C, $C_3$), 163.8 (C, $C_5$), 135.3 (CH, $C_1$), 114.0 (CH, $C_6$), 107.7 (CH, $C_2$), 104.5 (C, $C_4$), 56.2 (C, $C_8$). These data were in agreement with reported properties for **35** allowing its forward synthetic use.[126]

**4-Fluoro-2-hydroxy-benzaldehyde (36)**

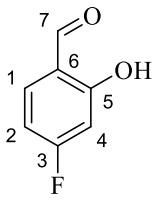


**36**

Synthesised according to **General Procedure B** using anhydrous magnesium chloride (2.86 g, 30.0 mmol), THF (80 ml), 3-fluorophenol (1.8 ml, 19.9 mmol), trimethylamine (10.6 ml, 76.0 mmol) and paraformaldehyde (4.20 g, 140.0 mmol) to afford the crude product as a pale pink oil in a quantitative yield (3.25 g, 23.2 mmol) which was identified *via* $^{1}$H NMR spectroscopy and used without further purification. **$R_f$** (8:1 pentane:ethyl acetate): 0.87; **$^{1}$H NMR** (400.1 MHz, $CDCl_3$): $\delta_H$ 11.36 (s, 1H, O*H*), 9.83 (s, 1H, C*H*O), 7.56 (dd, 1H, $^{3}J$ ($^{1}$H-$^{1}$H) = 8.6 Hz and $^{4}J$ ($^{1}$H-$^{1}$H) = 6.3 Hz, Ar*H*), 6.75-6.66 (m, 2H, Ar*H*); **$^{13}$C{$^{1}$H} NMR** (100.05 MHz, $CDCl_3$): $\delta_C$ 194.4 (C=O, $C_7$), 170.8 (C, $C_3$), 163.3 (C, $C_5$), 133.3 (CH, $C_1$), 116.5 (CH, $C_6$), 107.7 (CH, $C_2$), 104.8 (C, $C_4$). These data were in agreement with reported properties for **36** allowing its forward synthetic use.[203]

**Acetic acid hydrazide (37)**

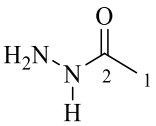


**37**

Compound **37** was prepared by a modification of a literature method,[204] as described below. A solution of hydrazine monohydrate (4.4 ml, 90.7 mmol) and ethyl acetate (10.0 ml, 102 mmol) in ethanol (20 ml) was heated at reflux for 24 h. Once cooled,

the solvents were removed *in vacuo* and the resulting oil was resuspended in hexane (to precipitate the product) which was once more removed *in vacuo* to give the product as a colourless solid in 83% yield (5.60 g, 75.6 mmol) which was used as obtained. **$^{1}$H NMR** (400.2 MHz, $CDCl_3$): $\delta_H$ 7.33 (br s, 1H, N*H*), 3.90 (br s, 2H, N$H_2$), 1.94 (s, 3H, C$H_3$); **$^{13}$C{$^{1}$H} NMR** (100.05 MHz, $CDCl_3$): $\delta_C$ 169.7 (C=O, $C_2$), 20.6 ($CH_3$, $C_1$). These data were in agreement with the reported spectroscopic properties of **37**.[204]

**General Procedure C**: **Synthesis of hydrazides**

A literature procedure[126] was used. A mixture of *o*-formyl-phenol derivatives (1 equiv.) and acetic acid hydrazide (1 equiv.) in ethanol (4.5 ml per mmol of phenol derivative) was heated to reflux for 18 h. After cooling, the solvent was removed *in vacuo* to yield the crude product which was washed with diethyl ether and then used without further purification. Typically, the hydrazides are isolated in near quantitative yield as mixture of interconverting (*E*)/(*Z*) conformational isomers.[126] In our examples peak separation was only seen for the OH resonances, the higher chemical shifts being assigned to the hydrogen bonded (*E*)-isomers:

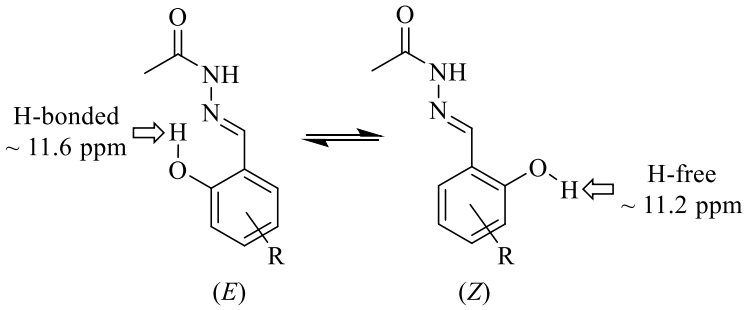


**38-40**

**(*2E*)-2-[(2-Hydroxy-4-methylphenyl)methylene]-acetic acid hydrazide (38)**

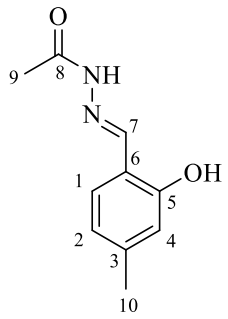


**38**

Synthesised according to **General Procedure C** using phenol **34** (3.02 g, 22.2 mmol) and **29** (1.64 g, 22.1 mmol) in ethanol (100 ml) to afford the crude product as a colourless solid in 96% yield (4.09 g, 21.3 mmol) which was identified *via* $^{1}$H NMR spectroscopy and used without further purification. **$R_f$** (ethyl acetate): 0.64; **$^{1}$H NMR** (400.2 MHz, DMSO-$d_6$): $\delta_{\mathbf{H}}$ 10.56 and 10.07 (2 × s, 1H, O*H*), 10.18 and 10.16 (2 × s, 1H, N*H*), 8.27 and 8.21 (2 × s, 1H, NC*H*), 7.47 and 7.35 (2 × d, 1H, $^{3}J$ ($^{1}$H-$^{1}$H) = 7.7 Hz, Ar*H*), 6.72-6.67 (m, 2H, Ar*H*), 2.26 and 2.24 (2 × s, 3H, ArC*H*$_3$), 2.15 and 1.96 (2 × s, 3H, COC*H*$_3$). These data were in agreement with reported properties for **38** allowing its immediate forward synthetic use.[126]

**(*2E*)-2-[(2-Hydroxy-4-methoxyphenyl)methylene]-acetic acid hydrazide (39)**

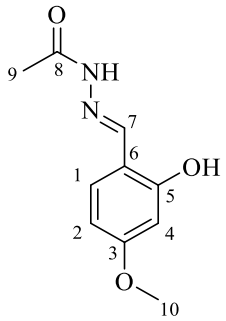


**39**

Synthesised according to **General Procedure C** using phenol **35** (3.20 g, 21.0 mmol) and **29** (1.56 g, 21.1 mmol) in ethanol (100 ml) to afford the crude product as a pale yellow solid in 88% yield (3.86 g, 18.5 mmol) which was identified *via* $^{1}$H NMR spectroscopy and used without further purification. **$R_f$** (ethyl acetate): 0.50; **$^{1}$H NMR** (400.2 MHz, DMSO-$d_6$): $\delta_H$ 11.49 and 11.09 (2 × s, 1H, O*H*), 11.47 and 10.30 (2 × s, 1H, N*H*), 8.22 and 8.14 (2 × s, 1H, NC*H*), 7.47 and 7.35 (2 × d, 1H, $^{3}J$ ($^{1}$H-$^{1}$H) = 8.5 Hz, Ar*H*), 6.51-6.41 (m, 2H, Ar*H*), 3.73 and 3.72 (2 × s, 3H, $OCH_3$), 2.12 and 1.93 (2 × s, 3H, COC$H_3$). These data were in agreement with reported properties for **39** allowing its immediate forward synthetic use.[126]

**(*2E*)-2-[(4-Fluoro-2-hydroxyphenyl)methylene]-acetic acid hydrazide (40)**

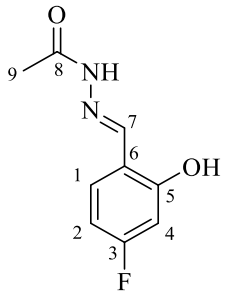


**40**

Synthesised according to **General Procedure C** using phenol **36** (3.26 g, 23.3 mmol) and **29** (1.70 g, 22.9 mmol) in ethanol (100 ml) to afford the crude product as a pale pink solid in 91% yield (4.10 g, 20.9 mmol) which was identified by $^{1}$H NMR spectroscopy and used without further purification. **$R_f$** (ethyl acetate): 0.32; **$^{1}$H NMR** (400.1 MHz, DMSO-$d_6$): $\delta_H$ 11.60 and 11.20 (2 × s, 1H, O*H*), 8.30 and 8.20 (2 × s, 1H, NC*H*), 7.66 and 7.55 (2 × dd, 1H, $^{3}J$ ($^{1}$H-$^{1}$H) = 8.4 Hz and $^{4}J$ ($^{1}$H-$^{1}$H) = 7.0 Hz, Ar*H*), 6.77 and 6.66 (m, 2H, Ar*H*), 2.15 and 1.95 (2 × s, 3H, COC$H_3$). These data were in agreement with reported properties for **40** allowing its immediate forward synthetic use.[126]

**General Procedure D: Synthesis of 2-acetyl-benzaldehyde derivatives**

A literature procedure was used with slight modifications.[126] To lead (IV) acetate (1.1 equiv.) was added THF (5 ml per mmol of hydrazide) followed by the portion wise addition of the hydrazide derivative (1 equiv.). After stirring at RT for 2 h, after which the majority of effervescence has ceased, the reaction was filtered through Celite®. The crude material was then diluted into ethyl acetate (100 ml), washed with saturated sodium hydrogen carbonate (50 ml) and water (50 ml) and dried over anhydrous magnesium sulfate. After removal of the solvent *in vacuo*, the crude

product was purified *via* flash column chromatography (eluent: 4:1 pentane:ethyl acetate) to yield the products which were typically used as obtained immediately, due to their high reactivity towards self-condensation.

**2-Acetyl-4-methyl-benzaldehyde (41)**

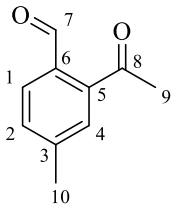


**41**

Synthesised according to **General Procedure D** using lead (IV) acetate (2.20 g, 4.96 mmol), hydrazide **38** (0.86 g, 4.47 mmol) and THF (22 ml) to give the product as a yellow oil in 47% yield (337 mg, 2.08 mmol). NOTE: The product is unstable at RT and will darken in colour if left. If stored at -20 °C, product was usable for up to 4 weeks and solidified to a low melting yellow solid. **$R_f$** (ethyl acetate): 0.86; **$^1$H NMR** (400.2 MHz, $CDCl_3$): $\delta_H$ 10.16 (s, 1H, C*H*O), 7.80 (d, 1H, $^3J$ ($^1$H-$^1$H) = 7.8 Hz, Ar*H*), 7.44 (m, 2H, Ar*H*), 2.63 (s, 3H, C$H_3$), 2.48 (s, 3H, C$H_3$); **$^{13}$C{$^1$H} NMR** (100.05 MHz, $CDCl_3$): $\delta_C$ 201.7 (C=O, $C_8$), 191.8 (CHO, $C_7$), 144.3 (C, $C_3$), 141.1 (C, $C_5$), 133.3 (C, $C_6$), 132.1 (CH, $C_2$), 130.1 (CH, $C_4$), 128.9 (CH, $C_1$), 29.1 ($CH_3$, $C_9$), 21.7 ($CH_3$, $C_{10}$). These data were in agreement with reported properties for **41** allowing its immediate forward synthetic use.[126]

**2-Acetyl-4-methoxy-benzaldehyde (42)**

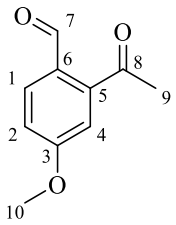


**42**

Synthesised according to **General Procedure D** using lead (IV) acetate (3.10 g, 6.99 mmol), hydrazide **39** (1.3 g, 6.24 mmol) and THF (31 ml) to give the product as a yellow solid in 56% yield (625 mg, 3.51 mmol). NOTE: The product is unstable at RT and will darken in colour if left. If stored at -20 °C, product was usable for up to 4 weeks. **$R_f$** (ethyl acetate): 0.86; **$^1$H NMR** (400.2 MHz, $CDCl_3$): $\delta_H$ 10.01 (s, 1H, C*H*O), 7.85 (dd, 1H, $^3J$ ($^1$H-$^1$H) = 8.4 Hz and $^4J$ ($^1$H-$^1$H) = 0.6 Hz, Ar*H*), 7.10-7.03 (m, 2H, Ar*H*), 3.88 (s, 3H, OC*H*$_3$), 2.56 (s, 3H, COC*H*$_3$); **$^{13}$C{$^1$H} NMR** (100.05 MHz, $CDCl_3$): $\delta_C$ 202.5 (C=O, $C_8$), 190.9 (CHO, $C_7$), 164.1 (C, $C_3$), 144.3 (C, $C_5$), 133.6 (CH, $C_1$), 128.4 (C, $C_6$), 115.8 (CH, $C_2$ or $C_4$), 114.5 (CH, $C_4$ or $C_2$), 56.3 ($CH_3$, $C_{10}$), 30.1 ($CH_3$, $C_9$ ). These data were in agreement with reported properties for **42** allowing its forward synthetic use.[126]

**2-Acetyl-4-fluoro-benzaldehyde (43)**

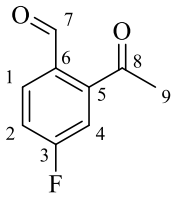


**43**

Synthesised according to **General Procedure D** using lead (IV) acetate (2.89 g, 6.52 mmol), hydrazide **40** (1.14 g, 5.81 mmol) and THF (29 ml) to give the product as a yellow solid in 60% yield (580 mg, 3.49 mmol). NOTE: The product is unstable at RT and will darken in colour if left. If stored at -20 °C, product was usable for up to 4 weeks. **$R_f$** (4:1 pentane:ethyl acetate): 0.58; **$^{1}$H NMR** (400.2 MHz, $CDCl_3$): $\delta_H$ 10.10 (s, 1H, C*H*O), 7.94 (dd, 1H, $^{3}J$ ($^{1}$H-$^{1}$H) = 8.5 Hz and $^{4}J$ ($^{1}$H-$^{1}$H) = 5.5 Hz, Ar*H*), 7.36-7.30 (m, 2H, Ar*H*), 2.61 (s, 3H, COC$H_3$); **$^{13}$C{$^{1}$H} NMR** (100.05 MHz, $CDCl_3$): $\delta_C$ 200.0 (C=O, $C_7$), 190.5 (CHO, $C_8$), 165.2 (C, $C_3$, d, $^{1}J$ ($^{13}$C-$^{19}$F) = 258.1 Hz), 143.6 (C, $C_5$, d, $^{3}J$ ($^{13}$C-$^{19}$F) = 7.1 Hz), 133.0 (CH, $C_1$, d, $^{3}J$ ($^{13}$C-$^{19}$F) = 9.1 Hz), 132.1 (C, $C_6$, d, $^{4}J$ ($^{13}$C-$^{19}$F) = 3.1 Hz), 118.7 (CH, $C_2$, d, $^{2}J$ ($^{13}$C-$^{19}$F) = 21.9 Hz), 115.8 (CH, $C_4$, d, $^{2}J$ ($^{13}$C-$^{19}$F) = 23.4 Hz), 29.22 ($CH_3$, $C_9$); **$^{19}$F NMR** (376.5 MHz, $CDCl_3$): $\delta_F$ -102.86 (ddd, $J$ = 8.2, 8.2, 5.5 Hz); **IR $\nu_{max}$** (neat): 3082, 2904, 1769 (C=O), 1676 (CHO), 1598, 1579, 1488, 1423, 1360, 1271, 1256, 1197, 968, 959, 914, 875, 842, 806, 731, 655, 574, 523, 475 cm$^{-1}$; **HRMS** found 189.0326 $C_9H_7O_2FNa^+$ requires 189.0322 (|σ| = 2.1 ppm).

## 4.5.4. Attempted complexation studies using ligands derived from 24

**Attempted preparation of *ansa* complex (24ae)**

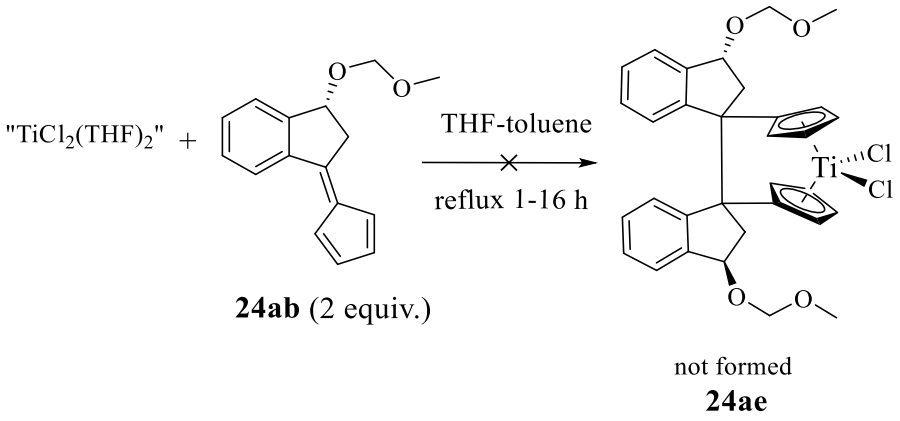


**24ab** (2 equiv.)

not formed
**24ae**

To a solution of titanium tetrachloride (0.5 equiv.) in toluene:THF (95:5) at -78 ºC was added *n*-BuLi (2 equiv.). To the resulted mixture, fulvene **24ab** in THF (200 mg, 0.83 mmol) was added and left for reflux for 1-16 h. Nothing could be isolated from the resultant complex mixtures.

**Preparation of cyclopentadienyl ligands (24ac) and (24ad)**

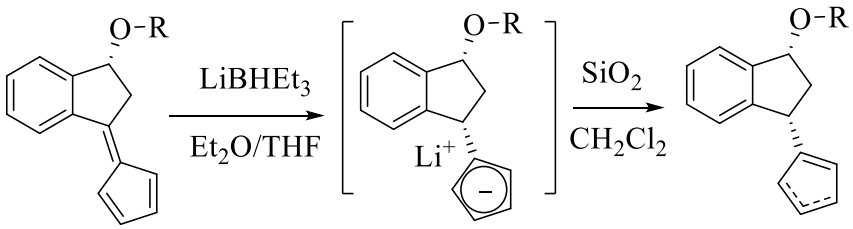


**24aa** R = TES
**24ab** R = MOM

**24ac** R = TES
**24ad** R = MOM

Cyclopentadienyl ligands **24ac** and **24ad** were provided by the procedure of Nouch,[116] in collaboration with that worker, as previously described.[116] Solutions of protected fulvenes (**24aa** or **24ab**)[116] (1 equiv., in THF:ether 2:1) were cooled to -45 ºC before dropwise addition of $LiBHEt_3$ (4 equiv. in $Et_2O$; prepared by THF removal from commercial THF solutions of $LiBHEt_3$ and addition of dry $Et_2O$ under nitrogen). The resulting fulvene mixtures were allowed to warm to 0 ºC and then to

RT over 1 h. The solvents were removed on a vacuum line and the resulting oils redissolved in dichloromethane. Purification by silica chromatography in the same solvent provided the products (colourless oils) as a 1:1 mixture of two double bond isomers, but with >16:1 stereoselectivity towards the *syn* products. Typical yields: **24ac** 74%, **24ad** 51%. Samples of **24ac** and **24ad** were noted to decompose after preparation (>25%, within 2-4 days at RT) to intractable uncharacterised species. They were thus always used as freshly prepared, when their NMR properties were identical to published values.[115] Alternatively, the crude reaction mixtures, containing the lithium cyclopentadienide intermediate were used directly.

For **24ac** (1:1 mixture of C=C tautomers): **$^1$H NMR** (400.1 MHz, $CDCl_3$): $\delta_H$ 7.39-7.35 (m, 2H, Ar*H*), 7.29-7.16 (m, 4H, Ar*H*), 7.06-7.00 (m, 2H, Ar*H*), 6.50-6.46 (m, 1H, Cp*H*), 6.46-6.43 (m, 2H, Cp*H*), 6.42-6.40 (m, 1H, Cp*H*), 6.35-6.32 (m, 1H, Cp*H*), 6.25-6.20 (m, 1H, Cp*H*), 5.26 (t, 1H, $^3J$ ($^1$H-$^1$H) = 8.0 Hz, C*H*O), 5.23 (t, 1H, $^3J$ ($^1$H-$^1$H) = 8.0 Hz, C*H*O), 4.11 (dd, 1H, $^3J$ ($^1$H-$^1$H) = 10.4, 7.0 Hz, C*H*Cp), 4.05 (dd, 1H, $^3J$ ($^1$H-$^1$H) = 10.4, 7.0 Hz, C*H*Cp), 3.06-2.69 (m, 2H, C$H_a$H$_b$ *anti* to OR and $CH_2$), 2.00-1.89 (m, 2H, CH$_a$C$H_b$ *syn* to OR), 1.05 (t, 18H, $^3J$ ($^1$H-$^1$H) = 7.9 Hz, $CH_2CH_3$), 0.73 (q, 12H, $^3J$ = 7.9 Hz, C$H_2$CH$_3$). The data were identical to an authentic sample.[116]

For **24ad** (1:1 mixture of C=C tautomers): **$^1$H NMR** (400.1 MHz, $CDCl_3$): $\delta_H$ 7.45-7.41 (m, 2H, Ar*H*), 7.30-7.23 (m, 4H, Ar*H*), 7.11-7.07 (m, 2H, Ar*H*), 6.49-6.41 (m, 3H, Cp*H*), 6.39-6.37 (m, 1H, Cp*H*), 6.34-6.30 (m, 1H, $^3J$ ($^1$H-$^1$H) = 5.4, 1.5 Hz, Cp*H*), 6.22-6.20 (m, 1H, Cp*H*), 5.17 (dd, 1H, $^3J$ ($^1$H-$^1$H) = 7.0, 7.0 Hz, C*H*O), 5.14 (dd, 1H, $^3J$ ($^1$H-$^1$H) = 7.0, 7.0 Hz, C*H*O), 4.89 (s, 2H, OC$H_2$O), 4.87 (s, 2H, OC$H_2$O), 4.16 (dd, 1H, $^3J$ ($^1$H-$^1$H) = 8.2, 8.2 Hz, C*H*Cp), 4.10 (dd, 1H, $^3J$ ($^1$H-$^1$H) = 8.2, 8.2 Hz,

C*H*Cp), 3.48 (s, 6H, OC$H_3$), 3.05-2.79 (m, 2H, C$H_a$C$H_b$ *anti* to OR and C$H_2$), 2.08-1.96 (m, 2H, C$H_a$C$H_b$ *syn* to OR). The data were identical to an authentic sample.[116]

Exposure of samples of **24ac** and **24ad** (0.1 M in THF or $Et_2O$) to *n*-BuLi (1.1 equiv.) followed by $D_2O$ quench led to net 1H reduction in the overall integral intensity across all CpH signals consistent with ready formation of the lithium cyclopentadienide similar to that postulated[128] for the $LiBHEt_3$ reduction above.

**Attempted complexation of cyclopentadienyl ligand 24ac *via* deprotonation**

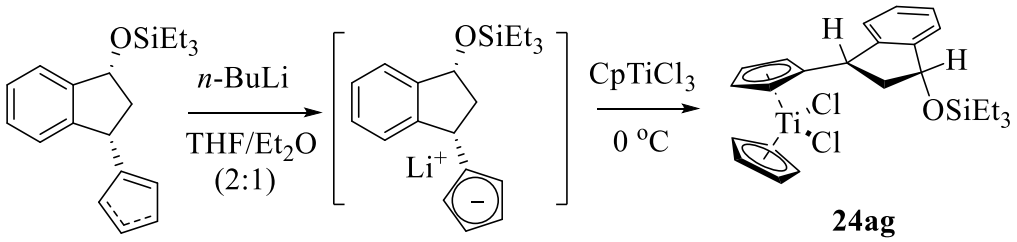


**24ac** **24ag** (at best trace in a complex mixture)

A solution of **24ac** (100 mg, 0.31 mmol) in THF:ether 2:1 (1 ml) was cooled to -78 °C before the addition of *n*-BuLi (1 equiv.) and the resultant mixture allowed to come to 0 °C. Solid (cyclopentadienyl)titanium trichloride (68 mg, 0.31 mmol) in THF (1 ml) was added at 0 °C and the mixture left to warm up at RT (reaction times 1 and 16 h were trialled). Analysis of the reaction mixtures by $^1$H NMR spectroscopy always revealed a complex mixture (see **Scheme 29**). All attempts to isolate putative **24ag** from such mixtures were unsuccessful. Similar observations were made for use of ligand **24ad**.

**Attempted complexation by interception of the $LiBHEt_3$ reduction product of 24ab**

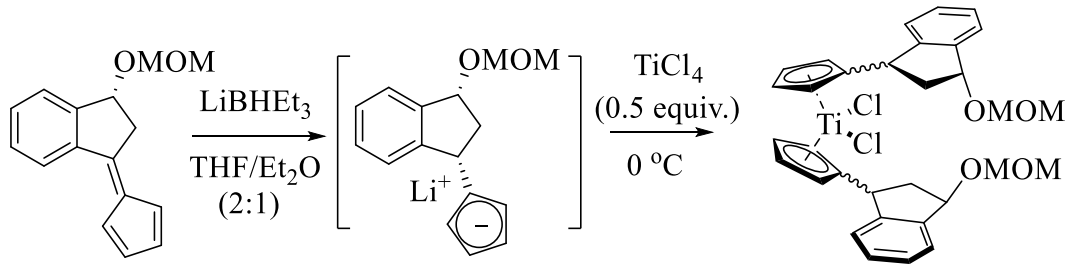


**24ab**

**24af**
(unstable, decomposes)

A solution of protected fulvene **24ab** (100 mg, 0.41 mmol) in THF:ether 2:1 (2 ml) was cooled to -45 °C before dropwise addition of $LiBHEt_3$ (4 equiv. 1 M in $Et_2O$; prepared by THF removal from commercial THF solutions of $LiBHEt_3$ and addition of dry $Et_2O$ under nitrogen). A solution of $TiCl_4$ (0.2 mmol) in $Et_2O$ (1 ml) was added and the resulting mixture allowed to warm to 0 °C and then to RT over 1 h. The solvents were removed on a vacuum line to afford a red oil. All attempts to isolate compound **24af** from these reaction mixtures led to the decomposition of the compounds observed in the crude reaction mixtures. However, on one occasion when nominal **24af** was formed we could attain $^1H$ NMR as shown in spectra below (see Results and Discussion p 65).

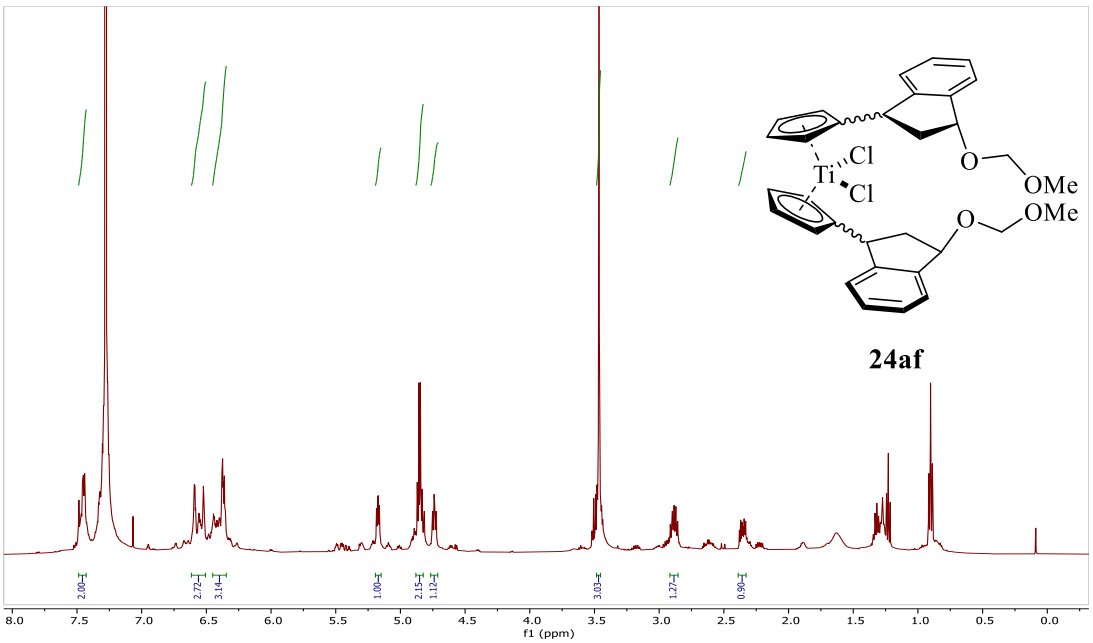

## 4.6. Experimental Data for Chapter 3

### *N*-(3-Chloro-4-hydroxyphenyl)isobutyramide (44)

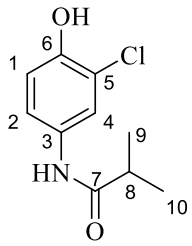


**44**

***44** recrystallised*

A solution of 4-amino-2-chlorophenol (953 mg, 6.64 mmol) and sodium acetate (570 mg, 6.90 mmol) in acetone (28 ml) was cooled to 0 °C before dropwise addition of isobutyryl chloride (726 µl, 738 mg, 6.93 mmol). The resulting mixture was stirred at RT for 5 h before being quenched *via* the addition of water (50 ml). Extraction with ethyl acetate (3 x 50 ml), drying over anhydrous sodium sulfate and the removal of solvents *in vacuo* yielded the crude product as a tan solid. The product was further purified *via* crystallisation (2:1 pentane:ether) to afford pale pink needles (1.21 g, 5.70 mmol, 87%). **M.p.**: 151-152 °C; **$^1$H NMR** (500.1 MHz, DMSO-$d_6$): $\delta_H$ 9.84 (s, 1H, ArN*H*), 9.69 (s, 1H, ArO*H*), 7.70 (d, 1H, $^4J$ ($^1$H-$^1$H) = 2.5 Hz, Ar*H*), 7.25 (dd, 1H, $^3J$ ($^1$H-$^1$H) = 8.9 Hz and $^4J$ ($^1$H-$^1$H) = 2.5, Hz, Ar*H*), 6.87 (d, 1H, $^3J$ ($^1$H-$^1$H) = 8.9 Hz, Ar*H*), 1.09 (s, 3H, *C*$H_3$), 1.07 (s, 3H, *C*$H_3$); **$^{13}$C{$^1$H} NMR** (125.025 MHz, DMSO-$d_6$): $\delta_C$ 175.2 (C=O, $C_7$), 149.1 (C, $C_6$), 132.4 (C, $C_3$), 121.20 (CH, $C_4$), 119.7 (CH, $C_2$), 119.5 (C, $C_5$), 116.9 (CH, $C_1$), 35.3 (CH, $C_8$), 20.0 ($CH_3$, $C_{9,10}$); **IR $\nu_{max}$** (neat): 3219 (NH), 3165 (OH), 3064, 2969, 1632 (C=O), 1500, 1411, 1294, 1281, 1232, 1160, 1095, 1050, 956, 819, 680, 533, 436 cm$^{-1}$; **HRMS** found 236.0452 $(M+Na)^+$ Calcd. for $C_{10}H_{12}ClNO_2$ 236.0449 ($|\sigma|$ = 1.27 ppm).

**4-(Hydroxymethyl)-2-methoxyphenol (45)**

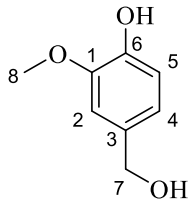


**45**

The compound was prepared by a literature method as described below.[205] To a solution of commercial vanillin (6.43 g, 42.3 mmol) in methanol (150 ml) was added portionwise an excess of sodium borohydride (3.20 g, 84.6 mmol, 2 equiv.) over 10-15 min. The resulting mixture was stirred at RT for 1 h. The reaction then was worked up by dilution with ethyl acetate (50 ml), washing with saturated $NH_4Cl$ (50 ml) and brine (50 ml), drying over anhydrous sodium sulfate, and the solvent removed *in vacuo* to afford colourless solid in 83% yield (5.38 g, 34.9 mmol). **$^1$H NMR** (500.1 MHz, DMSO-$d_6$): $\delta_H$ 8.76 (s, 1H, O*H*), 6.88 (app. s, 1H, Ar*H*), 6.74-6.67 (m, 2H, $^4J$ ($^1$H-$^1$H) = 2.3 Hz, Ar*H*), 4.98 (t, 1H, $^3J$ ($^1$H-$^1$H) = 5.7 Hz, O*H*), 4.37 (d, 2H, $^2J$ ($^1$H-$^1$H) = 5.6 Hz, Ar*C*$H_2$), 3.75 (s, 3H, ArO*C*$H_3$); **$^{13}$C{$^1$H} NMR** (125.0 MHz, DMSO-$d_6$): $\delta_C$ 147.8 (C, $C_6$), 145.7 (C, $C_1$), 134.0 (C, $C_3$), 119.5 (CH, $C_4$), 115.5 (CH, $C_5$), 111.5 (CH, $C_2$), 63.5 ($CH_2$, $C_7$), 56.0 ($CH_3$, $C_8$). These data were in agreement with reported properties for **45** allowing its forward synthetic use.[205] However, use of **45** in General Procedure E led only to decomposition.

**2-Methoxy-4-(((methylsulfonyl)oxy)methyl)phenyl methanesulfonate (45b)**

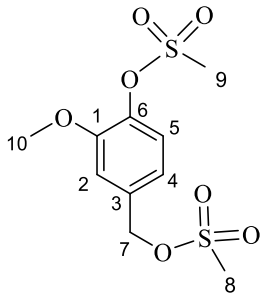


**45b**

To a solution of 4-(hydroxymethyl)-2-methoxyphenol **45** (200 mg, 1.30 mmol) in dichloromethane (10 ml) was added trimethylamine (0.54 ml, 3.90 mmol) and was left to stir for 10 min at RT. The mixture was cooled down to -10 $^{o}$C before the addition of mesyl chloride (0.30 ml, 3.90 mmol) and left to stir for 2 h at 0 $^{o}$C. The resulting brown reaction mixture was quenched *via* the addition of sodium hydrogen carbonate and water (50 ml) before being extracted with dichloromethane (3 × 25 ml), dried over anhydrous magnesium sulfate and the solvents removed *in vacuo* to afford the product as a tan oil in 73% yield (296 mg, 0.95 mmol). **$^{1}$H NMR** (500.1 MHz, $CDCl_3$): $\delta_H$ 7.35 (d, 1H, $^{3}J$ ($^{1}$H-$^{1}$H) = 8.2 Hz, Ar*H*), 7.06 (m, 2H, Ar*H*), 5.24 (s, 2H, ArC$H_2$), 3.96 (s, 3H, ArOC$H_3$), 3.23 (s, 3H, $CH_3$), 3.02 (s, 3H, $CH_3$); **$^{13}$C{$^{1}$H} NMR** (125.0 MHz, $CDCl_3$): $\delta_C$ 151.8 (C, $C_1$), 138.8 (C, $C_6$), 133.8 (C, $C_3$), 124.9 (CH, $C_4$), 121.3 (CH, $C_5$), 113.1 (CH, $C_2$), 70.4 ($CH_2$, $C_7$), 56.2 ($CH_3$, $C_{10}$), 38.5 ($CH_3$, $C_8$), 38.3 ($CH_3$, $C_9$). These data were in agreement with reported properties for **45b** allowing its forward synthetic use.[206] However, use of **45b** in General Procedure E led only to decomposition.

**4-Methoxy-2-methylphenol (46d)**

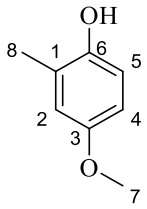


**46d**

The compound was prepared by a literature method as described below.[141] Hydrogen peroxide in water (0.6 ml of 100 volume aqueous solution, 5.8 mmol) and sulfuric acid (0.05 ml, ca. 0.1 g, 1.2 mmol) were added dropwise sequentially to a solution of 4-methoxy-2-methylbenzaldehyde (**45c**) (0.50 g, 3.33 mmol) in methanol (5.4 ml). The resulting orange mixture was stirred at RT for 20 h. The reaction was extracted with dichloromethane (3 × 25 ml) and washed with water. After drying over anhydrous sodium sulfate the solvent was removed *in vacuo*. The crude product was purified *via* flash column chromatography (eluent: chloroform) to afford the product as a pale tan oil in 98% yield (454 mg, 3.28 mmol). **M.p.**: 63-64 °C [Lit **M.p.**: 64-65 °C[207]]; **$^{1}$H NMR** (500.1 MHz, $CDCl_3$): $\delta_H$ 6.75-6.71 (m, 2H, Ar*H*), 6.65 (dd, 1H, $^{3}J$ ($^{1}$H-$^{1}$H) = 8.7 Hz and $^{4}J$ ($^{1}$H-$^{1}$H) = 3.0 Hz, Ar*H*), 4.41 (s, 1H, O*H*), 3.78 (s, 3H, O$CH_3$), 2.26 (s, 3H, $CH_3$); **$^{13}$C{$^{1}$H} NMR** (125.0 MHz, $CDCl_3$): $\delta_C$ 153.6 (C, $C_3$), 147.7 (C, $C_6$), 124.8 (C, $C_1$), 116.6 (CH, $C_2$), 115.5 (CH, $C_5$), 111.8 (CH, $C_4$), 55.7 ($CH_3$, $C_7$), 16.1 ($CH_3$, $C_8$). These data were in agreement with reported properties for **46d**.[208]

**2,4-Dimethoxyphenol (46e)**

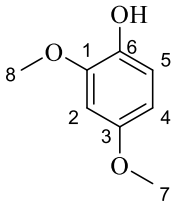


**46e**

The compound was prepared by a literature approach as described below.[209] Hydrogen peroxide in water (3.0 ml of 100 volume aqueous solution, 29 mmol) and sulfuric acid (0.3 ml, ca. 0.5 g, 5.5 mmol) were added dropwise sequentially to a solution of 2,4-dimethoxybenzaldehyde (**45d**) (3.0 g, 18 mmol) in methanol (30 ml). The resulting orange mixture was stirred at RT for 20 h. The reaction was extracted with dichloromethane (3 × 50 ml) and washed with water. After drying over anhydrous sodium sulfate the solvent was removed *in vacuo.* The crude product was purified *via* flash column chromatography (eluent: chloroform) to afford the product as a colourless oil in quantitative yield (2.7 g, 18 mmol). **$^{1}$H NMR** (500.1 MHz, $CDCl_3$): $\delta_H$ 6.86 (d, 1H, $^{3}J$ ($^{1}$H-$^{1}$H) = 8.7 Hz, Ar*H)*, 6.51 (d, 1H, $^{4}J$ ($^{1}$H-$^{1}$H) = 2.8 Hz, Ar*H*), 6.40 (dd, 1H, $^{3}J$ ($^{1}$H-$^{1}$H) = 8.7 Hz and $^{4}J$ ($^{1}$H-$^{1}$H) = 2.8 Hz, Ar*H*), 5.22 (s, 1H, Ar*OH*), 3.89 (s, 3H, O*CH*$_3$), 3.78 (s, 3H, O*CH*$_3$); **$^{13}$C{$^{1}$H} NMR** (125.0 MHz, $CDCl_3$): $\delta_C$ 153.5 (C, $C_3$), 147.0 (C, $C_1$), 139.7 (C, $C_6$), 114.0 (CH, $C_5$), 104.2 (CH, $C_4$), 99.4 (CH, $C_2$), 55.8 ($CH_3$, $C_7$ or $C_8$); **HRMS** found 177.0526 $(M+Na)^+$ Calcd. for $C_8H_{11}O_3$ 177.0522 ($|\sigma|$ = 2.26 ppm). These data were in agreement with reported properties for **46e** allowing its forward synthetic use.[141] It was used directly in General Procedure E.

**General Procedure E: synthesis of amine *bis*(phenolate) ligand derivatives**

The phenol **46** (1 equiv.) was dissolved with stirring (10 min) in toluene. To the resulting solution solid paraformaldehyde (1.5 equiv.) was added followed by methylamine (0.6 equiv. using a 40% w/w aqueous solution). The flask was equipped with water separator (Dean-Stark) and the mixture heated to reflux until water separation stopped (3-5 h). The solvent was removed *in vacuo* and the crude product oil was heated to 150 °C for 1 hour. The resulting oily material was crystallised from diethyl ether at 4 °C.

**6,6'-((Methylazanediyl)*bis*(methylene))*bis*(2,4-dimethylphenol) (47a)**

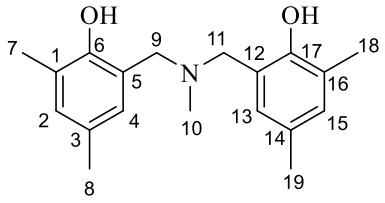


**47a**

Synthesised according to **General Procedure E** using toluene (30 ml), 2,4-dimethylphenol (**46a**) (7.68 ml, 62.8 mmol) and paraformaldehyde (2.82 g, 94.5 mmol) 40% w/w aqueous methylamine (2.60 ml, 36.0 mmol) to afford a colourless solid in 46% yield (4.3 g, 14.3 mmol). **$^{1}$H NMR** (400.1 MHz, $CDCl_3$): $\delta_H$ 6.90 (d, 2H, $^4J$ ($^1$H-$^1$H) = 2.1 Hz, *Ar*H), 6.76 (d, 2H, $^4J$ ($^1$H-$^1$H) = 2.1 Hz, *Ar*H), 3.64 (s, 4H, *Ar*$CH_2$N), 2.25 (s, 6H, *Ar*$CH_3$), 2.24 (s, 3H, *N*$CH_3$), 2.23 (s, 6H, *Ar*$CH_3$); **$^{13}$C{$^{1}$H} NMR** (100.0 MHz, $CDCl_3$): $\delta_C$ 152.0 (C, $C_6$ or $C_{17}$), 131.0 (CH, $C_2$ or $C_{15}$), 128.4 (C, $C_3$ or $C_{14}$), 128.3 (CH, $C_4$ or $C_{13}$), 124.3 (C, $C_5$ or $C_{12}$), 122.0 (C, $C_1$ or $C_{16}$), 59.4 ($CH_2$, $C_9$ or $C_{11}$), 41.11 ($CH_3$, $C_{10}$), 20.5 ($CH_3$, $C_8$ or $C_{19}$), 15.9 ($CH_3$, $C_7$ or $C_{18}$); **HRMS** found 300.1981 $[M+H]^+$ Calcd. for $C_{19}H_{26}NO_2$ 300.1958. The OH peaks were not observed due to exchange. These data were in agreement with reported

properties for **47a** allowing its forward synthetic use.[144] It was used directly in General Procedure F.

**6,6'-((Methylazanediyl)*bis*(methylene))*bis*(2-methoxy-4-methylphenol) (47b)**

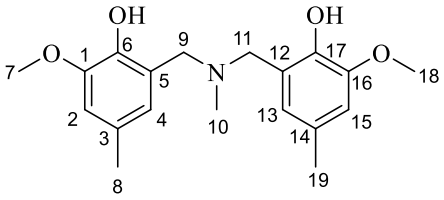


**47b**

Synthesised according to **General Procedure E** using toluene (15 ml), 2-methoxy-4-methylphenol (**46b**) (621 mg, 4.50 mmol) and paraformaldehyde (202 mg, 6.75 mmol) 40% w/w aqueous methylamine (206 µl, 2.84 mmol) to afford colourless columnar crystal in 80% yield (594 mg, 1.79 mmol). **M.p.**: 76-77 $^{o}$C; **$^{1}$H NMR** (500.1 MHz, $CDCl_3$): $\delta_H$ 8.42 (br s, 2H, O*H*), 6.63 (d, 2H, $^{4}J$ ($^{1}$H-$^{1}$H) = 1.8 Hz, Ar*H*), 6.55 (d, 2H, $^{4}J$ ($^{1}$H-$^{1}$H) = 1.8 Hz, Ar*H*), 3.87 (s, 6H, ArO$CH_3$), 3.70 (s, 4H, Ar$CH_2$N), 2.28 (s, 6H, Ar$CH_3$), 2.21 (s, 3H, N$CH_3$); **$^{13}$C{$^{1}$H} NMR** (125.0 MHz, $CDCl_3$): $\delta_C$ 147.0 (C, $C_1$ or $C_{16}$), 143.5 (C, $C_6$ or $C_{17}$), 128.2 (C, $C_3$ or $C_{14}$), 122.3 (C, $C_5$ or $C_{12}$), 122.1 (CH, $C_4$ or $C_{13}$), 111.3 (CH, $C_2$ or $C_{15}$), 58.5 ($CH_2$, $C_9$ or $C_{11}$), 55.9 ($CH_3$, $C_7$ or $C_{18}$), 40.8 (*N*$CH_3$, $C_{10}$), 21.0 ($CH_3$, $C_8$ or $C_{19}$); **IR $\nu_{max}$** (neat): 3381 (OH), 3008 ($NCH_3$), 2950 ($OCH_3$), 2913, 2848, 2806, 1605, 1497, 1460, 1418, 1365, 1297, 1236, 1210, 1194, 1156, 1121, 1086, 986, 966, 955, 922, 875, 841, 833, 787, 757, 740, 592, 566, 552 cm$^{-1}$; **HRMS** found 354.1660 $(M+Na)^+$ Calcd. for $C_{19}H_{25}NO_4$ 354.1676 (|σ| = 4.5 ppm); **Anal**: Calcd. (%) for $C_{19}H_{25}NO_4$: C, 68.86; H, 7.60; N, 4.23; found: C, 68.90; H, 7.62; N, 4.2.

**6,6'-((Ethylazanediyl)*bis*(methylene))*bis*(2-methoxy-4-methylphenol) (47c)**

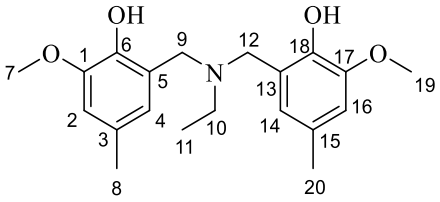


**47c**

Synthesised according to **General Procedure E** using toluene (25 ml), 2-methoxy-4-methylphenol (**46c**) (1.24 g, 9.00 mmol) and paraformaldehyde (405 mg, 13.5 mmol) 70% w/w aqueous ethylamine (0.30 ml, 3.78 mmol). The crude product was then purified *via* flash column chromatography (eluent 8:1 pentane:ethylacetate) to afford **47c** as a pale orange oil in 56% yield (875 mg, 2.53 mmol). **M.p.**: 95-96 $^{o}$C; **$^{1}$H NMR** (500.1 MHz, $CDCl_3$): $\delta_H$ 8.5 (br s, 2H, *OH*), 6.61 (d, 2H, $^{4}J$ ($^{1}$H-$^{1}$H) = 1.9 Hz, Ar*H*), 6.54 (d, 2H, $^{4}J$ ($^{1}$H-$^{1}$H) = 1.9 Hz, Ar*H*), 3.9 (s, 6H, ArO*CH*$_3$), 3.8 (s, 4H, Ar*CH*$_2$N), 2.60 (q, 2H, $^{3}J$ ($^{1}$H-$^{1}$H) = 7.1 Hz, N*CH*$_2$CH$_3$), 2.3 (s, 6H, ArO*CH*$_3$), 1.15 (t, 3H, $^{3}J$ ($^{1}$H-$^{1}$H) = 7.1 Hz, NCH$_2$*CH*$_3$); **$^{13}$C{$^{1}$H} NMR** (125.0 MHz, $CDCl_3$): $\delta_C$ 146.9 (C, $C_1$ or $C_{17}$), 143.5 (C, $C_6$ or $C_{18}$), 128.1 (C, $C_3$ or $C_{15}$), 122.3 (C, $C_5$ or $C_{13}$), 122.1 (CH, $C_4$ or $C_{14}$), 111.1 (CH, $C_2$ or $C_{16}$), 55.8 ($CH_2$, $C_9$ or $C_{12}$), 54.2 ($CH_3$, $C_7$ or $C_{19}$), 46.5 ($NCH_2$, $C_{10}$), 21.0 ($CH_3$, $C_8$ or $C_{20}$), 10.7 ($NCH_3$, $C_{11}$); **IR $\nu_{max}$** (neat): 3409 (OH), 2930 ($NCH_2$), 2833 ($OCH_3$), 1605, 1497, 1463, 1386, 1298, 1240, 1216, 1176, 1154, 1089, 942, 834, 788, 591, 555 cm$^{-1}$; **HRMS** found 368.1837 $(M+Na)^+$ Calcd. for $C_{20}H_{27}NO_4$ 368.1832 ($|\sigma|$ = 1.3 ppm); **Anal**: Calcd. (%) for $C_{20}H_{27}NO_4$: C, 69.54; H, 7.88; N, 4.05; found: C, 69.39; H, 7.96; N, 4.09.

**6,6'-((Methylazanediyl)*bis*(methylene))*bis*(4-methoxy-2-methylphenol) (47d)**

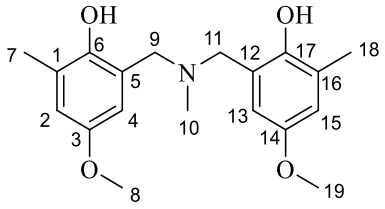


**47d**

Synthesised according to **General Procedure E** using toluene (15 ml), 4-methoxy-2-methylphenol (**46d**) (450 mg, 3.26 mmol) and paraformaldehyde (145 mg, 4.82 mmol) 40% w/w aqueous methylamine (0.14 ml, 2.00 mmol) to afford colourless rhomboidal crystals in 54% yield (289 mg, 0.872 mmol). **M.p.**: 109-110 $^{o}$C; **$^{1}$H NMR** (500.1 MHz, $CDCl_3$): $\delta_H$ 7.77 (br s, 2H, O*H*), 6.67 (d, 2H, $^{4}J$ ($^{1}$H-$^{1}$H) = 1.8 Hz, Ar*H*), 6.53 (d, 2H, $^{4}J$ ($^{1}$H-$^{1}$H) = 1.8 Hz, Ar*H*), 3.77 (s, 6H, ArO$CH_3$), 3.67 (s, 4H, Ar$CH_2$N), 2.26 (s, 3H, N$CH_3$), 2.25 (s, 6H, Ar$CH_3$). **$^{13}$C{$^{1}$H} NMR** (125.0 MHz, $CDCl_3$): $\delta_C$ 152.5 (C, $C_3$ or $C_{14}$), 148.1 (C, $C_6$ or $C_{17}$), 125.6 (C, $C_1$ or $C_{16}$), 122.7 (C, $C_5$ or $C_{12}$), 115.6 (CH, $C_2$ or $C_{15}$), 113.2 (CH, $C_4$ or $C_{13}$), 59.4 ($CH_2$, $C_9$ or $C_{11}$), 55.7 ($CH_3$, $C_8$ or $C_{19}$), 41.3 (*N*$CH_3$, $C_{10}$), 16.2 ($CH_3$, $C_7$ or $C_{18}$); **IR $\nu_{max}$** (neat): 3396 ($NCH_3$), 2992 (OH), 2832 ($OCH_3$), 1608, 1483, 1452, 1413, 1383, 1318, 1296, 1246, 1219, 1196, 1151, 1061, 1020, 989, 948, 863, 850, 836, 765, 743, 731 cm$^{-1}$; **HRMS** found 354.1673 $(M+Na)^+$ Calcd. for $C_{19}H_{25}NO_4$ 354.1676 ($|\sigma|$ = 0.8 ppm); **Anal**: Calcd. (%) for $C_{19}H_{25}NO_4$: C, 68.86; H, 7.60; N, 4.23; found: C, 68.87; H, 7.52; N, 4.36.

**6,6'-((Methylazanediyl)*bis*(methylene))*bis*(2,4-dimethoxyphenol) (47e)**

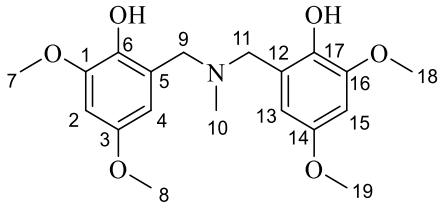


**47e**

Synthesised according to **General Procedure E** using toluene (20 ml), 2,4-dimethoxyphenol (**46e**) (2.66 g, 17.3 mmol) and paraformaldehyde (779 mg, 25.9 mmol) 40% w/w aqueous methylamine (0.75 ml, 10.4 mmol) to afford a fluffy colourless powder in 62% yield (1.94 g, 5.32 mmol). **M.p.**: 94-95 $^{o}$C; **$^{1}$H NMR** (400.1 MHz, $CDCl_3$): $\delta_H$ 8.14 (br s, 2H, O*H*), 6.44 (d, 2H, $^{4}J$ ($^{1}$H-$^{1}$H) = 2.8 Hz, Ar*H*), 6.27 (d, 2H, $^{4}J$ ($^{1}$H-$^{1}$H) = 2.8 Hz, Ar*H*), 3.86 (s, 6H, ArO$CH_3$), 3.77 (s, 6H, ArO$CH_3$), 3.71 (s, 4H, Ar$CH_2$N), 2.23 (s, 3H, N$CH_3$). **$^{13}$C{$^{1}$H} NMR** (100.0 MHz, $CDCl_3$): $\delta_C$ 152.5 (C, $C_3$ or $C_{14}$), 147.8 (C, $C_1$ or $C_{16}$), 140.0 (C, $C_6$ or $C_{17}$), 122.4 (C, $C_5$ or $C_{12}$), 105.2 (CH, $C_4$ or $C_{13}$), 98.9 (CH, $C_2$ or $C_{15}$), 58.7 ($CH_2$, $C_9$ or $C_{11}$), 56.0 ($CH_3$, $C_7$ or $C_{18}$), 55.8 ($CH_3$, $C_8$ or $C_{19}$), 41.0 (N$CH_3$, $C_{10}$); **IR $\nu_{max}$** (neat): 3483 ($NCH_3$), 2919 (OH), 2836 ($OCH_3$), 1614, 1500, 1455, 1384, 1151, 1090, 1045, 838, 779 cm$^{-1}$; **HRMS** found 364.1762 $(M+H)^+$ Calcd. for $C_{19}H_{25}N_1O_6$ 364.1755 ($|\sigma|$ = 1.9 ppm); **Anal**: Calcd. (%) for $C_{19}H_{25}N_1O_6$: C, 62.80; H, 6.93; N, 3.85; found: C, 62.81; H, 6.99; N, 3.88.

**6,6'-((Methylazanediyl)*bis*(methylene))*bis*(4-fluoro-2-methylphenol) (47f)**

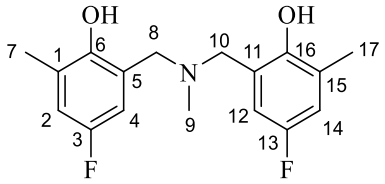


**47f**

Synthesised according to **General Procedure E** using toluene (15 ml), 4-fluoro-2-methylphenol (**46f**) (567 mg, 4.50 mmol) and paraformaldehyde (202 mg, 6.75 mmol) 40% w/w aqueous methylamine (0.19 ml, 2.70 mmol) to afford colourless needles in 55% yield (376 mg, 1.22 mmol). **M.p.**: 99-100 $^{o}$C; **$^{1}$H NMR** (400.1 MHz, $CDCl_3$): $\delta_H$ 7.94 (br s, 2H, *OH*), 6.79 (dd, 2H, $^{3}J$ ($^{1}$H-$^{1}$H) = 8.9 Hz and $^{4}J$ ($^{1}$H-$^{1}$H) = 2.8 Hz, Ar*H*), 6.66 (dd, 2H, $^{3}J$ ($^{1}$H-$^{1}$H) = 8.9 Hz and $^{4}J$ ($^{1}$H-$^{1}$H) = 3.0 Hz, Ar*H*), 3.67 (s, 4H, Ar$CH_2$N), 2.26 (s, 3H, N$CH_3$), 2.25 (s, 6H, Ar$CH_3$); **$^{13}$C{$^{1}$H NMR** (100.0 MHz, $CDCl_3$): $\delta_C$ 155.9 (d, C-F, $C_3$ or $C_{13}$, $^{1}J$ ($^{13}$C-$^{19}$F) = 237.1 Hz), 150.1 (d, C, $C_6$ or $C_{16}$, $^{4}J$ ($^{13}$C-$^{19}$F) = 1.9 Hz), 126.1 (d, C, $C_1$ or $C_{15}$, $^{3}J$ ($^{13}$C-$^{19}$F) = 7.4 Hz), 122.8 (d, C, $C_5$ or $C_{11}$, $^{3}J$ ($^{13}$C-$^{19}$F) = 7.3 Hz), 116.6 (d, CH, $C_2$ or $C_{14}$, $^{2}J$ ($^{13}$C-$^{19}$F) = 22.6 Hz), 113.9 (d, CH, $C_4$ or $C_{12}$, $^{2}J$ ($^{13}$C-$^{19}$F) = 22.7 Hz), 59.0 ($CH_2$, $C_8$ or $C_{10}$), 41.2 (*N*$CH_3$, $C_9$), 16.0 ($CH_3$, $C_7$ or $C_{17}$); **$^{19}$F NMR** (376.5 MHz, $CDCl_3$): $\delta_F$ -125.3 (app t, *J* = 7.5 Hz); **IR $\nu_{max}$** (neat): 3418 ($NCH_3$), 3043 (OH), 2950, 2851, 1472, 1443, 1220, 1189, 1123, 1028, 1000, 885, 867, 768 cm$^{-1}$; **HRMS** found 330.1273 $(M+Na)^+$ Calcd. for $C_{17}H_{19}F_2NO_2$ 330.1276 ($|\sigma|$ = 0.9 ppm).

**6,6'-((methylazanediyl)*bis*(methylene))*bis*(2-ethoxy-4-methylphenol) (47h)**

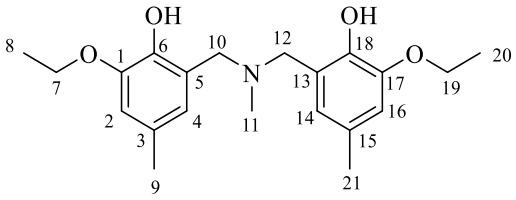


**47h**

Synthesised according to **General Procedure E** using toluene (15 ml), 2-ethoxy-4-methylphenol (**46h**) (500 mg, 3.28 mmol) and paraformaldehyde (148 mg, 4.92 mmol) 40% w/w aqueous methylamine (0.14 ml, 2.00 mmol) to afford pale yellow columnar crystals in 40 % yield (231 mg, 0.642 mmol). **M.p.**: 93-95 $^{o}$C; **$^{1}$H NMR** (500.1 MHz, $CDCl_3$): $\delta_H$ 8.44 (br s, 2H, *OH*), 6.62 (d, 2H, $^{4}J$ ($^{1}$H-$^{1}$H) = 1.9 Hz, Ar*H*), 6.53 (d, 2H, $^{4}J$ ($^{1}$H-$^{1}$H) = 1.9 Hz, Ar*H*), 4.90 (q, 4H, $^{3}J$ ($^{1}$H-$^{1}$H) = 7.0 Hz, ArO*CH*$_2$CH$_3$), 3.70 (s, 4H, Ar*CH*$_2$N), 2.27 (s, 6H, Ar*CH*$_3$), 2.19 (s, 3H, N*CH*$_3$), 1.47 (t, 6H, $^{3}J$ ($^{1}$H-$^{1}$H) = 7.0, ArOCH$_2$*CH*$_3$); **$^{13}$C{$^{1}$H} NMR** (125.0 MHz, $CDCl_3$): $\delta_C$ 146.2 (C, $C_1$ or $C_{17}$), 143.7 (C, $C_6$ or $C_{18}$), 128.0 (C, $C_3$ or $C_{15}$), 122.3 (C, $C_5$ or $C_{13}$), 122.1 (CH, $C_4$ or $C_{14}$), 112.1 (CH, $C_2$ or $C_{16}$), 64.4 ($CH_2$, $C_7$ or $C_{19}$), 58.7 ($CH_2$, $C_{10}$ or $C_{12}$), 40.7 ($NCH_3$, $C_{11}$), 21.0 ($CH_3$, $C_9$ or $C_{21}$), 15.0 ($CH_3$, $C_8$ or $C_{20}$); **IR $\nu_{max}$** (neat): 3291 ($NCH_3$), 2908 (OH), 2850 ($OCH_2CH_3$), 1706, 1501, 1440, 1377, 1287, 1215, 1202, 966, 945, 921, 855, 842, 830, 782, 760, 590, 556 cm$^{-1}$; **HRMS** found 360.2174 $(M+H)^+$ Calcd. for $C_{21}H_{29}N_1O_4$ 360.2171 ($|\sigma|$ = 0.9 ppm); **Anal**: Calcd. (%) for $C_{21}H_{29}N_1O_4$: C, 70.17; H, 8.13; N, 3.90; found: C, 70.26; H, 8.20; N, 3.96.

**General Procedure F: synthesis of *bis*(amine) *tetrakis*(phenolate) titanium(IV) complex derivatives**

Under the nitrogen atmosphere the *bis*phenol **47** (1 equiv.) was dissolved with stirring (10 min) in dry toluene. To the resulting solution titanium(IV) isopropoxide (0.6 equiv.) was added portion wise over 5 minutes and left to stir for 4 h at RT under nitrogen atmosphere. The solvent was then removed by trap-trap distillation to afford an orange solid. The product was recrystallised by liquid-liquid diffusion using suitable solvents (see individual preparations).

***Bis*((2,2'-((methylimino-*N*)*bis*(methylene))*bis*(4,6-dimethylphenolato-*O*)))titanium(IV) (48a)**

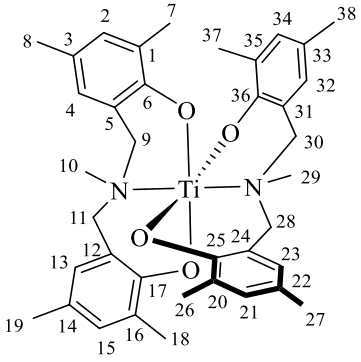

**48a**

Synthesised according to **General Procedure F** using toluene (10 ml), *bis*phenol **47a** (240 mg, 0.802 mmol), and titanium(IV) isopropoxide (0.14 ml, 136 mg, 0.48 mmol) to afford the product as a bright orange powder in 88% yield (225 mg, 0.350 mmol). **M.p.**: 254-255 °C; **$^{1}$H NMR** (500.1 MHz, $CDCl_3$): $\delta_H$ 6.92-6.83 (m, 3H, Ar*H*), 6.8 (s, 1H, Ar*H*), 5.05 (d, 1H, $^{2}J$ ($^{1}$H-$^{1}$H) = 13.1 Hz, C$H_aH_b$), 4.83 (d, 1H, $^{2}J$ ($^{1}$H-$^{1}$H) = 13.1 Hz, C$H_aH_b$), 3.34-3.32 (m, 2H, CH$_a$$H_b$), 2.43 (s, 3H, N-C$H_3$), 2.36 (s, 3H, Ar-C$H_3$), 2.24 (s, 3H, Ar-C$H_3$), 2.10 (s, 3H, Ar-C$H_3$), 1.53 (s, 3H, Ar-C$H_3$); **$^{13}$C{$^{1}$H} NMR** (125.0 MHz, $CDCl_3$): $\delta_C$ 160.1 (C, $C_6$ or $C_{17}$), 159.1 (C, $C_{25}$ or $C_{36}$), 131.5 (CH,

$C_2$ or $C_{15}$), 131.0 (CH, $C_{21}$ or $C_{34}$), 127.6 (CH, $C_4$ or $C_{13}$), 127.4 (CH, $C_{23}$ or $C_{32}$), 127.1 (C, $C_3$ or $C_{14}$), 127.0 (C, $C_{22}$ or $C_{33}$), 123.5 (C, $C_1$ or $C_{16}$), 123.2 (C, $C_{20}$ or $C_{35}$), 122.7 (C, $C_5$ or $C_{12}$), 122.6 (C, $C_{24}$ or $C_{31}$), 65.3 ($CH_2$, $C_9$ or $C_{11}$), 64.8 ($CH_2$, $C_{28}$ or $C_{30}$), 43.2 ($CH_3$, $C_{10}$ or $C_{29}$), 20.7 ($CH_3$, $C_8$ or $C_{19}$), 20.6 ($CH_3$, $C_{27}$ or $C_{38}$), 17.1 ($CH_3$, $C_7$ or $C_{18}$), 16.5 ($CH_3$, $C_{26}$ or $C_{37}$); **IR** $\nu_{max}$ (neat): 3002 ($NCH_3$), 2982 ($NCH_3$), 2914 (Ar*O)*, 2850 (Ar*O*), 1686, 1637, 1610, 1476, 1459, 1307, 1260, 1208, 1159, 1097, 1047, 970, 910, 884, 829, 737, 690, 593, 564 $cm^{-1}$; **HRMS** found 643.2999 $(M+Na)^+$ Calcd. for $C_{38}H_{47}O_4N_2Ti$ 643.3010 ($|\sigma|$ = 1.7 ppm). The compound could be recrystallised from (4:1 pentane:ether). These data were in agreement with reported properties for **48a**.[143]

***Bis*((2,2'-((methylimino-*N*)*bis*(methylene))*bis*(4-methyl-6-methoxylphenolato-*O*)))titanium(IV) (48b)**

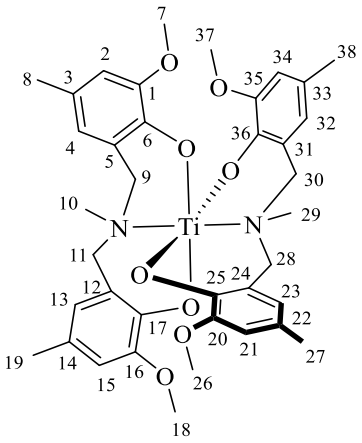


**48b**

Synthesised according to **General Procedure F** using toluene (7.0 ml), *bis*phenol **47b** (140 mg, 0.42 mmol), and titanium(IV) isopropoxide (76 µl, 71 mg, 0.3 mmol) to afford the product as a bright orange rhomboidal crystals in 66% yield (100 mg, 0.14 mmol). **M.p.**: 179-180 °C; **$^1$H NMR** (500.1 MHz, $CDCl_3$): $\delta_H$ 6.61 (d, 1H, $^4J$

($^{1}$H-$^{1}$H) = 1.8 Hz, Ar*H*), 6.54 (d, 1H, $^{4}J$ ($^{1}$H-$^{1}$H) = 1.8 Hz, Ar*H*), 6.47 (d, 1H, $^{4}J$ ($^{1}$H-$^{1}$H) = 1.8 Hz, Ar*H*), 6.44 (d, 1H, $^{4}J$ ($^{1}$H-$^{1}$H) = 1.8 Hz, Ar*H*), 4.85 (d, 1H, $^{2}J$ ($^{1}$H-$^{1}$H) = 12.8 Hz, C$H_a$H$_b$), 4.77 (d, 1H, $^{2}J$ ($^{1}$H-$^{1}$H) = 12.8 Hz, C$H_a$H$_b$), 3.46 (s, 3H, ArO$CH_3$), 3.41 (d, 1H, $^{2}J$ ($^{1}$H-$^{1}$H) = 12.8 Hz, CH$_a$$H_b$), 3.32 (s, 3H, ArO$CH_3$), 3.30 (d, 1H, $^{2}J$ ($^{1}$H-$^{1}$H) = 12.8 Hz, CH$_a$$H_b$), 2.55 (s, 3H, N$CH_3$), 2.30 (s, 3H, Ar$CH_3$), 2.24 (s, 3H, Ar$CH_3$); **$^{13}$C{$^{1}$H} NMR** (125.0 MHz, $CDCl_3$): $\delta_C$ 150.7 (C, $C_1$ or $C_{16}$), 150.6 (C, $C_{20}$ or $C_{35}$), 146.4 (2 × C, $C_{6,17}$ or $C_{25,36}$), 127.1 (C, $C_3$ or $C_{14}$), 126.9 (C, $C_{22}$ or $C_{33}$), 124.6 (C, $C_5$ or $C_{12}$), 123.7 (C, $C_{24}$ or $C_{31}$), 124.4 (CH, $C_4$ or C1$_3$), 124.3 (CH, $C_{23}$ or $C_{32}$), 113.0 (CH, $C_2$ or $C_{15}$), 112.6 (CH, $C_{21}$ or $C_{34}$), 55.7 (2 × $CH_3$, $C_{7,18}$ or $C_{26,37}$), 46.6 ($CH_2$, $C_9$ or $C_{11}$), 46.4 ($CH_2$, $C_{28}$ or $C_{30}$), 44.0 ($NCH_3$, $C_{10}$ or $C_{29}$), 21.1 ($CH_3$, $C_8$ or $C_{19}$), 21.0 ($CH_3$, $C_{27}$ or $C_{38}$); **IR $\nu_{max}$** (neat): 2981($NCH_3$), 2912 ($NCH_3$), 2850 (Ar*O*), 2832 (Ar*O*), 1580, 1485, 1457, 1259, 1154, 1100, 982, 928, 822, 581, 556, 530, 405 cm$^{-1}$; **HRMS** found 729.2624 $(M+Na)^+$ Calcd. for $C_{38}H_{46}N_2O_8Ti$ 729.2626 ($|\sigma|$ = 0.3 ppm); **Anal**: Calcd. (%) for $C_{38}H_{46}N_2O_8Ti$: C, 64.59; H, 6.56; N, 3.96; found: C, 64.31; H, 6.67; N, 3.90. The compound could be recrystallised from (4:1 pentane:ether).

***Bis*((2,2'-((ethylimino-*N*)*bis*(methylene))*bis*(4-methyl-6-methoxylphenolato-*O*)))titanium(IV) (48c)**

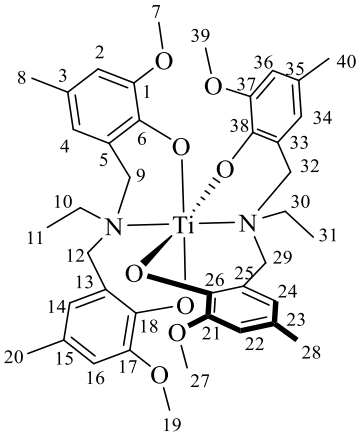


**48c**

Synthesised according to **General Procedure F** using toluene (12 ml), *bis*phenol **47c** (300 mg, 0.86 mmol), and titanium(IV) isopropoxide (156 µl, 146 mg, 0.51 mmol) to afford the product as orange rhomboidal crystals in 85% yield (270 mg, 0.37 mmol). **M.p.**: 171-172 °C; **$^{1}$H NMR** (500.1 MHz, $CDCl_3$): $\delta_H$ 6.63 (s, 1H, Ar*H*), 6.54 (s, 1H, Ar*H*), 6.48 (d, H, $^{4}J$ ($^{1}$H-$^{1}$H) = 1.45 Hz, Ar*H*), 6.45 (d, H, $^{4}J$ ($^{1}$H-$^{1}$H) = 1.45 Hz, Ar*H*), 4.67 (d, 1H, $^{2}J$ ($^{1}$H-$^{1}$H) = 13.0 Hz, C*H*$_a$H$_b$), 4.61 (d, 1H, $^{2}J$ ($^{1}$H-$^{1}$H) = 13.0 Hz, C*H*$_a$H$_b$), 3.68 (d, 1H, $^{2}J$ ($^{1}$H-$^{1}$H) = 12.9 Hz, CH$_a$*H*$_b$), 3.61 (d, 1H, $^{2}J$ ($^{1}$H-$^{1}$H) = 12.9 Hz, CH$_a$*H*$_b$), 3.51 (s, 3H, ArO*CH*$_3$), 3.34 (s, 3H, ArO*CH*$_3$), 3.13 (dq, 1H, $^{2}J$ ($^{1}$H-$^{1}$H) = 14.3 Hz and $^{3}J$ ($^{1}$H-$^{1}$H) = 7.0 Hz, NC*H*$_a$H$_b$), 3.02 (dq, 1H, $^{2}J$ ($^{1}$H-$^{1}$H) = 14.3 Hz and $^{3}J$ ($^{1}$H-$^{1}$H) = 7.0 Hz, NCH$_a$*H*$_b$), 2.27 (s, 3H, Ar*CH*$_3$), 2.22 (s, 3H, Ar*CH*$_3$), 1.00 (s, 3H, N*CH*$_3$); **$^{13}$C{$^{1}$H} NMR** (125.0 MHz, $CDCl_3$): $\delta_C$ 151.4 (C, $C_1$ or $C_{17}$), 151.1 (C, $C_{21}$ or $C_{37}$), 146.3 (C, $C_6$ or $C_{18}$), 146.2 (C, $C_{26}$ or $C_{38}$), 127.0 (C, $C_3$ or $C_{15}$), 126.8 (C, $C_{23}$ or $C_{35}$), 124.4 (C, $C_5$ or $C_{13}$), 123.7 (C, $C_{25}$ or $C_{33}$), 121.5 (CH, $C_4$ or $C_{14}$), 121.4 (CH, $C_{24}$ or $C_{34}$), 113.5 (CH, $C_2$ or $C_{16}$), 113.1 (CH, $C_{22}$ or $C_{36}$), 57.7 ($CH_2$, $C_9$ or $C_{12}$), 57.5 ($CH_2$, $C_{29}$ or $C_{32}$), 56.0 ($CH_3$, $C_7$ or $C_{19}$), 55.9 ($CH_3$, $C_{27}$ or $C_{39}$), 44.2

($CH_2$, $C_{10}$ or $C_{30}$), 21.2 ($CH_3$, $C_8$ or $C_{20}$), 21.0 ($CH_3$, $C_{28}$ or $C_{40}$), 5.7 ($CH_3$, $C_{11}$ or $C_{31}$); **IR** $\nu_{max}$ (neat): 2915 ($NCH_2CH_3$), 1580,1485, 1382, 1331, 1308, 1288, 1187, 1153, 1098, 821, 779, 740, 554, 529, 475 $cm^{-1}$; **HRMS** found 757.2930 $(M+Na)^+$ Calcd. for $C_{40}H_{50}N_2O_8Ti$ 757.2939 ($|\sigma|$ = 1.19 ppm); **Anal**: Calcd. (%) for $C_{40}H_{50}N_2O_8Ti$: C, 65.39; H, 6.86; N, 3.81; found: C, 65.27; H, 7.24; N, 3.81. The compound could be recrystallised from (4:1 pentane:ether).

***Bis*((2,2'-((methylimino-*N*)*bis*(methylene))*bis*(4-methoxy-6-methylphenolato-*O*)))titanium(IV) (48d)**

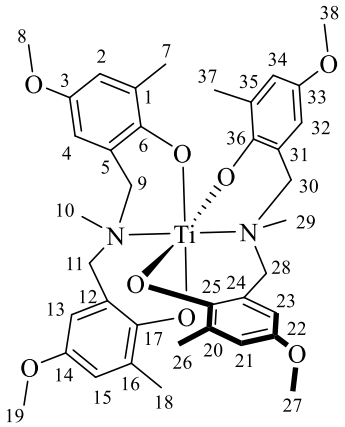


**48d**

Synthesised according to **General Procedure F** using toluene (7.0 ml), *bis*phenol **47d** (140 mg, 0.42 mmol), and titanium(IV) isopropoxide (76.0 µl, 71.0 mg, 0.25 mmol) to afford the product as a bright orange needles in 81% yield (120 mg, 0.17 mmol). **M.p.**: 179-180 °C; **$^1$H NMR** (500.1 MHz, $CDCl_3$): $\delta_H$ 6.69–6.60 (m, 3H, Ar*H*), 6.57 (d, 1H, $^4J$ ($^1$H-$^1$H) = 3.1 Hz, Ar*H*), 4.96 (d, 1H, $^2J$ ($^1$H-$^1$H) = 13.1 Hz, C$H_a$H$_b$), 4.73 (d, 1H, $^2J$ ($^1$H-$^1$H) = 13.1 Hz, C$H_a$H$_b$), 3.79 (s, 3H, ArO$CH_3$), 3.75 (s, 3H, ArO$CH_3$), 3.34 (app dd, 2H, $^2J$ ($^1$H-$^1$H) = 12.8 Hz and $^3J$ ($^1$H-$^1$H) 7.0 Hz, 2 × CH$_a$$H_b$), 2.44 (s, 3H, N$CH_3$), 2.09 (s, 3H, Ar$CH_3$), 1.57 (s, 3H, Ar$CH_3$); **$^{13}$C{$^1$H} NMR** (125.0 MHz, $CDCl_3$): $\delta_C$ 156.5 (C, $C_3$ or $C_{14}$), 155.5 (C, $C_{22}$ or $C_{33}$), 151.5 (C,

$C_6$ or $C_{17}$), 151.3 (C, $C_{25}$ or $C_{36}$), 124.4 (C, $C_1$ or $C_{16}$), 124.1 (C, $C_{20}$ or $C_{35}$), 123.0 (C, $C_5$ or $C_{12}$), 122.9 (C, $C_{24}$ or $C_{31}$), 116.0 (CH, $C_2$ or $C_{15}$), 115.5 (CH, $C_{21}$ or $C_{34}$), 112.5, (CH, $C_4$ or $C_{13}$), 112.3 (CH, $C_{23}$ or $C_{32}$), 65.1 ($CH_2$, $C_9$ or $C_{11}$), 64.8 ($CH_2$, $C_{28}$ or $C_{30}$), 56.0 ($CH_3$, $C_8$ or $C_{19}$), 55.8 ($CH_3$, $C_{27}$ or $C_{38}$), 43.1 ($NCH_3$, $C_{10}$ or $C_{29}$), 17.3 ($CH_3$, $C_7$ or $C_{18}$), 16.7 ($CH_3$, $C_{26}$ or $C_{37}$); **IR** $\nu_{max}$ (neat): 2918 ($NCH_3$), 2800, 1510, 1310, 1270, 1164, 1120, 976, 822, 581, 572, 555 $cm^{-1}$; **HRMS** found 729.2629 $(M+Na)^+$ Calcd. for $C_{38}H_{46}N_2O_8Ti$ 729.2626 ($|\sigma|$ = 0.4 ppm); **Anal**: Calcd. (%) for $C_{38}H_{46}N_2O_8Ti$: C, 64.59; H, 6.56; N, 3.96; found: C, 64.24; H, 6.66; N, 4.00. The compound could be recrystallised from (4:1 hexane:ether).

***Bis*((2,2'-((methylimino-*N*)*bis*(methylene))*bis*(4,6-dimethoxylphenolato-*O*)))titanium(IV) (48e)**

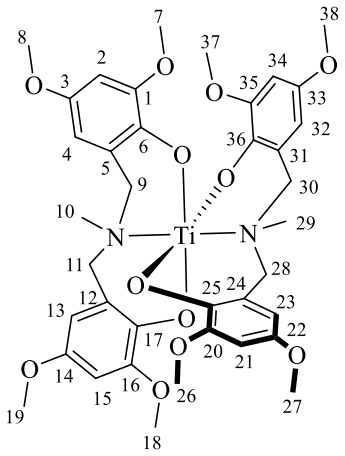


**48e**

Synthesised according to **General Procedure F** using toluene (10 ml), *bis*phenol **47e** (240 mg, 0.66 mmol), and titanium(IV) isopropoxide (0.12 ml, 112 mg, 0.39 mmol) to afford the product as a bright dark red rhomboidal crystals in 88% yield (224 mg, 0.350 mmol). **M.p.**: 117-118 °C; **$^1$H NMR** (500.1 MHz, $CDCl_3$): $\delta_H$ 6.36 (d, 1H, $^4J$ ($^1$H-$^1$H) = 2.8 Hz, Ar*H*), 6.30 (dd, 2H, $^3J$ ($^1$H-$^1$H) = 6.5 Hz and $^4J$ ($^1$H-$^1$H) = 2.8 Hz,

Ar*H*), 6.26 (d, 1H, $^{3}J$ ($^{1}$H-$^{1}$H) = 2.8 Hz, Ar*H*), 4.84 (d, 1H, $^{2}J$ ($^{1}$H-$^{1}$H) = 12.9 Hz, C*H*$_a$H$_b$), 4.77 (d, 1H, $^{2}J$ ($^{1}$H-$^{1}$H) = 12.9 Hz, C*H*$_a$H$_b$), 3.80 (s, 3H, ArO*CH*$_3$), 3.74 (s, 3H, ArO*CH*$_3$), 3.47 (s, 3H, ArO*CH*$_3$), 3.43 (d, 1H, $^{2}J$ ($^{1}$H-$^{1}$H) = 12.9 Hz, CH$_a$*H*$_b$), 3.37 (s, 3H, ArO*CH*$_3$), 3.31 (d, 1H, $^{2}J$ ($^{1}$H-$^{1}$H) = 12.9 Hz, CH$_a$*H*$_b$), 2.57 (s, 3H, N*CH*$_3$); **$^{13}$C{$^{1}$H} NMR** (125.0 MHz, $CDCl_3$): $\delta_C$ 152.0 (C, $C_3$ or $C_{14}$), 151.7 (C, $C_{22}$ or $C_{33}$), 147.5 (C, $C_1$ or $C_{16}$), 147.4 (C, $C_{20}$ or $C_{35}$), 147.3 (C, $C_6$ or $C_{17}$), 147.2 (C, $C_{25}$ or $C_{36}$), 124.3 (C, $C_5$ or $C_{12}$), 123.3 (C, $C_{24}$ or $C_{31}$), 104.7 (2 × CH, $C_{4,13}$ or $C_{23,32}$), 99.7 (CH, $C_2$ or $C_{15}$), 99.5 (CH, $C_{21}$ or $C_{34}$), 64.8 ($CH_2$, $C_9$ or $C_{11}$), 64.6 ($CH_2$, $C_{28}$ or $C_{30}$), 55.9 (2 × $CH_3$, $C_{7,18}$ or $C_{26,37}$), 55.7 ($CH_3$, $C_8$ or $C_{19}$), 55.6 ($CH_3$, $C_{27}$ or $C_{38}$), 44.1 ($CH_3$, $C_{10}$ or $C_{29}$); **IR** $\nu_{max}$ (neat): 3646 ($NCH_3$), 2930 ($OCH_3$), 2835, 1587, 1486, 1454, 1258, 1237, 1196, 1150, 1093, 1052,982, 828,592, 455 cm$^{-1}$; **HRMS** found 793.2409 $(M+Na)^+$ Calcd. for $C_{38}H_{46}N_2O_{12}Ti$ 793.2422 (|σ| = 1.6 ppm); **Anal**: Calcd. (%) for $C_{38}H_{46}N_2O_{12}Ti$: C, 59.22; H, 6.02; N, 3.64; found: C, 58.87; H, 6.01; N, 3.56. The compound could be recrystallised from (4:1 pentane:dichloromethane).

***Bis*((2,2'-((methylimino-*N*)*bis*(methylene))*bis*(4-fluoro-6-methylphenolato-*O*)))titanium(IV) (48f)**

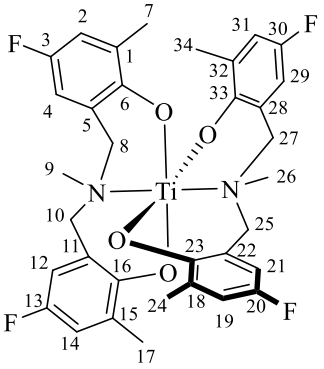

**48f**

Synthesised according to **General Procedure F** using toluene (6 ml), *bis*phenol **47f** (129 mg, 0.42 mmol), and titanium(IV) isopropoxide (76.0 µl, 71.0 mg, 0.25 mmol) to afford the product as a bright orange needles in 76% yield (104 mg, 0.16 mmol). **M.p.**: >250 °C; **$^{1}$H NMR** (400.1 MHz, $CDCl_3$): $\delta_H$ 6.86 – 6.69 (m, 4H, Ar*H*), 4.93 (d, 1H, $^{2}J$ ($^{1}$H-$^{1}$H) = 13.2 Hz, C*H*$_a$H$_b$), 4.70 (d, 1H, $^{2}J$ ($^{1}$H-$^{1}$H) = 13.2 Hz, CH$_a$*H*$_b$), 3.37 (app dd, 2H, $^{2}J$ ($^{1}$H-$^{1}$H) = 12.9, 4.6 Hz, 2 × CH$_a$*H*$_b$), 2.44 (s, 3H, N*CH*$_3$), 2.10 (s, 3H, Ar*CH*$_3$), 1.57 (s, 3H, Ar*CH*$_3$); **$^{13}$C{$^{1}$H} NMR** (100.0 MHz, $CDCl_3$): $\delta_C$ 157.8 (C, $C_3$ or $C_{13}$), 156.9 (C, $C_{20}$ or $C_{30}$), 156.3 (d, C, $C_1$ or $C_{15}$, $^{3}J$ ($^{13}$C-$^{19}$F) = 13.0 Hz), 154.0 (d, C, $C_{18}$ or $C_{32}$, $^{3}J$ ($^{13}$C-$^{19}$F) = 12.9 Hz), 125.0 (C, d, $C_5$ or $C_{11}$, $^{3}J$ ($^{13}$C-$^{19}$F) = 8.0 Hz), 124.7 (d, C, $C_{22}$ or $C_{28}$, $^{3}J$ ($^{13}$C-$^{19}$F) = 8.0 Hz), 123.0–122.5 (m, 2 × C, $C_{1,16}$ or $C_{23,33}$), 117.1 (d, CH, $C_2$ or $C_{14}$, $^{2}J$ ($^{13}$C-$^{19}$F) = 22.0 Hz), 116.7 (d, CH, $C_{19}$ or $C_{31}$, $^{2}J$ ($^{13}$C-$^{19}$F) = 22.0 Hz), 113.2 (d, CH, $C_4$ or $C_{12}$, $^{2}J$ ($^{13}$C-$^{19}$F) = 23.2 Hz), 112.9 (d, CH, $C_{21}$ or $C_{29}$, $^{2}J$ ($^{13}$C-$^{19}$F) = 23.2 Hz), 64.7 ($CH_2$, $C_8$ or $C_{10}$), 64.3 ($CH_2$, $C_{25}$ or $C_{27}$), 43.2 ($CH_3$, $C_9$ or $C_{26}$), 17.2 ($CH_3$, $C_7$ or $C_{17}$), 16.5 ($CH_3$, $C_{24}$ or $C_{34}$); **$^{19}$F NMR** (376.5 MHz, $CDCl_3$): $\delta_F$ -126.08 (app dt, $J$ = 12.0, 8.8 Hz); **IR $\nu_{max}$** (neat): 2913 ($NCH_3$), 1468, 1417, 1254, 1233, 1129, 852, 821, 595, 560, 405 cm$^{-1}$; **HRMS** found 681.1833

$(M+Na)^+$ Calcd. for $C_{34}H_{34}F_4N_2O_4Ti$ 681.1826 (|σ| = 1 ppm); **Anal**: Calcd. (%) for $C_{34}H_{34}F_4N_2O_4Ti$: C, 62.01; H, 5.20; N, 4.25; found: C, 61.58; H, 5.16; N, 4.21. The compound could be recrystallised from (4:1 pentane:dichloromethane).

***Bis*((2,2'-((methylimino-*N*)*bis*(methylene))*bis*(4,6-dichlorophenolato-*O*)))titanium(IV) (48g)**

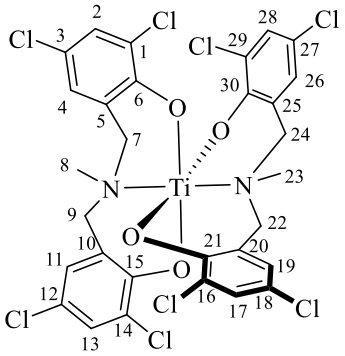


**48g**

Synthesised according to **General Procedure F** using toluene (27 ml). The crude *bis*phenol **47g** (650 mg, 1.70 mmol) was used directly as obtained, and titanium(IV) isopropoxide (325 µl, 304 mg, 1.07 mmol) to afford the product as orange powder in 83% yield (570 mg, 0.70 mmol). **M.p.**: >250 °C; **$^1$H NMR** (500.1 MHz, $CDCl_3$): $\delta_H$ 7.31 (d, 1H, , $^4J$ ($^1$H-$^1$H) = 2.4 Hz, Ar*H*), 7.28 (d, 1H, , $^4J$ ($^1$H-$^1$H) = 2.4 Hz, Ar*H*), 7.15 (d, 1H, $^4J$ ($^1$H-$^1$H) = 2.4 Hz, Ar*H*), 7.08 (d, 1H, $^4J$ ($^1$H-$^1$H) = 2.4 Hz, Ar*H*), 4.98 (d, 1H, $^2J$ ($^1$H-$^1$H) = 13.7 Hz, C$H_a$H$_b$), 4.83 (d, 1H, $^2J$ ($^1$H-$^1$H) = 13.7 Hz, C$H_a$H$_b$), 3.44 (app d, 2H, $^2J$ ($^1$H-$^1$H) = 13.7 Hz, 2 × CH$_a$$H_b$), 2.54 (s, 3H, N$CH_3$); **$^{13}$C{$^1$H} NMR** (125.0 MHz, $CDCl_3$): $\delta_C$ 157.1 (C, $C_6$ or $C_{15}$),155.9 (C, $C_{21}$ or $C_{30}$), 129.9 (CH, $C_2$ or $C_{13}$), 129.2 (CH, $C_{17}$ or $C_{28}$), 127.7 (2 × CH, $C_{4,11}$ or $C_{19,26}$), 125.5 (C, $C_3$ or $C_{12}$), 125.3 (C, $C_{18}$ or $C_{27}$), 123.7 (C, $C_5$ or $C_{10}$), 123.6 (C, $C_{20}$ or $C_{25}$), 120.8 (C, $C_1$ or $C_{14}$), 120.5 (C, $C_{16}$ or $C_{29}$), 64.1 ($CH_2$, $C_7$ or $C_9$), 63.8 ($CH_2$, $C_{22}$ or $C_{24}$), 43.8 ($CH_3$, $C_8$ or

$C_{23}$); **IR** $\nu_{max}$ (neat): 1453, 1319, 1240, 1215, 861, 769, 557, 521, 472 $cm^{-1}$; **HRMS** found 802.8641 $(M+H)^+$ Calcd. for $C_{30}H_{23}Cl_8N_2O_4Ti$ 802.8640 ($|\sigma|$ = 0.12 ppm).

***Bis*((2,2'-((methylimino-*N*)*bis*(methylene))*bis*(4-methyl-6 ethoxylphenolato-*O*)))titanium(IV) (48h)**

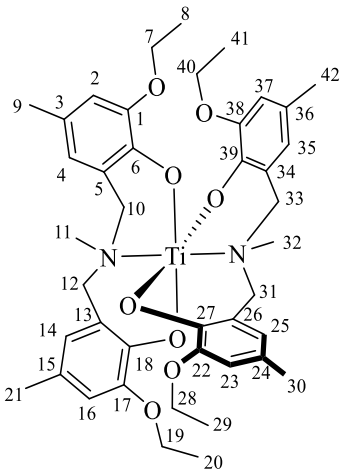

**48h**

Synthesised according to **General Procedure F** using toluene (6.0 ml), *bis*phenol **47h** (102 mg, 0.28 mmol), and titanium(IV) isopropoxide (52.0 µl, 48.0 mg, 0.17 mmol) to afford the product as a bright orange rhomboidal crystals in 89% yield (95 mg, 0.124 mmol). **M.p.**: 187-190 °C; **$^1$H NMR** (500.1 MHz, $CDCl_3$): $\delta_H$ 6.60 (app s, 2H, Ar*H*), 6.53 (app s, 2H, Ar*H*), 6.44 (app s, 4H, Ar*H*), 4.87 (d, 1H, $^2J$ ($^1$H-$^1$H) = 13.1 Hz, C$H_a$H$_b$), 4.76 (d, 1H, $^2J$ ($^1$H-$^1$H) = 13.1 Hz, C$H_a$H$_b$), 3.80-3.65 (m, 2H, ArO$CH_2$CH$_3$), 3.58-3.46 (m, 2H, ArO$CH_2$CH$_3$), 3.34 (d, 1H, $^2J$ ($^1$H-$^1$H) = 13.1 Hz, CH$_a$$H_b$), 3.31 (d, 1H, $^2J$ ($^1$H-$^1$H) = 13.1 Hz, CH$_a$$H_b$), 2.55 (s, 3H, N$CH_3$), 2.28 (s, 3H, Ar$CH_3$), 2.23 (s, 3H, Ar$CH_3$), 1.26 (t, 3H, ArOCH$_2$$CH_3$), 0.92 (t, 3H, ArOCH$_2$$CH_3$); **$^{13}$C{$^1$H} NMR** (125.0 MHz, $CDCl_3$): $\delta_C$ 150.9 (C, $C_1$ or $C_{17}$), 150.8 (C, $C_{22}$ or $C_{38}$), 145.8 (C, $C_6$ or $C_{18}$), 145.7 (C, $C_{27}$ or $C_{39}$), 127.0 (C, $C_3$ or $C_{15}$), 126.8(C, $C_{30}$ or $C_{42}$),

124.1 (C, $C_5$ or $C_{13}$), 123.9 (C, $C_{26}$ or $C_{34}$), 121.2 (CH, $C_4$ or $C_{14}$), 121.1 (CH, $C_{25}$ or $C_{35}$), 113.7 (CH, $C_2$ or $C_{16}$), 113.2 (CH, $C_{23}$ or $C_{37}$), 64.5 ($CH_2$, $C_7$ or $C_{19}$), 64.2 ($CH_2$, $C_{28}$ or $C_{40}$), 63.7 ($CH_2$, $C_{10}$ or $C_{12}$), 63.1 ($CH_2$, $C_{31}$ or $C_{33}$), 43.8 ($NCH_3$, $C_{11}$ or $C_{32}$), 21.1 ($CH_3$, $C_9$ or $C_{21}$), 21.0 ($CH_3$, $C_{30}$ or $C_{42}$), 15.0 ($CH_3$, $C_8$ or $C_{20}$), 14.3 ($CH_3$, $C_{29}$ or $C_{41}$); **IR** $\nu_{max}$ (neat): 2949 ($NCH_3$), 1971, 1533, 1462, 1303, 1226, 1188, 1105, 1044, 899, 770, 667, 597, 542, 523, 493, 472 $cm^{-1}$; **HRMS** found 763.3433 $(M+H)^+$ Calcd. for $C_{42}H_{54}N_2O_8Ti$ 763.3432 ($|\sigma|$ = 0.6 ppm); **Anal**: Calcd. (%) for $C_{42}H_{54}N_2O_8Ti$: C, 66.14; H, 7.14; N, 3.67; found: 66.28; H, 7.22; N, 3.72. The compound could be recrystallised from (4:1 pentane: dichloromethane).

**2,4-Dimethyl-*1H*-pyrrole (49)**

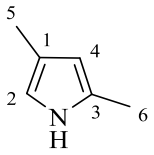


**49**

The reagent was prepared by a literature method as described below.[159] A solution of the diethyl 3,5-dimethyl-*1H*-pyrrole-2,4-dicarboxylate (3.00 g, 14.0 mmol) and potassium hydroxide (4.06 g, 72.0 mmol) in ethylene glycol (10 ml) were heated to reflux for 4 h at 160 $^oC$. The mixture was left to cool down and it was extracted with chloroform (4 × 25) and dried over sodium sulfate to afford yellowish oil. The crude was purified by distillation in vacuum (2 mbar, 1.5 mmHg, 82 °C) to afford tan oil in 45% yield (600 mg, 6.3 mmol); **$^1$H NMR** (500.1 MHz, $CDCl_3$): $\delta_H$ 7.63 (app br, 1H, N*H*), 6.43 (s, 1H, NC*H*), 5.78 (s, 1H, CH), 2.27 (s, 3H, $CH_3$), 2.11 (s, 3H, $CH_3$); **$^{13}$C{$^1$H} NMR** (125.0 MHz, $CDCl_3$): $\delta_C$ 127.7 (C, $C_3$), 119.2 (C, $C_1$),

113.8 (CH, $C_2$), 107.7 (CH, $C_4$), 13.0 ($CH_3$, $C_6$), 11.9 ($CH_3$, $C_5$). These data were in agreement with reported properties for **49** allowing its forward synthetic use.[159]

**4-Ethynylbenzaldehyde (50)**

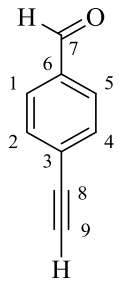


**50**

The 4-bromobenzaldehyde (1.00 g, 5.40 mmol), $Pd(PPh_3)_2Cl_2$ (37.8 mg, 0.054 mmol), CuI (21.6 mg, 0.113 mmol), $PPh_3$ (28.3 mg, 0.108 mmol), and KOH (160 mg, 2.85 mmol) were dissolved in (30 ml, 215 mmol) trimethylamine under nitrogen atmosphere. The mixture was left to stir at RT for about 10 min. To this ethynyltrimethylsilane (793.8 mg, 8.1mmol) was added *via* syringe and the mixture heated to reflux for 8 h at 94 $^oC$. The solvent was removed *in vacuo* and the resulting mixture was purified *via* flash column chromatography (eluent: 3:1 dichloromethane: petroleum ether) to afford the crude product as a yellow liquid. The crude mixture was dissolved in methanol (50 ml) and added potassium carbonate (1.6 g, 11.6 mmol) and left to stir at RT for 3 h. The solvent was removed *in vacuo* and the crude was re-dissolved in water and extracted with ether (3 × 25). The organic layer was collected and dried over sodium sulfate and solvent was removed *in vacuo* to give the product as a yellow solid in 83% yield (584 mg, 4.50 mmol). **$^1$H NMR** (500.1 MHz, $CDCl_3$): $\delta_H$ 10.04 (s, 1H, CO*H*), 7.87 (d, 2H, $^3J$ ($^1$H-$^1$H) = 8.2 Hz, Ar*H*), 7.67 (d, 2H, $^3J$ ($^1$H-$^1$H) = 8.2 Hz, Ar*H*), 3.32 (s, 3H, $CH_3$); **$^{13}$C{$^1$H} NMR** (125.0 MHz, $CDCl_3$): $\delta_C$ 191.4 (CHO, $C_7$), 136.0 (CH, $C_2$ or $C_4$), 132.7 (CH, $C_1$ or $C_5$), 129.5 (C, $C_6$), 128.3 (C, $C_3$),

82.6 (C, $C_8$), 81.1 (CH, $C_9$). These data were in agreement with reported properties for **50** allowing its forward synthetic use.[160]

**4,4-Difluoro-1,3,5,7-tetramethyl-8-(4-ethynylphenyl)boradiazaindacene(51)**

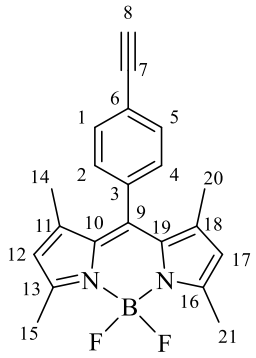


**51**

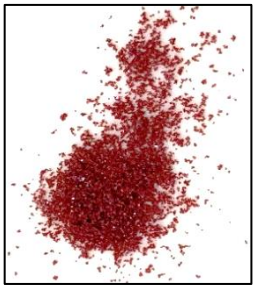

***51** recrystallised*

The fragment was prepared by a literature route, but with a modified purification procedure.[160] Under nitrogen atmosphere, to a solution of 4-ethynylbenzaldehyde (**50**) (130 mg, 1.00 mmol) and 2,4-dimethylpyrrole (**49**) (220 mg, 2.30 mmol) in dichloromethane (50 ml) was added trifluoroacetic acid (7.6 µl, 0.10 mmol). The mixture was stirred overnight at RT. To this mixture *p*-chloranil (245 mg, 1.00 mmol) in dichloromethane (10 ml) was added and left to stir for 30 min before the addition of boron trifluoride diethyl etherate (2.3 ml, 18.0 mmol, 2.60 g) and triethylamine (2.35 ml, 17.0 mmol), and the mixture was stirred for 6 h at RT. The mixture was washed with water (5 x 60 ml) and dried over sodium sulfate. The solvent was removed *in vacuo* and the crude was purified *via* flash column chromatography (eluent: 1:1dichloromethane:hexane) to afford the product as a dark purple solid in 26% yield (90 mg, 0.258 mmol). The product was then re-crystallised once again using hot methanol to give bright purple rhomboidal crystals. **$^1$H NMR** (400.1 MHz, $CDCl_3$): $\delta_H$ 7.65 (d, 2H, $^3J$ ($^1$H-$^1$H) = 8.2 Hz, Ar*H*), 7.30 (d, 2H, $^3J$ ($^1$H-$^1$H) = 8.2 Hz, Ar*H*), 6.01 (s, 2H, CH), 3.20 (s, 1H, CH), 2.58 (s, 6H, $CH_3$), 1.42 (s, 6H, $CH_3$); **$^{19}$F**

**NMR** (376.5 MHz, $CDCl_3$): $\delta_F$ -146.3 (dd, *J* = 65.9, 32.8 Hz). These data were in agreement with reported properties for **51** allowing its forward synthetic use.[160] Unfortunately, time restrictions prevented the coupling of **51** to any titanium complex.

## 4.7. Biology Section

### 4.7.1. Cell culture

All carcinoma cell lines were obtained from (ATCC) the American Type Tissue Cell Culture Collection and cultured in RPMI 1640 nutrient medium supplemented with 10% (v/v) foetal bovine serum (FBS), and 1% (v/v) glutamine. All cells were passaged twice weekly to preserve logarithmic growth. Thereafter, consumed culture medium was removed by aspiration, cells were washed with 1-2 ml sterilised PBS, as any trace of medium will minimise the ability of trypsin to detach adherent cells from the flask. The flask was then incubated for 5 min after adding 1 ml of trypsin-EDTA 1x solution to detach the cells from the bottom of the flask. When the majority of cells had dissociated, they were re-suspended in 7 ml of fresh medium to neutralise the effect of trypsin-EDTA solution. Subsequently, 0.25-0.5 ml of the cell suspension was added to new flasks containing 10 ml of fresh growth medium and incubated in an incubator at 37 °C with a 5% $CO_2$ atmosphere. The cells utilised in experiments were ≤30 passages (typically 4-16) to decrease genotypic/phenotypic drift. Milligram quantities of cisplatin and the other tested compounds were weighed using an Ultra Micro Balance (six significant figures, accurate to ±0.01 mg). Cisplatin and other compounds stock solutions (10 mM) were freshly prepared in DMSO directly before use. Dilution procedures were conducted adopting identical procedures (taking <1 h) followed by immediate use to minimise potential hydrolysis

of titanium, and other, agents. Colon cancer cell line (HCT-116), breast cancer cell line (MCF-7), and normal lung tissue (MRC-5) were used and all experiments were replicated ≥3 times.

#### 4.7.1.1. **MTT assay**

This technique was utilised to determine the growth of HCT-116 and MCF7 using the procedure presented in 1983 by Mosmann.[168] Cells were seeded in 96 well plates containing (180 µl per well) at density of 3000 cells per well and left for 24 h at 37 °C and 5% $CO_2$ to allow cells to adhere. Stock solutions of cisplatin and other tested compounds at 10 mM in DMSO were then made. Once the stock concentration solution was made, serial dilutions of concentrations were prepared in nutrient medium to achieve the final concentrations which were generally 0.05 µM, 0.1 µM, 0.5 µM, 1 µM, 5 µM, 10 µM, 20 µM, 50 µM, 100 µM, 200 µM respectively. The final concentrations of DMSO in the tested solutions were ≤0.1% v/v. Control studies indicated no effect for the DMSO presence at this level. Two vehicle plates were prepared for each cell and compound, one of T0 which was just the medium with the cancer cell line and another plate was treated with 20 µl of different concentrations of cisplatin and tested compounds as the concentrations above. The two plates were incubated: T0 for 24 h (plate was read at the time of test agent addition, in order to gain an accurate estimation of a) cell growth b) inhibition of cell growth by test agent over the ensuing 72 h period) and the experimental plates for 72 h time at 37 °C and 5% $CO_2$. All plates were treated with 20 µl of MTT solution (2 mg/ml in PBS) and were incubated for a further 2.5 h to allow metabolism of the MTT to purple formazan precipitates by viable cells. All supernatants were removed and DMSO (150 µl per well) added. Absorbance intensity was measured by the 2104 EnVision® Multilabelat plate reader at 550 nm wavelength. The intensity of the formazan colour

is proportional to the number of viable cells in a given well. Growth inhibition ($GI_{50}$) values were determined for each agent as below - [(OD of control - OD of T0)/2] + OD of T0 = OD at $GI_{50}$ and thereafter the $GI_{50}$ values were calculated by interpolation.[210]

#### 4.7.1.2. Clonogenic assay

Using a haemocytometer, 350-500 counted cells were seeded per well in 6-well plates with 2 ml of growth medium. The cells were allowed to attach to the wells for 24 h at 37 °C and 5% $CO_2$. Two wells were used as controls containing cells treated with the vehicle (medium) alone. The remaining wells contained cells treated with the compounds tested (1 and 5 µM assays in duplicate). Following 24 h exposure to test agents, the medium was aspirated along with the compound. Wells were washed with (1 ml) of cold PBS and 2 ml of fresh medium was added to each well. Plates were placed in the incubator at 37 °C and inspected daily until cells in control wells formed colonies of ≥50 cells. The cells were washed with (1 ml) of cold PBS before fixation with 100% methanol (0.5 ml) for 15 min. Colonies were stained with 0.7 ml of 0.05% methylene blue (1:1 water:methanol) for an additional 10 minutes. The colonies were washed, air dried, and counted.[176] The plating efficiency (PE) and survival fraction (SF) were calculated as below:

PE = (Number of colonies counted / Number of cells plated) × 100%

SF = (PE of treated sample / PE of control) × 100%

#### 4.7.1.3. Cell cycle assay

The method of Nicoletti *et al*. (1991)[211] was used for cell cycle assay. Cells were seeded in 10 cm petri dishes in 10 ml growth medium to provide cell densities of $7 \times 10^5$ (control and 24 h) and $4 \times 10^5$ (control, 48, and 72 h) cells per dish. Cells

were incubated at 37 °C for 24 h to allow time for adhesion of cells to the base of the dishes. Cells were then treated with desired concentrations of the tested compounds. After the required period of exposure, medium and floating cells were transferred to a labelled 15 ml falcon tube. Afterward, cells were harvested by addition of 0.5 ml of 1x trypsin-EDTA. Once the detached cells pooled together they were transferred with medium and centrifuged in a Beckman Coulter Allegro centrifuge at 1200 rpm for 5 min at 4 °C. The supernatant was discarded and the pellets were broken down by gently flicking the tube. Thereafter, (1 ml) cooled PBS was added and the tubes were vortexed and then the cells were centrifuged again. The supernatant was discarded and the pellet was broken down as before and the cells were re-suspended in 0.7 ml cold hypotonic fluorochrome solution (50 µg $ml^{-1}$ propidium iodide (PI), 0.1 mg $ml^{-1}$ ribonuclease A, 0.1% v/v Triton X-100, and 0.1% w/v sodium citrate in $dH_2O$). The cell suspension was transferred to a labelled fluorescence activated cell sorter tube (FACS) and stored overnight at 4 °C in the dark. Cells were vortexed to attain a single cell suspension. Events (15,000) were recorded for each sample, using a FC500 Beckman Coulter flow cytometer. The results obtained were analysed using WEASEL software.

#### 4.7.1.4. **Annexin-V assay**

The method of Qazzaz *et al*. (2017)[177] was used for the annexin V assay to determine apoptotic populations. Cells were seeded into 10 cm petri dishes using the normal medium 10 ml at a cell densities of $4 \times 10^5$ (control and 72 h). Cells were incubated for 24 h to allow cell attachment. Following treatment with test compound, cells were trypsinised with 300 µl of 1x trypsin-EDTA and pooled in a total of 1 ml complete normal medium. Afterward, the cells were resuspended in 2 ml of cold medium and decanted to labelled FACS tubes and kept on ice to recover from any damage caused

by trypsin. Cells were centrifuged at 1200 rpm (Beckman Coulter Allegro centrifuge) for 5 min at 4 °C. The supernatant was discarded and the pellet broken up by gently flicking the tube. Cold PBS (2 ml) was added and the cells were centrifuged as before. The supernatant was discarded and the pellet broken up by gently flicking the tube. Thereafter, 100 µl of 1x annexin binding buffer and 5 µl annexin-V FITC was added to each tube. The tubes were briefly vortexed and kept on ice for 15 min in the dark. Annexin binding buffer (400 µl; 1x) and 10 µl (50 µg/ml) of PI solution were added to each tube which was vortexed and kept for 10 min on ice in the dark prior to analysis on the flow cytometer. Samples were analysed within 1 h of completion of the above protocol to avoid sample deterioration. The samples were analysed by FC500 Beckman Coulter flow cytometer and 15,000 events were recorded for each sample. The results obtained were analysed using WEASEL software.

#### 4.7.1.5. **Determination of γ-H2AX foci perturbation:**

The method of Cini *et al.* (2016)[61] was used for γ-H2AX. Cells were seeded in 10 cm petri dishes at densities of $4 \times 10^5$ cells/dish in 10 ml medium. Following 72 h treatment with test compounds, the cells were harvested and pelleted by centrifugation, re-suspended and washed in (1 ml) PBS, pelleted by centrifugation and fixed in 500 µl 1% methanol-free formaldehyde in PBS (5 min; room temperature). Cells were permeabilised by adding 500 µl 0.4% Triton-X-100 in PBS. FBS (1% in PBS; 1 ml) was added to cells with gentle mixing before incubation at room temperature for 30 min. Cell suspensions were centrifuged and supernatants aspirated. Primary antibody (1$^o$ Ab, p-Histone γ-H2AX) solution (200 µl, 1:3333 in 1% FBS) was added to each tube and samples were incubated for 1.5 h. Additional PBS (1 ml) was added and samples were centrifuged and supernatants discarded. Secondary antibody (2$^o$ Ab, Alexa Flour 488 goat secondary anti-mouse) was

introduced (200 µl, 1:750 in 1% FBS) and samples incubated for 1 h at room temperature before addition of (1 ml) PBS. Samples were centrifuged and supernatant again discarded. Cells were re-suspended in PBS solution (300 µl) to which PI (50 µg $ml^{-1}$) and RNaseA (0.1 mg $ml^{-1}$) was added. Analyses of cells by flow cytometry followed immediately after an initial 10 min incubation period.

#### 4.7.1.6. **Caspase-3/7 activity assay**

An Apo-ONE® Homogeneous caspase 3/7 assay kit (Promega)[177] was used to determine caspase activity. Cells ($3 \times 10^3$ per well) were seeded in 96 well opaque white or black cell culture plates and incubated overnight at 37 °C. Compound **48b** (at 50, 20, 10, 5, 1, 0.5, 0.1, and 0.05 µM as required) was introduced into the wells and the plate incubated for 72 h. Thereafter, 100 µl of Apo-ONE® caspase 3/7 reagent (caspase substrate + Apo-ONE caspase 3/7 buffer) was added to each well with gentle mixing (300-500 rpm) for at least 30 seconds. Plates were incubated for 30 min at room temperature. Well fluorescence was measured using an EnVision multilabel plate reader (PerkinElmer) at wavelengths between 499 nm and 521 nm.

# 5. References


[1] W. B. Pratt, W. D. Ensminger, R. W. Ruddon, *The Anticancer Drugs*, Oxford University Press, USA, **1994**.

[2] R. L. Siegel, K. D. Miller, A. Jemal, *CA: Cancer J. Clin.* **2019**, *69*, 7-34.

[3] R. Hesketh, *Introduction to Cancer Biology*, Cambridge; New York: Cambridge University Press, **2013**.

[4] N. V. Krakhmal, M. V. Zavyalova, E. V. Denisov, S. V. Vtorushin, V. M. Perelmuter, *Acta Naturae* **2015**, *7*, 17-28.

[5] S. R. Hamilton, L. A. Aaltonen, *Pathology and Genetics of Tumours of the Digestive System*, IARC Press: Lyon, France, **2000**, pp. 1-314.

[6] E. C. Hayden, *Nature* **2009**, *458*, 686-687.

[7] E. Meggers, *Chem. Commun.* **2009**, 1001-1010.

[8] R. J. Papac, *Yale J Biol Med.* **2001**, *74*, 391-398.

[9] B. A. Chabner, T. G. Roberts, *Nat. Rev. Cancer* **2005**, *5*, 65-72.

[10] M. Balali-Mood, M. Abdollahi, *Basic and Clinical Toxicology of Mustard Compounds*, Springer Berlin Heidelberg, Berlin, Heidelberg, Germany, **2015**, pp. 1-416.

[11] V. T. DeVita, E. Chu, *Cancer Res.* **2008**, *68*, 8643-8653.

[12] G. M. Cragg, D. J. Newman, *J. Ethnopharmacol.* **2005**, *100*, 72-79.

[13] A. Saleem, G. D. Brown, F. Brady, E. O. Aboagye, S. Osman, S. K. Luthra, A. S. Ranicar, C. S. Brock, M. F. Stevens, E. Newlands, *Cancer Res.* **2003**, *63*, 2409-2415.

[14] J. Zhang, M. FG Stevens, T. D Bradshaw, *Curr. Mol. Pharmacol.* **2012**, *5*, 102-114.

[15] B. A. Weaver, *Mol. Biol. Cell* **2014**, *25*, 2677-2681.

[16] V. Martin, *Semin. Oncol. Nurs.* **1993**, *9*, 2-5.

[17] V. Chaudhry, E. K. Rowinsky, S. E. Sartorius, R. C. Donehower, D. R. Cornblath, *Ann. Neurol.* **1994**, *35*, 304-311.

[18] L. K. Shawver, D. Slamon, A. Ullrich, *Cancer Cell* **2002**, *1*, 117-123.

[19] A. van Niekerk, P. Chellan, S. F. Mapolie, *Eur. J. Inorg. Chem.* **2019**, *2019*, 3432-3455.

[20] K. J. Williams, *J. R. Soc. Med.* **2009**, *102*, 343-348.

[21] N. C. Lloyd, H. W. Morgan, B. K. Nicholson, R. S. Ronimus, *Angew. Chem.* **2005**, *44*, 941-944.

[22] R. A. Sánchez-Delgado, A. Anzellotti, *Mini-Rev. Med. Chem.* **2004**, *4*, 23-30.

[23] S. Gómez-Ruiz, D. Maksimovic-Ivanic, S. Mijatovic, G. Kaluđerović, *Bioinorg Chem Appl*, **2012**, *2012*, 1-14.

[24] S. Trzaska, *Chem. Eng. News* **2005**, *83*, 52.

[25] E. R. Jamieson, S. J. Lippard, *Chem. Rev.* **1999**, *99*, 2467-2498.

[26] C. R. R. Rocha, M. M. Silva, A. Quinet, J. B. Cabral-Neto, C. F. M. Menck, *Clinics* **2018**, *73*.

[27] S. A.-S. Adnan, K. Mika, *Curr. Med. Chem.* **2006**, *13*, 1337-1357.

[28] C. Mauro, N. Giovanni, *Anti-Cancer Agents Med. Chem.* **2007**, *7*, 111-123.

[29] M. Kartalou, J. M. Essigmann, *Mutat. Res.* **2001**, *478*, 23-43.

[30] B. J. Reedijk, *Platinum Met. Rev.* **2008**, *52*, 2-11.

[31] D. A. Delmastro, J. Li, A. Vaisman, M. Solle, S. G. Chaney, *Cancer Chemother. Pharmacol.* **1996**, *39*, 245-253.

[32] C. R. R. Rocha, C. C. M. Garcia, D. B. Vieira, A. Quinet, L. C. de Andrade-Lima, V. Munford, J. E. Belizário, C. F. M. Menck, *Cell Death Dis* **2014**, *5*, e1505.

[33] E. Meléndez, *Crit. Rev. Oncol. Hematol.* **2002**, *42*, 309-315.

[34] R. H. Crabtree, *The organometallic chemistry of the transition metals*, John Wiley & Sons, Hoboken, NJ, USA, **2009**.

[35] N. Hazari, P. Mountford, *Acc. Chem. Res.* **2005**, *38*, 839-849.

[36] a) E. Swan, K. Platts, A. Blencowe, *Beilstein J. Org. Chem.* **2019**, *15*, 2113-2132;

b) J. Thiele, *Chem. Ber.* **1900**, *33*, 666-673.

[37] K. Strohfeldt, M. Tacke, *Chem. Soc. Rev.* **2008**, *37*, 1174-1187.

[38] I. Erden, F.-P. Xu, A. Sadoun, W. Smith, G. Sheff, M. Ossun, *J. Org. Chem.* **1995**, *60*, 813-820.

[39] N. J. Sweeney, J. Claffey, H. Müller-Bunz, C. Pampillón, K. Strohfeldt, M. Tacke, *Appl. Organomet. Chem.* **2007**, *21*, 57-65.

[40] N. Sweeney, W. M. Gallagher, H. Müller-Bunz, C. Pampillón, K. Strohfeldt, M. Tacke, *J. Inorg. Biochem.* **2006**, *100*, 1479-1486.

[41] P. J. Chirik, J. E. Bercaw, *Group 3 Metallocenes*, Wiley-VCH Verlag GmbH, Germany, **2008**, pp. 111-152.

[42] H. Köpf, P. Köpf-Maier, *Angew. Chem. Int. Ed. Engl.* **1979**, *18*, 477-478.

[43] J. H. Toney, T. J. Marks, *J. Am. Chem. Soc.* **1985**, *107*, 947-953.

[44] P. Köpf-Maier, H. Köpf, *Bioinorganic Chemistry*, Springer Berlin Heidelberg, Berlin, Heidelberg, Germany, **1988**, pp. 103-185.

[45] P. Köpf-Maier, A. Hesse, *J. Cancer Res. Clin. Oncol.* **1984**, *108*, 254-255.

[46] A. M. Pizarro, A. Habtemariam, P. J. Sadler, in *Medicinal Organometallic Chemistry* (Eds.: G. Jaouen, N. Metzler-Nolte), Springer Berlin Heidelberg, Berlin, Heidelberg, Germany, **2010**, pp. 21-56.

[47] E. Y. Tshuva, J. A. Ashenhurst, *Eur. J. Inorg. Chem.* **2009**, *2009*, 2203-2218.

[48] D. P. Buck, P. M. Abeysinghe, C. Cullinane, A. I. Day, J. G. Collins, M. M. Harding, *Dalton Trans.* **2008**, 2328-2334.

[49] C. M. Manna, E. Y. Tshuva, *Dalton Trans.* **2010**, *39*, 1182-1184.

[50] M. Guo, Z. Guo, P. J Sadler, *J. Biol. Inorg. Chem.* **2001**, *6*, 698-707.

[51] M. Cini, T. D. Bradshaw, S. Woodward, *Chem. Soc. Rev.* **2017**, *46*, 1040-1051.

[52] M. Guo, H. Sun, H. J. McArdle, L. Gambling, P. J. Sadler, *Biochemistry* **2000**, *39*, 10023-10033.

[53] A. Erxleben, J. Claffey, M. Tacke, *J. Inorg. Biochem.* **2010**, *104*, 390-396.

[54] M. L. McLaughlin, J. M. Cronan, T. R. Schaller, R. D. Snelling, *J. Am. Chem. Soc.* **1990**, *112*, 8949-8952.

[55] P. Köpf-Maier, *Eur. J. Clin. Pharmacol.* **1994**, *47*, 1-16.

[56] G. Lümmen, H. Sperling, H. Luboldt, T. Otto, H. Rübben, *Cancer Chemother. Pharmacol.* **1998**, *42*, 415-417.

[57] S. Cuffe, C. M. Dowling, J. Claffey, C. Pampillón, M. Hogan, J. M. Fitzpatrick, M. P. Carty, M. Tacke, R. W. G. Watson, *The Prostate* **2011**, *71*, 111-124.

[58] a) O. R. Allen, A. L. Gott, J. A. Hartley, J. M. Hartley, R. J. Knox, P. C. McGowan, *Dalton Trans.* **2007**, 5082-5090; b) O. R. Allen, L. Croll, A. L. Gott, R. J. Knox, P. C. McGowan, *Organometallics* **2004**, *23*, 288-292.

[59] A. Deally, F. Hackenberg, G. Lally, M. Tacke, *Int. J. Med. Chem.* **2012**, *2012*, 1-13.

[60] I. de la Cueva-Alique, S. Sierra, A. Pérez-Redondo, I. Marzo, L. Gude, T. Cuenca, E. Royo, *J. Organomet. Chem.* **2019**, *881*, 150-158.

[61] M. Cini, H. Williams, M. W. Fay, M. S. Searle, S. Woodward, T. D. Bradshaw, *Metallomics* **2016**, *8*, 286-297.

[62] M. J. Romero, P. J. Sadler, *Bioorganometallic Chemistry* (Ed.: G. J. M. Salmain), Wiley, New York, USA, **2015**, pp. 85-116.

[63] F. Arnesano, A. Pannunzio, M. Coluccia, G. Natile, *Coord. Chem. Rev.* **2015**, *284*, 286-297.

[64] I. de la Cueva-Alique, S. Sierra, L. Muñoz-Moreno, A. Pérez-Redondo, A. M. Bajo, I. Marzo, L. Gude, T. Cuenca, E. Royo, *J. Inorg. Biochem.* **2018**, *183*, 32-42.

[65] C. M. Manna, G. Armony, E. Y. Tshuva, *Inorg. Chem.* **2011**, *50*, 10284-10291.

[66] M. Hogan, M. Tacke, in *Medicinal Organometallic Chemistry* (Eds.: G. Jaouen, N. Metzler-Nolte), Springer Berlin Heidelberg, Berlin, Heidelberg, Germany, **2010**, *32*, pp. 119-140.

[67] T. Schilling, K. B. Keppler, M. E. Heim, G. Niebch, H. Dietzfelbinger, J. Rastetter, A. R. Hanauske, *Invest. New Drugs* **1995**, *13*, 327-332.

[68] A. Vessières, M.-A. Plamont, C. Cabestaing, J. Claffey, S. Dieckmann, M. Hogan, H. Müller-Bunz, K. Strohfeldt, M. Tacke, *J. Organomet. Chem.* **2009**, *694*, 874-879.

[69] B. K. Keppler, C. Friesen, H. G. Moritz, H. Vongerichten, E. Vogel, in *Bioinorganic Chemistry*, Springer, Berlin, Heidelberg, Germany, **1991**, pp. 97-127.

[70] E. Dubler, R. Buschmann, H. W. Schmalle, *J. Inorg. Biochem.* **2003**, *95*, 97-104.

[71] R. M. Lord, J. J. Mannion, B. D. Crossley, A. J. Hebden, M. W. McMullon, J. Fisher, R. M. Phillips, P. C. McGowan, *ChemistrySelect* **2016**, *1*, 6598-6605.

[72] S. Frühauf, W. J. Zeller, *Cancer Res.* **1991**, *51*, 2943-2948.

[73] E. Y. Tshuva, M. Versano, I. Goldberg, M. Kol, H. Weitman, Z. Goldschmidt, *Inorg. Chem. Commun.* **1999**, *2*, 371-373.

[74] E. Y. Tshuva, I. Goldberg, M. Kol, Z. Goldschmidt, *Inorg. Chem.* **2001**, *40*, 4263-4270.

[75] K. Butsch, T. Günther, A. Klein, K. Stirnat, A. Berkessel, J. Neudörfl, *Inorg. Chim. Acta* **2013**, *394*, 237-246.

[76] W. J. Burke, E. L. M. Glennie, C. Weatherbee, *J. Org. Chem.* **1964**, *29*, 909-912.

[77] A. K. Bowser, A. M. Anderson-Wile, D. H. Johnston, B. M. Wile, *Appl. Organomet. Chem.* **2016**, *30*, 32-39.

[78] W. J. Burke, J. L. Bishop, E. L. M. Glennie, W. N. Bauer, *J. Org. Chem.* **1965**, *30*, 3423-3427.

[79] E. Y. Tshuva, D. Peri, *Coord. Chem. Rev.* **2009**, *253*, 2098-2115.

[80] S. H. Kim, J. Lee, D. J. Kim, J. H. Moon, S. Yoon, H. J. Oh, Y. Do, Y. S. Ko, J.-H. Yim, Y. Kim, *J. Organomet. Chem.* **2009**, *694*, 3409-3417.

[81] M. Shavit, D. Peri, C. M. Manna, J. S. Alexander, E. Y. Tshuva, *J. Am. Chem. Soc.* **2007**, *129*, 12098-12099.

[82] J. C. Pessoa, I. Correia, *Coord. Chem. Rev.* **2019**, *388*, 227-247.

[83] D. Peri, S. Meker, M. Shavit, E. Y. Tshuva, *Chem. Eur. J.* **2009**, *15*, 2403-2415.

[84] T. A. Immel, M. Debiak, U. Groth, A. Bürkle, T. Huhn, *ChemMedChem* **2009**, *4*, 738-741.

[85] S. Meker, O. Braitbard, M. D. Hall, J. Hochman, E. Y. Tshuva, *Chem. Eur. J.* **2016**, *22*, 9986-9995.

[86] H. Glasner, S. Meker, E. Y. Tshuva, *J. Organomet. Chem.* **2015**, *788*, 33-35.

[87] M. Miller, E. Y. Tshuva, *Eur. J. Inorg. Chem.* **2014**, *2014*, 1485-1491.

[88] A. Tzubery, E. Y. Tshuva, *Inorg. Chem.* **2011**, *50*, 7946-7948.

[89] A. Tzubery, E. Y. Tshuva, *Inorg. Chem.* **2012**, *51*, 1796-1804.

[90] D. Peri, S. Meker, C. M. Manna, E. Y. Tshuva, *Inorg. Chem.* **2011**, *50*, 1030-1038.

[91] A. Tzubery, E. Y. Tshuva, *Eur. J. Inorg. Chem.* **2017**, *2017*, 1695-1705.

[92] R. Manne, M. Miller, A. Duthie, M. F. C. Guedes da Silva, E. Y. Tshuva, T. S. Basu Baul, *Dalton Trans.* **2019**, *48*, 304-314.

[93] Z. Shpilt, R. Manne, M. A. Rohman, S. Mitra, E. R. T. Tiekink, T. S. Basu Baul, E. Y. Tshuva, *Appl. Organomet. Chem.* **2020**, *34*, e5309.

[94] P. Gong, S. Thangapandian, Y. Li, G. Idakwo, J. Luttrell IV, M. Chen, H. Hong, C. Zhang, in *Advances in Computational Toxicology: Methodologies and Applications in Regulatory Science* (Ed.: H. Hong), Springer International Publishing, New York, USA, **2019**, pp. 99-118.

[95] D. L. Eaton, E. P. Gallagher, in *Comprehensive Toxicology (Second Edition)* (Ed.: C. A. McQueen), Elsevier, Oxford, UK, **2010**, pp. 1-46.

[96] J. B. Waern, H. H. Harris, B. Lai, Z. Cai, M. M. Harding, C. T. Dillon, *J. Biol. Inorg. Chem.* **2005**, *10*, 443-452.

[97] M. Miller, O. Braitbard, J. Hochman, E. Y. Tshuva, *J. Inorg. Biochem.* **2016**, *163*, 250-257.

[98] C. M. Manna, O. Braitbard, E. Weiss, J. Hochman, E. Y. Tshuva, *ChemMedChem* **2012**, *7*, 703-708.

[99] C.-P. Tan, Y.-Y. Lu, L.-N. Ji, Z.-W. Mao, *Metallomics* **2014**, *6*, 978-995.

[100] D. Hanahan, Robert A. Weinberg, *Cell* **2011**, *144*, 646-674.

[101] S. W. Lowe, E. Cepero, G. Evan, *Nature* **2004**, *432*, 307-315.

[102] J. M. Adams, S. Cory, *Oncogene* **2007**, *26*, 1324-1337.

[103] M. G. Brattain, W. D. Fine, F. M. Khaled, J. Thompson, D. E. Brattain, *Cancer Res* **1981**, *41*, 1751-1756.

[104] H. D. Soule, J. Vazquez, A. Long, S. Albert, M. Brennan, *JNCI: Journal of the National Cancer Institute* **1973**, *51*, 1409-1416.

[105] A. S. Levenson, V. C. Jordan, *Cancer Res* **1997**, *57*, 3071-3078.

[106] W. L. Wang, W. Porter, R. Burghardt, S. H. Safe, *Carcinogenesis* **1997**, *18*, 925-933.

[107] S. Pathak, M. J. Siciliano, R. Cailleau, C. L. Wiseman, T. C. Hsu, *J. Natl. Cancer Inst.* **1979**, *62*, 263-271.

[108] R. Gradiz, H. C. Silva, L. Carvalho, M. F. Botelho, A. Mota-Pinto, *Sci. Rep.* **2016**, *6*, 21648.

[109] a) D. Martínez-Maqueda, B. Miralles, I. Recio, in *The Impact of Food Bioactives on Health: in vitro and ex vivo models* (Eds.: K. Verhoeckx, P. Cotter, I. López-Expósito, C. Kleiveland, T. Lea, A. Mackie, T. Requena, D. Swiatecka, H. Wichers), Springer International Publishing, New York, USA, **2015**, pp. 113-124; b) MRC-5 (ATCC® CCL-171™) Available from: https://www.lgcstandards-atcc.org/products/all/CCL-171.aspx?geo_country=gb#.

[110] P. Preethalayam, K. S. Krishnan, S. Thulasi, S. S. Chand, J. Joseph, V. Nair, F. Jaroschik, K. V. Radhakrishnan, *Chem. Rev.* **2017**, *117*, 3930-3989.

[111] G. Erker, *Organometallics* **2011**, *30*, 358-368.

[112] K. Chajara, H. Ottosson, *Tetrahedron Lett.* **2004**, *45*, 6741-6744.

[113] R. Beckhaus, *Coord. Chem. Rev.* **2018**, *376*, 467-477.

[114] R. Beckhaus, A. Lützen, D. Haase, W. Saak, J. Stroot, S. Becke, J. Heinrichs, *Angew. Chem. Int. Ed.* **2001**, *40*, 2056-2058.

[115] Y. Kim, Y. Han, Y. Do, *J. Organomet. Chem.* **2001**, *634*, 19-24.

[116] R. Nouch, Organocatalytic Synthesis of Pentfulvene Derivative and Kinetic Analysis of Copper Catalysed 1,4-Addition, Doctoral Dissertation, University of Nottingham, **2020**.

[117] a) J. Liu, L. Wang, *Synthesis* **2017**, *49*, 960-972; b) A. Masatoshi, *Bull. Chem. Soc. Jpn.* **1990**, *63*, 721-727.

[118] M. Marigo, T. C. Wabnitz, D. Fielenbach, K. A. Jørgensen, *Angew. Chem. Int. Ed.* **2005**, *44*, 794-797.

[119] Y. Hayashi, H. Gotoh, T. Hayashi, M. Shoji, *Angew. Chem. Int. Ed.* **2005**, *44*, 4212-4215.

[120] R. J. Comito, F. G. Finelli, D. W. C. MacMillan, *J. Am. Chem. Soc.* **2013**, *135*, 9358-9361.

[121] G. A. Molander, J. A. C. Romero, *Tetrahedron* **2005**, *61*, 2631-2643.

[122] V. Sandanayaka, B. Mamat, R. K. Mishra, J. Winger, M. Krohn, L.-M. Zhou, M. Keyvan, L. Enache, D. Sullins, E. Onua, J. Zhang, G. Halldorsdottir, H. Sigthorsdottir, A. Thorlaksdottir, G. Sigthorsson, M. Thorsteinnsdottir, D. R. Davies, L. J. Stewart, D. E. Zembower, T. Andresson, A. S. Kiselyov, J. Singh, M. E. Gurney, *J. Med. Chem.* **2010**, *53*, 573-585.

[123] K. Nobuoka, S. Kitaoka, T. Kojima, Y. Kawano, K. Hirano, M. Tange, S. Obata, Y. Yamamoto, T. Harran, Y. Ishikawa, *Org. Chem. Int.* **2014**, *2014*, 1-9.

[124] C. Piazza, P. Knochel, *Angew. Chem. Int. Ed.* **2002**, *41*, 3263-3265.

[125] L. Brandsma, Verkruijsse, Hermann D, *Preparative Polar Organometallic Chemistry*, Springer-Verlag, Berlin Heidelberg, Germany, **1987**, *1*, 1-233.

[126] D. H. T. Phan, B. Kim, V. M. Dong, *J. Am. Chem. Soc.* **2009**, *131*, 15608-15609.

[127] D. B. Knight, J. A. Harrelson, *ChemComm* **1987**, 116-117.

[128] N. J. Sweeney, O. Mendoza, H. Müller-Bunz, C. Pampillón, F.-J. K. Rehmann, K. Strohfeldt, M. Tacke, *J. Organomet. Chem.* **2005**, *690*, 4537-4544.

[129] S. Eger, T. A. Immel, J. Claffey, H. Müller-Bunz, M. Tacke, U. Groth, T. Huhn, *Inorg. Chem.* **2010**, *49*, 1292-1294.

[130] C. Saturnino, E. Sirignano, A. Botta, M. S. Sinicropi, A. Caruso, A. Pisano, R. Lappano, M. Maggiolini, P. Longo, *Bioorg. Med. Chem. Lett.* **2014**, *24*, 136-140.

[131] J. E. McMurry, *Acc. Chem. Res.* **1974**, *7*, 281-286.

[132] C. W. Schwietert, J. P. McCue, *Coord. Chem. Rev.* **1999**, *184*, 67-89.

[133] F. Caruso, M. Rossi, C. Pettinari, *Expert Opin. Ther. Pat.* **2001**, *11*, 969-979.

[134] M. Cini, T. D. Bradshaw, S. Woodward, W. Lewis, *Angew. Chem. Int. Ed.* **2015**, *54*, 14179-14182.

[135] T. A. Immel, U. Groth, T. Huhn, P. Öhlschläger, *PLOS ONE* **2011**, *6*, e17869-e17869.

[136] N. Ganot, O. Briaitbard, A. Gammal, J. Tam, J. Hochman, E. Y. Tshuva, *ChemMedChem* **2018**, *13*, 2290-2296.

[137] S. Meker, O. Braitbard, M. D. Hall, J. Hochman, E. Y. Tshuva, *Chem. Eur. J.* **2016**, *22*, 9986-9995.

[138] T. Pesch, H. Schuhwerk, P. Wyrsch, T. Immel, W. Dirks, A. Bürkle, T. Huhn, S. Beneke, *BMC Cancer* **2016**, *16*, 469.

[139] A. Lehtonen, R. Sillanpää, *Inorg. Chem.* **2004**, *43*, 6501-6506.

[140] J. Okuda, S. Fokken, H.-C. Kang, W. Massa, *Polyhedron* **1998**, *17*, 943-946.

[141] C. M. G. Azevedo, C. M. M. Afonso, J. X. Soares, S. Reis, D. Sousa, R. T. Lima, M. H. Vasconcelos, M. Pedro, J. Barbosa, L. Gales, M. M. M. Pinto, *Eur. J. Med. Chem.* **2013**, *69*, 798-816.

[142] a) C.-T. Chen, C.-A. Huang, B.-H. Huang, *Macromolecules* **2004**, *37*, 7968-7973; b) A. Lehtonen, H. Balcar, J. Sedláček, R. Sillanpää, *J. Organomet. Chem.* **2008**, *693*, 1171-1176.

[143] A. J. Chmura, M. G. Davidson, M. D. Jones, M. D. Lunn, M. F. Mahon, *Dalton Trans.* **2006**, 887-889.

[144] S. Kirschbaum, K. Landfester, A. Taden, *Macromolecules* **2015**, *48*, 3811-3816.

[145] C. Fan, S. Pu, G. Liu, T. Yang, *J. Photochem. Photobiol.* **2008**, *197*, 415-425.

[146] S. Meker, C. M. Manna, D. Peri, E. Y. Tshuva, *Dalton Trans.* **2011**, *40*, 9802-9809.

[147] T. Weyhermüller, R. Wagner, P. Chaudhuri, *Eur. J. Inorg. Chem.* **2011**, *2011*, 2547-2557.

[148] A. Peuronen, A. Lehtonen, *Top. Catal.* **2016**, *59*, 1132-1137.

[149] S. Phongtamrug, K. Tashiro, M. Miyata, S. Chirachanchai, *J. Phys. Chem. B* **2006**, *110*, 21365-21370.

[150] T. Weyhermüller, T. K. Paine, E. Bothe, E. Bill, P. Chaudhuri, *Inorg. Chim. Acta* **2002**, *337*, 344-356.

[151] D. Maity, J. Marek, W. S. Sheldrick, H. Mayer-Figge, M. Ali, *J. Mol. Catal. Chem.* **2007**, *270*, 153-159.

[152] S. Groysman, E. Y. Tshuva, I. Goldberg, M. Kol, Z. Goldschmidt, M. Shuster, *Organometallics* **2004**, *23*, 5291-5299.

[153] R. M. Lord, J. J. Mannion, A. J. Hebden, A. E. Nako, B. D. Crossley, M. W. McMullon, F. D. Janeway, R. M. Phillips, P. C. McGowan, *ChemMedChem* **2014**, *9*, 1136-1139.

[154] B. Bertrand, P.-E. Doulain, C. Goze, E. Bodio, *Dalton Trans.* **2016**, *45*, 13005-13011.

[155] G. W. Severin, C. H. Nielsen, A. I. Jensen, J. Fonslet, A. Kjær, F. Zhuravlev, *J. Med. Chem.* **2015**, *58*, 7591-7595.

[156] A. Martin, A. Byrne, C. Dolan, R. J. Forster, T. E. Keyes, *ChemComm* **2015**, *51*, 15839-15841.

[157] P. Farràs, A. C. Benniston, *Tetrahedron Lett.* **2014**, *55*, 7011-7014.

[158] O. Florès, A. Trommenschlager, S. Amor, F. Marques, F. Silva, L. Gano, F. Denat, M. P. Cabral Campello, C. Goze, E. Bodio, P. Le Gendre, *Dalton Trans.* **2017**, *46*, 14548-14555.

[159] Y. He, M. Lin, Z. Li, X. Liang, G. Li, J. C. Antilla, *Org. Lett.* **2011**, *13*, 4490-4493.

[160] W. Wu, L. Liu, X. Cui, C. Zhang, J. Zhao, *Dalton Trans.* **2013**, *42*, 14374-14379.

[161] L. P. Jameson, S. V. Dzyuba, *Beilstein J. Org. Chem.* **2013**, *9*, 786-790.

[162] C. Baylon, M.-P. Heck, C. Mioskowski, *J. Org. Chem.* **1999**, *64*, 3354-3360.

[163] C. Kim, T. G. Traylor, C. L. Perrin, *J. Am. Chem. Soc.* **1998**, *120*, 9513-9516.

[164] J. H. Lee, S. Gupta, W. Jeong, Y. H. Rhee, J. Park, *Angew. Chem. Int. Ed.* **2012**, *51*, 10851-10855.

[165] D. Bai, A. C. Benniston, J. Hagon, H. Lemmetyinen, N. V. Tkachenko, W. Clegg, R. W. Harrington, *Phys. Chem. Chem. Phys.* **2012**, *14*, 4447-4456.

[166] K. M. Buettner, A. M. Valentine, *Chem. Rev.* **2012**, *112*, 1863-1881.

[167] J. A. Plumb, in *Cancer Cell Culture: Methods and Protocols* (Ed.: S. P. Langdon), Humana Press, Totowa, NJ, USA, **2004**, pp. 165-169.

[168] T. Mosmann, *J. Immunol. Methods* **1983**, *65*, 55-63.

[169] J. van Meerloo, G. J. L. Kaspers, J. Cloos, in *Cancer Cell Culture: Methods and Protocols* (Ed.: I. A. Cree), Humana Press, Totowa, NJ, USA, **2011**, pp. 237-245.

[170] S. A. Loza-Rosas, M. Saxena, Y. Delgado, K. Gaur, M. Pandrala, A. D. Tinoco, *Metallomics* **2017**, *9*, 346-356.

[171] C. Hansch, A. Leo, R. W. Taft, *Chem. Rev.* **1991**, *91*, 165-195.

[172] R. B. Badisa, S. F. Darling-Reed, P. Joseph, J. S. Cooperwood, L. M. Latinwo, C. B. Goodman, *Anticancer Res.* **2009**, *29*, 2993-2996.

[173] a) A. Tzubery, N. Melamed-Book, E. Y. Tshuva, *Dalton Trans.* **2018**, *47*, 3669-3673; b) S. J. Lucas, R. M. Lord, A. M. Basri, S. J. Allison, R. M. Phillips, A. J. Blacker, P. C. McGowan, *Dalton Trans.* **2016**, *45*, 6812-6815.

[174] N. A. P. Franken, H. M. Rodermond, J. Stap, J. Haveman, C. van Bree, *Nature Protocols* **2006**, *1*, 2315-2319.

[175] H. Rafehi, C. Orlowski, G. T. Georgiadis, K. Ververis, A. El-Osta, T. C. Karagiannis, *J. Vis. Exp.* **2011**, 2573.

[176] A. Munshi, M. Hobbs, R. E. Meyn, in *Chemosensitivity: Volume 1 In Vitro Assays* (Ed.: R. D. Blumenthal), Humana Press, Totowa, NJ, USA, **2005**, pp. 21-28.

[177] M. E. Qazzaz, V. J. Raja, K.-H. Lim, T.-S. Kam, J. B. Lee, P. Gershkovich, T. D. Bradshaw, *Cancer Lett.* **2016**, *370*, 185-197.

[178] V. J. Raja, K.-H. Lim, C.-O. Leong, T.-S. Kam, T. D. Bradshaw, *Invest. New Drugs* **2014**, *32*, 838-850.

[179] P. Pozarowski, Z. Darzynkiewicz, in *Checkpoint Controls and Cancer: Volume 2: Activation and Regulation Protocols* (Ed.: A. H. Schönthal), Humana Press, Totowa, NJ, USA, **2004**, pp. 301-311.

[180] C. Riccardi, I. Nicoletti, *Nat. Protoc.* **2006**, *1*, 1458-1461.

[181] Z. Darzynkiewicz, G. Juan, E. Bedner, *Curr Protoc Cell Biol* **1999**, *1*, 8.4.1-8.4.18.

[182] D. Yang, J. Reedijk, G. A. van der Marel, A. H. J. Wang, *J. Biomol. Struct. Dyn.* **1996**, *13*, 989-998.

[183] I. Vermes, C. Haanen, H. Steffens-Nakken, C. Reutellingsperger, *J. Immunol. Methods* **1995**, *184*, 39-51.

[184] L. J. Kuo, L.-X. Yang, *In Vivo* **2008**, *22*, 305-309.

[185] J. Wang, M. J. Lenardo, *J. Cell Sci.* **2000**, *113*, 753-757.

[186] J. Li, J. Yuan, *Oncogene* **2008**, *27*, 6194-6206.

[187] R. U. Jänicke, *Breast Cancer Res. Treat.* **2009**, *117*, 219-221.

[188] C. Hansch, J. P. Björkroth, A. Leo, *J. Pharm. Sci.* **1987**, *76*, 663-687.

[189] D. Screnci, M. McKeage, P. Galettis, T. Hambley, B. Palmer, B. Baguley, *Br. J. Cancer* **2000**, *82*, 966-972.

[190] Y. Asano, H. Ito, K. Hara, M. Sawamura, *Organometallics* **2008**, *27*, 5984-5996.

[191] a) K. V. Zaitsev, M. V. Bermeshev, A. A. Samsonov, J. F. Oprunenko, A. V. Churakov, J. A. L. Howard, S. S. Karlov, G. S. Zaitseva, *New J. Chem.* **2008**, *32*, 1415-1431; b) Y. Hong, S.-D. Mun, J. Lee, Y. Do, Y. Kim, *J. Organomet. Chem.* **2008**, *693*, 1945-1951.

[192] S.-d. Mun, S. H. Kim, J. Lee, H.-J. Kim, Y. Do, Y. Kim, *Polyhedron* **2010**, *29*, 379-383.

[193] D. Cousin, J. Zhang, M. G. Hummersone, C. S. Matthews, M. Frigerio, T. D. Bradshaw, M. F. G. Stevens, *MedChemComm* **2016**, *7*, 2332-2343.

[194] Preliminary discussion with Dr. David Boocock, Nottingham Trent University, see also https://www.ntu.ac.uk/staff-profiles/science-technology/david-boocock.

[195] S. Woodward in *Transition Metals in Organic Synthesis* (Ed.: S. E. Gibson, née Thomas), Oxford University Press, Oxford, UK, **1997**, pp. 1-34.

[196] U. Albrecht, T. H. Van Nguyen, P. Langer, *J. Org. Chem.* **2004**, *69*, 3417-3424.

[197] S. Saha, A. Sarbajna, J. K. Bera, *Tetrahedron Lett.* **2014**, *55*, 1444-1447.

[198] C. K. Mahato, S. Mukherjee, M. Kundu, A. Pramanik, *J. Org. Chem.* **2019**, *84*, 1053-1063.

[199] Parthasaradhi Reddy. Bandi, *C-3 Novel Triterpenone with C-28 Amide Derivatives As HIV Inhibitors*, **2018**, 20180237472.

[200] F. An, B. Maji, E. Min, A. R. Ofial, H. Mayr, *J. Am. Chem. Soc.* **2020**, *142*, 1526-1547.

[201] P. Canonne, J. Plamondon, M. Akssira, *Tetrahedron* **1988**, *44*, 2903-2912.

[202] B. Liu, X. Zhou, *Chin. Chem. Lett.* **2019**, *30*, 725-728.

[203] W. Chen, Z.-H. Zhou, H.-B. Chen, *Org. Biomol. Chem.* **2017**, *15*, 1530-1536.

[204] C. I. Someya, S. Inoue, E. Irran, S. Krackl, S. Enthaler, *Eur. J. Inorg. Chem.* **2011**, *2011*, 2691-2697.

[205] Z. Lu, C. Hu, J. Guo, J. Li, Y. Cui, Y. Jia, *Org. Lett.* **2010**, *12*, 480-483.

[206] M. Altamura, E. Perrotta, *J. Org. Chem.* **1993**, *58*, 272-274.

[207] C. D. Selassie, R. P. Verma, S. Kapur, A. J. Shusterman, C. Hansch, *J. Chem. Soc., Perkin Trans. 2*, **2002**, 1112-1117.

[208] C. Viglianisi, M. G. Bartolozzi, G. F. Pedulli, R. Amorati, S. Menichetti, *Chem. Eur. J.* **2011**, *17*, 12396-12404.

[209] M. Matsumoto, K. Kobayashi, Y. Hotta, *J. Org. Chem.* **1984**, *49*, 4740-4741.

[210] A. I. Kuruppu, The Role of HER Family Signalling in Breast Cancer, Doctoral Dissertation, University of Nottinghm **2015**.

[211] I. Nicoletti, G. Migliorati, M. C. Pagliacci, F. Grignani, C. Riccardi, *J. Immunol. Methods* **1991**, *139*, 271-279.

# 6. Appendix

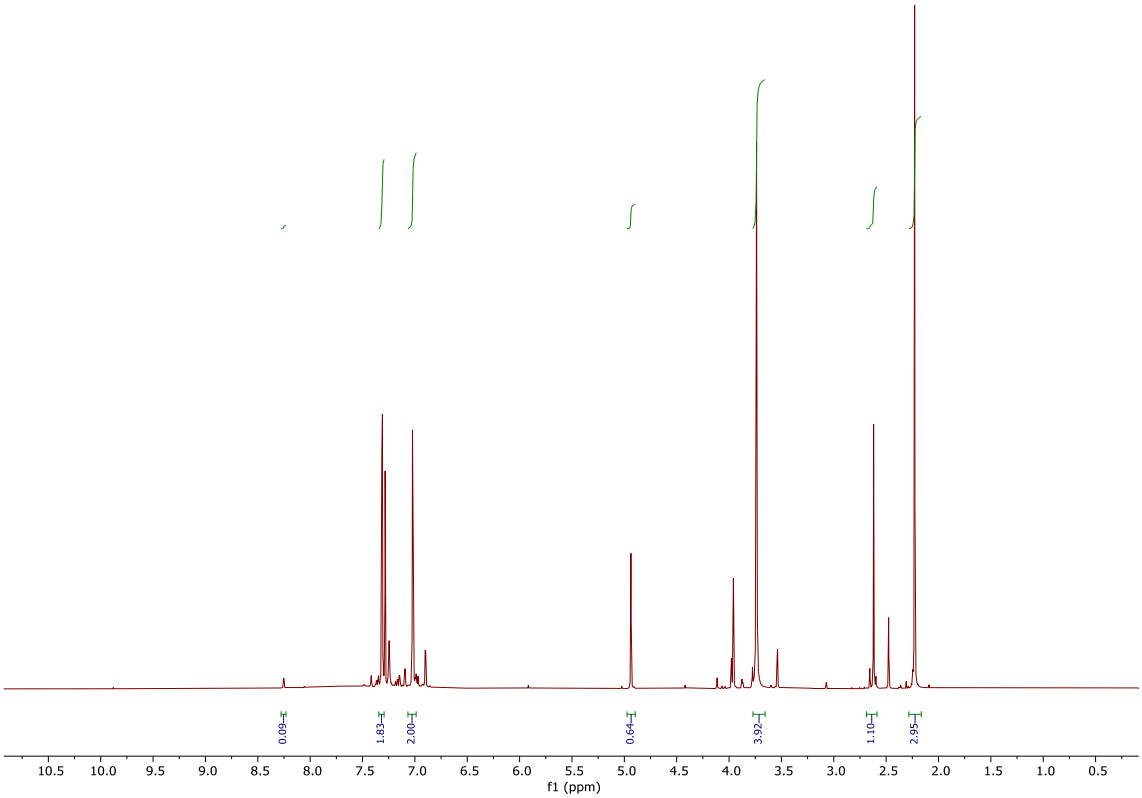


**Figure S1. $^{1}$H NMR** spectrum of **47g** in the crude mixture.

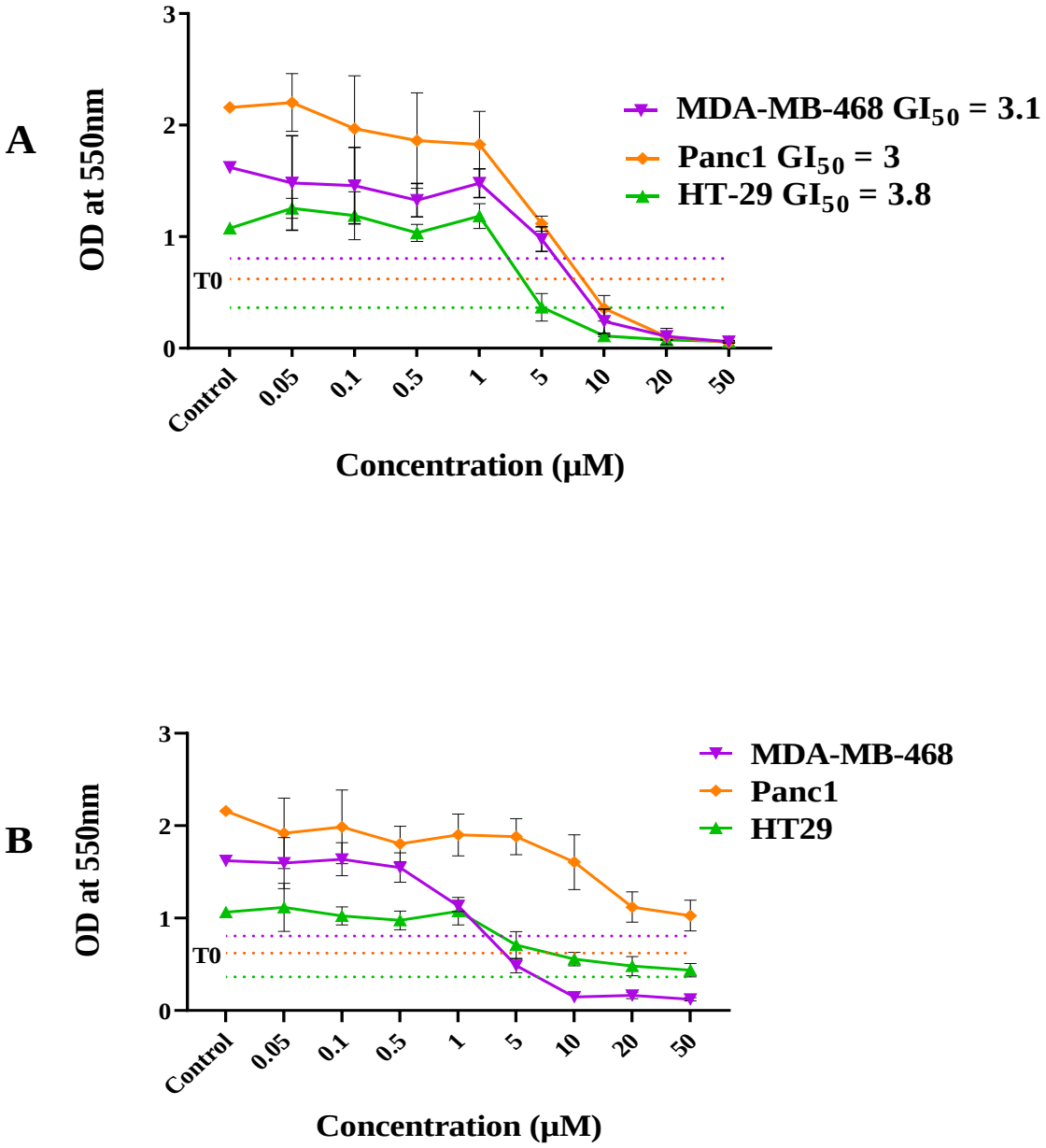


**Figure S2.** Representative dose-dependent growth inhibitory properties of **48b** (**A**) and cisplatin (**B**) against MDA-MB-468, Panc1 and HT-29 carcinoma cell lines. Data points depict mean ± S.D. n = 8; ≥3 independent trials were conducted.

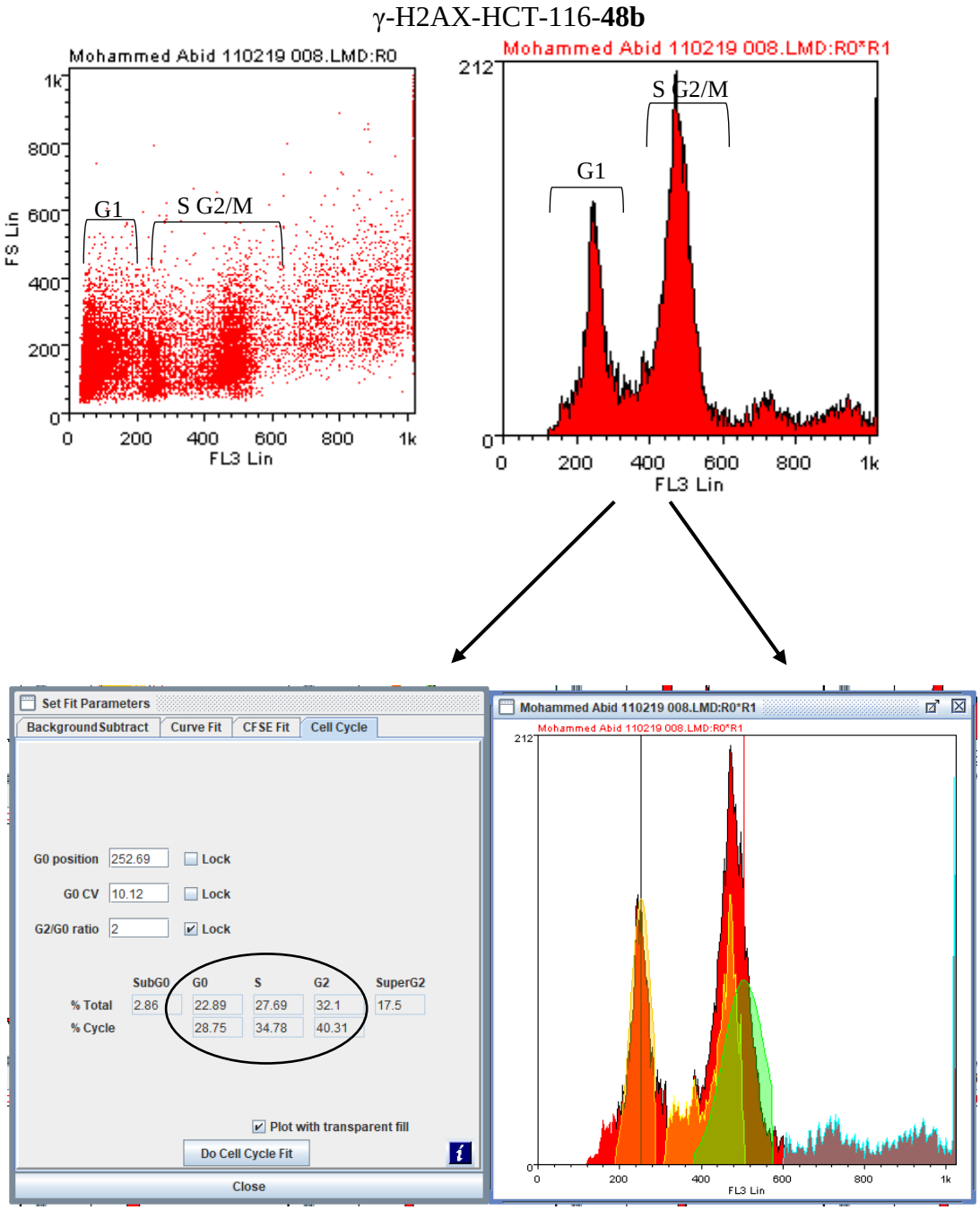


**Figure S3.** Shows the event of γ-H2AX with HCT-116 after the addition of **48b**.

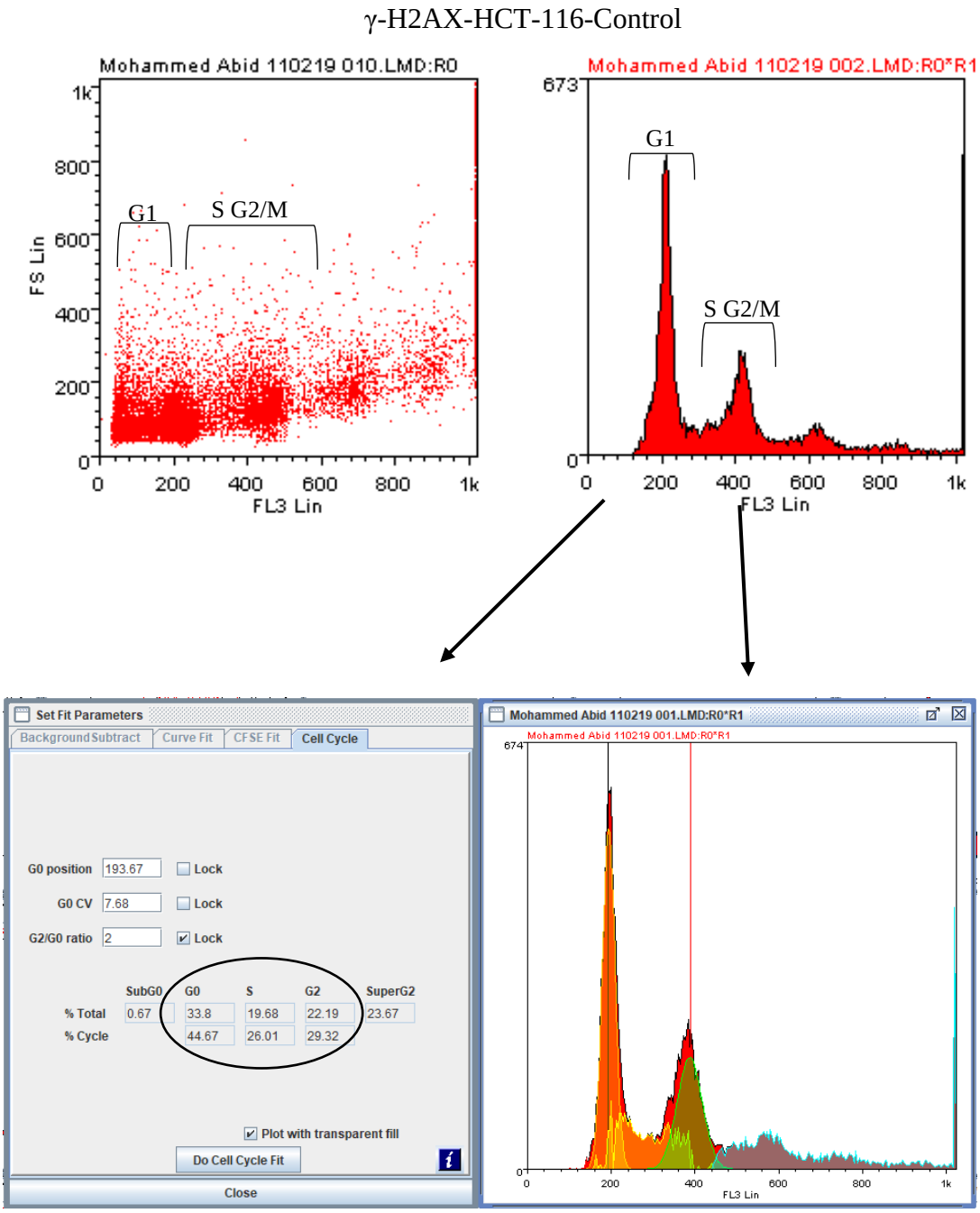


**Figure S4.** Shows the event of γ-H2AX with HCT-116 before addition of titanium agent (control).

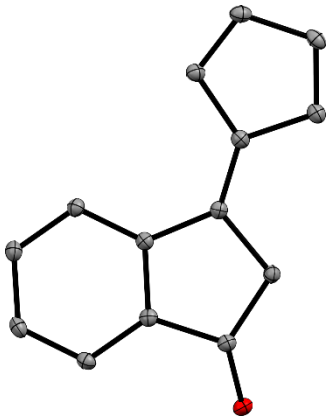

**(*R*)-24**

| | |
|---|---|
| Identification code | MCSWCI |
| Empirical formula | $C_{14}H_{14}O_1$ |
| Formula weight | 196.24 |
| Temperature/K | 120(2) |
| Crystal system | trigonal |
| Space group | P3 |
| a/Å | 21.5126(16) |
| b/Å | 21.5126(16) |
| c/Å | 5.7918(5) |
| α/° | 90 |
| β/° | 90 |
| γ/° | 120 |
| Volume/Å$^3$ | 2321.3(4) |
| Z | 9 |
| $\rho_{calc}$g/cm$^3$ | 1.263 |
| μ/mm$^{-1}$ | 0.609 |
| F(000) | 936.0 |
| Crystal size/mm$^3$ | 0.4071 × 0.3698 × 0.1057 |
| Radiation | CuKα (λ = 1.54184) |
| 2Θ range for data collection/° | 14.262 to 148.276 |
| Index ranges | -23 ≤ h ≤ 18, -22 ≤ k ≤ 26, -6 ≤ l ≤ 6 |
| Reflections collected | 3166 |
| Independent reflections | 1618 [$R_{int}$ = 0.0176, $R_{sigma}$ = 0.0227] |
| Data/restraints/parameters | 1618/1/140 |
| Goodness-of-fit on F$^2$ | 1.053 |
| Final R indexes [I>=2σ (I)] | $R_1$ = 0.0245, $wR_2$ = 0.0635 |
| Final R indexes [all data] | $R_1$ = 0.0248, $wR_2$ = 0.0638 |
| Largest diff. peak/hole / e Å$^{-3}$ | 0.12/-0.12 |
| Flack parameter | -0.02(15) |

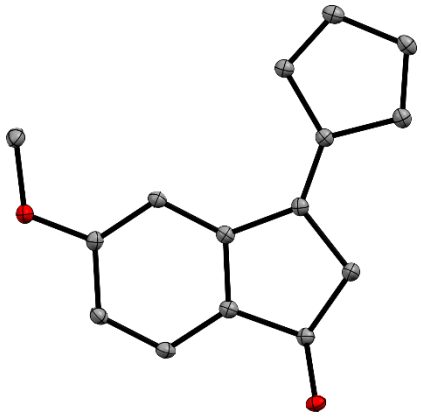

**(*R*)-27**

| | |
|---|---|
| Identification code | RJNSWA |
| Empirical formula | $C_{15}H_{14}O_2$ |
| Formula weight | 226.26 |
| Temperature/K | 120(2) |
| Crystal system | trigonal |
| Space group | $P3_1$ |
| a/Å | 12.3941(4) |
| b/Å | 12.3941(4) |
| c/Å | 6.5877(2) |
| α/° | 90 |
| β/° | 90 |
| γ/° | 120 |
| Volume/Å$^3$ | 876.39(6) |
| Z | 3 |
| $\rho_{calc}$g/cm$^3$ | 1.286 |
| μ/mm$^{-1}$ | 0.673 |
| F(000) | 360.0 |
| Crystal size/mm$^3$ | 0.081 × 0.068 × 0.038 |
| Radiation | CuKα (λ = 1.54184) |
| 2Θ range for data collection/° | 8.238 to 147.166 |
| Index ranges | $-14 \leq h \leq 13$, $-15 \leq k \leq 11$, $-7 \leq l \leq 8$ |
| Reflections collected | 4587 |
| Independent reflections | 2264 [$R_{int}$ = 0.0237, $R_{sigma}$ = 0.0301] |
| Data/restraints/parameters | 2264/1/156 |
| Goodness-of-fit on $F^2$ | 1.068 |
| Final R indexes [I>=2σ (I)] | $R_1$ = 0.0303, $wR_2$ = 0.0716 |
| Final R indexes [all data] | $R_1$ = 0.0322, $wR_2$ = 0.0728 |
| Largest diff. peak/hole / e Å$^{-3}$ | 0.11/-0.14 |
| Flack parameter | 0.03(15) |

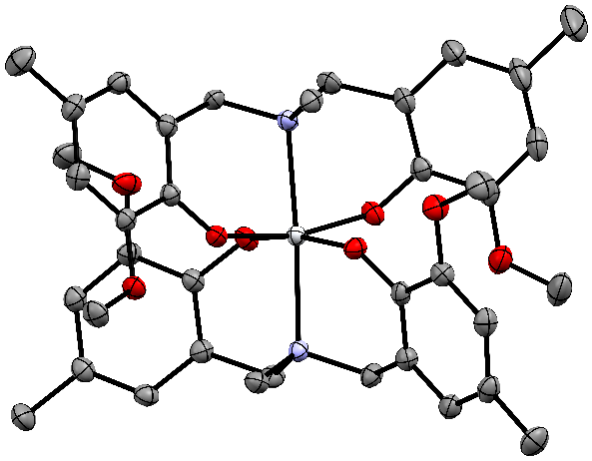

**48b**

| | |
|---|---|
| Identification code | MAASWA |
| Empirical formula | $C_{38}H_{46}N_2O_8Ti$ |
| Formula weight | 706.67 |
| Temperature/K | 120(2) |
| Crystal system | monoclinic |
| Space group | $P2_1$ |
| a/Å | 11.21970(19) |
| b/Å | 23.2053(4) |
| c/Å | 14.0298(2) |
| α/° | 90 |
| β/° | 105.8538(17) |
| γ/° | 90 |
| Volume/Å$^3$ | 3513.81(10) |
| Z | 4 |
| $\rho_{calc}$g/cm$^3$ | 1.336 |
| μ/mm$^{-1}$ | 2.519 |
| F(000) | 1496.0 |
| Crystal size/mm$^3$ | 0.286 × 0.169 × 0.085 |
| Radiation | CuKα (λ = 1.54184) |
| 2Θ range for data collection/° | 6.55 to 148.884 |
| Index ranges | $-14 \leq h \leq 13$, $-28 \leq k \leq 28$, $-15 \leq l \leq 17$ |
| Reflections collected | 28369 |
| Independent reflections | 13947 [$R_{int}$ = 0.0271, $R_{sigma}$ = 0.0356] |
| Data/restraints/parameters | 13947/1/904 |
| Goodness-of-fit on $F^2$ | 1.021 |
| Final R indexes [I>=2σ (I)] | $R_1$ = 0.0374, $wR_2$ = 0.0958 |
| Final R indexes [all data] | $R_1$ = 0.0391, $wR_2$ = 0.0976 |
| Largest diff. peak/hole / e Å$^{-3}$ | 1.04/-0.24 |
| Flack parameter | 0.457(5) |

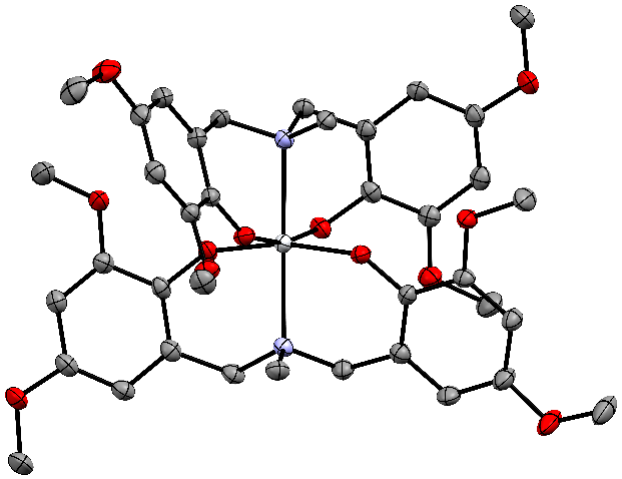

**48e**

| | |
|---|---|
| Identification code | MAASWD |
| Empirical formula | $C_{39}H_{48}N_2O_{12}Cl_2Ti$ |
| Formula weight | 855.59 |
| Temperature/K | 120(2) |
| Crystal system | monoclinic |
| Space group | $P2_1/n$ |
| a/Å | 13.7166(2) |
| b/Å | 21.9379(3) |
| c/Å | 14.14825(19) |
| α/° | 90 |
| β/° | 110.9940(16) |
| γ/° | 90 |
| Volume/Å$^3$ | 3974.78(10) |
| Z | 4 |
| $\rho_{calc}$g/cm$^3$ | 1.430 |
| μ/mm$^{-1}$ | 3.614 |
| F(000) | 1792.0 |
| Crystal size/mm$^3$ | 0.118 × 0.084 × 0.054 |
| Radiation | CuKα (λ = 1.54184) |
| 2Θ range for data collection/° | 7.704 to 150.324 |
| Index ranges | $-17 \leq h \leq 17$, $-27 \leq k \leq 26$, $-16 \leq l \leq 17$ |
| Reflections collected | 33174 |
| Independent reflections | 7985 [$R_{int}$ = 0.0543, $R_{sigma}$ = 0.0429] |
| Data/restraints/parameters | 7985/0/515 |
| Goodness-of-fit on $F^2$ | 1.008 |
| Final R indexes [I>=2σ (I)] | $R_1$ = 0.0364, $wR_2$ = 0.0916 |
| Final R indexes [all data] | $R_1$ = 0.0470, $wR_2$ = 0.0980 |
| Largest diff. peak/hole / e Å$^{-3}$ | 0.72/-0.52 |

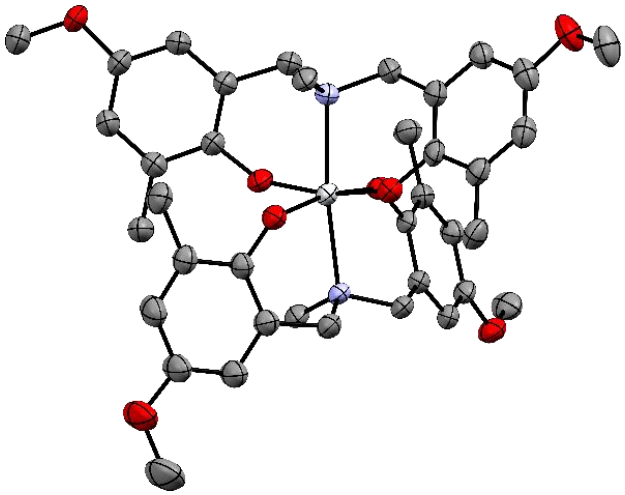

**48d**

| | |
|---|---|
| Identification code | MAASWG_tw |
| Empirical formula | $C_{40.5}H_{52}N_2O_8Ti$ |
| Formula weight | 742.74 |
| Temperature/K | 120(2) |
| Crystal system | triclinic |
| Space group | P-1 |
| a/Å | 14.7859(5) |
| b/Å | 16.7001(7) |
| c/Å | 18.4355(9) |
| α/° | 64.736(5) |
| β/° | 68.608(4) |
| γ/° | 89.619(3) |
| Volume/Å$^3$ | 3772.6(3) |
| Z | 4 |
| $\rho_{calc}$g/cm$^3$ | 1.308 |
| μ/mm$^{-1}$ | 2.370 |
| F(000) | 1580.0 |
| Crystal size/mm$^3$ | 0.152 × 0.084 × 0.014 |
| Radiation | CuKα (λ = 1.54184) |
| 2Θ range for data collection/° | 7.974 to 155.212 |
| Index ranges | -18 ≤ h ≤ 18, -18 ≤ k ≤ 21, -20 ≤ l ≤ 23 |
| Reflections collected | 15336 |
| Independent reflections | 15336 [$R_{int}$ = ?, $R_{sigma}$ = 0.0531] |
| Data/restraints/parameters | 15336/0/951 |
| Goodness-of-fit on F$^2$ | 1.050 |
| Final R indexes [I>=2σ (I)] | $R_1$ = 0.0900, w$R_2$ = 0.2636 |
| Final R indexes [all data] | $R_1$ = 0.1146, w$R_2$ = 0.2870 |
| Largest diff. peak/hole / e Å$^{-3}$ | 1.25/-0.91 |

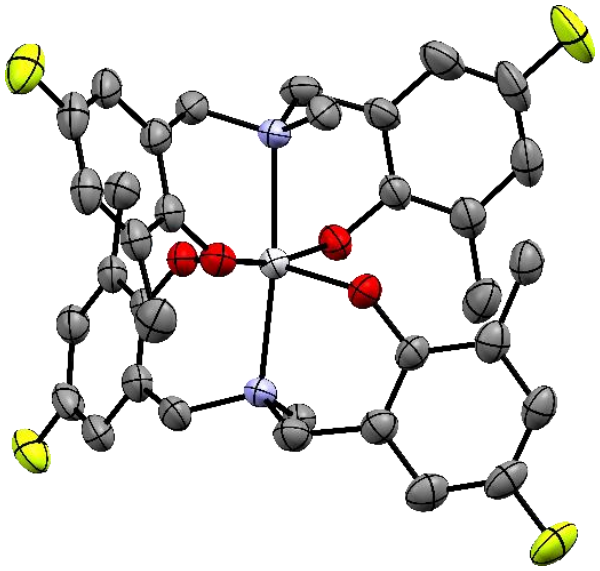

**48f**

| | |
|---|---|
| Identification code | MAASWF |
| Empirical formula | $C_{34.5}H_{35}ClF_4N_2O_4Ti$ |
| Formula weight | 700.99 |
| Temperature/K | 120(2) |
| Crystal system | triclinic |
| Space group | P-1 |
| a/Å | 12.6700(8) |
| b/Å | 16.5527(13) |
| c/Å | 16.5998(7) |
| α/° | 97.696(5) |
| β/° | 91.062(4) |
| γ/° | 110.178(6) |
| Volume/Å$^3$ | 3230.4(4) |
| Z | 4 |
| $\rho_{calc}$g/cm$^3$ | 1.441 |
| μ/mm$^{-1}$ | 3.568 |
| F(000) | 1452.0 |
| Crystal size/mm$^3$ | 0.403 × 0.403 × 0.072 |
| Radiation | CuKα (λ = 1.54184) |
| 2Θ range for data collection/° | 7.452 to 151.696 |
| Index ranges | -15 ≤ h ≤ 9, -20 ≤ k ≤ 20, -20 ≤ l ≤ 19 |
| Reflections collected | 24487 |
| Independent reflections | 12780 [$R_{int}$ = 0.0920, $R_{sigma}$ = 0.0969] |
| Data/restraints/parameters | 12780/77/878 |
| Goodness-of-fit on F$^2$ | 1.052 |
| Final R indexes [I>=2σ (I)] | $R_1$ = 0.1013, $wR_2$ = 0.2617 |
| Final R indexes [all data] | $R_1$ = 0.1239, $wR_2$ = 0.3094 |
| Largest diff. peak/hole / e Å$^{-3}$ | 2.01/-1.00 |

ChemPubSoc Europe

DOI: 10.1002/chem.201704247

CHEMISTRY A European Journal Communication

Synthetic Methods

# Enantioselective Synthesis of 6,6-Disubstituted Pentafulvenes Containing a Chiral Pendant Hydroxy Group

Ryan Nouch,[a] Melchior Cini,[a] Marc Magre,[b] Mohammed Abid,[a] Montserrat Diéguez,*[b] Oscar Pàmies,[b] Simon Woodward,*[a] and William Lewis[a]

**Abstract:** Simple enantioselective synthesis of 6,6-disubstituted pentafulvenes bearing chiral pendant hydroxy groups are attained by cascade reactivity using commercially available proline-based organocatalysts. Condensation of cyclopentadiene with the acetyl function of a 1,2-formylacetophenone, followed by cyclization of a resulting fulvene-stabilized carbanion with the formyl group, generates bicyclic chiral alcohols with initial *er* values up to 94:6. Exceptional enantio-enrichment of the resultant alcohols results upon crystallization—even near racemic samples spontaneously de-racemize. This enables new families of substituted cyclopentadienes that are both enantiomerically and diastereomerically pure to be rapidly attained.

Synthetic methodology for pentafulvene formation has not altered significantly since these were first prepared by Thiele in 1900 by sodium ethoxide-facilitated condensation of cyclopentadiene with ketones (Scheme 1).[1] Although improved by Little[2] and Ottosson,[3] among others, none of these allows access to chiral fulvenes. Little's method uses pyrrolidine catalysis to increase the reactivity of the ketone, while Ottosson's method uses sodium cyclopentadienide as a more reactive source of the cyclopentadiene nucleophile. Both approaches allow for the reaction of more hindered or less activated carbonyls. Across the board, examples of syntheses of pentafulvenes bearing chiral pendant functional groups are almost unknown, one rare example being Togni's condensation of sodium cyclopentadienide with a homochiral amide (Scheme 1).[4] Unfortunately, this method was limited in scope as only two chiral examples of singly substituted 6-derivatives could be accessed. Despite a complete lack of effective stereoselective syntheses, pentafulvenes remain a commonly used compound class. Frequent applications include: cycloadditions to generate complex, polycyclic scaffolds[5,6] and their use as intermediates in the synthesis of substituted (sometimes chiral) cyclopentadienyl derivatives by nucleophilic addition to the exocyclic C=C bond as a route to (asymmetric) cyclopentadiene units.[7–9] Herein we describe a simple approach to families of asymmetric 6,6-disubstituted pentafulvenes bearing chiral pendant hydroxy groups (for further functionalization) by straightforward organocatalytic methodology. The pentafulvenes are useful as intermediates in the synthesis of substituted cyclopentadienes as single enantiomers and diastereomers.

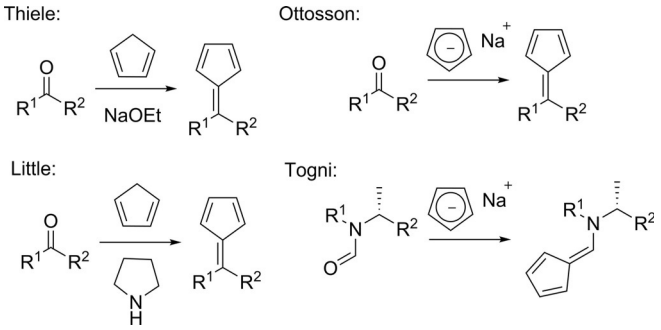


**Scheme 1.** Traditional approaches to (chiral) 6,6- and 6-substituted pentafulvenes.

To develop a route to new chiral pentafulvenes bearing pendant hydroxy groups, we investigated the reaction between 2-acetyl-benzaldehyde and cyclopentadiene in the presence of organocatalysts (Table 1). Reference samples of (±)-**2a** were prepared via pyrrolidine catalysed reactions, although these were slower than the later enantioselective reactions (see Table S1 in the Supporting Information). Interestingly, we noted that (±)-**2a** de-racemizes exceptionally readily, with each crystal being a single enantiomer, in the same manner as the classical tartrate crystals of Pasteur.[10,11] Individual crystals of (*R*) or (*S*)-**2a** are readily attained stochastically from initially racemic (±)-**2a**. This occurs predictably for scalemic **2a** making exceptional enantio-enrichment possible. Conglomerate crystal formation in **2a** is driven by a strongly stereodirecting helical hydrogen bonding array in its packing (see Figure S5 in the Supporting Information). Simple (L)-proline gave only low yields of **2a**, but greater success was had with derivatives of (*S*)-2-pyrrolidinemethanol ($\mathbf{L_A}$). Smaller amounts of achiral **3** and aldol product **4** could also be isolated from the reaction. Compound **4** is a known product of **1a** (formed in low *er* in asymmetric aldol chemistry)[12] but the preparation of pentaful-

[a] R. Nouch, Dr. M. Cini, M. Abid, Prof. Dr. S. Woodward, Dr. W. Lewis
GlaxoSmithKline Carbon Neutral Laboratories for Sustainable Chemistry
University of Nottingham
6 Triumph Road, Nottingham, NG7 2GA (UK)
E-mail: simon.woodward@nottingham.ac.uk

[b] Dr. M. Magre, Prof. Dr. M. Diéguez, Prof. Dr. O. Pàmies
Departament de Química Física i Inorgànica
Universìtat Rovira i Virgili
Campus Sescelades, Marcel, lí Domingo 1-43007, Tarragona (Spain)
E-mail: montserrat.dieguez@urv.cat

Supporting information and the ORCID identification number(s) for the author(s) of this article can be found under https://doi.org/10.1002/chem.201704247.

**Table 1.** Summary of optimization for enantioselective preparation of pentafulvene **2a**.[a]

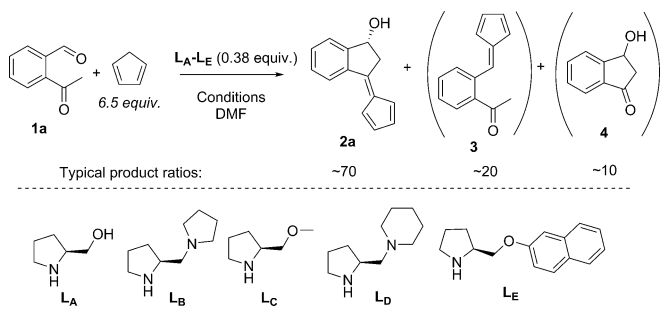


| Catalyst | Acid [equiv.] | *t* [h] | *T* [°C] | Yield [%][b] | *er* |
|---|---|---|---|---|---|
| $L_A$ | AcOH (0.38) | 24 | 25 | 90[c] | 79:21 |
| $L_B$ | AcOH (0.38) | 2 | 25 | 71 | 86:14 |
| $L_B$ | AcOH (0.26) | 2 | 22 | 76 | 89:11 |
| $L_B$ | AcOH (0.13) | 6 | 15 | 78 | 94:6 |
| $L_C$ | AcOH (0.13) | 24 | 22 | 69 | 80:20 |
| $L_D$ | AcOH (0.13) | 2 | 22 | 71 | 90:10 |
| $L_E$ | AcOH (0.13) | 4 | 22 | < 5 | n.d.[d] |

[a] Carried out on **1a** (0.39 mmol) in DMF (1 mL); for full details of optimization see Supporting Information. [b] Isolated yield unless otherwise stated. [c] Conversion determined by $^1$H NMR spectroscopy with no internal standard present (mass balance of > 90% confirmed independently). [d] Not determined.

**Table 2.** Substrate scope for chiral pentafulvene (**2**) formation.[a]

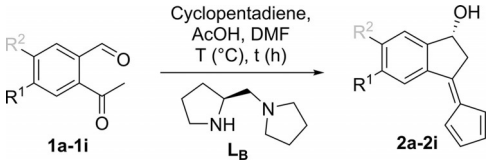


| Cmpd. | $R^1$ | $R^2$ | *T* [°C] | *t* [h] | Yield [%][b] | Initial *er* | Recrystallized *er* |
|---|---|---|---|---|---|---|---|
| **2a** | H | H | 15 | 6 | 78 | 94:6 | > 99:1 |
| (*S*)-**2a**[d] | H | H | 15 | 6 | 65 | 94:6 | 98:2 |
| **2b** | Ph | H | 15 | 4.5 | 53 | 88:12 | > 99:1 |
| **2c** | *t*Bu | H | 22 | 2.5 | 91 | 82:18 | –[c] |
| **2d** | Me | H | 15 | 6 | 72 | 91:9 | –[c] |
| **2e** | OMe | H | 15 | 5 | 54 | 91:9 | > 99:1 |
| **2f** | F | H | 25 | 4.5 | 39 | 92:8 | > 99:1 |
| **2g** | H | Me | 15 | 6 | 67 | 89:11 | –[c] |
| **2h** | H | F | 25 | 3 | 52 | 88:12 | > 99:1 |
| (*S*)-**2h**[d] | H | F | 25 | 3 | 39 | 90:10 | > 99:1 |
| **2i** | H | Cl | 25 | 3 | 38 | 91:9 | 99:1 |
| (*S*)-**2i**[d] | H | Cl | 25 | 2.5 | 30 | 89:11 | 99:1 |

[a] Carried out on **1** (0.6–2.1 mmol) with AcOH (0.13 equiv) and $L_B$ (0.38 equiv) in DMF (1–5 mL); for full details see Supporting Information. [b] Isolated yield. [c] Could not be enriched by recrystallization. [d] Synthesized under identical conditions but providing the (*S*)-pentafulvene using (*R*)-$L_B$.

vene products of type **2** is unprecedented, as far as we are aware. Catalysts bearing too much steric bulk, such as $L_E$ or the bulky diaryl derivatives developed by Jørgenson[12] and Hayashi,[13] proved ineffective as did the imidazolidinone derivatives of Macmillan.[14] Optimal results were attained with (2*S*)-1-(pyrrolidin-2-ylmethyl)pyrrolidine ($L_B$),[15,16] with a reduced number of equivalents of acetic acid (0.13 vs. 0.38 equiv). Below 0.38 equivalents of catalyst $L_B$ the reaction conversion suffered but the *er* remained high. Alternative acids were also trialed but all performed worse than acetic acid in the reaction (see Table S1 in the Supporting Information). The reaction could be scaled to gram quantities without any significant negative yield or *er* effects (see Experimental section). Excesses of cyclopentadiene were employed, as it is cheap and easily removed during purification, to ensure reliability of the reaction and to hinder the production of by-product **4** as much as possible.

The precursor 2-acetyl-benzaldehydes (**1a**–**1i**) needed for generalization of the reaction are easily prepared on multigram scales via two routes. Directed lithiation of a range of benzyl alcohols followed by reaction with acetaldehyde and subsequent oxidation provides **1a**–**c** in two steps. Alternatively, Phan's phenol formylation, followed by acyl hydrazide formation and subsequent acyl transfer was used for **1d**–**i**.[17] The optimal catalyst $L_B$ is commercially available, but also readily and efficiently prepared on multi-gram scales, starting from low cost L-proline using our optimized method (see Supporting Information). The generality of the reaction was thus explored (Table 2).

Fulvene formation is tolerant of a range of electronic substituent effects in the 5-position (**2d**–**f**) but is more sensitive to steric factors (runs **2b**,**c**). The opposite situation applies to substitution in the 6-position (runs **2g**–**i**). The poorer yields obtained for halogen containing **2f** and **2i** appear to be due to the decreased stability of the product rather than lower conversion based on control experiments. Modification of the reaction conditions allowed isolation of the two by-products **3** and **4** in useful quantities. Reduction of the reaction temperature to 0 °C provided condensation by-product **3** in 45% yield after 48 hours. We propose that this is due to the lower temperature strongly disfavoring the less reactive keto functionality, allowing for an increase in condensation between the more reactive aldehyde and cyclopentadiene at longer reaction times. Running the reaction under its optimized conditions (Table 1, Run 4) but without added cyclopentadiene resulted in a 55% isolated yield of aldol by-product (*S*)-**4** (*er* < 85:15). Isolation of these by-products enabled us to unambiguously define the reaction mechanism for pentafulvene formation (Scheme 2). Pathway A can be discounted as intermediate **5** would produce aldol by-product **4**, however, resubmission of isolated **4** to the reaction conditions produces no fulvene products discounting cyclopentadiene condensation at the keto group of **4**. In addition, HPLC confirmed the chiral centre in (*S*)-**4** is of opposite configuration to the (*R*)-**2** provided by $L_B$, eliminating **4** as a simple precursor to **2**.[18,19] Similarly, pathway C can be discounted on the fact that resubmission of isolated **3** to the reaction conditions also produces no **2**, disavowing potential intermediates in the H-shift pathway **7a**,**b**. In addition, pathway C would provide regioisomeric **2′** (Scheme 2) if appropriately substituted (regardless of the sense of asymmet-

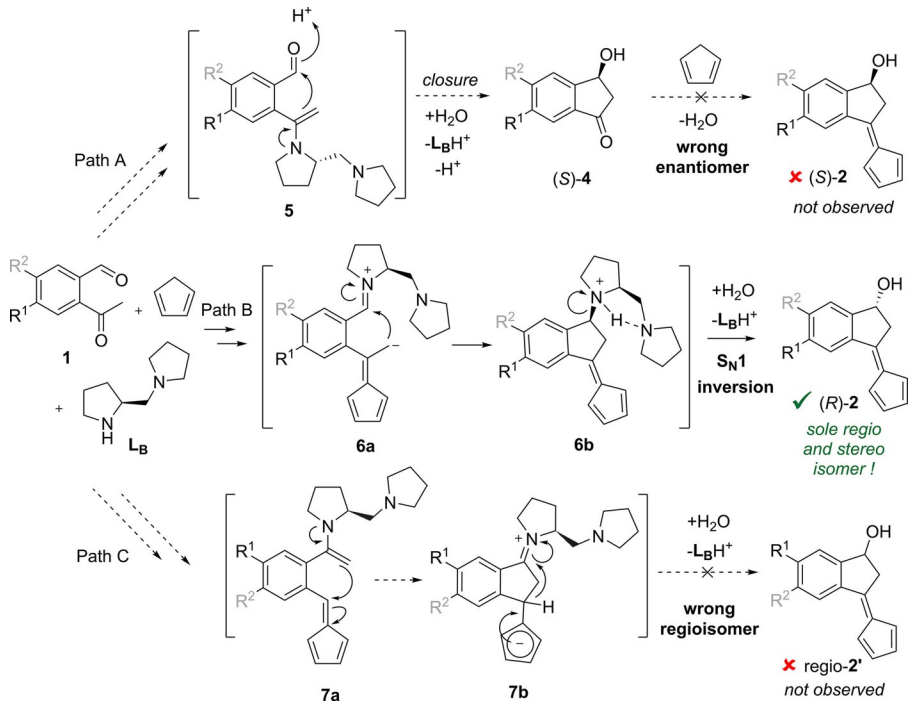


**Scheme 2.** Mechanistic possibilities for the formation of pentafulvene **2a**.

ric induction). Only pathway B, in which condensation of cyclopentadiene with the acetyl ketone occurs first, correctly accounts for both the regiochemistry and sense of stereochemistry observed in the reaction. The acidity of the α-methyl fulvene group ($pK_a$ ca. 22.1 in DMSO)[20] and the subsequent inversion in the $S_N1$-like cleavage of the amine both have precedent.[21–23] Intermediates **6a**,**b** could not be isolated or detected but remain the only viable option consistent with the experimental data. Large leaving groups, as in **6b**, strongly favour inversion outcomes in $S_N1$ hydrolysis reactions and an ability for additional protonation of the pyrrolidine nitrogen may account for the improved performance of $\mathbf{L_B}$.

Preliminary studies show that, following functionalization of the pendant hydroxy group, pentafulvenes of type **2** can be reduced, in the manner of Tacke,[24] using $LiBEt_3H$. One example of this is shown in Scheme 3. The reduction proceeds with very high diastereoselectivity (>25:1 as the other diastereomer is not visible in the $^1$H NMR spectrum) following functionalization of pentafulvene **2a** with triethylsilyl chloride (TESCl). The silyl ether moiety acts as a blocking group, forcing the hydride to add *anti* to it, resulting in the synthesis of *syn*-cyclopentadiene **9** (see Supporting Information, Figure S2, for an explanation of the structural assignment of **9**).

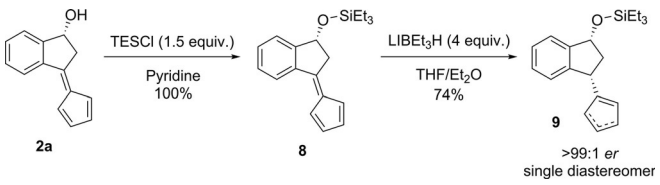


**Scheme 3.** Synthesis of protected pentafulvene **8**, via the reaction of pentafulvene **2a** with TESCl, which is then reduced to *syn*-cyclopentadiene **9**. The double bond tautomers of **9** are removed upon metal complexation.

To conclude, we have presented an efficient synthesis of chiral 6,6-disubstituted pentafulvenes bearing a functionalizable chiral pendant hydroxy group in moderate to good yields and enantiomeric ratios. These pentafulvenes possess the interesting and useful characteristic of crystallizing as conglomerates, often giving the products in >99:1 *er* at gram scales. Once functionalized, these chiral pentafulvene derivatives can then be converted into substituted cyclopentadienes essentially as both single enantiomers and diastereomers.

## Experimental Section

### Representative procedure for synthesis of pentafulvene (R)-2a

Commercially available 2-acetyl-benzaldehyde (1.29 g, 78% purity, 6.79 mmol) and cyclopentadiene (3.6 mL, 42.8 mmol) were dissolved in DMF (16.0 mL) before the addition of acetic acid (47 μL, 0.82 mmol) and dropwise addition of commercially available *(2S)*-1-(pyrrolidin-2-ylmethyl)pyrrolidine (411 μL, 2.52 mmol). This was then stirred at 15 °C for 6 hours, after which the reaction was diluted into ethyl acetate (250 mL) and washed with pH 7.4 phosphate buffer (3×100 mL). The solvent was removed in vacuo before purification via flash column chromatography (eluent: dichloromethane) to yield the crude product as a bright orange solid in 64% yield (850 mg, 4.33 mmol); yield range on 0.1-1 g scales: 64–78%. Purification from $CH_2Cl_2$/pentane, or dimethoxyethane readily afforded (*R*)-**2a** as red needles (590 mg, 3.01 mmol, 70% recovery) with >99:1 *er*. M.p.: 130–140 °C (darkens from this temperature); $R_f$ (dichloromethane): 0.30; $^1$H NMR (400.2 MHz, $CDCl_3$): $\delta_H$ = 7.96 (dd, *J* = 6.6, 1.9 Hz, 1H, Ar*H*), 7.58–7.55 (m, 1H, Ar*H*), 7.48–7.38 (m, 2H, Ar*H*), 6.92 (app ddd, *J* = 5.3, 1.7, 1.7 Hz, 1H, Cp*H*), 6.59–6.55 (m, 1H,

Cp*H*), 6.53–6.49 (m, 2H, Cp*H*), 5.35 (ddd, $J=7.0$, 7.0, 3.7 Hz, 1H, C*H*OH), 3.72 (dd, $J=17.5$, 7.0 Hz, 1H, $CH_aH_b$ *anti* to OH), 3.09 (dd, $J=17.5$, 7.0 Hz, 1H, $CH_aH_b$ *syn* to OH), 2.01 ppm (d, $J=3.7$ Hz, 1H, O*H*); $^{13}C$ NMR (100.05 MHz, $CDCl_3$): $\delta_C=151.2$ (C), 149.5 (C), 139.4 (C), 138.7 (C), 132.8 (CH), 131.1 (CH), 131.0 (CH), 129.4 (CH), 126.5 (CH), 125.4 (CH), 123.4 (CH), 120.0 (CH), 72.9 (CH), 44.0 ppm ($CH_2$); ($CHCl_3$): $\tilde{\nu}_{max}=3614$, 3590, 3070, 3045, 3008, 2960, 2927, 2873, 1630, 1476, 1458, 1389, 1368, 1239, 1050, 1021, 997 $cm^{-1}$; HRMS found 197.0959 $C_{14}H_{13}O^+$ requires 197.0961 ($|\sigma|=1.0$ ppm); HPLC (before crystallization): Chiralpak AD-H; mobile phase, hexane:2-propanol (4:1 *v*/*v*); flow rate, 0.5 mL $min^{-1}$; retention times (*S*)-enantiomer: 11.8 min (6.2%), (*R*)-enantiomer: 14.2 min (93.8%), *er* 94:6; $[\alpha]_D^{23}$: +68.0 (*er* > 99:1, $c=0.50$ in $CHCl_3$); Elemental analysis (%): Calcd. for $C_{14}H_{12}O$ C, 85.68; H, 6.16; found C, 85.20; H, 6.47.

## Acknowledgements

We thank the Edith Johnson Bequest Fund and Aesica Pharmaceuticals for partial support of the University of Nottingham studentships of M.C. and R.N. respectively. M.A. is grateful to the University of Anbar (Iraq) for PhD study leave (award IDB600032695). MM, MD and OP thank the Spanish Ministry of Economy and Competitiveness (CTQ2016-74878-P) and European Regional Development Fund (AEI/FEDER, UE), the Catalan Government (2014SGR670), and the ICREA Foundation (ICREA Academia award to MD) for financial support.

## Conflict of interest

The authors declare no conflict of interest.

**Keywords:** carbanions · asymmetric catalysis · fulvenes · organocatalysis · synthetic methods

[1] J. Thiele, *Ber. Dtsch. Chem. Ges.* **1900**, *33*, 666–673.
[2] K. J. Stone, R. D. Little, *J. Org. Chem.* **1984**, *49*, 1849–1853.
[3] K. Chajara, H. Ottosson, *Tetrahedron Lett.* **2004**, *45*, 6741–6744.
[4] H. C. L. Abbenhuis, U. Burckhardt, V. Gramlich, A. Togni, A. Albinati, B. Mueller, *Organometallics* **1994**, *13*, 4481–4493.
[5] Z. Zhou, Z.-X. Wang, Y.-C. Zhou, W. Xiao, Q. Ouyang, W. Du, Y.-C. Chen, *Nat. Chem.* **2017**, 1–5.
[6] Z. J. Jia, C. Merten, R. Gontla, C. G. Daniliuc, A. P. Antonchick, H. Waldmann, *Angew. Chem. Int. Ed.* **2017**, *56*, 2429–2434; *Angew. Chem.* **2017**, *129*, 2469–2474.
[7] M. Cini, T. D. Bradshaw, W. Lewis, S. Woodward, *Eur. J. Org. Chem.* **2013**, 3997–4007.
[8] M. Cini, T. D. Bradshaw, S. Woodward, W. Lewis, *Angew. Chem. Int. Ed.* **2015**, *54*, 14179–14182; *Angew. Chem.* **2015**, *127*, 14385–14388.
[9] N. J. Sweeney, J. Claffey, H. Müller-Bunz, C. Pampillón, K. Strohfeldt, M. Tacke, *Appl. Organomet. Chem.* **2007**, *21*, 57–65.
[10] L. Pasteur, *Ann. Chim. Phys.* **1850**, *28*, 56–99.
[11] Y. Tobe, *Mendeleev Commun.* **2003**, *13*, 93–94.
[12] M. Marigo, T. C. Wabnitz, D. Fielenbach, K. A. Jørgensen, *Angew. Chem. Int. Ed.* **2005**, *44*, 794–797; *Angew. Chem.* **2005**, *117*, 804–807.
[13] Y. Hayashi, H. Gotoh, T. Hayashi, M. Shoji, *Angew. Chem. Int. Ed.* **2005**, *44*, 4212–4215; *Angew. Chem.* **2005**, *117*, 4284–4287.
[14] R. J. Comito, F. G. Finelli, D. W. C. Macmillan, *J. Am. Chem. Soc.* **2013**, *135*, 9358–9361.
[15] M. Asami, *Bull. Chem. Soc. Jpn.* **1990**, *63*, 721–727.
[16] J. Liu, L. Wang, *Synthesis* **2016**, 960–972.
[17] D. H. T. Phan, B. Kim, V. M. Dong, *J. Am. Chem. Soc.* **2009**, *131*, 15608–15609.
[18] J. Moritani, Y. Hasegawa, Y. Kayaki, T. Ikariya, *Tetrahedron Lett.* **2014**, *55*, 1188–1191.
[19] T. Suzuki, K. Ghozati, T. Katoh, H. Sasai, *Org. Lett.* **2009**, *11*, 4286–4288.
[20] D. B. Knight, J. A. Harrelson, *J. Chem. Soc. Chem. Commun.* **1987**, 116–117.
[21] R. M. Pagni, *Found. Chem.* **2011**, *13*, 131–143.
[22] P. Brewster, E. D. Hughes, C. K. Ingold, P. A. D. S. Rao, *Nature* **1950**, *166*, 179–180.
[23] S. M. E. D. Hughes, C. K. Ingold, *J. Chem. Soc.* **1935**, 1196–1200.
[24] N. J. Sweeney, O. Mendoza, H. Müller-Bunz, C. Pampillón, F. J. K. Rehmann, K. Strohfeldt, M. Tacke, *J. Organomet. Chem.* **2005**, *690*, 4537–4544.

Manuscript received: September 10, 2017
Accepted manuscript online: October 30, 2017
Version of record online: November 20, 2017

ChemPubSoc Europe

DOI: 10.1002/ejic.201900510

EurJIC European Journal of Inorganic Chemistry

Full Paper

Anti-cancer Ti Complexes

# Tripodal O-N-O *Bis*-Phenolato Amine Titanium(IV) Complexes Show High in vitro Anti-Cancer Activity

Mohammed Abid,[a,b] Ryan Nouch,[b] Tracey D. Bradshaw,[c] William Lewis,[b][‡] and Simon Woodward*[b]

**Abstract:** The octahedral titanium(IV) complexes *trans,mer*-[Ti{$R^3N(CH_2C_6H_2$-2-O-4-$R^2$-6-$R^1)_2$}$_2$] ($R^1$ = Me, OMe, Cl; $R^2$ = Me, OMe, F, Cl; $R^3$ = Me, Et; not all combinations) are synthesised in two steps from simple phenols in 36–53 % overall yield. The highly crystalline (4 X-ray structures) complexes are active against MCF-7 (breast) and HCT-116 (colon) cancer cell lines showing widely varying $GI_{50}$ values in the range 1–100 μM depending on $R^1$–$R^3$. Highest activities are realised when $R^1$ = OMe and $R^2$, $R^3$ = Me ($GI_{50}$ ca. 1 μM for MCF-7 and 2–3 μM for HCT-116). These are respectively 8× and 3× times greater than the activities of cisplatin in the same cell lines. These titanium complexes show some significant selectivity for cancer cell lines; up to 7× higher in MCF-7 compared to non-cancer (MRC-5) fibroblast cells. Details of cellular mode of action indicators (cell cycle perturbation, Annexin V, γ-H2AX, and caspase studies) that point to an apoptosis mode for the most active compound ($R^1$ = OMe and $R^2$, $R^3$ = Me) are also reported.

## Introduction

In 1969, cisplatin [*cis*-diamminedichloroplatinum(II)] first emerged as a cancer therapy, subsequently becoming one of the most popular antineoplastic (cytotoxic) agents employed against human ovarian, testicular, head, neck and bladder carcinomas. Although cisplatin possesses potential against most carcinomas, its toxic side-effects (myelotoxicity and nephrotoxicity) and problems with resistance soon became apparent.[1] Because of such issues, alternative metal complexes have also been explored for anti-cancer activity.[2] These related metal complexes can show mechanisms of action other than the DNA binding seen for cisplatin depending on their metal acidity/oxidation state and their supporting ligands.[3] In particular, titanium(IV) complexes have recently appeared showing activities higher or comparable to cisplatin and its Pt-based derivatives and these are thought to be promising anti-cancer drug candidates.[4] Unfortunately, progress towards potential clinical candidates has been hindered by a lack of understanding of the mechanism(s) of action of titanium agents.[5] Initial investigations in this area focused on titanocene dichloride $Cp_2TiCl_2$ (Cp = η-$C_5H_5$) and this candidate reached clinical trial (although its low efficacy did not allow it to progress beyond phase II). One of the problems in deriving the cellular mode of action of $Cp_2TiCl_2$, and related titanium(IV) complexes, is that while partial ligand hydrolysis is apparently vital in attaining the biological activity such reactions rapidly cascade providing complex mixtures of species. Thus, correlation of the observed cellular outcomes to a particular titanium species becomes difficult. With the aim of slowing down and controlling such hydrolysis events Tshuva has introduced polydentate phenolato ligands of type $\mathbf{L_A}$ and $\mathbf{L_B}$ (Scheme 1).[6,7] We became intrigued as to why the related ligand cores $\mathbf{L_C}$, after coordination to titanium(IV), had not been trialled in anti-cancer studies (even though exam-

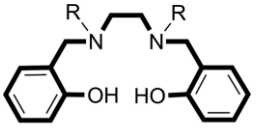


$\mathbf{L_A}$ R = Me
$\mathbf{L_B}$ R = $CH_2CH_2OH$

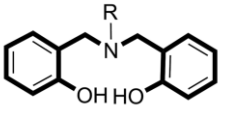


$\mathbf{L_C}$ R = Me,Et

Scheme 1. Previously screened ($\mathbf{L_A}$, $\mathbf{L_B}$) and an untried class $\mathbf{L_C}$ phenolato-amine ligand cores (shown in bold) for anti-cancer trials of titanium(IV) complexes.

[a] *Department of Chemistry, College of Science, University of Anbar, Western side of Ramadi City, Anbarshire, Republic of Iraq*
*E-mail: aboyazenabid@gmail.com*
*mohammed.abid@nottingham.ac.uk*
[b] *GSK Carbon Neutral Laboratories for Sustainable Chemistry, University of Nottingham, Triumph Road, Nottingham, NG7 2TU United Kingdom*
*E-mail: simon.woodward@nottingham.ac.uk*
*https://www.nottingham.ac.uk/~pczsw/SWGroup/*
[c] *School of Pharmacy, Centre for Biomolecular Sciences, University Park, Nottingham, NG7 2RD United Kingdom*
*E-mail: tracey.bradshaw@nottingham.ac.uk*
[‡] Present address: Dr. W. Lewis
School of Chemistry, The University of Sydney, Eastern Avenue, Sydney, NSW 2006 Australia
E-mail: w.lewis@sydney.edu.au

*Supporting information and ORCID(s) from the author(s) for this article are available on the WWW under https://doi.org/10.1002/ejic.201900510.*

ples of such complexes have been known in the fields of coordination chemistry and catalysis since 1970s).[8] We were particularly interested to see if use of ligand of type **L$_C$** (Scheme 1) could lead to highly active titanium(IV) complexes suitable for subsequent mechanistic investigations.

## Results and Discussion

### Ligand and Complex Formation and Stability

While over 5000 examples of entities containing the sub structure core of **L$_C$** (shown in bold) are known,[8] it is desirable for biological studies (e.g. for oxidative stability) to block sites *ortho* and *para* to the phenol (OH) function and to restrict R to a simple methyl unit. Only 35 examples of such structures (**2**, Scheme 2) are known, where R$^1$ and R$^2$ are restricted to Br, Cl, Me, *t*Bu and adamantyl.[8] Importantly, *no examples* of **2** have been reported containing electron-releasing OMe units, which we postulated would be the most biologically active when R$^3$ = Me. We thus prepared a small library of 4,6-substituted versions of **L$_C$ 2a–f** (Scheme 2) using simple Mannich chemistry. Five moderate electron-rich ligands **2a–e** containing methyl ($\sigma_p$ = –0.17) and methoxy ($\sigma_p$ = –0.27) units were prepared of which only **2a** was previously known.[9] Non-commercial phenols (**1d–e**) are accessed by simple Bayer–Villiger oxidations of the parent aldehydes (see Supporting Information). Crude yields for **2a–e** were in the range 50 to 80+% and analytically pure materials were attained by layering pentane onto their ether solutions. Attempts to prepare 4,6-substituted **L$_C$** from nitrogen containing **1h** were unsuccessful (Supporting Information). For comparison electron deficient **2f** (F, $\sigma_p$ = +0.06) and **2g** (Cl, $\sigma_p$ = +0.23) were also targeted. While **2f** is prepared in moderate yield **2g** could not be isolated pure in our hands, although it is described in the literature.[10] However, compound **2g** is clearly present in the crude mixture and this could be used for subsequent complexation studies (see later).

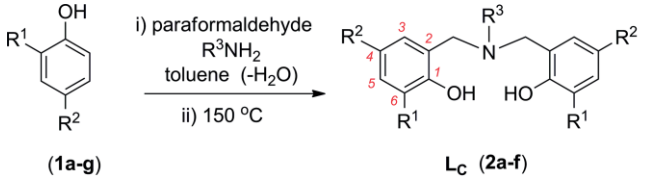


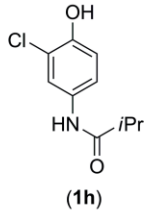


| L$_C$ | R$^1$ | R$^2$ | R$^3$ | Recrystallised yield (%) | Ref |
|---|---|---|---|---|---|
| **2a** | Me | Me | Me | 46 | [9] |
| **2b** | MeO | Me | Me | 62 | |
| **2c** | MeO | Me | Et | 80 | |
| **2d** | Me | MeO | Me | 54 | |
| **2e** | MeO | MeO | Me | 55 | |
| **2f** | Me | F | Me | 56 | |
| **2g** | Cl | Cl | Me | - | [10] |

Scheme 2. 4,6-substituted ligand **Lc** library prepared in this study.

Reaction of ligands **2** at a 2:1 stoichiometry with Ti(O*i*Pr)$_4$ in toluene at ambient temperature leads to intense red coloured solutions from which complexes **3** can be isolated in good yield as rhomboidal crystals or orange powders upon removal of the toluene and recrystallisation from optimal solvents (see Supporting Information) (Scheme 3).

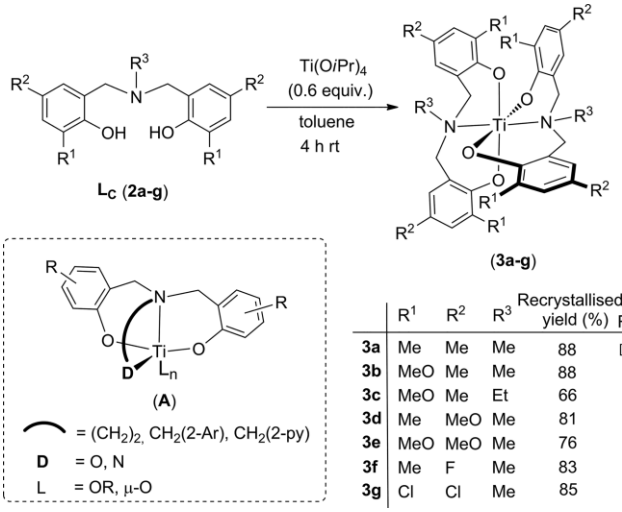


| | R$^1$ | R$^2$ | R$^3$ | Recrystallised yield (%) | Ref |
|---|---|---|---|---|---|
| **3a** | Me | Me | Me | 88 | [17] |
| **3b** | MeO | Me | Me | 88 | |
| **3c** | MeO | Me | Et | 66 | |
| **3d** | Me | MeO | Me | 81 | |
| **3e** | MeO | MeO | Me | 76 | |
| **3f** | Me | F | Me | 83 | |
| **3g** | Cl | Cl | Me | 85 | |

Scheme 3. Titanium complexes **3** library prepared in this study and comparison to the more commonly targeted motifs (**A**).

Ligands of type **2** (**L$_C$**) complex readily to a wide variety of transition metals including: Zr,[11] V,[12] Mo,[13] Mn,[14] Fe,[15] and Cu[16] However, for titanium only the preparation of **3a** is known[17] together with three Ti(substituted-**L$_C$**)$_2$ complexes using ligands related to **2** with R$^1$, R$^2$ = Me (or its 3-isomer), *t*Bu and R$^3$ = Et, *n*Pr, $CH_2CH_2NMe_2$.[18] Other than that, the nearest related titanium complexes we could identify (ca. 180 examples[8]) were those showing the motifs (**A**) (Scheme 3), which have been prepared mostly for studies of alkene polymerisation catalysis.[8] Complexes **3** are chiral (but racemic) and this causes observation of characteristic diastereotopic aryl C-H (four $^4J$ coupled doublets in the range $\delta_H$ 6.61–6.44) and $NCH_2$ (at $\delta_H$ 4.85–3.30 showing $^2J$ ca. 12.8 Hz or second order behaviour) signals. Conveniently, complexes **3** are all highly crystalline so that they can be easily brought to analytical purity for both biological and mechanistic studies (see Supporting Information for individual compounds). All of the compounds **3** are stable in [D$_6$]DMSO solution (10 mM) for at least 5 days at ambient conditions. Addition of excess $D_2O$, simulating the serial dilutions carried out in the biological assessments (see later), indicated that species **3** form colloidal suspensions and that hydrolysis to afford ligands **2** as the major solution species is a slow process (>1 day, see Supporting Information).

### Crystallographic Studies

The molecular structure of complex **3b** was determined by X-ray studies and is shown in (Figure 1). The same *trans*,*mer* geometry is also seen in related crystallographic studies of **3d**, **3e**, **3f** (see Supporting Information) and for the literature structure of **3a**.[17] The ligands in these series **3** contain a common $CH_2NMeCH_2$ linker so that electronic effects on bonding to $TiO_4N_2$ core induced by the aryl substituents can be examined. Comparing the bond length and angle data for these five com-

plexes (Table 1) reveals a very similar range of geometries. No significant structural correlation of the pro-drug structures of **3** to their cytotoxic activity (see later) was observed, implying that the observed structure-activity-relationship is due only to ligand electronic effects on the electron density in in vitro formed titanium species. At best for precursors **3** a slight distortion of N-Ti–N angles correlated with the anti-cancer activity. However, the latter may be due to crystal packing rather than substituent effects. Complexes **3d–f** were found to crystallise as solvates, but these are readily lost in the absence of supporting solvent and all subsequent biological studies were carried out on samples of **3** assayed as solvent free (NMR) and analytically pure (CHN).

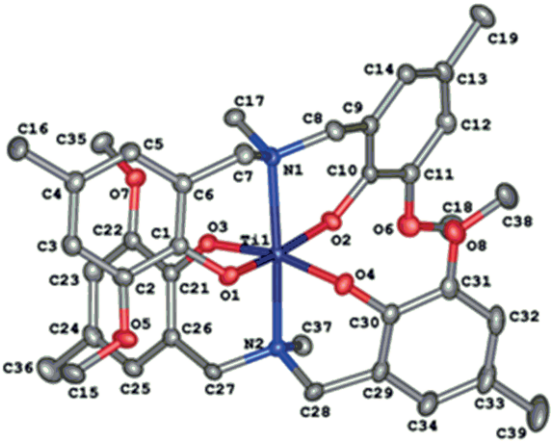


Figure 1. Molecular structure of titanium complex **3b**.

*Table 1.* Selected comparison of bond length and angle data for titanium complexes **3a**–**3b** and **3d**–**f** for their $TiO_4N_2$ cores.[a]

| Complex | **3a**[b] | **3b**[c] | **3d**[c] | **3e** | **3f** |
|---|---|---|---|---|---|
| $R^1$ (*ortho*) | Me | MeO | Me | OMe | Me |
| $R^2$ (*para*) | Me | Me | OMe | OMe | F |
| **Bond lengths [Å]** | | | | | |
| Ti(1)–O(1) | 1.892 | 1.909 | 1.881 | 1.921 | 1.880 |
| Ti(1)–O(2) | 1.882 | 1.859 | 1.889 | 1.874 | 1.876 |
| Ti(1)–O(3) | 1.892 | 1.873 | 1.894 | 1.867 | 1.880 |
| Ti(1)–O(4) | 1.882 | 1.900 | 1.878 | 1.887 | 1.876 |
| Ti(1)-$O_{ave}$ | 1.887 | 1.885 | 1.885 | 1.887 | 1.878 |
| Ti(1)–N(1) | 2.264 | 2.244 | 2.244 | 2.272 | 2.247 |
| Ti(1)–N(2) | 2.264 | 2.267 | 2.265 | 2.251 | 2.247 |
| Ti(1)-$N_{ave}$ | 2.264 | 2.255 | 2.256 | 2.262 | 2.247 |
| **Bond angles (°)** | | | | | |
| O(1)–Ti(1)–O(2) | 168.6 | 167.5 | 167.1 | 165.2 | 167.9 |
| O(3)–Ti(1)–O(4) | 168.6 | 167.6 | 167.9 | 166.4 | 167.9 |
| N(1)–Ti(1)–N(2) | 179.7 | 174.7 | 173.8 | 173.6 | 179.8 |

[a] The $TiO_4N_2$ donor set is numbered in all cases as for **3b** in Figure 1 (see also Supporting Information). [b] Based on the published SEFZIN structure.[17] [c] Average of two independent molecules within unit cell.

## Growth Inhibitory Activity of 3b–e Against MCF-7 and HCT-116

In vitro antitumour activity of all compounds (**3**) was assessed using the MTT assay against two human-derived cancer cell lines: MCF-7 (breast) and HCT-116 (colon), with cisplatin as a positive control for all tests, using standard protocols (see Supporting Information). Compound **3a** has been previously reported in the literature,[17] but its anti-cancer properties were not determined. Trials of **3a** revealed unremarkable activity ($GI_{50}$ values 35–40 μM) against both these cell lines. Exchange of a single methyl for methoxy group in complex **3b** resulted in >10-fold increase in anti-cancer activity. The growth inhibitory activities of **3a** and **3b** are compared in Figure 2. The $GI_{50}$ values of the electronically diverse complexes **3b–f** were similarly screened by MTT assay. Complex **3b** was confirmed as the most active with $GI_{50}$ values of ca. 1 μM for MCF-7 and ca. 3.4 μM for HCT-116 (Table 2). Other compounds in the series showed moderate to good anti-cancer activity (Figure 3 and Table 2). Typically, no structural modifications were made to the compounds at the nitrogen donor (e.g. $R^3$), as preliminary studies changing the methyl group within **3b** to the ethyl derivative **3c** negatively affected the compound class, reducing potency. The activity of **3c** is similar to cisplatin, whose control $GI_{50}$ values in our studies were 6.6 μM for MCF-7 and 9.2 μM for HCT-116 (Figure 3A–B). We suspect **3c** of being less soluble in aqueous media leading to reduced activity. Our results show that Ti(IV) complexes **3b–f** are among the most active reported in the literature[4–7] and that this activity is strongly dependent on the ligand structure. While **3b** is the most potent compound, **3d** showed good activity with $GI_{50}$ values of 2 μM and 3 μM against MCF-7 and HCT-116 cell lines respectively (Figure 3A–B and Table 2). Complex **3e** showed lower potency than **3b** and **3d** against the same cell lines ($GI_{50}$ values ca. 8.5 μM against both MCF-7 and HCT-116 cells; Figure 3A–B and Table 2). Complex **3f** revealed reduced activity with $GI_{50}$ values of 11.7 μM for MCF-7 and 22 μM for HCT-116 (Figure 3A–B and Table 2).

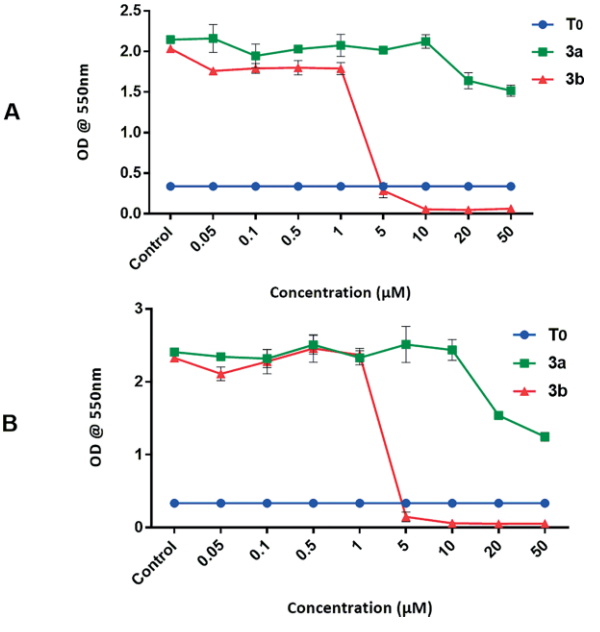


Figure 2. Representative MTT graphs displaying the dose-dependent growth inhibitory properties of **3a–b** against MCF-7 (**A**) and HCT-116 (**B**) cell lines. Cells were seeded in 96-well plates at a density of $3 \times 10^3$ cells/well. After allowing 24 h to adhere, cells were treated with the specified compound and incubated for 72 h. Data points depict mean ±S.D. n = 8; MTT assays were repeated >3 times. Line$T_0$ is a control run: using just media and cancer cell line.

Table 2. Activity of complexes **3** ($GI_{50}$ values in μM by MTT assay) against MCF-7 and HCT-116 cancer cell lines and normal MRC-5 fibroblast cells. Data were generated from ≥3 independent trials; n = 8 per experimental condition per trial.

| **3** | $R^1$ | $R^2$ | $R^3$ | $\sigma_p(R^1)$[a] | $\sigma_p(R^2)$[a] | $GI_{50}$ (MCF-7) (μM)[b] | $GI_{50}$ (HCT-116) (μM)[b] | $GI_{50}$ (MRC-5) (μM)[b] |
|---|---|---|---|---|---|---|---|---|
| **3a** | Me | Me | Me | –0.17 | –0.17 | 36.3±0.1 | 38.6±0.1 | >50 |
| **3b** | MeO | Me | Me | –0.27 | –0.17 | 1.0±0.04 | 3.4±0.07 | 7.33±0.04 |
| **3c** | MeO | Me | Et | –0.27 | –0.17 | 6.6±0.07 | 9.2±0.09 | 15.23±0.01 |
| **3d** | Me | MeO | Me | –0.17 | –0.27 | 2.2±0.06 | 3.0±0.05 | 8.38±0.04 |
| **3e** | MeO | MeO | Me | –0.27 | –0.27 | 8.4±0.1 | 8.6±0.15 | 16.0±0.1 |
| **3f** | Me | F | Me | –0.17 | +0.06 | 11.7±0.05 | 22±0.031 | 34±0.03 |
| **3g** | Cl | Cl | Me | +0.23 | +0.23 | 51.5±0.1 | 64.8±0.07 | >100 |
| Cis-Pt[c] | – | – | – | – | – | 7.8±0.04 | 8.4±0.06 | 7.6±0.09 |

[a] Hammett parameter value for para substituent.[20] [b] As determined by MTT assay (3 duplicates). [c] Cisplatin.

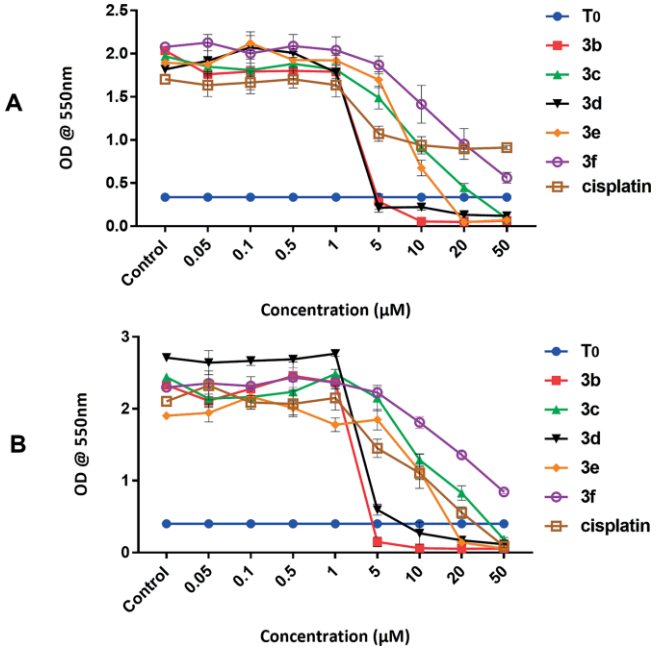


Figure 3. Representative MTT graphs displaying the dose-dependent growth inhibitory properties of **3b–f** against MCF-7 (**A**) and HCT-116 (**B**) cell lines. Cells were seeded in 96-well plates at a density of $3 \times 10^3$ cells/well. After allowing 24 h to adhere, cells were treated with the specified compound and incubated for 72 h. Data points depict mean ±S.D. n = 8; MTT assays were repeated >3 times. Line$T_0$ is a control run: using just media and cancer cell line.

Tetrachloro analogue **3g** showed the lowest activity amongst the new derivatives of **3** screened and was comparable to complex **3a**. The **3g** $GI_{50}$ values were: 51.5 μM for MCF-7 and 64.8 μM for HCT-116 (Figure S4, see Support Information). The selectivity of **3b** for cancerous cells was evaluated by measuring its growth inhibitory activity in non-cancerous MRC-5 human lung fibroblast (Figure S5–A, see Support Information). Complex **3b** showed reduced activity (cytotoxicity) toward these cells, implying a degree of cancer cell selectivity.[19] The $GI_{50}$ value of **3b** in MRC-5 cells was higher at 7.3 μM (Table 2), indicating ca. 7-fold selectivity when compared to activity against MCF-7 breast cancer cells. The activities of all Ti(IV) complexes **3** were similarly assessed against MRC-5 and consistently, reduced activities were observed against these non-tumourigenic fibroblasts; the $GI_{50}$ values for **3e**, **3f** and **3g** were ca. 16 μM, 34 μM and >100 μM respectively. This was in complete contrast to cisplatin controls, which were equi-active across all three cell lines (cancerous MCF-7 and HCT-116 and benign MRC-5 fibroblasts). Thus, the novel Ti(IV) complexes **3** demonstrate significant cancer cell selectivity (Table 2 and Figure S5–B in Supporting Information).

The in vitro growth inhibitory activity of complexes **3a–g** are summarised in Table 2. An interesting correlation is seen between the electronic properties of the phenolic substituents vs. the cellular cytotoxic activity. Moderate donation ($R^1$, $R^2$ = Me, MeO) into the phenolate results in increased activity, but if this is either further increased (**3e**) or decreased (**3a**, **3f**, **3g**) the biological activity falls. Bulky substitution of $R^3$ (**3b** vs. **3c**) also has a negative effect on biological performance.

## Effect of 3b and 3d–f on MCF-7 and HCT-116 Colony Formation

Having established that Ti(IV) analogues **3** cause selective growth inhibitory activity in two cancer cell lines, we sought to evaluate whether these cancer cells could survive a brief challenge of 24 h exposure to 1 μM or 5 μM of representative Ti complexes **3** and retain their proliferative capacity. To this end, clonogenic assays were set up. Clonogenic assays are a recognised technique for determining the cytotoxic potential of a test agent and results are typically represented as a survival fraction (%) vs. control cell colony populations of non-treated cells. Both **3b** and **3d** significantly inhibited colony formation after 24 h treatment of cells at concentrations of 1 and 5 μM (Figure 4A–B). Complexes **3b** and **3d** inhibited MCF-7 colony formation cell at 1 and 5 μM by 40–45 % and 100 % respectively. Despite the fact that MCF-7 and HCT-116 showed variable sensitivities to **3b** and **3d** ($GI_{50}$ 1.0 μM and 3.4 μM respectively), similar inhibition of HCT-116 colony formation was observed, 51 % and 100 % by 1 and 5 μM values respectively (Figure 4A–B). Complexes **3e** and **3f** also inhibited the colony formation in MCF-7 cells by 25 % and 29 % (1μM), and 57 % and 48 % (5 μM) respectively. The same agents inhibited HCT-116 colony formation by 16 % and 22 % (1 μM **3e** and **3f**) and 49 % and 28 % (5 μM **3e** and **3f**; Figure 4A–B). Complete (100 %) inhibition of colony formation was observed in HCT116 cells and MCF-7 exposed to 5 μM **3b** and **3d**, reflecting potency and cytotoxicity of these complexes (Figure S6 C and D, see Support Information). These data indicate that the cancer cells have lost their ability to form progeny colonies or have been killed (Fig-

ure S6–C, see Support Information).[21] Representative colonies are shown (Figure S6 C-D, see Support Information). In contrast, at the concentrations adopted, **3e** and **3f** demonstrated reduced potency, therefore exposure of MCF-7 or HCT-116 cells to 1 μM or 5 μM **3e** and **3f** failed to inhibit colony formation by >50 %.[22]

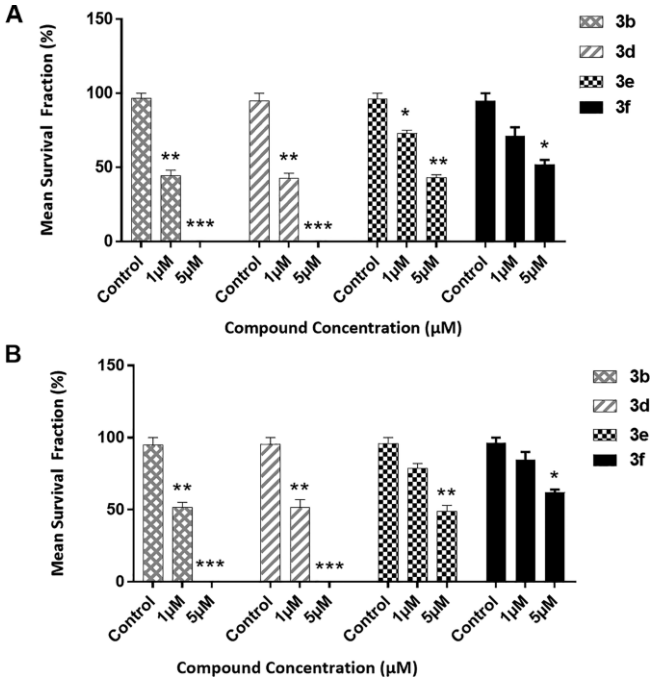


Figure 4. Effect **3b**, **3d**, **3e**, and **3f** on **A**) MCF-7, **B**) HCT-116 colony formation. A + B Mean survival fraction of % control represented of mean ±SEM of 5 independent trials (n = 2 per trial). Complexes **3b** and **3d** exhibited significant reduction in colony formation while **3e** and **3f** showed modest activity by comparison ($p < 0.0001$, n = 2).

## Cell Cycle Analysis

Based on MTT and clonogenic assays, the complexes **3** compromise cancer cell viability and growth. Led by these observations, we examined the effect of **3b**, **3f** (as efficient and modest agents, i.e. $GI_{50}$ values of ca. 3 and 22 μM against the HCT-116 cell line respectively), and cisplatin (as a positive control) on cell cycle perturbation by flow cytometry. An HCT-116 control cell cycle distribution profile demonstrated: 53.4 %, 24.9 % and 15.3 % events for the G1, S, G2/M phases[5] respectively. Negligible events can be detected in the preG1 compartment reflecting a healthy HCT-116 population (Figure S7, see Supporting Information). In contrast, following 72 h exposure of these cells to 10 μM (ca. 1.5 × $GI_{50}$) cisplatin, a substantial pre-G1 population is evident (25.5 % events) indicative of cells undergoing apoptosis. It is known that cisplatin causes DNA inter- and intra-strand crosslinks,[23] blocking DNA replication; alerted DNA repair mechanisms fail to repair cisplatin-induced DNA damage (initially) initiating apoptosis. As DNA replication is blocked and repair is attempted, the cell cycle is halted during S and G2 phases. After 72 h of continued treatment, DNA repair failure triggers programmed cell death. No preG1 peak is evident in HCT-116 cells exposed to 10 μM (ca. 3 × $GI_{50}$) **3b**; this Ti(IV) analogue caused a profound accumulation of events in the G2/M phases, indicating a different/delayed mechanism of action. If the arrested cell cycle occurs as a result of DNA damage, its onset may be later than that caused by cisplatin.[24] In contrast, complex **3f** (at 10 μM; <0.5 × $GI_{50}$) caused negligible apparent cell cycle perturbation. MCF-7 cells exposed to cisplatin, **3b** or **3f** demonstrated modest increase in late S/G2/M events (Supplementary Figure S8).

## Induction of Apoptosis in Cancer Cells

Annexin-V/PI apoptosis assays[5] were performed to explore the apoptosis-inducing properties of **3b** and **3f**; cisplatin being used as a positive control. MCF-7 and HCT-116 cells were exposed to both complexes (5 μM and 10 μM; 72 h). Apoptotic populations were confirmed by dual annexin V-FITC/PI staining (Figure 5). The majority (65 %) of cells exposed to 10 μM cisplatin (72 h) were undergoing apoptosis. Both **3b** and **3f** revealed profound apoptotic MCF-7 and HCT-116 populations at the concentrations tested. However, while early and late apoptosis were evident in HCT-116 cells treated with **3b**, exposure to **3f** for 72 h revealed a larger proportion of cells undergoing early apoptosis – indicating later onset of programmed cell death (Figure 5, and Figures S9, S10 Supporting Information).

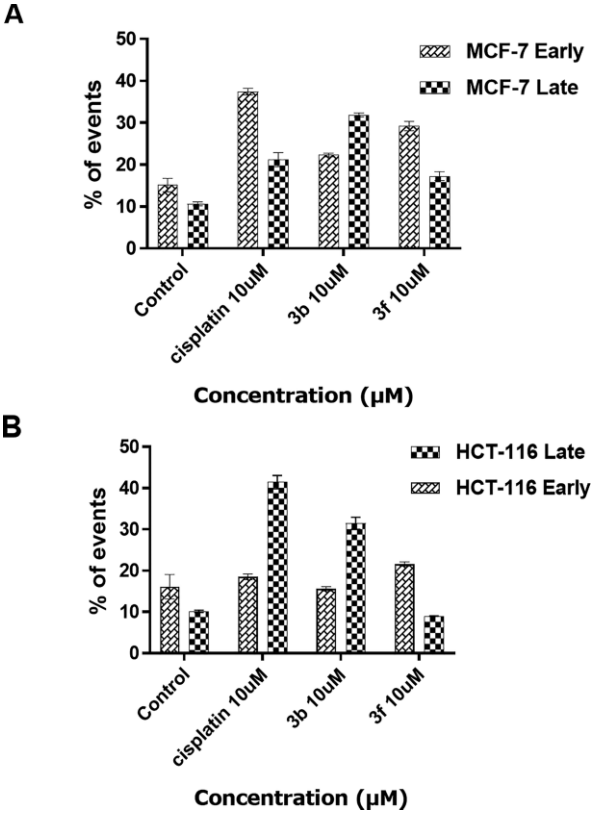


Figure 5. Apoptotic effects of **3b**, **3f**, and cisplatin on **A**) MCF-7 and **B**) HCT-116 cells at 10 μM. Cells were treated with 10 μM for 72 h. Annexin-V/PI apoptosis assay was adopted to determine the percentage of apoptotic cells.

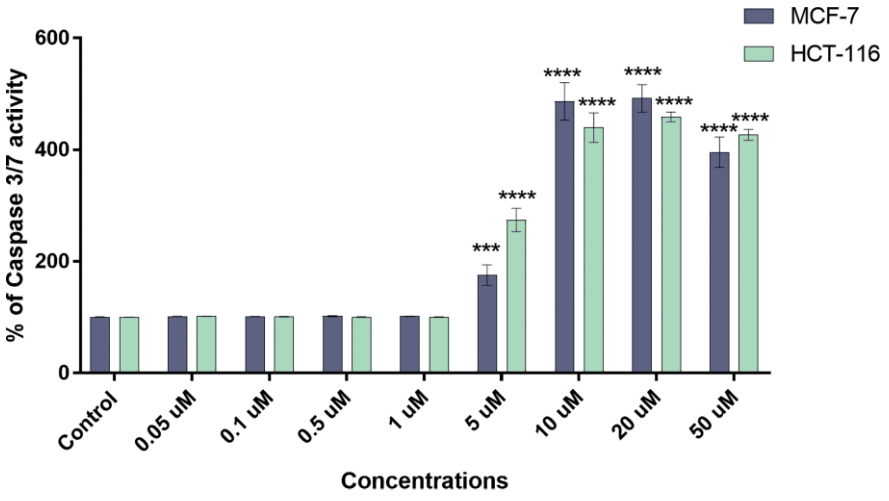


Figure 6. Dose-dependent elevation of caspase 3/7 activity in HCT-116 and MCF-7 cells following 72 h exposure of cells to Ti *complex* **3b**. Data points are mean ±S.D; ($p < 0.0001$, $n = 8$).

### Induction of DNA Damage

To determine whether apoptosis is triggered by DNA double strand breaks (DSBs), flow cytometric analyses of control, cisplatin-, **3b-** and **3f-**treated HCT-116 and MCF-7 populations were performed following co-incubation with PI (propidium iodide) and a 1° Ab (primary antibody) recognising γ-H2AX;[5] γ-H2AX foci appear at sites of DNA DSBs.[25] It is known that cisplatin causes DNA damage: inter/intrastrand DNA crosslinks, and DNA monoadducts that lead to DNA DSBs. These harbingers of apoptosis are largely responsible for Pt-drug antitumour activity.[1,23] Thus, co-incubation of cell populations with PI and 1° Ab recognising γ-H2AX, prior to flow cytometry analyses, allows cell-cycle-specific detection of sites of DNA DSBs. Consistent with cell cycle analyses, dual PI/ γ-H2AX labelling of HCT-116 cells supported **3b**-induced G2/M cell cycle arrest. Interestingly, HCT-116 G2/M events comprised a population heavily positively stained γ-H2AX+ve (53 %) suggestive of the presence of DNA DSBs. Complex **3f**, in contrast (consistent with HCT-116 cell cycle analysis and reduced potency) revealed neither G2/M arrest, nor γ-H2AX-+ve events associated with this cell phase. Rather a minority proportion of G1 events appeared to have incurred DNA DSB damage and were γ-H2AX+ve. Validating these analyses, accumulation of G2/M cell cycle events following exposure of HCT-116 cells to cisplatin (10 μM; 72 h was observed accompanied by γ-H2AX +ve events at sites of DNA DSBs (Figure S11, Support Information). Obvious γ-H2AX +ve events were detected in G1 and G2 cell cycle phases following exposure of MCF-7 cells to cisplatin, **3b** or **3f** (Supporting Information, Figure S12). Interestingly, chiral cyclopentadienyl complexes did not halt the cell cycle in treated cells and DNA DSBs (γ-H2AX foci) were similarly not detected.[26] Instead, antitumour activity of this compound was a consequence of paraptotic cell death, involving MAP kinase signal transduction. In contrast, current Ti complexes **3b** and **3f** clearly evoke apoptosis.

### Caspase Activation

Taken together, our data suggest that potent Ti complex **3b** causes later-onset apoptosis compared to cisplatin. To irrefutably confirm an apoptotic cell fate for cells exposed to **3b**, a caspase 3/7 activation assay was performed following exposure of HCT-116 and MCF-7 cells to escalating concentrations of **3b**. Dose-dependent significant caspase activation (≥5 μM **3b** $p < 0.0001$; Figure 6) was detected following 72 h exposure of cells to **3b** consistent with apoptosis-induction. As a positive control, 50 μM cisplatin was to confirm the assay raised caspase activation (e.g. by ca. 350 % in HCT-116 populations; not shown). These data confirm that after 72 h exposure, **3b** triggers apoptotic cell death (Figure 6).[27]

## Conclusion

A series of Ti(IV) complexes (**3**) has been synthesised and their structures confirmed by X-ray crystallography. Complex **3b** evoked potent cancer-selective growth inhibitory and cytotoxic activity. Cell cycle analyses indicated late-onset G2/M cell cycle arrest, which at 10 μM (representing ca. $3 \times GI_{50}$) triggered an apoptotic cell fate. Experiments are underway to determine modes of cell death and molecular targets of this promising class of titanium anti-cancer agents.

## *Acknowledgments*

M. A. is grateful to the University of Anbar (Iraq) for a PhD study leave (award IDB600032695). R. N. is grateful to Aesica and the School of Chemistry for support of a studentship. We thank Dr Huw E. Williams, Dr Thomas Macinally, Mr Mustapha Musa and the reviewers for helpful suggestions.

**Keywords:** Antiproliferation · Cytotoxicity · Titanium · Substituent effects

[1] For leading overviews of Pt-agents see: a) E. R. Jamieson, S. J. Lippard, *Chem. Rev.* **1999**, *99*, 2467–2498; b) J. S. Saad, M. Benedetti, G. Natile, L. G. Marzilli, *Inorg. Chem.* **2010**, *49*, 5573–5583 and citations thereof.
[2] For introductions to metal (including non-Pt) Anti-cancer agents see: a) *Metal-based Anticancer Agents* (Eds.: A. Casini, A. Vessières, S. M. Meier-Menches), Royal Society of Chemistry, Cambridge, UK, **2019**, pp. 500; b) U. Ndagi, N. Mhlongo, M. E. Soliman, *Drug Des. Dev. Ther.* **2017**, *11*, 599–616; c) M. J. Clarke, F. Zhu, D. R. Frasca, *Chem. Rev.* **1999**, *99*, 2511–2534.
[3] D. R. Williams, *Chem. Rev.* **1972**, *72*, 203-213.
[4] For overviews of titanium anti-cancer agents see: a) E. Y. Tshuva, J. A. Ashenhurst, *Eur. J. Inorg. Chem.* **2009**, 2203–2218; b) K. Strohfeldt, M. Tacke, *Chem. Soc. Rev.* **2008**, *37*, 1174–1187; c) K. M. Buettner, A. M. Valentine, *Chem. Rev.* **2012**, *112*, 1863–1881; d) S. A. Loza-Rosas, M. Saxena, Y. Delgado, K. Gaur, M. Pandrala, A. D. Tinoco, *Metallomics* **2017**, *9*, 346–356.
[5] M. Cini, T. D. Bradshaw, S. Woodward, *Chem. Soc. Rev.* **2017**, *46*, 1040–1051.
[6] a) M. Shavit, D. Peri, C. M. Manna, J. S. Alexander, E. Y. Tshuva, *J. Am. Chem. Soc.* **2007**, *129*, 12098–12099; b) D. Peri, S. Meker, M. Shavit, E. Y. Tshuva, *Chem. Eur. J.* **2009**, *15*, 2403–2415; c) S. Meker, O. Braitbard, M. D. Hall, J. Hochman, E. Y. Tshuva, *Chem. Eur. J.* **2016**, *22*, 9986–9995.
[7] For recent relevant developments in the titanium anti-cancer agent area see: a) R. Manne, M. Miller, A. Duth, M. F. C. G. da Silva, E. Y. Tshuva, T. S. B. Baul, *Dalton Trans.* **2019**, *48*, 304–314; b) N. Ganot, O. Briaitbard, A. Gammal, J. Tam, J. Hochman, E. Y. Tshuva, *ChemMedChem* **2018**, *13*, 2290–2296; c) M. Miller, E. Y. Tshuva, *Nat. Sci. Rep.* **2018**, *8*, 9705; d) S. A. Loza-Rosas, A. M. Vazquez-Salgado, K. I. Rivero, L. J. Negron, Y. Delgado, J. A. Benjamin-Rivera, A. L. Vazquez-Maldonado, T. B. Parks, C. Munet-Colon, A. D. Tinoco, *Inorg. Chem.* **2017**, *56*, 7788–7802; e) S. Barroso, A. M. Coelho, S. Gómez-Ruiz, M. J. Calhorda, Z. Zizak, G. N. Kaluđerović, A. M. Martins, *Dalton Trans.* **2014**, *43*, 17422–17433.
[8] Substructures $\mathbf{L_C}$ were identified through Scifinder (May 2019). Prepared by simple Mannich chemistry, their use in attaining catalysts for the polymerisation of alkenes and lactones is common; representative examples: a) A. Lehtonen, R. Sillanpaeae, *Inorg. Chem.* **2004**, *43*, 6501–6506; b) C.-T. Chen, C.-A. Huang, B.-H. Huang, *Macromolecules* **2004**, *37*, 7968–7973; c) C. M. Silvernail, L. J. Yao, L. M. R. Hill, M. A. Hillmyer, W. B. Tolman, B. William, *Inorg. Chem.* **2007**, *46*, 6565–6574; d) A. Lehtonen, H. Balcar, J. Sedlacek, R. Sillanpaeae, *J. Organomet. Chem.* **2008**, *693*, 1171–1176.
[9] W. J. Burke, J. L. Bishop, E. L. Mortensen Glennie, W. N. Bauer, *J. Org. Chem.* **1965**, *30*, 3423–3427.
[10] W. J. Burke, E. L. M. Glennie, C. Weatherbee, *J. Org. Chem.* **1964**, *29*, 909–912.
[11] For example: A. J. Chmura, M. G. Davidson, M. D. Jones, M. D. Lunn, M. F. Mahonc, *Dalton Trans.* **2006**, 887–889.
[12] For example: D. Maity, J. Marek, M.-F. Sheldrick, M. Ali, *J. Mol. Catal. A* **2007**, *270*, 153–159.
[13] For example: A. Peuronen, A. Lehtonen, *Top. Catal.* **2016**, *59*, 1132–1137.
[14] For example: T. Weyhermüller, T. K. Paine, E. Bothe, E. Eberhard, E. Bill, P. Chaudhuri, *Inorg. Chim. Acta* **2002**, *337*, 344–356.
[15] For example: T. Weyhermüller, R. Wagner, P. Chaudhuri, *Eur. J. Inorg. Chem.* **2011**, 2547–2557.
[16] S. Phongtamrug, K. Tashiro, M. Miyata, S. Chirachanchai, *J. Phys. Chem. B* **2006**, *110*, 21365–21370.
[17] a) see ref.[11]; b) Y. Chung, Y. Kim, *Acta Crystallogr., Sect. E* **2013**, *69*, m222; c) The Cambridge Crystallographic Data Centre (www.ccdc.cam.ac.uk) codes for these published structures of **3a** are SEFZIN and WHIMAD respectively.
[18] D. Peri, S. Meker, C. M. Manna, E. Y. Tshuva, *Inorg. Chem.* **2011**, *50*, 1030–1038. This includes the CCDC structures REZRET: Ti{$\mathbf{L_C}$(**2**)}$_2$ $R^1 = R^2$ = Me; $R^3$ = Et; REZRIX: Ti{$\mathbf{L_C}$(**2**) $\mathbf{L_C}$(**2′**)} first ligand with $R^1 = R^2$ = Me; $R^3$ = Et and second ligand with $R^1 = R^2$ = *t*Bu; $R^3$ = Et and REZRUJ: Ti{$\mathbf{L_C}$(**2**) $\mathbf{L_C}$(**2′**)} first ligand with $R^1$ = Me (but in 3-position) $R^2$ = Me; $R^3$ = $CH_2CH_2NMe_2$ and second ligand with $R^1 = R^2$ = *t*Bu; $R^3$ = Et.
[19] For a related selectivity study see ref. 6c.
[20] C. Hansch, A. Leo, R. W. Taft, *Chem. Rev.* **1991**, *91*, 165–195.
[21] For a related example see: M. E. Qazzaz, V. J. Raja, K.-H. Lim, T.-S. Kam, J. B. Lee, P. Gershkovich, T. D. Bradshaw, *Cancer Lett.* **2016**, *370*, 185–197.
[22] For a related example see: V. J. Raja, K.-H. Lim, C.-O. Leong, T.-S. Kam, T. D. Bradshaw, *Invest. New Drugs* **2014**, *32*, 838–850.
[23] For an overview of DNA-drug interactions see: D. Yang, J. Reedijk, G. A. van der Marel, A. H. J. Wang, *J. Biomol. Struct. Dyn.* **1996**, *13*, 989–998.
[24] For a recent related G2 block observation see: T. Pesch, H. Schuhwerk, P. Wyrsch, T. Immel, W. Dirks, A. Bürkle, T. Huhn, S. Beneke, *BMC Cancer* **2016**, *16*, 469.
[25] L. J. Kuo, L.-X. Yang, In vivo **2008**, *22*, 305–309.
[26] a) M. Cini, T. D. Bradshaw, S. Woodward, W. Lewis, *Angew. Chem. Int. Ed.* **2015**, *54*, 14179–14182; *Angew. Chem.* **2015**, *127*, 14385; b) M. Cini, H. Williams, M. W. Fay, M. S. Searle, S. Woodward, T. D. Bradshaw, *Metallomics* **2016**, *8*, 286–297.
[27] R. U. Jänicke, *Breast Cancer Res. Treat.* **2009**, *117*, 219–221.

Received: May 7, 2019